KU LEUVEN

ARENBERG DOCTORAL SCHOOL
FACULTY OF SCIENCE

Detection and analysis of forest cover dynamics with Landsat satellite imagery

Application in the Romanian Carpathian Ecoregion

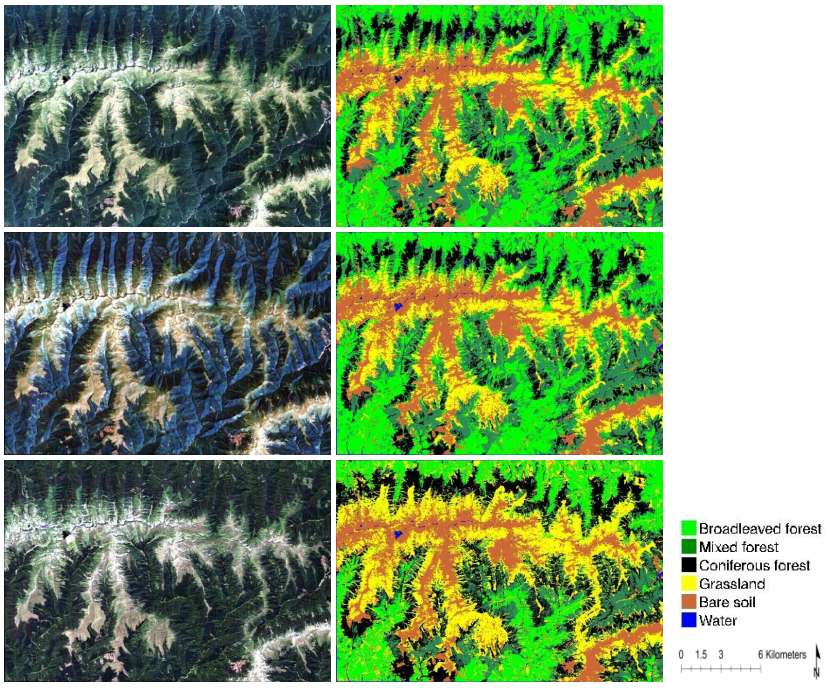

Ir. Steven VANONCKELEN

Supervisor:
Prof. Dr. A. Van Rompaey

Dissertation presented in partial fulfilment of the requirements for the degree of Doctor in Science

February 2014

DETECTION AND ANALYSIS OF FOREST COVER DYNAMICS WITH LANDSAT SATELLITE IMAGERY

APPLICATION IN THE ROMANIAN CARPATHIAN ECOREGION

Ir. Steven VANONCKELEN

Supervisor:
Prof. dr. A. Van Rompaey

Members of the Examination Committee:
Prof. dr. G. Govers (chair)
Prof. dr. P. Hostert
Prof. dr. ir. B. Muys
Prof. dr. V. Vanacker
Prof. dr. ir. J. Van Orshoven

Dissertation presented in partial fulfilment of the requirements for the degree of Doctor in Science

February 2014

Uitgegeven in eigen beheer, STEVEN VANONCKELEN, LEUVEN

ISBN 978-90-8649-697-6
D/2014/10.705/6

“Think globally, act locally, change personally”

Dankwoord

At the end of the journey of my PhD thesis, I would like to thank a number of people who helped me realizing this work. Hierbij geef ik graag toe dat ik me de keuze voor een doctoraat nooit beklaagd heb. Zo heb ik enorm veel bijgeleerd op professioneel gebied, maar zeker ook op persoonlijk vlak.

Vooreerst wil ik Prof. Anton Van Rompaey bedanken om me de kans te bieden om in het verlengde van mijn thesis een doctoraat te starten. Prof. Van Rompaey, de leerzame discussies en je advies waren onontbeerlijk bij het verwezenlijken van dit doctoraat. Anton, bedankt voor de fijne momenten tijdens het veldwerk (denk maar de nachtelijke rit door de Karpaten en het verlies van een reservewiel), maar vooral tijdens de begeleiding van mijn doctoraat. Ik neem ook van je mee dat werk belangrijk is, maar dat je vooral gelukkig moet zijn (en daarbij kan taart altijd helpen).

Ten tweede dien ik Stef Lhermitte - een zeer gedreven 'post-doc' waarvan ik hoop dat hij academisch kan verder gaan - enorm te bedanken. Stef, merci voor de hulp bij het programmeren, publicaties schrijven, maar voornamelijk bedankt om me altijd bij te staan (ook al kon ik soms dingen opnieuw en opnieuw vragen). Also many thanks to Patrick Griffiths, you have really helped me out with inspiring research ideas, programming in IDL and the construction of the pixel based-composites. This PhD is also partly your work! Furthermore, thanks for the interesting and nice research stay in Berlin.

Moreover, my great appreciation goes to Prof. Patrick Hostert and the entire team from Humboldt-Universität zu Berlin (e.g. Jan Knorn and Benjamin Jakimow). You are really doing high-level research in a pleasant way! Thanks for the interesting discussions and the support with advice and accurate data. Verder dien ik ook de projectpartners van de UCL te Louvain-La-Neuve te bedanken. Hierbij denk ik voornamelijk aan Vincent Balthazar voor de aangename samenwerking. Maar zeker bedankt aan Prof. Veerle Vanacker, Prof. Eric Lambin en Dr. Patrick Meyfroidt. En niet te vergeten het 'Belgian Federal Science Policy Office' voor de kans om deze leerrijke en interuniversitaire samenwerking te ondersteunen.

Iris, Hanne en Jacky dien ik zeker ook te bedanken voor de fijne momenten in de Roemeense Karpaten. Door weer, wind, bramen, kilo's vleesgerechten, jägermeisters en mogelijk beren het veld in; het schept een band! Ook dank aan Annelien en Lien voor hun werk aan de Bachelor proeven.

Natuurlijk dien ik ook de andere leden van mijn jury die ik nog niet vermeld heb te bedanken. Vooreerst Gerard, een man met een visie en altijd een gedegen en onderbouwde mening. Ook dank aan Prof. Jos Van Orshoven voor o.a. de kans die ik kreeg om mijn loopbaan te starten bij SADL en aan Prof. Bart Muys voor de bosbouwkundige inbreng in mijn doctoraat.

Bedankt aan alle collega's voor de fijne werksfeer en discussies in de 200E. Daarbij in het bijzonder merci aan m'n bureaugenoten Hanne, Bert, Nils en Bastiaan. Ook merci aan Karolien en Annemarie, met wie ik samen van start ging, doe dat nog goed! Bedankt Yann voor de grappige PhD mails die af en toe over en weer verzonden werden. Merci ook aan m'n nieuwe collega's bij het ANB voor de nieuwe uitdaging, zo wist ik wat te doen tijdens mijn weekends in 2014 (jawel, mijn doctoraat afwerken).

Dankjewel aan alle huisgenoten, studie- en scoutsvrienden doorheen de jaren! De scouts van Diependaal, geweldig!

Mike, Buffel en andere goede vrienden; voor de squash partijen, pintjes en goeie babbels (ook in de toekomst!).

Nele, om al zoveel jaren lang m'n beste vriendin te zijn. Karen, bedankt om er altijd voor me te zijn.

Bedankt aan alle familie, maar toch vooral aan oma, opa, moeke en vake (die trots op me zou zijn). Ook al ben ik misschien (te) vaak druk bezig, ik zie jullie graag!

En dan dank ik uiteraard nog mijn twee mega-broers die het elk op hun eigen manier aan het maken zijn. Dieter, ik kom nog wel eens een pint drinken in Chengdu, als jij tijd maakt tenminste! Maarten, en Karolien, bedankt voor de fijne momenten en de extra energie en warmte die Warre en Lenthe in de familie brachten!

Maar bovenal, dankjewel mama en papa, voor de kansen die jullie me geven, voor jullie onvoorwaardelijke steun en enthousiasme bij alles wat ik ondernomen heb en nog zal ondernemen!

Jullie allen bezorgden me de kracht, het enthousiasme en de drijfveer om een werk als deze thesis te realiseren.

Steven Vanonckelen
Leuven, februari 2014

This research was funded by the Belgian Science Policy, Research Program for Earth Observation Stereo II, contract SR/00/133, as part of the FOMO project (remote sensing of the forest transition and its ecosystem impacts in mountain environments).

Abstract

Forest cover changes have essential implications on a variety of landscape functions and their associated ecosystem services. Globally, contrasting forest trends are present: some countries are greening, while others are still in a deforestation phase. The detection and mapping of forest dynamics is rather challenging since landscapes in the transition phase typically consist of patchy structures and often occur in inaccessible areas such as highlands, which impedes mapping approaches based on fieldwork. Furthermore, forest cover changes in the turnover phase are characterized by subtle up- and downward trends.

Remote sensing techniques seem to be adequate tools for the analysis of forest cover changes in mountain areas. Over the past half century, remote sensing imagery has been acquired by a range of multispectral and hyperspectral sensors. Many regional long-term vegetation (change) maps have been derived from medium to low resolution imagery such as the Landsat sensor with a spatial resolution of 30m. Despite recent developments, remote sensing methods for the detection and analysis of forest cover dynamics at regional scale still suffer from methodological challenges: (1) recorded reflectance values are disturbed by atmospheric effects, (2) differences between illuminated and shadowed slopes occur in mountain areas, and (3) regional scale analyses require that multiple images are mosaicked to construct homogeneous image composites. During the last decades, a range of simple empirical and more advanced physically-based preprocessing techniques has been developed to solve these problems. At present, however, it is not clear what the added value of these techniques is for the detection of regional scale forest cover change.

The main objective of this PhD research was to evaluate, compare and improve the methods for regional scale detection and analysis of forest cover dynamics. The Romanian Carpathians Mountains, which are characterized by significant forest cover dynamics related to a land decollectivization process were selected as the study area. In order to address the main objective of this thesis, the following specific research questions were formulated:

1. To what extent do available atmospheric and topographic correction techniques improve the land surface reflectance values derived from medium resolution imagery in mountain areas? Do complex physically-based methods perform better than simplified empirical approaches?
2. Does image preprocessing improve land cover classification?
3. Does topographic correction and pixel-based compositing improve large area (change) mapping?
4. What is the pattern and what are the controlling factors of forest cover changes in the Romanian Carpathians?

This first research question was addressed by comparing the results of 15 combinations of atmospheric and topographic correction methods. The analyses were performed on a Landsat footprint in the Romanian Carpathian mountains. First, results showed a reduction of the differences between average illuminated and shaded reflectance values after correction. Significant improvements were found for methods with a pixel-based Minnaert (PBM) or a pixel-based C (PBC) topographic correction. Secondly, the analysis of the coefficients of variation showed that the homogeneity for selected forest pixels increased after correction. Finally, the dependency of reflectance values on terrain illumination was reduced after implementation of an atmospheric correction combined with a PBM or PBC correction. Considering overall results, this analysis showed

that the most advanced correction methods produced the most accurate results, but these methods were also the most difficult to automate in a processing chains. Furthermore, the added value of advanced topographic methods was found to be high, while the added value of advanced atmospheric methods was found to be rather limited.

In order to address the second research question, all preprocessed imageres (15 combinations) were used as an input for a Maximum Likelihood (ML) land cover classification. The resulting land cover maps, showing e.g. urban area, arable land, grassland, coniferous, broadleaved and mixed forest, were validated by comparison with field observations. Validation results showed that the land cover maps derived from preprocessed images were more accurate than the land cover maps derived from the unpreprocessed images. Furthermore, it was found that class accuracies of especially the coniferous and mixed forest classes were enhanced after correction. Moreover, combined correction methods appeared to be the most efficient on weakly illuminated slopes ($\cos \theta \leq 0.65$). Considering all results, the best overall classification results were achieved after the application of the combination of an atmospheric correction method based on transmittance functions and a PBM or PBC topographic correction. Results of this study also indicated that the topographic component had a higher influence on classification accuracy than the atmospheric component.

The third research question was addressed by the application of a pixel-based compositing algorithm developed by Griffiths et al. (2013b). Composites were developed with 3 degrees of freedom: (1) the classifier (Maximum Likelihood or Support Vector Machine, SVM), (2) number of delineated land cover classes (4 or 8), and (3) the topographic correction (uncorrected or corrected). Land cover maps were produced for the years 1985, 1995 and 2010. The accuracy of the resulting land cover maps was evaluated by comparing the classified land cover with references data collected by field observation or visual inspection of very high resolution imagery. The map validation showed that the SVM classifier resulted in a more accurate land cover classification than the ML classifier. Preprocessing increased the accuracy of the classification even more, but its impact showed to be less important than the selection of the classifier. The overall accuracy of the maps depicting 8 land cover classes was between 66% and 82% for all years. The classification accuracy was further increased by lowering the number of land cover classes. The highest overall accuracies were found for the maps with 4 land cover classed based on preprocessed imagery using a SVM classifier: respectively 85% (1985), 83% (1995) and 91% (2010). By comparing the maps of 1985, 1995 and 2010, land cover change could be detected. Both afforestation and deforestation patterns were detected but it was concluded that overall the Romanian Carpathians were gradually greening between 1985 and 2010 since the first process was dominant.

In a final step, an attempt was done to detect the controlling factors of the forest cover dynamics between 1985-1995 and 1995-2010. Therefore, multiple logistic regression models were calibrated in which accessibility, demographic evolution, land use policy and biophysical characteristics were linked with the observed deforestation and afforestation patterns. The results showed that both deforestation and afforestation were more likely to occur at high elevations, but far from nearby secondary roads. No significant correlation could be found between population change at the level of communes and forest cover dynamics.

Samenvatting

Veranderingen van bosareaal en bossamenstelling hebben belangrijke gevolgen voor verschillende landschapsfuncties en hun bijbehorende ecosysteemdiensten. Wereldwijd zijn contrasterende trends in de evolutie van het bosareaal geobserveerd: sommige landen zijn aan het vergroenen, terwijl andere landen nog in een duidelijke fase van ontbossing zijn. De detectie en kartering van veranderingen van bossen is niet vanzelfsprekend omdat het vaak gaat over landschappen in een overgangsfase die worden gekenmerkt door onregelmatige temporele fluctuaties en een gefragmenteerde ruimtelijke structuur. Bovendien worden de grootste bosdynamieken vaak waargenomen in afgelegen berggebieden, wat nauwkeurige detectie en inventarisatie op basis van veldwerk bemoeilijkt.

Teledetectie technieken lijken de meest aangewezen technieken om dynamieken in het bosareaal te detecteren en te kwantificeren. Gedurende de voorbije 50 jaar werden een grote hoeveelheid beelden opgenomen door multispectrale en hyperspectrale satellietsensoren. Op basis van deze beelden werden verschillende pogingen ondernomen om vegetatieve bedekking en veranderingen hierin in kaart te brengen. Hiervoor werden vaak satellietbeelden met een gemiddelde tot lage ruimtelijke resolutie aangewend, zoals de Landsat sensor met een ruimtelijke resolutie van 900 m². Ondanks recente verbeteringen in beeldclassificatiemethoden is er nog steeds geen eenduidige methode om het bosareaal in kaart te brengen, mede omdat er nog een aantal belangrijke methodologische uitdagingen blijven bestaan: (1) de gedetecteerde reflectantiewaarden worden verstoord door atmosferische effecten, (2) er zijn belangrijke verschillen tussen belichte en beschaduwde hellingen in berggebieden, en (3) het blijft bijzonder moeilijk om meerdere beelden naadloos samen te voegen tot homogene beeldcomposieten die nodig zijn voor regionale analyses. Gedurende de laatste decennia werd er een reeks van eenvoudige empirische en geavanceerde fysisch-gebaseerde 'preprocessing' technieken ontwikkeld om deze problemen op te lossen. Momenteel is het echter niet duidelijk wat de toegevoegde waarde van deze technieken is voor de detectie van regionale veranderingen van het bosareaal.

Het voornaamste doel van dit doctoraatsonderzoek was dan ook om methoden voor de detectie en de analyse van bosveranderingen op regionale schaal te evalueren, te vergelijken en te verbeteren waar mogelijk. De Roemeense Karpaten , die gekarakteriseerd worden door significante veranderingen van het bosareaal gerelateerd aan het proces van decollectivisatie, werden gekozen als studiegebied. Om de belangrijkste doelstelling van dit proefschrift te onderzoeken, werden de volgende onderzoeksvragen geformuleerd:

1. In welke mate verbeteren de beschikbare atmosferische en topografische correcties de reflectantiewaarden in berggebieden die gedetecteerd werden door satellietbeelden met een ruimtelijke resolutie van 30 meter? Leiden geavanceerde fysisch-gebaseerde technieken tot betere resultaten dan eenvoudige empirische technieken?
2. Verbetert 'image preprocessing' de landgebruiksclassificatie?
3. Verbetert topografische correctie en 'pixel-based compositing' de kartering van dynamieken in het bosareaal voor een groot gebied?
4. Wat is het patroon en wat zijn de sturende factoren van bosdynamieken in de Roemeense Karpaten?

Deze eerste onderzoeksvraag werd beantwoord door de resultaten van 15 combinaties van atmosferische en topografische correcties te vergelijken. De analyses werden uitgevoerd op een Landsat satellietbeeld dat een deel van de Roemeense Karpaten bedekt. De resultaten toonden ten eerste een vermindering van de verschillen tussen de gemiddelde verlichte en beschaduwde reflectantiewaarden na correctie. Significante verbeteringen werden gevonden voor de technieken met een 'pixel-based Minnaert (PBM)' of een 'pixel-based C (PBC)' topografische correctie. Ten tweede toonde de analyse van de variatiecoëfficiënten aan dat de homogeniteit van de geselecteerde bospixels verhoogd werd na correctie. Tenslotte werd de afhankelijkheid tussen de reflectantiewaarden en de terreinverlichting verminderd na de combinatie van een atmosferische correctie met een PBM- of PBC-correctie. Rekening houdend met alle resultaten bleek uit deze analyse dat de meest geavanceerde correcties tot de meest nauwkeurige resultaten leidden, maar deze technieken waren ook het moeilijkst om te automatiseren. Bovendien was de toegevoegde waarde van geavanceerde topografische technieken hoog, terwijl de toegevoegde waarde van de atmosferische technieken eerder beperkt was.

Om de tweede onderzoeksvraag te beantwoorden, werden alle gecorrigeerde satellietbeelden (15 combinaties) gebruikt als invoer voor een 'Maximum Likelihood (ML)' landgebruiksclassificatie. De resulterende landgebruikskaarten die onder andere stedelijk gebied, akkerland, grasland, naaldhout, loofhout en gemengd bos bevatten, werden gevalideerd door een vergelijking met veldwaarnemingen. De validatie resultaten toonden aan dat de landgebruikskaarten afgeleid van gecorrigeerde satellietbeelden nauwkeuriger waren dan de landgebruikskaarten afgeleid van de ongecorrigeerde satellietbeelden. Verder waren de gecombineerde correcties het meest efficiënt op zwak verlichte hellingen ($\cos \beta \leq 0{,}65$). Rekening houdend met alle resultaten werden de beste classificatieresultaten behaald na de toepassing van een combinatie van een atmosferische correctie gebaseerd op transmissiefuncties met een PBM of PBC topografische correctie. De resultaten van deze studie toonden ook aan dat de topografische component een grotere invloed had op de nauwkeurigheid van classificatie dan de atmosferische component.

Om een antwoord te vinden op de derde onderzoeksvraag, werd er een 'pixel-based compositing' algoritme toegepast dat ontwikkeld werd door Griffiths et al. (2013b). Composieten werden ontwikkeld met 3 vrijheidsgraden: (1) de classificatiemethode (Maximum Likelihood of Support Vector Machine, SVM), (2) het aantal landgebruiksklassen (4 of 8), en (3) de topografische correctie methode (ongecorrigeerd of gecorrigeerd). Vervolgens werden er landgebruikskaarten geproduceerd voor de jaren 1985, 1995 en 2010. De nauwkeurigheid van de resulterende landgebruikskaarten werd beoordeeld door een vergelijking tussen de landgebruikskaarten en referentiegegevens verzameld via veldobservatie of visuele inspectie van zeer hoge resolutie beelden. Uit de kaart validatie bleek dat de SVM classificatiemethode resulteerde in een meer accurate classificatie van de landgebruiksklassen dan de ML classificatiemethode. Preprocessing technieken verhoogden de nauwkeurigheid van de classificatie verder, maar het effect was minder belangrijk dan de selectie van de classificatiemethode. De nauwkeurigheid van de kaarten met 8 landgebruiksklassen varieerde tussen 66% en 82% voor de drie jaren. De nauwkeurigheid werd verder verhoogd door het verlagen van het aantal landgebruiksklassen. De hoogste nauwkeurigheden werden bereikt voor de kaarten met 4 landgebruiksklassen en gebaseerd op gecorrigeerde beelden met behulp van een SVM classificatiemethode: de nauwkeurigheden waren respectievelijk 85% (1985), 83% (1995) en 91% (2010). Verder werden de landgebruiksveranderingen gedetecteerd door de vergelijking te maken

tussen de kaarten van 1985, 1995 en 2010. Zowel bebossings- als ontbossingspatronen werden waargenomen, maar er werd een gestage vergroening van de Roemeense Karpaten tussen 1985 en 2010 vastgesteld aangezien het eerste proces dominant was.

In een laatste stap werd er getracht om de verklarende variabelen van de bosveranderingen tussen 1985-1995 en 1995-2010 te detecteren. Hiervoor werden meervoudige logistische regressie modellen gebruikt waarin de verklarende variabelen toegankelijkheid, demografische evolutie, beleid en biofysisch milieu gelinkt werden aan de waargenomen bebossings- en ontbossingspatronen. De resultaten toonden aan dat zowel bebossing als ontbossing vaker optreden op grote hoogten, maar ver van nabijgelegen secundaire wegen. Verder kon er geen significante correlatie gevonden worden tussen de demografische veranderingen op het gemeentelijk niveau en de verandering van het bosareaal.

List of abbreviations

AC	Atmospheric correction
AFFOR	Afforestation
AR	Arable land
ASTER	Advanced spaceborne thermal emission and reflection radiometer
AUV	Area under the curve
AVHRR	Advanced very high resolution radiometer
AVIRIS	Airborne visible and infrared imaging spectrometer
AWiFS	Advanced wide field sensor
BELSPO	Belgian science policy office
BL	Broadleaved forest
BRDF	Bidirectional reflectance distribution function
BS	Bare soil
CF	Coniferous forest
CEO	Carpathians environment outlook
CERI	Carpathian ecoregion initiative
CORINE	Coordination of information on the environment
DE	Demographic evolution
DEFOR	Deforestation
DEM	Digital elevation model
DN	Digital number
DNS	Distance to nearby settlement
DOS	Dark object subtraction method
DOY	Day of year
DPR	Distance to primary roads
DSR	Distance to secondary roads
E	Empirical
ERTS	Earth resources technology satellite
ETM+	Enhanced thematic mapper plus
EU	European Union
EV	Elevation
EVI	Enhanced vegetation index
EXT	Extensification
FAO	Food and agriculture organization
FMASK	Function of mask
FRA	Forest resoruces assessment
FRMPI	Forest research and management planning institute
FSC	Forest stewardship council
GCP	Ground control point
GDP	Gross domestic product
GLCC	Regional land cover characterization
GRASS	Grassland
GSD	Ground sampling distance

GVI	Green vegetation index
HRG	High resolution geometry
HRV	High resolution visible
HRVIR	High resolution visible and infrared
IUCN	International union for conservation of nature
LG	Lambertian geometrical
Landsat	Land remote sensing satellite program
LEDAPS	Land ecosystem disturbance adaptive processing system
LOWTRAN	Low resolution atmospheric transmission
LULCC	Land use and land cover change
ML	Maximum likelihood
MLR	Multiple logistic regression
MODIS	Moderate resolution imaging spectroradiometer
MODTRAN	Moderate resolution atmospheric transmission
MX	Mixed forest
NASA	National aeronautics and space administration
NDVI	Normalized difference vegetation index
NFA	National forest administration
NIR	Near infrared
NIS	National institute of statistics
NLG	Non-Lambertian geometrical
NOAA	National oceanic and atmospheric administration
NUTS	Nomenclature of territorial units for statistics
OA	Overall accuracy
OK	Overall kappa
PA	Producer's accuracy
PBC	Pixel-based C-correction
PBIC	Pixel-based image compositing
PFA	Protected forest areas
PES	Payments for ecosystem services
PROBA-V	Project for on-board autonomy - vegetation
PVI	Perpendicular vegetation index
REDD	Reduced emissions from deforestation and forest degradation
ROC	Relative operation characteristic
SAVI	Soil-adjusted vegetation index
SBI	Soil brightness index
SCI	Area of special conservation interest
SF	Stable forest
SG	Slope gradient
SLC	Scan line corrector
SPA	Special protection area
SPOT	Satellite pour l'observation de la terre
SRTM	Space shuttle radar topography mission
ST	Soil type
TC	Topographic correction

TF	Transmittance function
TM	Thematic mapper
TSAVI	Transformed soil-adjusted vegetation index
UA	User's accuracy
UN	United Nations
UR	Urban land
US	United States
USGS	US geological survey
VCI	Vegetation condition index
VI	Vegetation index
WRB	World reference base for soil resources
WT	Water surface
WWF	World wide fund for nature

Table of Contents

List of Figures

List of Tables

PART 1: INTRODUCTION

Chapter 1: Problem statement and research objectives

1.1 Forest cover dynamics

Quantification of global forest change has been lacking despite the recognized importance of forest ecosystem services. For the definition of forest, the Global Forest Resources Assessment (FRA) adopted a threshold of 10 percent minimum crown cover (FAO, 2010). Forest is defined as land spanning larger than 0.5 hectares with trees higher than 5 meters and a canopy cover of more than 10 percent, or trees able to reach these thresholds insitu (FAO, 2010). This definition does not include land that is predominantly under agricultural or urban land use and includes both natural forests and forest plantations. However, it excludes stands of trees established primarily for agricultural production (e.g. fruit tree plantations). Furthermore, afforestation is defined as the transformation from non-forest to forest, i.e., the planting of trees on land that was not previously classified as forest, or through natural expansion of forest, i.e., natural successions on land that was previously under another land use (e.g., forest succession on agricultural land; FAO, 2010). The definition of deforestation used in FRA 2010 is “the conversion of forest to another land use orthe long-term reduction of the tree canopy cover below the minimum 10 percent threshold” (FAO, 2010).

The quantification of global forest change is challenging since a standardized technique needs to be feasible for all regional and local scenarios. A worldwide forest inventory was developed in FAO (2010), containing all 233 countries. The total forest area in 2010 was estimated on 4 billion hectares, or 31% of the total land area. This corresponds to an average of 0.6 ha per capita. Figure 1.1 shows that the forested area is unevenly distributed. The forests of five countries account for more than half of the total forest area (53%): the Russian Federation, Brazil, Canada, the United States of America and China. In contrast, 64 countries, with a combined population of 2 billion people, own less than 10% forested land (FAO, 2010). The data of the Global Forest Resources Assessment for 1990, 2000, 2005 and 2010 are based on FAO land resource questionnaires (FAO, 2010). The data are transparent and the reports provide in considerable detail information on forest cover and characteristics at the national and regional levels. However, due to the limited availability of recent inventory and survey data, the accuracy of estimates and the quality of data was not always assured (Matthews and Grainger, 2002). Furthermore, countries in the temperate region (e.g. Romania) pointed out that differences in national forestry definitions and systems of measurement, and the use of different reference periods, were causing problems (FAO, 2008).

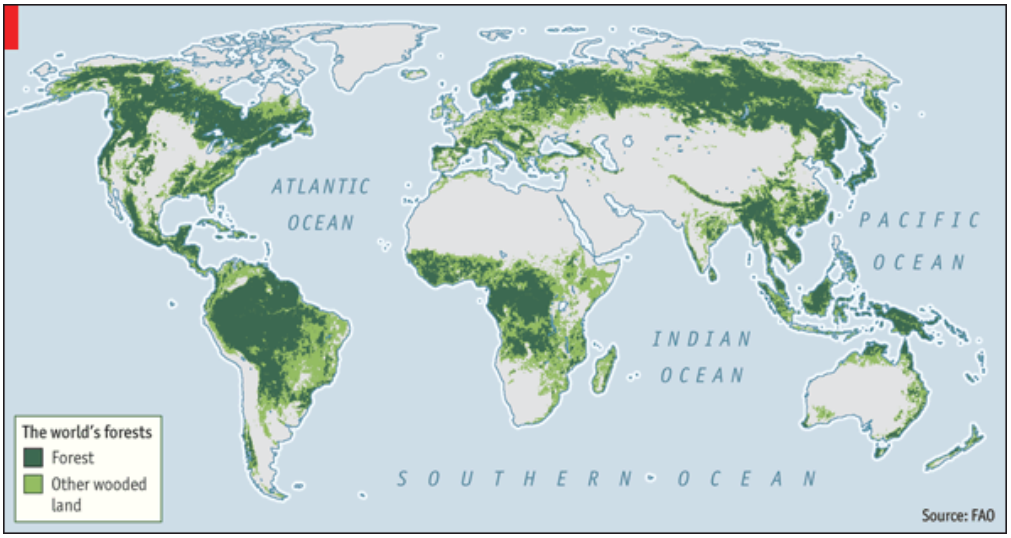

Figure 1.1.: The world's forests (tree cover data were derived from 2005 MODIS data; FAO, 2010).

The most recent worldwide forest inventory was performed between 2000 and 2012 by Hansen et al. (2013) and used Earth observation Landsat satellite data with at a spatial resolution of 30 meters. The tropics were the only climate domain to exhibit a clear trend, with forest loss increasing by 210,100 ha per year. Furthermore, Brazil's well-documented reduction in deforestation was compensated by increasing forest loss in Paraguay, Bolivia, Zambia, Indonesia, Malaysia, Angola, and elsewhere (Hansen et al., 2013). Moreover, boreal forest losses were largely triggered by fire (Potapov et al., 2008; Hansen et al., 2013).

At a global scale, forests are disappearing despite the establishment of forest policies and laws supporting sustainable forest management. The annual forest area decreased with 0.20% (8,327,000 ha/yr) between 1990 and 2000, and with 0.13% (5,211,000 ha/yr) between 2000 and 2010 (FAO, 2010). Furthermore, Hansen et al. (2013) mapped a global forest loss of 230 million ha and a global forest gain of 80 million ha between 2000 and 2012 (Hansen et al., 2013). The statistics of both studies - FAO (2010) and Hansen et al. (2013) - demonstrate that the forest decline slowed down during the last decade. At continental level, South America suffered the largest net loss of forests between 1990-2000 and 2000-2010, about 4 million hectares per year (Figure 1.2; FAO, 2010). Hansen et al. (2013) also documented that the tropical dry forests of South America had the highest rate of tropical forest loss between 2000 and 2012, especially due to deforestation dynamics in the Chaco woodlands of Argentina, Paraguay and Bolivia. The high deforestation in South America was followed by Africa, which lost 3.4 million hectares annually between 2000 and 2010 (Figure 1.2; FAO, 2010). In contrast, Hansen et al. (2013) only reported an annual loss of 53,600 ha per year in the African tropical moist deciduous forest between 2000 and 2012.

Oceania also reported a net loss of forest of about 700,000 ha per year over the period 2000–2010, mainly due to large forest losses in Australia where severe drought and forest fires have exacerbated the loss of forest since 2000 (FAO, 2010). The forest area in North and Central America was estimated almost equal in 2000 and 2010 (FAO, 2010). However, North American subtropical forests of the southeastern United States are unique in terms of change dynamics due to short-cycle tree planting and harvesting (Hansen et al., 2013). In Europe, the forest area continued to expand, though

at a slower rate (700,000 ha per year) than in the 1990s (900,000 ha per year; FAO, 2010). Forest gain between 2000 and 2012 was substantial in the boreal zone, with Eurasian coniferous forests having the largest area of gain of all global ecozones during the study period, due to forestry, agricultural abandonment and forest recovery after fire (Prishchepov et al., 2013; Hansen et al., 2013). Asia, which had a net loss of forest of some 600,000 ha annually in the 1990s, reported a net gain of forest ±2.2 million hectares per year in the period 2000–2010, primarily due to the large scale afforestation reported by China and despite continued high rates of net loss in many countries in south and southeast Asia (FAO, 2010). These results depict that the assessed global forest cover trends are consistent, although regional differences between different studies are possible depending on the implemented techniques. An accurate assessment of regional forest cover trends is essential since it is relevant national policy makers.

The recent Millennium Development Goals Report (2013) stated that accelerated progress and actions are needed for forest conservation. At present, about 75% of the world's forests are covered by national forest programmes. However, in many cases, deforestation is caused by factors beyond a programme's control. One of the primary deforestation drivers is the conversion of forests into agricultural land to feed the world's growing population (Millennium Development Goals Report, 2013). In the Report of the High-Level Panel of Eminent Persons on the Post-2015 Development Agenda (2013), some universal goals and national targets were implemented. One of the goals is the reduction of deforestation and the increase of reforestation. Thereby, each country is responsible to define their own targets (Report of the High-Level Panel of Eminent Persons on the Post-2015 Development Agenda, 2013).

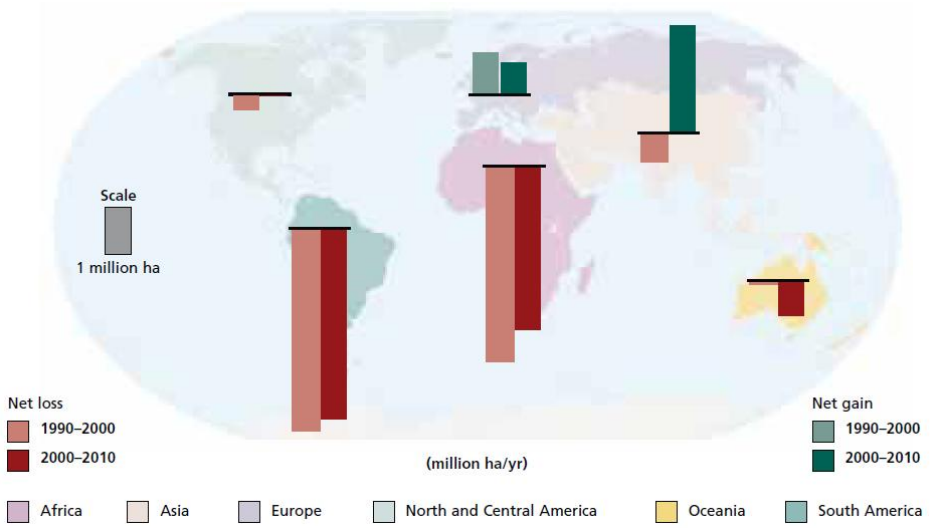

Figure 1.2.: Annual change in forest area by region between 1990, 2000 and 2010 (FAO, 2010).

1.2 Controlling factors of forest cover dynamics

Forest cover dynamics are controlled by multiple socio-economic and biophysical variables and therefore vary through space and time. Current socio-economic controlling factors of land cover change such as urbanization and economic and population growth are producing two contrasting

land-use trends. In an attempt to join various worldwide observed and often opposing forest cover trends, the concept of forest transition was introduced by Mather (1992). A forest transition is defined as a process in which the forested area in a given region or country changes from decreasing to expanding. Forest transitions are typically driven by globalization processes in which self subsistence farming is gradually replaced by market-oriented agriculture, whereby land units with a low productivity will be abandoned and agricultural activities are intensified on the most productive land units. This process is often accompanied by urbanization, industrialization and economic growth.

At present, most studies on forest transition are country-specific and only focus on the national forest cover. In contrast, a forest cover decrease in one country is able to trigger a major import of forest products and consequently an increase in deforestation in another country (Rudel et al., 2005; Meyfroidt et al., 2010). Importing wood is the economic equivalent of exporting ecological impacts (Mayer et al., 2005; Mayer et al., 2006). The international timber trade thus creates illusory images of conservation by preserving forests in accessible, affluent political jurisdictions while extracting natural resources from remote places with permissive or poorly enforced environmental policies (Berlik et al., 2002; Meyfroidt et al., 2010). For example, a forest cover increase in Vietnam between 1992 and 2005 triggered wood imports and illegal deforestation in Cambodia and Laos (Barney, 2005; Global Witness, 1999; Meyfroidt and Lambin, 2010). Therefore, transboundary studies that incorporate worldwide connections and trades in wood need to be performed.

Figure 1.3 shows a general and conceptual forest transition curve based on Mather (1992). The forest transition curve demonstrates a conceptual irregular trend since forest cover change is a non-linear process. The length of the time-axis in Figure 1.3 varies from shorter to longer periods (Rudel et al., 2010). Different controlling factors that influence a forest transition are explained in section 1.1.2. The transition can be divided in three phases: a phase of decrease, a turnover phase and a phase of forest cover increase (Mather and Needle, 1998). The conceptual figure shows a decline in forest cover over time until a turnover phase is reached. After this turnover phase, an increase in total forest cover occurs.

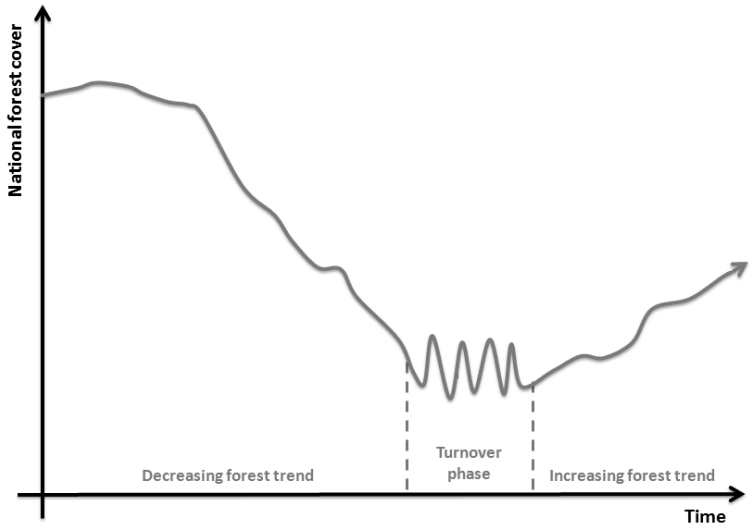

Figure 1.3.: The conceptual forest transition curve with indication of different transition phases: decreasing forest trend, turnover phase and forest increase (based on Mather, 1992).

An overview of documented worldwide forest transitions is presented in Table 1.1. At present, most of the developing countries are situated on the left part of the curve since these countries experience a net forest cover loss. Whereas more developed countries (e.g. USA and Europe) went through a phase with minimal forest percentage and are now located on the upward part of the curve. Especially in several European countries with temperate forests, transition occurred over the last centuries. More recent cases of forest transition occurred in tropical countries such as Vietnam, India and the Philippines (Meyfroidt and Lambin, 2010; DeFries and Pandey, 2010; Vu et al., 2013). In some places, economic development created enough off-farm jobs to pull farmers away from the land, inducing a natural forest regeneration on abandoned fields. In other places, a scarcity of forest products stimulated governments and landowners to plant trees on agricultural lands. Pathways and patterns of deforestation and forest transitions vary geographically (Perz, 2007; Lambin and Geist, 2006; Rudel et al., 2009). The first forest transition studies focused on western European countries with a temperate climate. In these countries, worldwide industrialization became less crucial to explain reforestation in the second half of the 20th century. In contrast, afforestation through tree plantation gained importance (Rudel, 2009).

Table 1.1.: Worldwide forest transition studies: cases, references, turning point and forest cover at turning point as a percentage (based on: Meyfroidt and Lambin, 2010 and 2011; Van Dessel, 2010).

Case	**References**	**Turning point**	**Forest cover at turning point (%)**
Europe			
Austria	Krausmann (2001)	circa 1880	circa 40
Belgium (Flanders)	Van Rompaey et al., 2002	1930	circa 30
Belgium (Wallonia)	Petit and Lambin (2002)	mid 19th century	/
Bulgaria	Ionov et al. (2000)	< 1950	circa 31
Czech Republic	Bicik et al. (2001)	before 1845	circa 29
Denmark	Mather and Needle (1998), Mather (2001)	1800-1810	circa 4
European Russia	Kauppi et al. (2006)	1930s	circa 28
Finland	Myllyntaus and Mattila (2002), Siiskonen (2007)	circa 1900	< 86
France	Freeman (1994), Mather et al. (1999), Mather (2001), Liébault et al. (2005)	1830 – 1900	circa 13-70
Germany	Kandler (1992), Radkau (2008)	19th century	circa 22
Hungary	Mather (1992)	between 1800 and 1925	< 12
Hungary (Balaton)	Jordan et al. (2005)	circa 1945	circa 18
Ireland	Rudel et al. (2005)	circa 1920-1930	circa 0
Italy	Piussi and Pettenella (2000)	< 1925	< 18
Norway	Staaland et al. (1998), FAO (2010)	before 1990	/
Poland	Kozak et al. (2007a)	19t century	
Portugal	Kauppi et al. (2006)	before 1870	circa 7
Scotland	Mather (2004) Rudel et al. (2005)	circa 1750	circa 5 or less
Slovenia	Petek (2002)	before 1896	circa 40
Sweden	Ericsson et al. (2000), Bradshaw	1850-1900	circa 30

	(2004)		
Switzerland	Mather and Fairbairn (2000)	19th century, before 1860	< 20
Ukraine	Solovoi (2000), Kuemmerle et al. (2010)	1920-1950	circa 12
United Kingdom	Aldhous (1997), Osborn (2003), West (2003)	1925	circa 5
Asia - Pacific			
Bhutan	FAO (2010), Meyfroidt and Lambin (2010)	circa 1975-1990	circa 65
China	Zhang (2000), Zhang et al. (2000,) Wenhua (2004), Mather (2007), Wang et al. (2007), Xu et al. (2007), Song and Zhang (2009)	1970-1980	circa 13
India	Mather (2007)	1950-1980	15-20
Japan	Knight (2000), Chhabra (2002), Foster and Rosenzweig (2003), Tsutsui (2003), Chhabra and Dadhwal (2004), Kauppi et al. (2006), DeFries and Pandey (2010)	1950-1960	50-60
New Zealand	Stubbs (2008), Wood and Pawson (2008), Knight (2009)	early 20th century	/
Philippines	FAO (2010), Preston (1998), Shively (2001), Grainger and Malayang (2006), Kastner (2009)	after 1988	circa 22
South Korea	Klock (1995), Kim and Kim (2005), Youn (2009), Young and Kwang (2009)	1945-1960	10-30
Vietnam	Meyfroidt and Lambin (2008a, 2008b, 2010); Vu et al. (2013)	1991-1993	25-31
America			
Chile	Hyde et al. (1996), Clapp (2001), Echeverria et al. (2008), Schulz et al. (2010), Diaz et al. (2011)	1950s	/
Costa Rica	Kleinn et al. (2002), Kull et al. (2007)	circa 1990	20-30
Cuba	FAO (2010), Diaz-Briquets and Perez-Lopez (2000)	circa 1960s-1970s	circa 14
El Salvador	Hecht et al. (2006), Hecht and Saatchi (2007)	1980s-1990s	/
Puerto Rica	Rudel et al. (2000), Grau et al. (2003), Grau et al. (2004), Lugo and Helmer (2004)	1950	circa 9
United States (48 conterminous states)	Clawson (1979), Pisani (1985), Pisani (1993), Foster (1992), Foster et al. (1998), Rudel (2001)	1920	circa 24
United States (all)	MacCleery (1994), Houghton and Hackler (2000), Ramankutty et al. (2010)	1920	circa 27
Uruguay	FAO (2010), Baldi and Paruelo (2008), Vega et al. (2009)	before 1990	circa 5
Africa			
Gambia	FAO (2010)	before 1990	circa 46
Morocco	FAO (2010)	2001	circa 11

Rwanda	FAO (2010)	before 1990	circa 12
Tunisia	FAO (2010)	before 1990	circa 2-3

Notes: cases are grouped by continent. If no dates are provided for the end of the deforestation or the start of forest recovery period, the dates directly precede or follow after the turning point.

A forest transition is a complex process which is never triggered by two linearly related controlling factors (Mather et al., 1999). In contrast, forest transitions are driven by a combination of socio-economic and ecological changes associated with loss of forest cover, as well as policies that are linked to forest scarcity (Rudel et al., 2005; Angelsen and Rudel, 2013). Other possible controlling factors for forest transitions are the following: nature protection, production of biofuels, changes in land use intensity, etc.

Rudel et al. (2005) identified two main forest transition pathways based on a cross-national study for the 1990s: a forest scarcity and an economic development path. First, in the forest scarcity pathway, deforestation caused by agricultural expansion or wood extraction creates a scarcity of forest products. Furthermore, the forest scarcity is reinforced by the increasing demand for wood products through economic growth (Rudel et al., 2005). As a consequence, governments and land owners are incited to establish afforestation programs (Lambin and Meyfroidt, 2010). In this first pathway, economic and political changes arise as a response to the adverse impacts of deforestation. Furthermore, investments in forestry research, sustainable management practices and fuelwood substitution are promoted (Meyfroidt and Lambin, 2010 and 2011). Secondly, in some cases, labor scarcity rather than forest product scarcity is the controlling factor of forest conversion. The loss of farm laborers stems from urbanization and economic development (Mather, 1992). Farm workers leave the countryside for better paying off-farm jobs. Consequently, farmers start to abandon their remote and less productive fields which convert slowly to forests. This forest transition pathway is called the economic development path.

The forest scarcity pathway is more crucial in densely populated and poorer countries, e.g. in Asia. In contrast, the economic development pathway is more logical in richer and less populated countries such as in Europe and northern America (Rudel et al., 2005). Recent studies suggested that these two pathways are insufficient to explain forest transitions in countries such as: Bhutan, Chile, China, Costa Rica, El Salvador, India, Puerto Rico and Vietnam (Hecht, 2010; Mather, 2007; Meyfroidt and Lambin, 2011; Figure 1.4). Therefore,Lambin and Meyfroidt (2010) identified three additional pathways of forest transition: (a) globalization; (b) state forest policy; and (c) smallholder, tree-based land-use intensification pathways. The globalization pathway is a modern version of the economic development pathway in which national economies are increasingly integrated into and influenced by global markets and ideologies. In the state forest policy pathway, national forest policies, triggered by factors outside and within the forestry sector, exert an essential role in forest transition. This state forest policy pathway was crucial in several Asian countries (e.g. China, India and Vietnam) which experienced a forest cover increase that was strongly promoted by the state since the 1990s (Mather, 2007). Finally, forest transitions driven by land use planning in economies rather isolated fromglobal markets and dominated by smallholders tend to an expansion of natural forests that provide multiple ecosystem goods and services, as illustrated by Bhutan (Lambin and Meyfroidt, 2010).

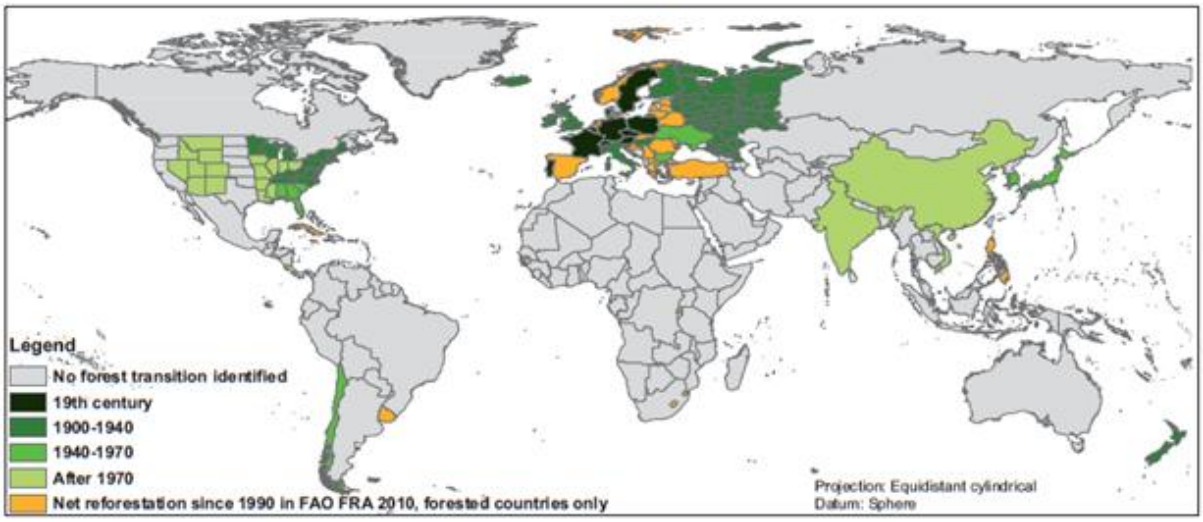

Figure 1.4.: Periods of recent forest transitions. When there was no reliable study confirming the forest transition, data from the Forest Resources Assessment (FRA; FAO, 2010) were used to identify countries with net reforestation since at least 1990–2010 (note that reforestation may have started before 1990). The class 'no forest transition identified' indicates the countries in which a forest transition was not yet documented. For a number of countries, the 2010 FAO data reported a net reforestation. However, these data were not confirmed by other studies or contradictory evidence from other source was found. (based on Meyfroidt and Lambin, 2011).

Each particular case of forest transition involves interactions between elements of the above pathways. However, the concept of forest transition describes a process at an aggregated scale, e.g. regional scale. Cases of sub-national or local forest regrowth are contributing to the understanding of forest transitions (Meyfroidt and Lambin, 2011). In Table 1.2, the main relationships between the five forest transition pathways and their explanatory frameworks of land use transitionsare summarized.

Table 1.2.: Main relationships between forest transition pathways and explanatory frameworks of land use transitions (based on Lambin and Meyfroidt, 2010).

Explanatory frameworks	**Forest transition pathway**				
	Forest scarcity	State policy	Economic Dev.	Globalisation	Smallholder Int.
Socio-ecological feedbacks					
Resource-limited growth	X				
Land scarcity, intensification	X				X
Land use adjustment		X	X		X
Socio-economic changes					
Economic modernization			X	X	
Market access		X	X	X	X
Land ownership		X		X	X
Global trade				X	
Diffusion of conservation ideas		X		X	

Generally, forest transitions are complex processes which are often linked to a gradual extensification process such as land abandonment (Van Dessel, 2010). Extensification is described as the process of removing production from land areas that were previously used for more intensive purposes (Izac et al., 1991). Historical analyses of European forest transitions in the 19th century highlighted a broad set of interrelated political, institutional, economic and cultural processes (Mather, 1992; Mather et al., 1998; Mather, 1998; Mather et al., 1999; Mather and Fairborn, 2000;

Mather, 2004). The controlling factors of forest transitions were dependent on the historical and geographical contexts. In central and eastern Europe, the recent political history exerted a significant influence on forest cover (Bicik et al., 2001; Van Rompaey et al., 2007; Kuemmerle et al., 2010). Along with forest regeneration, disturbances triggered by logging and fragmentation affected the forests in this region (Kuemmerle et al., 2007). Targets for forest conservation are defined on a regional and local scale. For example, the Flemish region in Belgium has the ambitious goal to plant 10 million trees by 2020 (BOS+, 2013). In Europe, the establishment of the Natura 2000 network was a major achievement. Special Protection Areas designated under the Birds Directive need to be managed in accordance with the ecological needs of the bird's habitats. According to the EU nature directives, the conservation objectives should be achieved in agreement with economic, social, cultural and recreational requirements. Therefore, member states establish appropriate methods and instruments to implement the directives and to achieve the conservation objectives of Natura 2000 sites (European Commission, 2013b).

1.3 Impact of forest dynamics

Among the main effects of human activities on the environment are land use and resulting land cover changes. Such changes impact the capacity of ecosystems to provide goods and services to the human society (Burkhard et al., 2012). This supply of multiple goods and services by nature should match the demands of the society, if self-sustaining human–environmental systems and a sustainable utilization of natural capital are to be achieved. Hereby, ecosystem services only have a value when a demand exist for this service. While several authors (e.g. van Berkel and Verburg, 2011; Maes et al., 2011. Haines-Young et al., 2012; Liquete et al., 2013; Stürck et al., 2014) have mapped ecosystem services at the continental scale, mapping the demand and supply of ecosystem services has been attempted predominately at the local and regional scale, e.g. Burkhard et al. (2012). By linking land cover information from remote sensing and land surveys with data from monitoring, statistics, modeling or interviews, ecosystem service supply and demand can be assessed and transferred to different spatial and temporal scales (Burkhard et al., 2012).

In the future, global change will alter the supply of ecosystem services that are vital for human well-being. Schröter et al. (2005) investigated the ecosystem service supply during the 21st century in Europe by a range of ecosystem models and scenarios of climate and land-use change. Results indicated that large changes in climate and land use typically resulted in large changes in ecosystem service supply (Schröter et al., 2005). Some of the determined trends were positive (e.g. increases in forest area and productivity) or offered opportunities (e.g. extra land for agricultural extensification and bioenergy production).

Forest cover dynamics play an essential role within the context of global environmental change and hydrological and biogeochemical cycles (Global Land Project, 2005). Changes in forest cover, e.g. afforestation and deforestation, are irreversible processes due to their inherent hysteresis. Thereby, anthropogenic changes drive the Earth system into a qualitatively different state and ecosystem services are unable to recover. Higgins and Scheiter (2012) documented that Earth system scientists are particularly concerned about tipping elements: large-scale components of the Earth system that

can be switched into qualitatively different states by small perturbations. Land use extensification and forest cover dynamics are generally associated with positive feedbacks on ecosystem goods and services (Costanza et al., 1997). However, a net forest cover increase is not necessarily translated in an increase of forest biomass, biodiversity or ecosystem services (Garcia-Quijano et al., 2007). Forest cover changes have an impact on the ecosystems services that regulate provisional (e.g. food), regulatory (e.g. climate regulation), cultural (e.g. education) and supporting (e.g. nutrient cycle) functions (Millennium Ecosystem Assessment, 2003). Forests can be viewed as striving to produce a portfolio of ecosystem services to provide the greatest overall benefit to the public and nature within a landscape's capacity (Kline and Mazzotta, 2012). However, there is always a trade-off between the different ecosystem services since they are interrelated and even conflicting.The impact forest cover change on ecosystem services mainly depends on the forest cover trajectory and the type of forest cover change (e.g. native vs. exotic plantations and plantations vs. revegetation).
Generally, a decreasing forest cover has a negative impact on different ecosystem services: soil conservation (Chazdon, 2008), air quality (Krieger, 2001), biodiversity (Dupouey et al., 2002; Hall et al., 2012), carbon sequestration (Philips et al., 1998), soil fertility (Cole et al., 1989), water retention (Molina et al., 2012), climate regulation (Costanza et al., 1997; Schröter et al., 2005; World Health Organization, 2005), etc. In contrast, an increasing forest cover exerts a positive influence on these ecosystem services. For example, Molina et al. (2012) analyzed the impact of forest change on water and sediment fluxes in a highly degraded Andean catchment. Different pathways of land cover change between 1963 and 2007 were observed and deforestation increased landslide activity in the higher, more remote parts. In contrast, a recovery and reforestation was observed in the middle and lower parts where agricultural and bare land was prevalent.

Considering global warming, positive forest cover dynamics are able to decrease the amount of greenhouse gases in the atmosphere by an enhanced carbon sequestration (Houghton et al., 2000). Generally, deforested lands are carbon-poor. The regeneration of a secondary forest increases the sequestration of carbon. Furthermore, a forest cover increase and a consecutive lower runoff rate has a positive effect on the hydrological cycle. Consequently, a decrease in soil erosion causes a lower sediment load in the rivers, which results in an improved water quality (Ammer et al., 1995). A study in Greece by Bakker et al. (2005) indicated that abandonment of arable land was triggered by a declining productivity. Path analysis showed that erosion was a crucial controlling factor for the abandonment and reallocation of cereals. Results of a recent study in the Ecuadorian Andes indicated that human activities significantly increased the landslide hazard (Vanacker et al., 2013). An increase in the occurrence of landslides was observed after deforestation and road construction. Furthermore, various authors suggest that the impact of forest cover change strongly depends on the initial state of the ecosystem (Scott et al., 2005; Chazdon, 2008; Hofstede, 2011) and the type of land cover established during the transition (e.g. natural forest regeneration versus plantation).

1.4 Responses from policy makers

In response to changes in forest cover, policy makers worldwide have developed a wide range of policy instruments that aim to steer human-environment interactions towards more sustainable development pathways. For example, global protected areas network has been expanding rapidly

over the last decades (Jenkings and Joppa, 2009), and various parts of the world's natural resources receive some kind of protection status, also referred to as land zoning. Furthermore, land users and local governments are encouraged to preserve and strengthen the delivery of bundles of ecosystem services by financial incentives. Payments for ecosystem services (PES) are incentives offered to farmers in exchange for managing their land to provide some sort of ecological service (Jack et al., 2008). There exists a wide range of often nationally-implemented PES programmes of which the most expensive programmes are the 'Unites States Conservation Reserve Programme' (Ribaudo et al., 2001) and the Chinese 'Grain for Green Programme' (Zhou et al., 2009) in which farmers are paid to remove production of environmentally sensitive land. Another mechanism that was launched is environmental certification, whereby a company or a farmer can voluntary choose to comply with predefined processes or objectives set forth by the certification service. Thereby, the production standards are defined through commodity roundtables, by NGOs, or by private corporations, and these standards can be enforced by governments. Widely adopted environmental certificates are the 'Forest Stewardship Council' (FSC) which promotes the responsible management of forests on an international scale and 'Rainforest Alliance' certifying sustainable forestry, farming and tourism in tropical areas. Finally, in an attempt to address the need to take meaningful actions to reduce emissions from deforestation and forest degradation, the REDD and REDD+ programmes were set up in which national governments receive financial grants if carbon emissions are reduced through avoidance of deforestation and forest degradation (REDD) and if additional local environmental and socioeconomic benefits are captured (REDD+; Strasburg et al., 2010).

1.5 Research challenges

Assessing and monitoring the state of the Earth's surface is a key requirement for global change research (Committee on Global Change Research, National Research Council, 1999; Jung et al. 2006; Lambin et al., 2001; Goudie, 2013). Classifying and mapping vegetation is an essential technical task for managing natural resources as vegetation provides a base for all living beings and plays an essential role in global climate change (Xiao et al., 2004). Vegetation mapping also presents valuable information for understanding the natural and man-made environments through quantifying vegetation cover from local to global scales at a given time or over a continuous period. Thereby, it is critical to obtain current states of vegetation cover in order to initiate vegetation protection and restoration programs (Egbert et al., 2002; He et al., 2005). Frequently updated data on vegetation cover is preferred in order to better assess the environment (Knight et al., 2006) and to evaluate the efficiency of adopted land policy instruments.

There is a need for reliable instruments to detect forest cover dynamics and to evaluate the efficiency of policy measures. Although, forest cover detection and mapping is rather challenging since the definition of forest is varying between different countries. Moreover, landscapes in the transition phase typically consist of patchy structures and dependent on the quality and the uncertainties of the assessed forest data. Hereby, certain land units are still degrading, while others are in various stages of regeneration. Furthermore, forest cover changes in the turnover phase are characterized by up- and downward trends (as shown in Figure 1.3), and subtle variations in

vegetation which are hard to detect. Finally, large forests are present in inaccessibility of places which are difficult to monitor and where a lack of validation data exists.

Spaceborne remote sensing techniques seem to offer a practical and economical mean to study vegetation cover changes, especially over large and remote areas (Langley et al., 2001; Nordberg and Evertson, 2003). However, remote sensing imagery has been acquired by a range of multispectral and hyperspectral sensors over the past half century. Hereby, satellite imagery is especially used to monitor and detect vegetation cover characteristics (Coppin et al., 2001). The interest in Land Use and Land Cover Change (LULCC) analyses accelerated the development of mosaicking techniques, which integrate several images to construct one large radiometrically balanced image without visible boundaries between the original images (Inampudi, 1998). Recent methods adopt pixel-based compositing algorithms which select a subset of data from a large data archive. This selection of the data is based in the scope of the study, e.g. cloud masking or atmospheric correction (Qi and Kerr, 1997). Further information on the development of pixel-based image composites (PBICs) is described in Chapter 2.

Despite these recent developments, remote sensing methods for the analysis of forest cover dynamics at regional scale still suffer from methodological challenges due to atmospherical, topographical and shadowing effects. During the last decades, various techniques have been developed to correct satellite imagery for geometric, atmospheric and topographic distortions on mountainous surfaces. The available techniques range from empirical procedures to process-based models. Sophisticated techniques are particularly difficult to apply in streamlined processing schemes since site-specific calibration is required. At present, however, the added value of complex preprocessing techniques compared to empirical methods and the impact of more sophisticated processing on subsequent analyses is unclear. Furthermore, ideal images or pixels for specific applications can be selected by mosaicking or compositing techniques. Finally, most studies lack an evaluation of the automation potential of the different preprocessing techniques. The automation potential determines the difficulty to automate a technique and depends on the availability, amount and complexity of the input parameters. For example, the automation potential of different correction techniques decreases with the number and complexity of input parameters. In long-term vegetation studies that implement medium resolution imagery, techniques require a straightforward implementation in order to allow for chain processing.

1.6 Research objectives

Apparent research gaps and opportunities for the detection of forest cover dynamics are still present. The major scientific and policy challenges are the following:

- Reliable forest assessments with standardized procedures that allow evaluation of land management techniques, policy interventions and implementation of financial compensation regulations, especially in remote and inaccessible areas. Hereby, possible translocation processes which trigger deforestation trends in other countries should be take into account included;

- Detection of forest cover dynamics which are characterized by fluctuating forest cover trends and patchy landscapes;
- Improvement of mapping procedures and optimization of trade-offs between the complexity of the mapping procedure and its automation potential;
- Impact assessment of forest cover dynamics on ecosystem services such as carbon sequestration, biodiversity, and soil and water conservation.

Given the major scientific challenges in the broad research domain, the main objective of this PhD research is the methodological improvement of regional scale detection and analysis of forest cover dynamics by means recently developed image preprocessing techniques. Therefore, this thesis aims at a better understanding of the impact of atmospheric and topographic correction techniques on the detection of forest cover dynamics. These techniques are essential in mountain areas since highly elevated areas are often very sensitive to changes in environmental drivers and are prone to shadowing effects due to elevation differences. Furthermore, the thesis develops an optimal preprocessing chain for semi-automatic change analyses of satellite data covering mountainous terrain. Since the Romanian Carpathians Mountains still harbor extended areas of virgin forests and have a large range in elevation, these mountain range was selected to develop, calibrate and validate the different preprocessing techniques. Finally, the produced maps were implemented to analyze the spatial pattern of forest cover changes in the Romanian Carpathians.

In order to address the main objective of this thesis, the following specific research questions were formulated:

1. To what extent do available atmospheric and topographic corrections improve the homogeneity of reflectance values of distorted medium resolution imagery in mountain areas? Do complex procedures perform better than simplified approaches?
2. Does image preprocessing lead to more accurate land cover classification?
3. To what extent does topographic correction and pixel-based compositing improve large area (change) mapping?
4. What is the pattern and what are the controlling factors of forest cover changes in the Romanian Carpathians?

1.7 Thesis outline

The structure of this thesis is shown in Table 1.3. The parts and chapters are ordered from literature study to field observation analysis, preprocessing and multi-temporal analysis towards the general discussion and overall conclusions. Major parts of this thesis have been published as individual research papers. Therefore some overlap may occur between the different chapters.

The first, introductory part consists of three chapters. Chapter 1 provides a general introduction to the concept of forest transition and also the research objectives are identified. Chapter 2 consists of a thorough literature overview of the available sensors for forest detection. Furthermore, an overview is provided of the existing compositing techniques, atmospheric and topographic correction methods. The third chapter describes the study area in which the research for this thesis has been

conducted. Furthermore, available data on land use change, forest cover dynamics and their controlling factors in the Romanian Carpathians is presented. This chapter serves as the background upon which the later chapters rely for comparison.

The second part deals with the preprocessing of satellite imagery in the Romanian Carpathians. In Chapter 4, a range of atmospheric and topographic correction methods is selected and automated in the ENVI/IDL software. Furthermore, the performance of all combined corrections is evaluated in a study area of 185 x 185 km. Subsequently, in Chapter 5, the effect of atmospheric and topographic correction methods on land cover classification accuracy is discussed.

In the third part, a multi-temporal analysis is performed in the Romanian Carpathians. Chapter 6 deals with the integration of topographic correction in a pixel-based compositing algorithm and forest cover change analysis in the Romanian Carpathian Ecoregion (±107,000 km²). Chapter 7 includes the analysis of the forest cover change controlling factors in the Romanian Carpathian Ecoregion. The final part consists of a general discussion of the main results, along with the overall conclusions. Finally, as far from all research opportunities were unaddressed in this thesis, a number of future recommendations are listed.

Table 1.3.: Thesis outline.

Part 1: Introduction
Chapter 1: Problem statement and research objectives
Chapter 2: State of the art and challenges for forest cover dynamics detection with medium resolution satellite imagery
Chapter 3: Study area, forest cover dynamics and their controlling factors in the Carpathians
Part 2: Atmospheric and topographic correction
Chapter 4: Performance of atmospheric and topographic correction methods on Landsat imagery in mountain areas
Chapter 5: Effect of atmospheric and topographic correction methods on land cover classification accuracy in mountain areas
Part 3: Multi-temporal analysis
Chapter 6: Integration of topographic correction in a pixel-based compositing algorithm and forest cover change detection in the Romanian Carpathian Ecoregion
Chapter 7: Controlling factors of forest cover changes in the Romanian Carpathian Ecoregion
Part 4: General discussion and conclusions
Chapter 8: General discussion and conclusions

Chapter 2: State of the art and challenges for forest cover dynamics detection with medium resolution satellite imagery

2.1 Monitoring changes in vegetation cover

Traditional methods (e.g. field surveys, literature reviews, map interpretation and ancillary data analysis) are ineffective to assess the state of vegetation cover at a regional scale level, especially in remote areas. These conventional methods are time consuming, labor intensive and often too expensive. Remote sensing techniques offer a practical and economical means to study vegetation cover changes, especially over large areas (Langley et al., 2001; Nordberg and Evertson, 2003). First, aerial photographs were acquired from a relatively low altitude (up to 6 km) above the Earth's surface. Aerial photography has advantages over ground level photographs. The aerial view enables the observation of a large area and are fast tools to map inaccessible regions. Furthermore, objective comparison of selected areas are possible. Without overlapping photography and a stereoscopic viewing instrument, detailed variations in terrain features are invisible. Consequently, the interpretation of aerial photography requires training to allow good interpretation (Xie et al., 2008).

Secondly, satellite remote sensing techniques have been developed for land cover mapping at regular time intervals. In an effort to monitor major fluctuations in vegetation, scientists started using satellite remote sensors about 30 years ago to measure and map the density of green vegetation over the Earth. Especially in inaccessible regions, satellite imagery is used to obtain data on a cost and time effective basis. Remotely sensed data are generated by various sensor types that are attached to different platforms. All sensors capture data at various heights and at different times of day. By applying remote sensing imagery, significant efforts have been made by researchers to delineate vegetation cover from local to global scale.

Wavelengths of satellite imagery range from visible to microwave, with spatial resolutions varying from sub-meter to kilometers and temporal frequencies varying from 30 minutes to weeks or months. Typically, the spatial resolution of available remote sensing imagery is divided in four categories: (1) low spatial resolution is defined as pixels with ground sampling distance (GSD) of 30 m or greater, (2) medium spatial resolution is GSD in the range of 2–30 m, (3) high spatial resolution is GSD 0.5–2 m, and (4) very high spatial resolution is pixel sizes <0.5 m GSD. Despite the availability of a wide range of remote sensors, field forest inventories remain crucial for the assessment of Ground Control Points (GCPs) for validation.

Most long-term vegetation mapping projects have been achieved with medium to low spatial resolution imagery. Typical medium spatial resolution sensors are Landsat (Land remote sensing satellite program) and Satellite Pour l'Observation de la Terre (SPOT). Examples of low spatial resolution sensors are the Moderate Resolution Imaging Spectroradiometer (MODIS) and SPOT-VEGETATION. Medium to very high spatial resolution scanners can be used to map the Earth’s cover by means of categorical land cover classes such a forest, grassland and arable land whereby the spectral signature of a pixel is used for identification. This approach is impractical for low spatial

resolution sensors since their pixels often cover more than one land cover type. Therefore, a whole set of Vegetation Indices (VI) were developed to quantify the concentrations of green leaf vegetation around the globe. By combining the daily VIs into 8-, 16-, or 30-day composites, detailed maps of the Earth's green vegetation density were created (NASA, 2013a). Furthermore, maps derived from the different sensors are proper tools for land cover analysis, such as the European land cover and forest maps compiled in the Coordination of Information on the Environment (CORINE; EEA, 1995), the Global Land Cover Facility datasets (NASA, 1997) and the global maps constructed by Hansen et al. (2013). The major drawback of these applications is the lack of repeated observations over a longer period and problems originating from geometric, atmospheric and topographic distortions (Singh et al., 2011). Therefore, preprocessing techniques are an essential step to improve interpretation of satellite imagery. A comprehensive overview of the frequently used remote sensors, their derived vegetation indices, advantages and disadvantages is provided in the following sections.

2.1.1 Remote sensors

A remote sensor is a device that captures the unique spectral characteristics of the Earth's surface. The spectral radiances in the red and near-infrared regions are incorporated into spectral vegetation indices that are directly related to the intercepted fraction of photosynthetically active radiation (Asrar et al., 1984). The different spectral signatures of photosynthetically and non-photosynthetically active vegetation are shown in Figure 2.1 (Beeri et al., 2007; Xie et al., 2008).

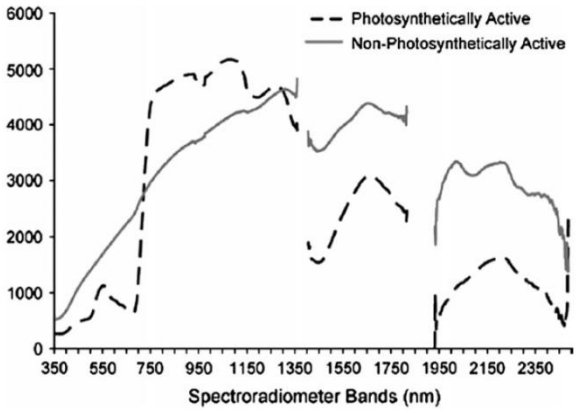

Figure 2.1.: Typical spectral signatures of photosynthetically active and non-photosynthetically active vegetation (Beeri et al., 2007).

Since different sensors have different spatial, temporal, spectral and radiometric characteristics; the selection of appropriate sensors is crucial for mapping vegetation cover. The selection of images acquired by adequate sensors is mainly determined by five related factors: (1) mapping objective, (2) spatial and temporal resolution, (3) cost of images, (4) climate conditions (especially atmospheric conditions), and (5) the technical issues related to image interpretation (Xie et al., 2008). First, the mapping objective concerns what is to be mapped and what mapping accuracy is expected. Thereby, images with higher spatial resolution are implemented for fine scale vegetation classification (e.g. WorldView-2 and QuickBird). Secondly, the spatial and temporal resolution determine the level of detail and the number of repeated observations. Thirdly, the cost of remote sensing imagery is definitely a consideration when choosing imagery (e.g. Landsat imagery is free for download while

the WorlView-2 sensor with high resolution is expensive). Fourthly, cloud-free image series from different sources need to be obtained over an extended period (Soudani et al., 2006). Finally, a number of technical specifics need to be considered regarding image quality, preprocessing and interpretation (e.g. all Landsat standard data products are preprocessed using the Level 1 Product Generation System).

Frequently applied sensors for vegetation mapping include Landsat, SPOT, MODIS, AVHRR, IKONOS and QuickBird. The temporal and spatial characteristics of these sensors are summarized in Figure 2.2. Further information is provided in Table 2.1 which is ordered from very high to low spatial resolution and described below, based on the research of Xie et al. (2008).

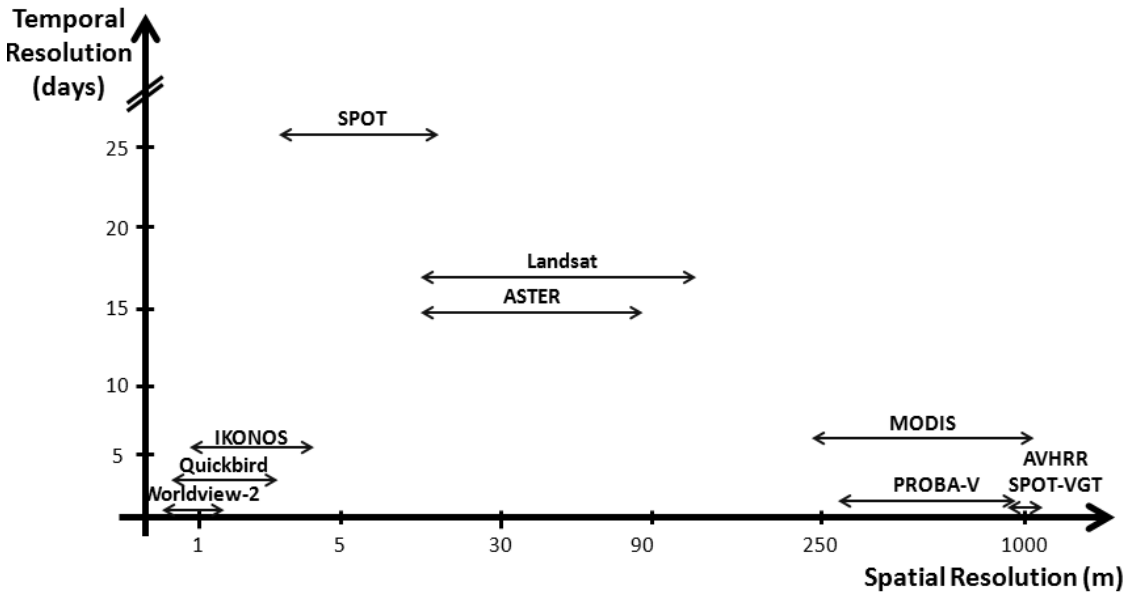

Figure 2.2.: Overview of satellite sensors for vegetation and forest mapping with indication of the temporal (days) and spatial resolution (m). Note: the division of the x and y axis is not linearly scaled.

Table 2.1.: Main features of image products from different satellite sensors, ordered from very high to low spatial resolution (based on Xie et al., 2008).

Products (sensors)	Spatial resolution and operating time	Footprint size	Spectral bands	Temporal resolution
WorldView-2	46 cm Panchromatic resolution and 1.85 meter multispectral resolution (2009 to present).	16.4 x 16.4 km	8	1.1 days on average
QuickBird	High resolution (0.6-2.4m) and panchromatic and multispectral imagery (2001 to present).	16.5 x 16.5 km	4	1–3.5 days depending on latitude
IKONOS	High resolution imagery at 1 m (panchromatic) and 4 m resolution (multispectral bands) (1999 to present).	11 x 11 km	4	3 days
SPOT	A full range of medium spatial resolutions from 20 m down to 2.5 m. SPOT 1, 2, 3, 4, 5 and 6 were launched in the year of	60 x 60 km for RV/HRVIR/HRG	4-5	26 days

	1986, 1990, 1993, 1998, 2002 and 2012, respectively.			
ASTER	Medium spatial resolution (15–90 m) image with 14 spectral bands from the Terra Satellite (1999 to present). Visible to near-infrared bands have a spatial resolution of 15 m, 30 m for short wave infrared bands and 90 m for thermal infrared bands.	60 x 60 km	15	16 days
Landsat TM	Medium to coarse spatial resolution with multispectral data (120 m for thermal infrared band and 30 m for multispectral bands) from Landsat 4 and 5 (1982 to present).	185 x 185 km	7	16 days
Landsat ETM+ (Landsat 7)	Medium to coarse spatial resolution with multispectral data (15 m for panchromatic band, 60 to 120 m for thermal infrared and 30 m for multispectral bands) (1999 to present).	185 km x 185 km	7	16 days
MODIS	Low spatial resolution (250–1,000 m) and multispectral data from the Terra Satellite (2000 to present) and Aqua Satellite (2002 to present).	2,330 km x 10 km	36	1–2 days
PROBA-V	300 m (VNIR), 600 m (SWIR) and 1 km (VNIR and SWIR) (2013 to present)	2,250 x 2,2250 km	4	± once a day
SPOT-VGT	Medium spatial resolution of 1 km (1998 and 2002 to present)	2,250 x 2,250 km	4	1 day
AVHRR	1 and 5 km with multispectral data from the NOAA satellite series (1981 to present).	2,400 x 6,400 km	4	Twice per day

WorldView-2

The WorldView-2 sensor was the first high resolution 8-band multispectral commercial satellite and provides 46 cm panchromatic resolution and 1.85 meter multispectral resolution (Puetz et al., 2009).

QuickBird

Similar to IKONOS, QuickBird offers highly accurate and high resolution imagery with panchromatic imagery at 60–70 cm resolution and multispectral (4 bands) imagery at 2.4 and 2.8 m resolution (Toutin and Cheng, 2002). QuickBird images are normally applied to study special topics in relatively small areas. Due to the high cost and rigid technical parameters, QuickBird imagery is impractical for applications in large areas (Parcak, 2009).

IKONOS

IKONOS is a commercial sun-synchronous Earth observation satellite launched in 1999 and was the first to collect publicly available high resolution imagery at 1 and 4 m resolution (Dial et al., 2003). IKONOS has two imaging sensors: the panchromatic sensor collects images of 1 m resolution, while the multispectral bands have a spatial resolution of 4 m. Both sensors have a swath width of 11 km and a 3 day revisit interval (Dial et al., 2003). The IKONOS observations are at a spatial scale equivalent to field measurements typically carried out in ecological and land cover research (Goetz et al., 2003). However, for long term mapping, IKONOS satellite imagery is very expensive (Parcak, 2009).

SPOT

Six SPOT satellites have been launched so far, from SPOT 1 to SPOT 6 in 1986, 1990, 1993, 1998, 2002 and 2012, respectively. SPOT imagery comes in a full range of resolutions from 1 km (SPOT vegetation imagery) down to 2.5 m (Courtois and Weill, 1985; ASTRIUM, 2013). Two HRV (High Resolution Visible) imaging instruments on SPOT 1, 2 and 3 and the corresponding instruments of HRVIR (High Resolution Visible and Infrared) on SPOT 4 and HRG (High Resolution Geometry) on SPOT 5 scan in either panchromatic or multispectral modes (5 spectral bands; Chevrel et al., 1980; ASTRIUM, 2013). In addition, SPOT 4 and 5 also have a second imaging instrument referred to as SPOT vegetation (VGT) instrument that collects data at a spatial resolution of 1 km and a temporal resolution of 1 day (ASTRIUM, 2013). SPOT 6 was launched in 2012 and the proposed launch date for SPOT 7 is in 2014 (ASTRIUM, 2013). SPOT VGT images are useful for observing and analyzing the evolution of land surfaces and understanding land cover changes over large areas (Maggi and Stroppiana, 2002). Due to the presence of multiple sensor instruments and the high revisit frequency, SPOT satellites are capable to obtain low resolution daily image of any place on Earth (Maggi and Stroppiana, 2002).

ASTER

Advanced Spaceborne Thermal Emission and Reflection Radiometer (ASTER) is an imaging instrument orbiting on the Terra platform. ASTER acquires images with spatial resolutions between 20 and 256 m (Epiphanio, 2005; Ponzoni et al., 2006) and has been applied to obtain detailed land surface and elevation maps (Tuttle et al., 2006). An advantage of ASTER is the availability of 15 spectral bands which allow for studies on snow cover, water, vegetation and minerals.

Landsat TM and ETM+

The Landsat series of satellites started with the launch of ERTS-1 (Earth Resources Technology Satellite, later renamed Landsat 1) in 1972 and continues to this day with Landsat 8, providing the world's longest continuously acquired collection of space-based land remote sensing data. Therefore, the Landsat sensor has a long history and wide application for monitoring the Earth from space (USGS, 2013b). Since the first Landsat satellite was launched in 1972, a series of more sophisticated multispectral imaging sensors with 7 spectral bands, named TM or Thematic Mapper, have been launched. The Landsat sensors range from Landsat 1 (1972-1978), Landsat 2 (1975-1981), Landsat 3 (1978-1983), Landsat 4 (1982-1993), 5 (1984-2013), 6 (1993, launch failed), 7 (1999-now; Enhanced Thematic Mapper Plus, ETM+, scan-line corrector failure since 2003) to the Landsat Data Continuity Mission (LDCM or Landsat 8) in 2013 (USGS, 2013b). The Landsat TM and ETM+ imaging sensors have archived millions of images with a nearly continuous record of global land surface data since its

launch. Landsat provides medium to coarse spatial resolution images (USGS, 2013b). For example, Landsat ETM+ imagery has a spatial resolution of 30 m for the multispectral bands and 60 to 120 m for the thermal infrared band (USGS, 2013b). The long Landsat history is helpful to map long-term vegetation cover and to study spatiotemporal vegetation changes. Therefore, Landsat products have been applied in vegetation mapping mainly at regional scales. For example, nearly 20-year Landsat TM/ETM+ image datasets (19 images) covering western Oregon were applied to detect and characterize changes in early forest succession (Schroeder et al., 2006). The different characteristics of Landsat spectral sensors require a spectral reflectance correction between these images (Schroeder et al., 2006).

MODIS

MODIS is a key instrument aboard of the Terra and Aqua satellites. Terra MODIS and Aqua MODIS together are able to visit the entire Earth's surface every 1–2 days. The gathered images from MODIS with spatial resolutions between 250 m and 1 km are mainly applied to map vegetation dynamics and processes at a large scale (Xie et al., 2008). Due to the coarse spatial resolution, vegetation mapping at a local or regional scale is discouraged (Justice et al., 1998; Giri et al., 2005). An advantage of MODIS is the availability of 36 spectral bands, including thermal bands that allow to monitor water vapour and evapotranspiration (Sader and Jin, 2006) .

PROBA-V

In order to ensure data continuity after the decommissioning of VEGETATION, a new mission under the name of Project for On-Board Autonomy - Vegetation (PROBA-V) has been prepared by the European Space Agency. The satellite and the instrument were developed and built by Belgian contractors and was launched on May 7 2013. PROBA-V is a small satellite, assuring the succession of the VEGETATION instruments on board the French SPOT-4 and SPOT-5 Earth observation missions (BELSPO, 2011). PROBA-V was initiated by the Space- and Aeronautics department of the Belgian Science Policy Office (BELSPO). Traditional vegetation products generated by the VEGETATION instruments include the 1-day Synthesis products and the 10-day Synthesis products, both with a ground resolution of about 1 km (1 km x 1 km pixel size; VITO, 2013b). Despite the fact that the VEGETATION instrument onboard PROBA-V has a higher spatial resolution (smaller ground pixels) than the VEGETATION instruments on board the SPOT satellites, the long time series (15 years) of the traditional Vegetation products will be continued by PROBA-V (ESA, 2012). Thus, PROBA-V will also generate the traditional vegetation products at approximately 1 km x 1 km ground resolution and support applications such as land use, worldwide vegetation classification, crop monitoring, famine prediction, food security, disaster monitoring and biosphere studies (ESA, 2012). Another advantage is that products older than 3 months are downloadable free of charge (BELSPO, 2011).

SPOT-VEGETATION

The SPOT-VEGETATION programme is a space collaboration between various European partners: Belgium, France, Italy, Sweden and the European Commission. It consists of two observation instruments in orbit, VEGETATION 1 and VEGETATION 2 (VITO, 2013a). The first satellite component (VEGETATION 1) of the programme was launched on March 24 1998 onboard SPOT 4, while the second instrument was launched onboard SPOT 5 on May 4 2002. They deliver measurements specifically tailored to monitor parameters of land surfaceswith a frequency of about once a day on a global basis and a medium spatial resolution of one km (VITO, 2013a).

AVHRR

Carried on the NOAA's Polar Orbiting Environmental Satellite series, the AVHRR sensor is a broadband scanning radiometer in the visible, near infrared and thermal infrared spectrum. AVHRR image data have two spatial resolutions: ~1.1 km for local area coverage and 5 km for global area coverage (Ho and Asem, 1986). AVHRR is widely applied to study and monitor vegetation conditions in ecosystems, land cover mapping and production of large scale maps (Johnson et al., 1987; Ehrlich et al., 1994; Loveland et al., 2000). One of the advantages of AVHRR is the low cost and the high probability of obtaining a cloud-free view of the land surface in e.g. a monthly composite (Eidenshink and Faundeen, 1994) due to the high temporal resolution. Since AVHRR has an image archive with long history since 1981, it is useful to study long-term changes of vegetation (Teuber, 1990). However, AVHRR imagery suffers certain limitations in calibration, geometry, orbital drift, limited spectral coverage (4 bands) and variations in spectral coverage especially in the early acquisitions (Wu et al., 2010; Devasthale et al., 2012; Latifovic et al., 2012). One of the main advantages of the AVHRR instrument is that it provides a long term reflectance data sets to monitor the land surface (Maggi and Stroppiana, 2002).

Hyperspectral sensors and applications

Besides the above mentioned sensors, many other sensors are available. Hyperspectral sensors collect hundreds of spectral bands. Note that the principle for mapping vegetation cover from remote sensing images relies on the unique spectral features of different vegetation types. Thus, hyperspectral imagery contains more vegetation information and is applied for more accurate vegetation mapping (Fisher et al., 1998). The Airborne Visible Infrared Imaging Spectrometer (AVIRIS), for example, collects images with 224 spectral bands. A disadvantage from this sensor is the irregular temporal resolution that depends on weather conditions at target sites (Xie et al., 2008).

Furthermore, the International Geosphere–Biosphere Program started a global land cover mapping in the development of the Global Land Cover Characterization (GLCC) Database that was based on 1 km Advanced Very High Resolution Radiometer (AVHRR) image data in 1992 (USGS, 2013a). Similarly, in collaboration with over 30 research teams from around the world, the Joint Research Centre of the European Commission in Italy implemented the Global Land Cover 2000 project (GLC2000) in 1999 to map global land cover and build up the VEGA2000 dataset by extracting the data from 1 km SPOT4-VEGETATION imagery (European Commission, 2013a). Two years later, US National Aeronautics and Space Administration (NASA) released the database of global MODIS land cover based on monthly composites from Terra MODIS Levels 2 and 3 images between January and December 2001 (Xie et al., 2008). Next to these initiatives at the global and continental scales, numerous programs started to map vegetation at regional scale. An example is the USGS – National Park Service Vegetation Mapping, that started in 1994 with the aim to produce detailed and computerized maps of the vegetation for ~250 national parks across the United States. Inventories were performed by processing Airborne Visible and Infrared Imaging Spectrometer (AVIRIS) imagery along with ground sampling references.

2.1.2 Indices derived from low and medium resolution imagery

Indices derived from medium to low resolution sensors are a proper tool for land cover analysis. Vegetation indices (VIs) have a long history over a wide range of applications such as: vegetation monitoring, climate and hydrologic modeling, agricultural activities, drought studies and public health issues (Bannari et al., 1995; Elvidge and Chen, 1995; Huete et al., 1997; Huete et al., 2002). Vegetation capture the unique spectral signatures, which evolve with the plant life cycle. VIs are dimensionless radiometric measures that combine information from different channels, particularly in the red and near infrared (NIR) portions of the spectrum, to enhance the vegetation signal. Such indices allow reliable spatial and temporal inter-comparisons of terrestrial photosynthetic activity and canopy structural variations (Eumetrain, 2010). VIs are generally computed for all pixels in time and space, regardless of biome type, land cover condition and soil type (Huete et al., 2002). Due to their simplicity and ease of application, vegetation indices have a wide range of usage within the user community. In the following paragraphs, the main VIs are summarized (Gutman, 2012).

Normalized Difference Vegetation Index (NDVI)

The amount of red and NIR reflectance is related to the amount of vegetation present on the ground (Huete et al., 1999). Reflected red energy decreases with plant development due to the chlorophyll absorption within actively photosynthetic leaves. Reflected NIR energy, on the other hand, will increase with plant development through scattering processes in healthy leaves (Eumetrain, 2010).

The most widely used VI is the NDVI which consists of a normalized ratio of the NIR and red bands (Rouse, 1973; Equation 2.1):

$$NDVI = \frac{\rho_{NIR} - \rho_{red}}{\rho_{NIR} + \rho_{red}} \tag{2.1}$$

where ρ_{red} and ρ_{NIR} are reflectance measurements in % for the red and NIR bands, respectively. NDVI values range from 1 to -1. For land targets, the index ranges from 0 for arid or barren areas to 1 for densely vegetated areas. Negative NDVI values usually correspond to urban areas. The NDVI over water surfaces is close to -1 due to their low reflectance in the NIR band. NDVI's main advantage is the simple computation without assumptions regarding to land cover classes, soil type or climatic conditions. Furthermore, long time series of more than 20 years are available. There are also a number of disadvantages: additive noise effects, asymptotic (saturated) signals over high biomass condition and sensitivity to canopy background brightness (Huete et al., 2002). Furthermore, the NDVI is not a structural property of land surface areas.

Enhanced Vegetation Index (EVI)

The EVI was developed by the MODIS Science Team to take full advantage of the sensor capabilities (Liu and Huete, 1995; Equation 2.2):

$$EVI = \mathrm{G}\ \frac{\rho_{NIR} - \rho_{red}}{\rho_{NIR} + C_1 x \rho_{red} - C_2 x \rho_{blue} + L} \tag{2.2}$$

Where ρ are atmospherically corrected reflectances values for Rayleigh and ozone absorption, L is the canopy background adjustment, C_1 and C_2 are coefficients related to aerosol correction and G is a

gain factor. In order to increase the sensitivity to the vegetation signal, the index implements measurements in the red and near infrared bands (as in the case of NDVI), and also in the visible blue band, which allows for an extra correction of aerosol scattering. EVI also performs better than NDVI over high biomass areas, since it does not saturate as easily (Huete et al., 2002). The blue band is used to remove residual atmosphere contamination caused by smoke and thin clouds. EVI's main advantage is the good performance under high aerosol loads and biomass burning conditions (Huete et al., 2002). Some disadvantages are comparable with the NDVI: it is not a structural property of land surface areas and it features an inherent nonlinearity since it is a ratio based index. Other disadvantages are the relatively low values in all biomes and also lower ranges over semiarid sites to compensate for the effects of NDVI saturation over high biomass areas (Eumetrain, 2010).

Othervegetation indices

Several other vegetation indices have been developed, the equations of five VIs are provided underneath. Furthermore, a extensive variety of other VIs is available for different purpose (Veraverbeke et al., 2010; Vina et al., 2011; Huete, 2012).

- Perpendicular Vegetation Index (PVI*;* Richardson and Wiegand, 1977; Equation 2.3)

$$PVI = \sqrt{(0.355\rho_{NIR} - 0.149\rho_{red})^2 - (0.355\rho_{red} - 0.852\rho_{NIR})^2} \quad (2.3)$$

- Vegetation Condition Index (VCI; Kogan,1995; Equation 2.6):

$$VCI = 100 \text{ x } \frac{(NDVI - NDVI_{\min})}{(NDVI_{max} - NDVI)} \quad (2.4)$$

where $NDVI_{min}$ and $NDVI_{max}$ are NDVI multi-year absolute maximum, and minimum, respectively.

- Soil Brightness Index (SBI*;* Richardson and Wiegand, 1977 *;* Equation 2.4)

$$SBI = a_1\rho_{green} + b_1\rho_{red} + c_1\rho_{NIR} + d_1\rho_{NIR} \quad (2.5)$$

where ρ_{green} is the reflectance measurement for the visible green band and a_1, b_1, c_1 and d_1 are coefficients.

- Soil-Adjusted Vegetation Index (SAVI; Huete, 1988; Equation 2.7):

$$SAVI = (1 + l) \frac{(\rho_{NIR} - \rho_{red})}{(\rho_{NIR} + \rho_{red} + l)} \quad (2.6)$$

where *l* is the soil brightness correction factor. The value of *l* varies by the amount or cover of green vegetation: *l*=0 in very high vegetation regions and *l*=1 in areas without green vegetation.

- Transformed Soil-Adjusted Vegetation Index (TSAVI; Baret et al., 1989; Equation 2.7):

$$TSAVI = \frac{(a(\rho_{NIR} - a\rho_{red} - b))}{(a\rho_{NIR} + \rho_{red} - (ab) + x(1 + a^2))} \quad (2.7)$$

where a = slope of the soil line, b = intercept of the soil line, x = adjustment factor.

2.2 Preprocessing and compositing of remote sensing imagery

Figure 2.3 provides an overview of the different preprocessing steps that should be applied prior to image compositing, interpretation and classification. Remote sensors capture electromagnetic radiance values which are recorded in digital numbers. In a first step, the geometric correction, the pixels are placed in a planimetric reference system. Secondly, clouded pixels are detected and masked out. Finally, a radiometric correction is carried out which includes the correction for disturbances in the atmosphere and for differential illumination effects due to topography. At-surface reflectance values can then be used for image interpretation and classification. For large scale studies, an additional compositing step may be required, in which multiple images are mosaicked or pixels are composited. In the following sections, these different steps are documented.

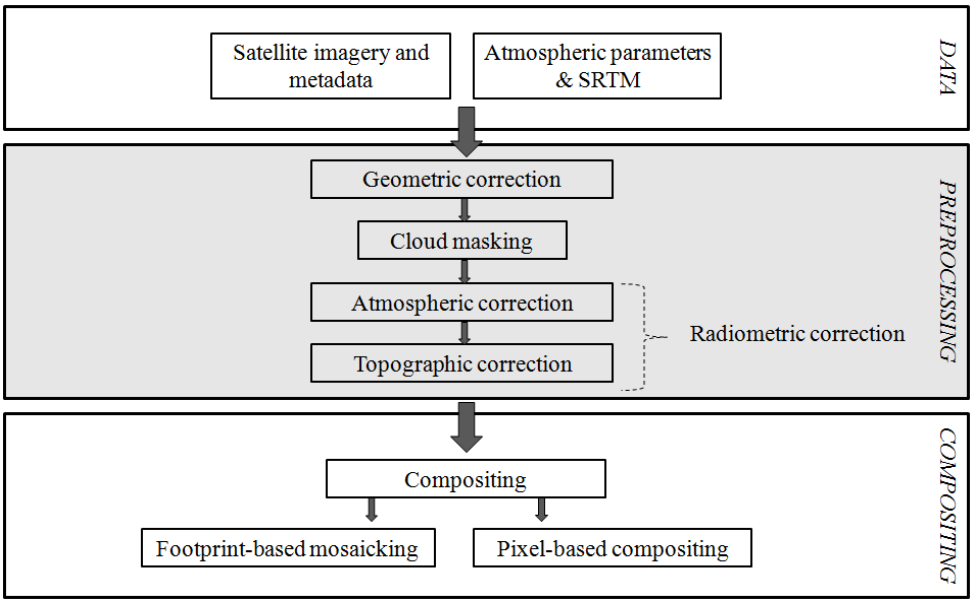

Figure 2.3.: Overview of different input data, and preprocessing steps prior to compositing: geometric correction, cloud masking, and atmospheric and topographic correction. The SRTM is the shuttle radar topography mission.

2.2.1 Geometric correction

Remote sensors record information about the Earth's surface by measuring the transmission of energy from the surface in different portions of the electromagnetic (EM) spectrum and store the information in digital numbers (often coded with one byte resulting in 256 levels). The digital numbers (DN; eight-bit) of each spectral band need to be converted to at-satellite radiances ($L_{as,\lambda}$, in W/(m^{2}µm); Equation 2.8) by means of a calibration. This calibration includes gain and offset values describing the sensitivity of the sensor and are obtained from the calibration file in the metadata (where L_{as} refers to the at-satellite radiances and λ to the band wavelength in m):

$$L_{as,\lambda} = \text{DN} \times \text{gain} + \text{offset} \quad (2.8)$$

Geometric correction aims to place the registered pixels in a uniform planimetric reference system. This requires corrections for tilting and tipping of the sensor and an orthorectification that includes displacements due to off-nadir viewpoints and the topography of the terrain. In most cases,

providers of satellite imagery deliver geometrically corrected imagery. For example, all Landsat images in the freely available USGS archive are orthorectified with precision terrain correction level L1T. This correction provides the geometric accuracy by incorporating ground control points while employing a Digital Elevation Model (DEM) for topographic accuracy (NASA, 2013b).

2.2.2 Cloud masking

To correctly interpret results, clouds and cloud shadows are often masked out by different procedures: visually (Knorn et al., 2012a; Prishchepov et al., 2012; Vicente-Serrano et al., 2008), by image differencing with a cloud-free reference image (Kennedy et al., 2010) or by using a specifically developed algorithm, such as the Function of mask (FMASK) algorithm (Zhu and Woodcock, 2012). Most of the cloud detection and masking algorithms are designed for implementation on a global (Gardner, 1993; Ackerman et al., 2002; Asmala and Shaun, 2012; Prishchepov et al., 2012; Zhu and Woodcock, 2012) or regional scale (Saunders, 1986; Logar et al., 1998; Knorn et al., 2012a). However, the practical implementation is often unsuccessful in the equatorial regions, especially southeast Asia (Franya and Cracknell, 1995; Bendix et al., 2004; Asmala and Shaun, 2012).

2.2.3 Atmospheric correction (AC)

Atmospheric correction is usually the first step in a radiometric correction in which the radiance received at the satellite is corrected for scattering, absorbing, and refraction of light by molecules in the atmosphere (Gao and Zhang, 2009). Atmospheric correction aims at the isolation of the solar direct irradiance from other radiance fluxes that enter the sensor: the path radiance, the sky diffuse irradiance and the adjacent terrain reflected irradiance (Jensen, 2005; Lillesand et al., 2004; Figure 2.4).

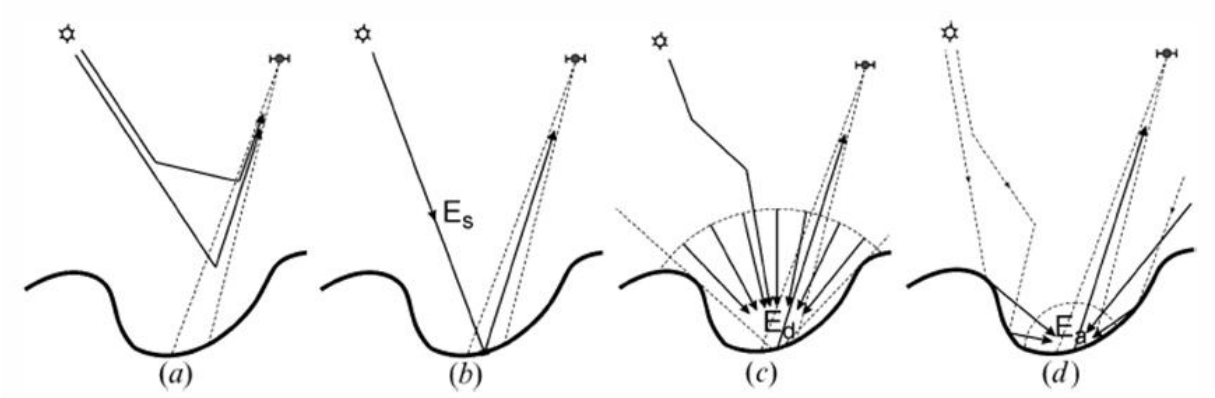

Figure 2.4.: Process of solar (ir)radiance entering a sensor: (a) path radiance, (b) solar direct irradiance, (c) sky diffuse irradiance, and (d) adjacent terrain reflected irradiance (Van Beek, 2011).

AC methods can be divided in two major types: (1) empirical methods and (2) methods based on radiative transfer models (Gao et al., 2009). An overview of frequently implemented atmospheric correction algorithms, their type, references and abbreviations is provided in Table 2.2. Empirical methods assess atmospheric disturbances based on parameters derived from the recorded radiance values. In contrast to more advanced AC methods, empirical corrections don't require external

atmospheric parameters collected by in-situ field measurements during the satellite flight. The most popular empirical AC methods are the dark object subtraction (DOS; Vincent, 1972; Chavez, 1975) and the empirical line method (Conel et al., 1987).

The DOS correction assumes that the atmospheric scattering or path radiance is equal to the radiance captured in the darkest object or pixel of the image (Vincent, 1972; Chavez, 1975; Chavez, 1996). The correction for scattering is implemented by subtracting the radiance value of the darkest object from all pixels of the image (Chavez, 1996). The empirical line method is based on regression analyses between the infrared band and other bands, whereby it is assumed that the infrared band is less susceptible to atmospheric scattering than the bands capturing shorter wavelengths (Conel et al., 1987). The empirical AC correction methods are relatively easy to apply since they only require the observed radiance values stored in the pixels of the image. However, these methods remain rough approximations of the underlying physical processes happening in the atmosphere, and their results are often of low quality (Moran et al., 1992; Thome et al., 1993).

The second type of methods are based on radiative transfer models which implement parameters that describe the atmospheric condition at the moment of image capture (Gao et al., 2009). A wide range of radiative transfer models has been developed that physically describe the pathways and the interaction of the electromagnetic radiance with different wavelengths through the atmosphere (Table 2.2). Most models include the following parameters: water vapour, ambient atmospheric pressure value and aerosol concentration (Berk et al., 1998; Richter, 1996; 1998; Kobayashi and Sanga-Ngoie, 2008). The main disadvantage of correction methods based on radiative transfer models is the need to capture these parameters during each satellite flight (Chavez, 1996). In many cases, the required parameters need to be derived from look-up tables or need to be assessed by means of regression between the captured parameters. Table 2.2 summarizes frequently implemented AC methods, in which the methods are ordered chronologically by year of publication. The AC methods applied in this PhD thesis are described in detail in Chapter 4.

Table 2.2.: Atmospheric correction (AC) algorithms, type, reference and explained abbreviation.

Correction	**Type**	**Reference**	**Abbreviation (explained)**
Flat field	Empirical	Roberts et al., 1986	
Empirical line	Empirical	Conel et al., 1987, Smith and Milton, 1999	
LOWTRAN	Radiative transfer	Kneizys et al., 1988	Low resolution atmospheric transmission
IAR	Empirical	Kruse, 1988	Internal Average Reflectance
MODTRAN	Radiative transfer	Berk et al., 1989	Moderate resolution atmospheric transmission
Cloud shadow	Empirical	Reinersman et al., 1998; Lee et al., 2005; Filippi et al., 2006	
RTCs, image-based procedures and DOS	Radiative transfer and empirical	Moran et al., 1992	Radiative transfer codes
ATREM	Radiative transfer	Gao et al., 1993	Atmosphere Removal algorithm
Inverse technique	Radiative transfer	Gilabert et al., 1994	
SMAC	Radiative transfer	Rahman and Dedieu, 1994	Simplified method for AC
DOS	Empirical	Chavez, 1996	Dark object subtraction method

ATCOR2	Radiative transfer	Richter, 1996	Acronym for atmospheric correction
SDAS	Radiative transfer	Staenz et al., 1998	Imaging Spectrometer Data Analysis System
FLAASH	Radiative transfer	Adler-Golden et al., 1999	Fast Line-of-sight Atmospheric Analysis of Spectral Hypercubes
DOS, DDV and modified DDV	Empirical	Song et al., 2001	Dense Dark Vegetation
AC with look-up tables	Radiative transfer	Liang et al., 2001; Liang and Fang, 2004	
LEDAPS	Radiative transfer	Wofsy and Harriss, 2002; Masek et al., 2006	Landsat Ecosystem Disturbance Adaptive Processing System
HATCH	Radiative transfer	Qu et al., 2003	High-accuracy Atmospheric Correction for Hyperspectral Data
QUAC	Radiative transfer	Bernstein et al., 2005	Quick Atmospheric Correction
6S	Radiative transfer	Sriwongsitanon et al., 2011; Vermote et al., 1997; Zhao et al., 2000; Burns and Nolin, 2014	Second simulation of a satellite signal in the solar spectrum
ACORN	Radiative transfer	Kruse, 2004	Atmosphere Correction Now
Transmittance functions (TF)	Radiative transfer	Kobayashi and Sanga-Ngoie, 2008	This method is the AC part of the combined radiometric correction
COST and MADCAL	Empirical and radiative transfer	Kennedy et al., 2010 ; Main-Knorn et al., 2012a	Multivariate Alteration Detection and Calibration
COST and ATCOR2	Empirical and radiative transfer	Broszeit and Ashraf, 2013	

2.2.4 Topographic correction (TC)

After atmospheric correction, the at-satellite radiance is converted to at-surface reflectance ($\rho_{T,\lambda}$) which includes variations in Earth-sun distance, the mean exo-atmospheric solar irradiance and the solar zenith angle. Equation 2.9 proposed by Markham and Barker (1986) is the most frequently adopted to carry this conversion.

$$\rho_{t,\lambda} = \frac{\pi L_{s,\lambda} d^2}{ESUN_\lambda \cos\theta_s} \quad (2.9)$$

where: λ = band wavelength; t = terrain; $\rho_{t,\lambda}$ = observed surface reflectance on an inclined surface (%,); $L_{s,\lambda}$ = at-satellite radiance after atmospheric correction (W/(m^2 µm)); d = Earth–sun distance (astronomical units); ϑ_s= solar zenith angle (degrees) and ESUN$_\lambda$= mean exo-atmospheric solar irradiance (W/(m^2 µm)).

In a final preprocessing step, the at-surface reflectance values are normalized. This step is essential in mountainous areas where pixels receive differential illumination depending on different illumination angles at the moment of image acquisition. Hereby, a Lambertian surface is an ideal diffuse reflection which reflects the incoming radiation equally into all directions of the hemisphere (Figure 2.5a).The apparent brightness of such a surface to an observer is the same regardless of the observer's angle of

view (Jensen, 1996). In contrast, the process when reflected light rays is scattered unequally in all directions for a rough surface is called non-Lambertian reflection (Figure 2.5b).

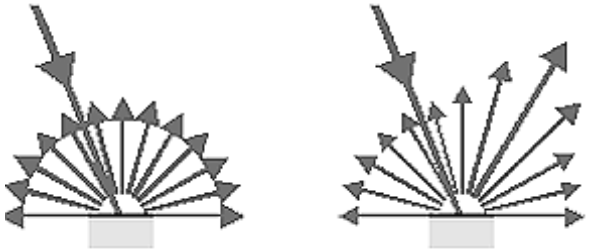

Figure 2.5.: (a) Lambertian reflection, and (b) non-Lambertian reflection (Jensen, 1996).

Due to the differences in illumination, comparable vegetation types show a dissimilar reflectance response on different hill slopes, where shaded areas have lower than expected reflectance, and the opposite effect is observed on brightly illuminated areas (Figure 2.6, Riaño et al., 2003).

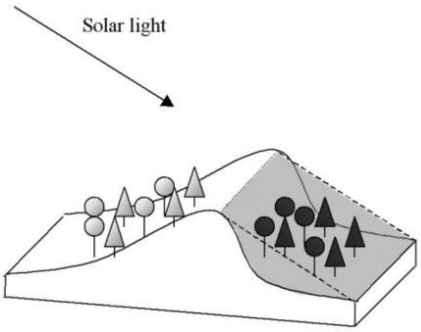

Figure 2.6.: Differences in illumination due to topographic effects (Riaño et al., 2003).

Topographic normalization aims at removing these differential illumination effects by assessing the theoretical reflectance for a horizontal surface ($\rho_{H,\lambda}$; Veraverbeke et al., 2010). Figure 2.7 shows the different angles that explain differential illumination: solar zenith angle (ϑ_s), the slope angle of the terrain (ϑ_n, in degrees), the solar azimuth angle (ϕ_t, in degrees) and the aspect angle of the terrain (ϕ_a, in degrees). Furthermore, the incident solar angle θ (degrees) is the angle between the normal to the ground surface and the solar zenith direction (Civco, 1989).

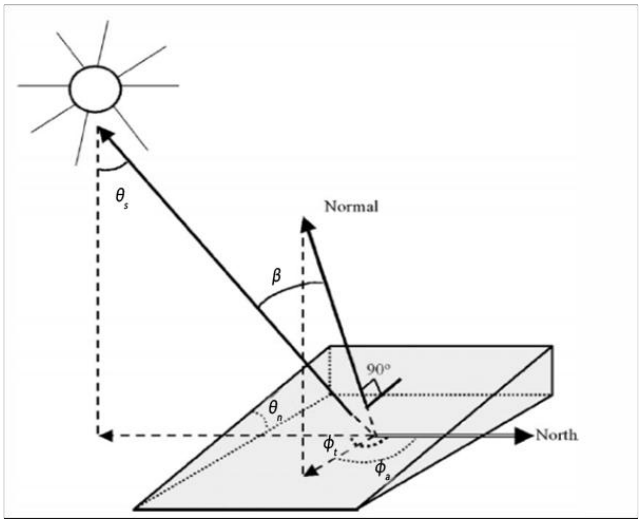

Figure 2.7.: The different angles involved in topographic correction.

The normalized reflectance of a horizontal surface ($\rho_{H,\lambda}$) can be calculated using different topographic corrections. An overview of frequently implemented topographic correction algorithms, their type, references and abbreviations is provided in Table 2.3. Three major types of topographic correction methods have been developed: (1) empirical methods, (2) Lambertian geometrical methods, and (3) non-Lambertian geometrical methods.

Empirical methods assume that induced illumination variations are wavelength-independent (Crippen, 1988). For example, band ratioing removes the differential illumination by dividing the recorded reflectance value of an individual pixel in a specific band by the average of the recorded reflectance values of all bands (Colby, 1991; Ono et al., 2007). The major advantage of empirical topographic correction methods is that the complex illumination geometry is included in the calculations. Empirical methods have shown their efficiency in removing relative over- or under-illumination, but in many applications image artifacts occurred (Ekstrand, 1996; Hantson and Chuvieco, 2011).

Geometrical methods are based on a reconstruction of the incoming radiance, given the incidence angle of the sun and the aspect of the slope (Figure 2.7). A straightforward correction is the cosine correction that assesses the observed reflectance on a horizontal terrain ($\rho_{H,\lambda}$; Equation 2.10)

$$\rho_{h,\lambda} = \rho_{t,\lambda} \frac{\cos\theta_s}{\cos\beta} \tag{2.10}$$

Where $\rho_{t,\lambda}$ is the observed reflectance on an inclined terrain (%,), λ is the wavelength, ϑ_s is the solar zenith angle and β the incident solar angle**.** The incident solar angle β is calculated with the metadata of the image, which will be explained in Chapter 4 (Civco, 1989). The cosine correction is a frequently implemented geometrical correction which assumes Lambertian reflection and includes the direct solar irradiance on the ground (Teillet et al., 1982). In this method, the illumination geometry of each pixel is derived with a co-registered digital elevation model (DEM). A disadvantage of the cosine correction is the ignorance of the diffuse irradiance from the sky and adjacent terrain reflected irradiance (Teillet et al., 1982). Furthermore, the effectiveness of geometric corrections depends on the accuracy and the resolution of the DEM (Conese et al., 1993). The cosine correction also often results in an overcorrection of the brightness since pixels in the shade still receive radiance due to diffuse skylight (Moran et al., 1992; Dengsheng et al., 2008; Soenen et al., 2008; Richter et al., 2009).

Therefore, an improved cosine correction was proposed in which an empirical coefficient C_λ was added to equation 2.10 as follows:

$$\rho_{h,\lambda} = \rho_{t,\lambda} \frac{\cos\theta_s + C_\lambda}{\cos\beta + C_\lambda} \tag{2.11}$$

The coefficient C_λ is dependent on wavelength and on the intensity of diffuse sky irradiance and should be calibrated empirically (Teillet et al., 1982; Meyer et al., 1993).

More advanced topographic correction procedures also include the observation angle of the sensor. In the case of Lambertian reflection in which the incident radiance is reflected homogeneously in the hemisphere, the observation angle is of no importance. However, the majority of the Earth's surface

behaves as a near-perfect diffuse reflector. Minnaert (1941) was the first to propose a solution for this problem by adding an empirical coefficient *k*, describing the reflection type, to a standard cosine resulting in Equation 2.12:

$$\rho_{h,\lambda} = \rho_{t,\lambda} \left(\frac{\cos\theta_s}{\cos\beta}\right)^k \quad (2.12)$$

whereby $k = 1$ in the case of perfect Lambertian reflection and $k > 1$ in the case of semi-diffuse or semi specular reflection.

The Minnaert procedure is attractive from conceptual point of view but, is difficult to implement since it requires an assessment of the *k* value for each pixel. Different ways for computing the *k* value have been developed. A simple way is to use a single global *k* value for an entire image (Colby and Keating, 1998; Garcia-Haro et al., 2001; Mitri and Gitas, 2004; Gitas and Deverux, 2006). This calculation is based on the assumption that the anisotropic nature of reflectance is homogeneous over the study area. However, this assumption is invalid due to topography and land cover variations (Bishop and Colby, 2002). In reality, a global *k* value cannot result in accurate correction for all slopes and aspects due to differences in topographic impacts on the land surface reflectance (Ekstrand, 1996; Bishop and Colby, 2002). A second approach computes individual pixel-based *k* values for each land cover class, based on NDVI values or on a regression analysis between reflectance values and cos *ϐ* (Bishop and Colby, 2002; Bishop et al., 2003; Blesius and Weirich, 2008). Finally, *k* values are derived for each band and different slope groups (Lu et al., 2008). These advanced geometrical corrections account for the non-Lambertian behavior by the implementation of bidirectional reflectance distribution functions (BRDFs; Zhang and Gao, 2009). The major disadvantage of these advanced methods is the requirement of additional parameters that need to be derived from regression analyses, look-up tables or land cover maps (Aspinall, 2002; Hansen et al., 1994; Lu et al., 2008). The requirement to collect these additional input data hampers the inclusion of advanced topographic correction methods in automated processing chains which are necessary in large scale mapping (Rogan and Chen, 2004; Rogan et al.; 2008).

Table 2.3. provides an overview of frequentlyimplemented TC methods that were described in recent literature, ordered chronologically by year of publication. The algorithms were classified in three different groups: (1) empirical (E), (2) geometrical assuming Lambertian reflection (LG), and (3) geometrical assuming non-Lambertian reflection (NLG). The TC methods applied in this PhD thesis are described in detail in Chapter 4.

Table 2.3.: Topographic correction (TC) algorithms, type, reference and explained abbreviation.

Correction	Type	Reference	Abbreviation (explained)
Minnaert	NLG*	Minnaert, 1941; Smith et al., 1980; Bishop and Colby, 2002; Lu et al., 2008;	
Cosine	LG*	Teillet et al., 1982	
C	NLG	Teillet et al., 1982 ; Meyer et al., 1993; Jensen, 1996; Bishop et al., 2003	
Two stage topographic normalization	E*	Civco, 1989	
Band ratios	E	Colby, 1991; Ono et al.,	

		2007	
Minnaert with changing constant and correction based on empirical function	NLG and E	Ekstrand, 1996	
SCS	NLG	Gu and Gillespie, 1998	Sun-canopy-sensor topographic correction
Statistical Approach	LG	Gu et al., 1999	
Band ratio, Minnaert, aspect partitioning and combinations of these corrections	E, NLG, LG and combinations	Hale and Rock, 2003	
C-Huang Wei	NLG	Huang et al., 2008	
PBC and PBM	NLG	Kobayashi and Sanga-Ngoie, 2008	Pixel-based Minnaert and pixel-based C-correction
Empirical line, cosine, C, Minnaert, statistical-empirical, SCS, b, SCS+C and MFM-TOPO	E, LG, NLG, NLG, E, NLG, NLG, NLG and NLG	Soenen et al., 2008	MFM-TOPO is a canopy reflectance model-based TC
Empirical, cosine, C and Minnaert	E, LG, NLG and NLG	Wu et al., 2008	
Cosine, SCS, b and VECA	LG, NLG, NLG and NLG	Gao and Zhang, 2009	VECA is the variable empirical coefficient algorithm
C, modified Minnaert and Gamma	NLG, NLG and NLG	Richter et al., 2009	
Simplified normalization	E	Cuo et al., 2010	
Modified C-correction	NLG	Veraverbeke et al., 2011	
Cosine, C, Minnaert, modified Minnaert and empiric–statistic correction	LG, NLG, NLG, NLG, NLG, and E	Hantson and Chuvieco, 2011	
Cosine, C, smooth C, SCS+C, C-Huang Wei and slope matching	LG, NLG, NLG, NLG, NLG, and E	Singh et al., 2011	
Three-factor+C	NLG	Zhang and Gao, 2011	
Cosine, Minnaert , C, SCS, two stage topo normalization and slope matching	LG, NLG, NLG, NLG, E, and E	Zhang et al., 2011	
C, statistical-empirical and VECA	NLG, E and NLG	Li et al., 2013	
C, improved Cosine, Minnaert, statistical-empirical and VECA	NLG, NLG, NLG, E and NLG,	Szantoi and Simonetti, 2013	
Minnaert	NLG	Crawford et al., 2013	
Empirical rotation model	E	Tan et al., 2013	
C, SCS+C, Minnaert SCS, slope-matching and VECA	NLG, NLG, NLG, E and NLG		

* E is empirical, LG is Lambertian geometrical and NLG is non-Lambertian geometrical.

One may expect that the more advanced topographic correction methods deliver more accurate results. However, including additional parameters also introduces additional uncertainty in the

model calculations through propagation of errors in the input data. Van Rompaey and Govers (2002) showed that the quality of the available input data determined the model complexity and that the most complex models were not necessarily producing the best results due to error propagation. The question whether or not these more advanced topographic correction methods have an added value for the detection and mapping of forest cover dynamics will be addressed in the following chapters.

2.2.5 Combined topographic and atmospheric correction

AC and TC methods are both components of the radiometric correction and are often implemented subsequently in a preprocessing chain. In some cases, the atmospheric and the topographic components of radiometric corrections are interacting. This is for example the case in a *C*-correction (Equation 2.11), whereby an extra coefficient is introduced to describe the diffuse sky irradiance. An independent atmospheric correction preceding a *C*-correction would result in lower *C*-values since part of the diffuse sky-irradiance is already removed. In this study, we refer to this type of models as 'combined methods' which combine an AC and TC method with or without any interaction between both components.

Many radiometric correction methods described in literature are presented as 'integrated', but are no more than a sequential application of independent AC and TC methods. So far, a maximum of five individual atmospheric and/or topographic methods has been combined and compared by Riaño et al. (2003) and Vicente-Serrano et al. (2008). The combination of a specific AC and TC models is often given a model name such as e.g. MODTRAN, ATCOR or LOWTRAN. The major disadvantage of these radiometric correction models with a predefined combination of a specific AC and TC component is the lack of flexibility. For certain applications, other combinations of AC and TC that those offered in existing models may be suited. Moreover, the fixed combination of AC and TC components hinders the interpretation, validation and comparison of results. A certain combined model may perform poor, but it will be impossible for an end user to attribute these results to the AC or TC component of the model. Therefore, in this study, all combined models will be split up in a topographic and an atmospheric component. This has two advantages: (1) evaluation of the performance of each component individually, and (2) creation of many more new combinations of AC and TC methods.

An overview of frequently implemented combined corrections, and their acronyms are provided in Table 2.4, ordered chronologically by year of publication. Many of these models are implemented in remote sensing software and it is up to the user to select an appropriate combined radiometric correction method given the characteristics of the study area, available data, computing time and the goal of the image processing.

Table 2.4.: Combined correction, reference and explained abbreviation.

Combined correction	Reference	Abbreviation (explained)
Inverse technique + band ratios	Conese et al., 1993	
ATCOR2 + DEM [ATCOR3]	Richter, 1997; Richter and Schäpfler, 2002; Richter and Schäpfler, 2011	
6S + DEM	Sandmeier and Itten, 1997	
DOS + Minnaert, C and variation of C	Riaño et al., 2003	
DOS + cosine and SCS	Vincini and Frazzi, 2003	

ATCOR2 + Minnaert	Mitri and Gitas, 2004	
LOWTRAN-7 + Minnaert	Gitas and Devereux, 2006	
MODTRAN + SCS	Huang et al., 2008	
TF + PBC	Kobayashi and Sanga-Ngoie, 2008	
DTA and 6S + cosine and C	Vicente-Serrano et al., 2008	DTA is the dark target approach
MODTRAN-4 + AMARTIS and SIERRA	Lenot et al., 2009	AMARTIS is advanced modeling of atmospheric radiative transfer for inhomogeneous surfaces; SIERRA is spectral reflectance image extraction from radiance with relief and AC
DOS + Minnaert and SCS	Gao and Zhang, 2009	
Parameterized BRDFs	Wen et al., 2009	Bidirectional reflectance distribution function
6S + C-correction	Burns and Nolin, 2014	

2.2.6 Compositing

For large scale studies, an additional compositing step may be required, in which multiple images or footprints are mosaicked or in which pixels are composited (see Figure 2.3). If the study area exceeds one sensor's footprint, it is necessary to mosaic different images. A major challenge in this process is the development of unitemporal, homogeneous and radiometric consistent composites (Hansen and Loveland, 2012). In the hypothetical case of perfect radiometric correction of the footprints, a simple mosaicking of images would be sufficient. In reality, this leads to patched composites with stitch lines clearly visible (Gutman et al., 2008).

In order to address this problem, pixel-based image compositing (PBIC) algorithms have been composed in which 'the most suitable pixel' for each cell in terms of observation time and radiometric disturbance is selected from an image archive. A clouded pixel on one footprint may for example be replaced by an unclouded pixel from a footprint of the year before. Figure 2.8 shows the principle of PBIC with an archive of 3 images. In reality, archives of thousands of images can be used. In the first step, all available images are collected and georeferenced (Figure 2.8a). Next, for each cell, all available pixels in the archive are ranked according to their suitability. Finally, the composite is composed by selecting the best or most suitable pixels for each cell (Figure 2.8b). Each pixel of the composite consists of a single value and not an average value, since pixel and footprint specific metadata (solar zenith angle, solar azimuth angle, etc.) need to be stored for further analysis, e.g. topographic correction.

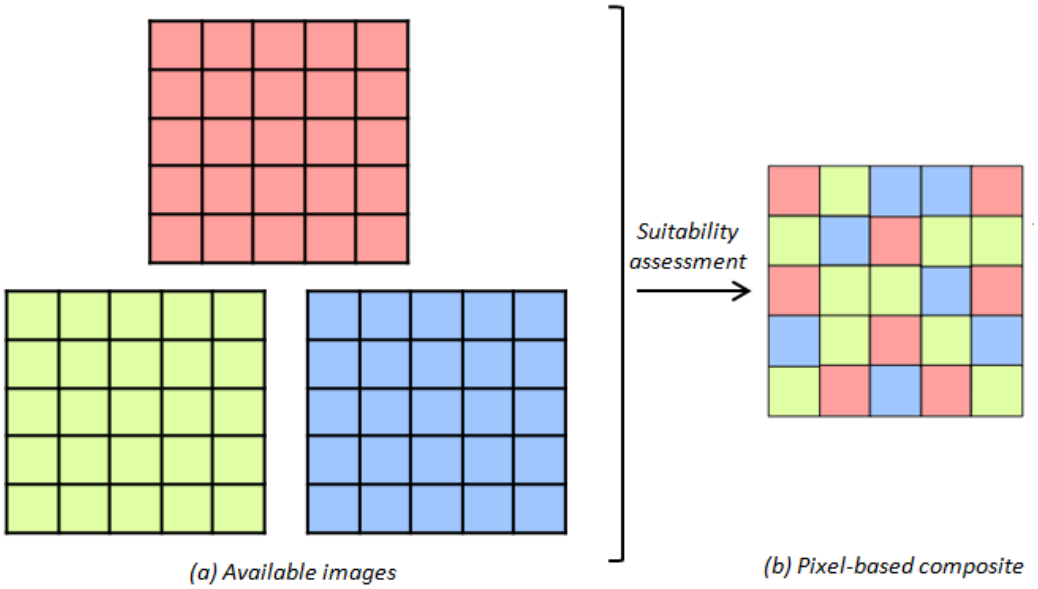

Figure 2.8.: Pixel-based compositing with (a) selection of all available images (in this example there are only 3 images available), and (b) construction of the pixel-based composite with selection of the best pixel for each cell after a suitability assessment.

The conversion from footprint-based mosaicking to pixel-based compositing was initially developed for wide-swath sensor data, which suffered from cloud disturbances (Cihlar et al., 1994; Holben, 1986). PBIC methods can be classified according to different suitability criteria. Initial PBIC methods aimed at developing cloud-free composites and implemented the parameter 'distance from cloud' as a criterion (Hansen et al., 2008; Roy et al., 2010). For example, the South Dakota State University approach works with all available Landsat data based on a cloud cover metadata threshold (Broich et al., 2011; Hansen et al., 2011; Potapov et al., 2011 and 2012). Other PBIC methods were developed for the removal of the missing lines in Landsat-7 imagery (Goward et al., 1999; Arvidson et al., 2001; Arvidson et al., 2006). The Cropland Data Layer product combines the Advanced Wide Field Sensor (AWiFS) and Landsat ETM+ and TM data in characterizing annual crop types (Johnson and Mueller, 2010). Kennedy et al. (2007) developed a change detection algorithm which selects idealized pixels based on the temporal trajectory of spectral values. Furthermore, Huang et al. (2010) developed a similar algorithm for forest cover change mapping. This Vegetation Change Tracker (VCT) is based on the spectral–temporal characteristics of land cover and forest change processes. In 2010, Kennedy et al. (2010) presented the Landsat-based detection of trends in disturbance and recovery (LandTrendr) approach which implements change detection algorithms to perform temporal segmentation and fitting of Landsat time series. This approach was also used in eastern Europe by Griffiths et al. (2013a).

Griffiths et al. (2013b) implemented a PBIC algorithm to produce cloud-free and best observation composites of leaf-on phenology. Suitability of a given pixel was based on a parametric decision function which included: (1) the acquisition year, (2) the acquisition day-of-year, and (3) the pixel's distance to the next cloud/shadow. For each unique acquisition, scores across the parameters were summed up and for a given pixel all spectral band values of the acquisition with the highest total score were written into the final best observation composite (Griffiths et al., 2013b). The most recent worldwide forest change inventory between 2000 and 2012 by Hansen et al. (2013) was also based

on a per-pixel set of cloud-free image observations. The spatially homogeneous pixel-based image composites also offer other advantages: (1) avoidance of artificial partitioning into footprints, (2) observation frequency increase by across track overlap exploitation, (3) reduction of large scale mappingcosts, and (4) improved large area LULCC analyses (Masek et al., 2006). The major drawback is the dependency on storage and computational power as pixels of thousands of images need to be evaluated at the same time.

Pixel-based image compositing clearly offers new possibilities for the large scale analysis of land and forest cover dynamics. The homogeneous image composites can be classified and analyzed in a single operation resulting in consistent land cover (change) maps. It is clear that the image compositing algorithms interact to some extent with the topographic and atmospheric correction methods described above. If in a first step all the images from the archive are preprocessed, different pixels may be selected for the composite as some distorted pixels may become suitable after correction. An alternative procedure would consist of firstly constructing the composite and secondly applying radiometric correction. In this case, the added value of topographic and atmospheric correction would probably be lower since pixels with major disturbances are already removed. The possible interaction between pixel-based compositing and radiometric corrections and their consequences for the accuracy of the resulting maps are not yet examined at present and will be addressed in the following chapters.

Chapter 3: Study areas, forest cover dynamics and their controlling factors in the Carpathians

3.1 Biophysical setting of the Carpathians

The Carpathian mountain range connects eight eastern European countries: from Serbia and Romania in the south through Ukraine, Poland, Hungary, Czech Republic, Slovakia and Austria in the north (Björnsen et al., 2009). Covering an area of ±209,256 km², the Carpathian Mountains are one of Europe's most remarkable natural regions with unique forest ecosystems (Badea et al., 2004; WWF, 2012). Formed during the early Tertiary period, the Carpathians are relatively young mountains with elevations varying from 300 to 2,655 m above sea level (Webster et al., 2001). The mountains are mainly composed of sequences of sandy rocks formed of layers of alternating sandstone and shale. Other parts of the Carpathians are formed of limestone, or, as in the case of the Tatras, magmatic rock such as granite (Webster et al., 2001). The biodiversity of this region is unique in Europe. Due to its function as a refuge in the last ice age, an incredibly high natural diversity of species is present, including many endemic ones (about 12% of the total flora). Overall, this region harbors over one third of all European vascular plant species (Oszlányi et al., 2004). Furthermore, the Carpathians region serves as the last refuge for large predators such as the brown bear (*Ursus arctos*), the wolf (*Canis lupus*) and the lynx (*Lynx lynx*) (Oszlányi et al., 2004). Apart from this enormous diversity, Europe's largest natural mountain beech and conifer mixed forest ecosystems are found here, along with Europe's largest old-growth natural and unmanaged virgin forests. More than half of the mountainous region is covered by natural or planted forest (Webster et al., 2001). The Carpathian forest is an essential corridor for the dispersal of species, since it links the European southern, northern and western forests (Carpathian Ecoregion Initiative, 2001).

Several recent studies describe the major landscape transitions that occurred in eastern Europe (Bicik et al., 2001; Feranec et al., 2000; Kuemmerle, 2006 and 2008a; Van Dessel et al., 2010). The following transition phases can be identified: (1) the communist collectivization process triggered an arable land increase and the disappearance of small fields; (2) the decollectivization after the communist period induced the conversion of less fertile soils into permanent grassland or forests and a more intensive agricultural use of the most suitable soils. The fall of the Iron Curtain brought substantial changes in the region's socio-economic and institutional structures. This triggered widespread land use changes which in turn affected local livelihoods, biodiversity and the provision of ecosystem services.

In order to secure the unique characteristics of the Carpathian Mountians, several areas have been protected over the last decades. In 1999, the Carpathian Ecoregion Initiative (CERI) was formed and aims for better protection and conservation of the area (Carpathian Ecoregion Initiative, 2012). In Figure 3.1, the total Carpathian Ecoregion is delineated in light blue. Detailed biodiversity and socio-economic assessment has been undertaken to provide the basis for a long term biodiversity vision for core areas, complemented by a range of specific local projects aiming at sustainable forms of rural diversification. CERI is innovative since such a large scale long-term approach has never been attempted in the region. It is a unique international partnership with contributions from governments and international donor agencies such as the European Commission, the United

Nations Development Programme and the World Bank (Turnock, 2001). Since the analyses of Chapters 4 to 7 are implemented on two scale levels in the Romanian Carpathians, a regional or large scale and a local or small scale area in the Romanian Carpathians are chosen as study areas. In the next sections, the Romanian forest history, management and protections is described.

Figure 3.1.: The Carpathian Ecoregion in a light blue color, covering part of eight different countries (Carpathian Ecoregion Initiative, 2007).The regional scale study area was explored in three contrasting study sites: Gheorgheni (northern polygon), Brașov (central polygon) and Făgăraș (western polygon).

3.1.1 Forest types and history

Due to the variety of climatic conditions and altitude above sea level, Romania is the most varied country for vegetation and forest growth in temperate Europe (Veen et al., 2010). The conditions vary from the east-mediterranean (Black Sea) till continental climates and from lowland floodplain and coastal sites till high mountains with forest and shrub formations along and above the timberline in the central and southern Carpathians. At the beginning of the Neolithic period (some 8,000 years BC), forests covered ca. 80% of the present day Romanian territory (Biriş et al., 2006). Three historical periods of massive forest cuttings are known: the Dacian Kingdom and its succession (100 BC–105 AD), the Ottoman Empire (thirteenth to nineteenth century), and the Inter-bellum (first half of the twentieth century). By the end of the nineteenth century, only 40% of the country was covered by forests. This means that 50% of the forested area was removed and changed mostly into agricultural land. In 1940, forests were reduced till 28% of the country area. Since that time, the total forest cover remained more or less stable with 27% forest cover present day (Veen et al., 2010).

In 2005, Romanian forests covered a total surface of 6,3 million hectares, representing about 27% of Romania's land area (WWF, 2005). Two third of the forest area was located in the mountain area, 24% in the hilly area and 10% in lowlands. According to forest inventories data of 2010, broadleaved tree species cover 70%, while conifers 30%. The most widespread species are European beech (*Fagus silvatica*, 32%; Figure 3.2a), Norway spruce (*Picea abies*, 23%; Figure 3.2b), oak species (*Quercus*sp., 17%) and silver fir (*Abies alba*, 15%) (Stancioiu and O'Hara, 2006; ASFOR, 2010). Furthermore, also pine (*Pinus sylvestris*), European larch (*Larix decidua*), sycamore maple (*Acer pseudoplatanus*), rowan (*Sorbus aucuparia*), birch (*Betula sp.*) and pioneer species such as willow (*Salix sp.*) occur frequently.

Figure 3.2.: (a) Typical broadleaved European beech stand, and (b) old grown coniferous forest (photos: Iris Deliever, 2012).

After the fall of the communist regime, the wood harvesting and processing sector was fully privatized. Over 650 enterprises are members of the Romanian Forestry Association (ASFOR), a professional organization which represents the forestry and the woodworking industry. ASFOR was founded in 1994 with the mission to promote and protect the general interests of its members on both national and international levels (ASFOR, 2010). Since 2004, ASFOR has been a member of the European Organization of the Sawmill Industry *(*EOS). Skidders, cable cranes, horses and gravitation are the currently used means for harvesting in Romania (NIS Romania, 2013). The development of the forest sector is closely linked to the usage of cable cranes and the building of new forest roads (ASFOR, 2010). Unlike other countries in Central Europe, Romania has a very poorly developed forest road net. The current density of the Romanian forest road net is 6.2 m per ha, as opposed to 18 – 35 m per ha in other European countries (ASFOR, 2010). In 2010, Romania remained the main hardwood lumber producer within the EOS, accounting for 25.3% of the total production (ASFOR, 2010). Along with France which produced 23.7% of the entire EOS volume, Romania covered half of the hardwood lumber production.

3.1.2 Forest management and silvicultural systems

Matthews (1989) and the British Colombia Ministry of Forests (2001) grouped the different silvicultural management systems in even-aged systems (e.g. clear-cut, shelterwood, coppice or patch cut systems) and uneven-aged systems (selection system). The silvicultural regime refers to the system of technical, economic and legal regulations issued by the Central Public Authority (Dumitriu et al., 2003). In Romania, The National Forest Administration Romsilva (NFA) was established in 1990 and manages all state owned forests with 41 County branches. NFA Romsilva performs the State forest inventory and undertakes forest management on private or community owned forests on contractual basis (WWF, 2005). The private and local public administration forests can be managed by:

- Private Forest Districts established by private forest owners or local public administration;
- NFA – County Forest Directorates through their Forest Districts, on a contractual base;
- Individuals with a limitation to specific activities.

The Forest Code of 1996 stipulated the main characteristics of the forest management. Under the Forestry Code of 1996, a forest area was defined as an area larger than 0.25 ha and covered with forest trees (FAO, 1997). Furthermore, the forests should be managed through management plans issued either by private companies or by the Forest Research and Management Planning Institute (FRMPI) and approved by a Technical Committee of the State Authority for Forests (WWF, 2005). The main characteristics of Romanian forest management plans were: management rules in accordance with the forest type and forest site; maintenance of natural composition in forests; use of natural regeneration; maintenance of a high-level rotation age for native forest species; clear-cutting only in pure stands of spruce, pine, acacia, poplar and willow for areas smaller than 3 ha with an absolute exceptional maximum area of 5 ha; a coppice regime is allowed only in poplar and willow forests; natural regeneration or forestation of these areas within a maximum of two years; adequate wood harvesting technical solutions in order to maintain the ecological balance; and an evolution towards multi-use forests (FAO, 1997; WWF, 2005). Law 120/2004 regarding the forestry regime and forest administration rules modified and completed the previous Law 141/1999 (FAO, 1997). This 1999 Law enforced a legal framework for sustainable forest management in both state owned and private forests. The recent Law 120/2004 stipulated that all forest operations should be executed in accordance with the management plans and the implementation is the responsibility of the State Authority for Forests and the National Control Authority through their local bodies (FAO, 1997). However, a lack of resources led to inadequate enforcement, directly influencing illegal logging (WWF, 2005).

According to the Romanian Forest Code of 1996, cleared patches are supposed to be regenerated in two to three years. When regeneration after the second year is insufficient, trees must be planted in order to afforest the area. These species are cultivated in nurseries and planted in the field after three or four years (Figure 3.3a and b). A disadvantage of the reseeded monocultures, often grown by foreign seed, is the resulting poorer habitat diversity. Consequently, these new forest are more vulnerable to natural disasters such as diseases and storms.

Figure 3.3: (a) Norway spruce and other coniferous species nursery, and (b) Norway spruce sapling planted recently on a cleared forest plot in Gheorgheni (photos: Steven Vanonckelen, 2012).

Forest management plans are developed in accordance with sustainable forest management criteria and revised every 10 years (FAO, 1997; Lawrence, 2009). These plans are the basis for all forest management activities, including the annual cutting allowance per surface units and species. Before 1989, management plans were developed only by FRMPI, but starting 12 years ago, there was an

increased number of private companies which produced or revised forest management plans (WWF, 2005). The forest management plans are the basis to establish regional and national inventory of forested areas and wood harvested volumes. Table 3.1 shows the historical annual allowable cut and wood harvest in Romania between 1962 and 2004 (Bud, 2000; Borlea et al., 2004). This data are calculated by cumulating the allowable cut for each forest district of the national forest area (state owned forest and private forest). The data show that the calculation of the annual allowable cut was influenced by the political and economic context. In 1986, the forest management started to be directed as 'close-to-nature forestry' with an interdiction of clear-cuttings on areas larger than 3 ha and only in spruce forests (WWF, 2005).

Table 3.1.: Annual allowable cut and wood harvest in Romania between 1962 and 2004 (in million m^3; Bud, 2000; Borlea et al., 2004)

Year	Annual allowable cut (million m^3)	Annual wood harvest (million m^3)
1962-1975	24	25-27
1976-1980	21	22
1981-1985	21	23
1986-1990	18	18,5
1991	19	15,3
1993	15	13,6
1994	14,5	12,9
1995	14,4	13,8
1996	14,6	14,8
1997	14,8	14,5
1998	15,2	12,6
1999	15,5	13,7
2000	15,8	14,2
2001	17	13,4
2002	17	16,8
2003	16	15
2004	18	17,5

Romanian forests have been generally well-managed over the years so that certification in line with the standards set by the Forest Stewardship Council (FSC) is achieved in certain forest management units, e.g. in the Persani Mountains near Brasov (Turnock, 2001; Ioras et al., 2009; WWF, 2010). Such a better management maintains biodiversity and secures higher prices for the harvested timber. Certification is also relevant since the main demand for Romanian timber is shifting from Arabian and Chinese markets to western Europe which is demanding FSC certified timber (Turnock, 2001).

3.1.3 Forest ownership and restitution

Before 1989, almost the entire Romanian forest area was owned by the state. Starting in 1991, large areas of forest were returned to the former owners, according to three consecutive land restitution laws in 1991, 2000 and 2005 (Abrudan et al., 2009). Law 18/1991 returned up to one hectare to historically entitled private individuals (350,000 ha in total), irrespective of historic location or extend (Vasile and Mantescu, 2009). After the second phase in 2000, the restituted area was restricted to 1 ha. Many owners were uncertain of their property rights, feared to loose their land again in the next restitution phase and as a consequence, more unsustainable logging was observed after this second phase (Olofsson et al., 2011). Most of the restituted forests were immediately cleared by the new

owners and this tendency was further clear-cuttings were stimulated by weakened institutions and increased economic hardship (Mantescu and Vasile, 2009; Knorn et al., 2012a). The law of 2005 favored public owners while constraining the restituted forest area for individuals (10 ha), churches (30 ha), and community members (20 ha; Griffiths et al., 2012). This law stated that all forested areas which were privately owned before World War II should be restituted, including protected forests and resulting in a process which is still going on (Abrudan et al., 2009; Olofsson et al., 2011). Since 2005, the third law aimed at returning all remaining pre-World War II not state-owned forest property. Once complete, up to 70% of Romanian forests will have been restituted, increasing the number of non-state forest owners to 800,000 (Ioras and Abrudan, 2006; Lawrence, 2009; Lawrence and Szabo, 2005). The restitution process led to the current structure of forest ownership as presented below (WWF, 2005):

- 65% of forest area is owned by the Romanian State and managed by the National Forest Administration (NFA);
- 24% of forest area is owned by various entities/institutions, including local public administration and managed by private and public forest districts or contracted under the management of the NFA;
- Individual owners own 11% of the forest area. Part of individual owners is managing the forest by themselves while some of them are gathered in owner associations or other forms of group management. Individuals own areas from less than 1 ha to 10 ha.

3.1.4 Natural and human impact on forests

Extreme events such as windstorms affect the Romanian Carpathian Ecoregion. In February 2006, an intense windstorm affected the area and a small scale hurricane moved across the Romanian Carpathian Ecoregion during the summer of 2009. Small scale wind events occur rather often, affecting small areas of forest by wind-throw (Anfodillo et al., 2008; Keeton and Crow, 2009). Furthermore, extensive salvage logging occurs after wind-throws (Macovei, 2009) (Figure 3.4).

Figure 3.4.: Wind-thrown area with a huge clear-cut afterwards (Gheorgheni; photos: Steven Vanonckelen, 2012).

Pests such as insect infestations have enormous impacts on forest stands. The spruce bark beetle (*Ips typographus*) sickens Norway spruce stands with large scale clear-cutting as a remedy (Keeton and Crow, 2009). The spruce bark beetles nestle just underneath the bark of tree and feed themselves

from the tree saps until eventually the tree dies (Figure 3.5a). In order to kill the insects and to prevent further infestation, beetle traps are placed in the affected areas (Figure 3.6b).

Figure 3.5: (a) Spruce bark beetle pattern on a dead tree trunk, and (b) Beetle trap (Gheorgheni; photos: Iris Deliever, 2012).

Unsustainable and/or illegal logging is a major environmental and economic problem in eastern Europe and increased after the breakdown of socialism (Kuemmerle et al., 2009a). During the study visits in Romania, traces of illegal logging were observed. Figure 3.6a shows a tree stem that was cut with an axe at chest height. The trees were cut at chest height in order to keep an eye on the surroundings and trees were dragged out of the forest by horse power (Figure 3.6b).

Figure 3.6.: Logging by gypsies with (a) tree cut with an axe, and (b) tree harvesting by horse power (Braşov; photo: Iris Deliever, 2012).

In Romania, most footslopes and plateaus are used for arable farming and cattle herding. In many areas, transhumance is still applied by bringing herds of sheep, goat and cows above the tree line for summer grazing. Figure 3.7 shows a herder with cattle that is grazing on the higher mountain parts in Braşov.

Figure 3.7.: Typical scene of transhumance (Braşov; photo: Iris Deliever, 2012).

3.1.5 Virgin forests and forest protection

Virgin forests or old growth forests are forests which have not been influenced directly by man in their development and are the last places where nature survives in its purest state (Brünig and Mayer, 1980; Schuck et al., 1994; Parviainen, 2005). These virgin forests play a key role in maintaining biodiversity and are irreplaceable for sustaining biodiversity (Gibson et al., 2011). Moreover, old-growth forests play an important part in the response to climate change since they continue to sequester carbon for long time periods and store more carbon per unit area than any other ecosystem or forest successional stage (Luyssaert et al., 2008; Knohl et al., 2009; Wirth, 2009; Keeton et al., 2011; Knorn et al., 2012b). Old-growth forests in the Carpathian Mountains store high carbon levels in comparison to younger and managed forests (Holeksa et al., 2009; Keeton et al., 2010). Despite their ecological importance, old-growth forests around the globe are vanishing at an alarming rate mainly due to deforestation, unsustainable logging practices and increases in fire frequency (Achard et al., 2009). Of the total forest area in central Europe, only 0.2% of old-growth forests have survived, mainly in remote mountainous areas or within nature reserves (Frank et al., 2009; Schulze et al., 2009; Knorn et al., 2012b).

Romania's forests represent up to 65% of the virgin forests still remaining in Europe, outside of Russia, 80% of which are still unprotected (WWF, 2012). The area of existing virgin forests in Romania declined dramatically in the last century. The assessed 2 million ha of virgin forests at the end of the nineteenth century and based on forest inventory data was reduced to 700,000 ha and 400,000 ha in respectively 1945 and 1984 (WWF, 2012). Inventories organized by Veen et al. (2010) in Romania found 218,494 ha of remaining virgin forests. Hereby, the identified virgin forests sites were mainly located in the southern part of the mountain region. In the 1990s, virgin forests were protected within the national nature protection policy. Today, most of the remaining old-growth forests are included in the system of protected areas (Biriş and Veen, 2005; Knorn et al., 2012b). These protected forests represent ca. 12.5% of the total Romanian forested area. Moreover, there is a lack of similar and complete inventories of virgin forests in the Romanian Carpathians (Muys et al., 2011). In May 2011, the Parties to the Carpathian Convention approved a protocol to protect Carpathian natural forests (COP3, 2011). Romanian virgin forest sites should all be protected as nature reserves to avoid their commercial exploitation and to allow scientific research (Muys et al., 2011). Surprisingly, Knorn et al. (2012b) concluded that 72% of the old-growth forest disturbances between

2000 and 2010 were found within protected areas. Logging in old-growth forests was partially related to the institutional reforms, insufficient protection and ownership changes since the collapse of communism in 1989. The majority of harvesting activities in old-growth forest areas were in accordance with the law. However, the future of Romania's old-growth forests and the provided ecosystem services remains uncertain without improvements to their governance.

The first official forest protection measure was taken in the fourteenth century, by means of the 'Carti de paduri oprite' (Letters of forbidden forests; Veen et al., 2010). The letter mentions 'branişti,' which means forests in which nobody had the right to cut trees, mow hay or graze cattle; also hunting, fishing or picking fruits was forbidden. These areas may be seen as the first precursors of later forest reserves. Regular forest protection started first in the Banat region in the eighteenth century (1739). In Transylvania, a law on forest use was published in 1781. Similar regulations followed later in other parts of the country (Bucovina in 1786; Moldavia in 1792; Wallachia in 1793). In the nineteenth century, however, the Treaty of Adrianople (1829) had a new, strongly negative impact on lowland forests. Between 1856 and 1890, about 3 million hectares of remaining forests were changed into arable land to cultivate cereals. In the Inter-bellum period, the forest area was further reduced by 1.3 million hectares (Veen et al., 2010). In the 1930s, under the influence of the modern Central European forestry ideas, the old practice of unscrupulous forest exploitation was stopped. Further reduction of the forested area was forbidden and forestry planning was introduced. Within this development, one of the most important tasks of leading foresters of that time was the exploitation of virgin forests and introduction of organized forestry.

The nature conservation activity throughout the last 80 years can be divided into three periods (Biriş et al., 2006):

- Before 1944: the establishment of Retezat National Park (1935, about 10,000 ha of which 7,500 ha is forest) and 55 small-protected areas (about 5,515 ha) of which 30 are Protected Forest Areas (PFA; approximately 4,352 ha).
- Between 1944 and 1989: the Retezat National Park is extended to about 22,500 ha (20,000 ha in the forest fund), with a strict protected area of 9,600 ha. The number of small-protected areas increased to 75 with a total surface area of 64,196 ha, 40 of these areas are located in the forest fund with an area of 21,702 ha.
- After 1990: the number of large protected areas increased to 13 in 1994 with an area of 397,000 ha and to 17 in 2000. The number of small-protected areas located outside of the large areas increased to 693, covering ±102,000 ha. The 17 large protected areas consist of:
  - 11 national parks with a total area of 300,544 ha (221,263 ha is forest), having 49 strict protected areas (60,119 ha) of which 46 are PFA (52,977 ha);
  - 5 natural parks with a total area of 251,632 ha (181,000 ha of forests), having 74 strict protected areas (17,866 ha) of which 65 are PFA (11,108 ha);
  - 1 Biosphere Reserve with a total area of 580,000 ha (17,539 ha of forest), having 19 strict protected areas (52,160 ha) of which 3 are PFA (5,125 ha).

Today, about 20% of Romanian territory and about 10% of the country's forests are under some form of protection (Ioja et al., 2010). The national network of protected areasis organized in accordance with the first five categories of the International Union for Conservation of Nature (IUCN): scientific reserve, national park, natural monument, nature reserve and natural park (Oszlanyi et al., 2004;

Biriş et al., 2006; IUCN, 2008). Besides the categories of protected areas included in the national network of protected areas, Romania recognizes the categories of protection stipulated through international or EU legislation (Diaci et al., 1998; Biriş et al., 2006):

- Biosphere Reserves;
- Ramsar Sites – Wetlands of International Importance;
- World Heritage Natural Sites;
- Natura 2000. In order to fulfill the accession criteria imposed by the EU, the Romanian state was obliged to create or adjust different laws that had a major impact on the land regulation and the forest protection policy. The global EU nature conservation strategy was implemented in the Birds and Habitats Directives of respectively 1979 and 1992.These Directives are the legal framework of the Natura 2000 network, which influences sustainable development, forest management and forest protection. Romania accessed the EU in 2007 and participated since 2001 in the Natura 2000 network (Natura 2000, 2012). The Natura 2000 network includes two different protection zones: Special Protection Areas (SPAs) and Areas of Special Conservation Interest (SCIs). The Birds Directive requires SPAs and the Habitats Directive requests the establishment of SCIs for species other than birds and also habitats on itself. In the Romanian SPAs, 105 birds species were identified, comprising 70% of the Romanian ornitofauna (Timisescu, 2009). The Romanian SCI zones consist of 6 forest habitats, 4 natural and semi-natural grassland formations and 2 other types of habitats (freshwater habitats and running water). In total, 34,830 km^2 or 18% of Romania is covered by these two protection zones (Matei, 2011). Implementing the Natura 2000 network in Romania is rather difficult due to the lack of trained experts, data availability and/or their chaotic dispersion. At the governmental level difficulties consist of budget constraints, human resources limitations and insufficient experience concerning protected areas management and monitoring requirements. Difficulties at the local and county level include limited integration of environmental issues, less importance given to biodiversity and interests focused mainly on economic development (Biriş et al., 2006).

While the recent increase in protected areas is a milestone for biodiversity conservation in Romania, considerable concerns about the status of nature protection remain: protected areas are sometimes subject to illegal logging and poaching, and many protected areas lack professional management, financing, and scientific support (Soran et al., 2000; Ioja et al., 2010; Knorn et al., 2012a).

3.2 Landscape changes in Romania

In post-war eastern Europe, a state-organized collective farming system was installed. Following the example of the Soviet Union, individual fields were merged in order to create fields with a size and shape that enabled mass production technologies (Van Dessel, 2010). When the communist system collapsed in December 1989, drastic socio-economic and political changes occurred with a transition from state-commanded to market-driven economies (Kuemmerle et al., 2007). Former collective agricultural entities were divided to return the land units to the former and legitimate landowners. However, many new landowners were living in cities and no longer interested in cultivating arable lands on the countryside. Consequently, fragmented marginal fields were abandoned and changed to grassland and forest (Kuemmerle et al., 2006 and 2008a). In Romania, several natural and

anthropogenic factors have influenced the forest cover changes. Land reforms affected large areas of forest land that altered from state-owned to private ownership.

3.2.1 Forest dynamics

Remote sensing data are implemented as an independent information source to monitor vegetation. The land cover pattern in central and eastern Europe is the result of different periods of intensive land cover change due to a succession of different stages in economic and political situation (Lowicki, 2008; Van Dessel, 2010). Generally, there was an overall trend of a more stable forest cover in Romania since the 1970s (Bennet, 2000). Based on the annual FAO land resource questionnaires, national Romanian forest statistics for 1990, 2000, 2005 and 2010 were presented in Figure 3.8 (FAO, 2010; FAOSTATS, 2013a; Worldbank 2013). The total forest area was respectively 6,371,000 ha in 1990 and 6,573,000 ha in 2010. Between 1990 and 2000, the forested area declined slightly with ±5,000 ha. After a minor forest increase of ±25,000 ha between 2000 and 2005, there was a major forest increase of 200,000 ha between 2005 and 2011 (Figure 3.8).

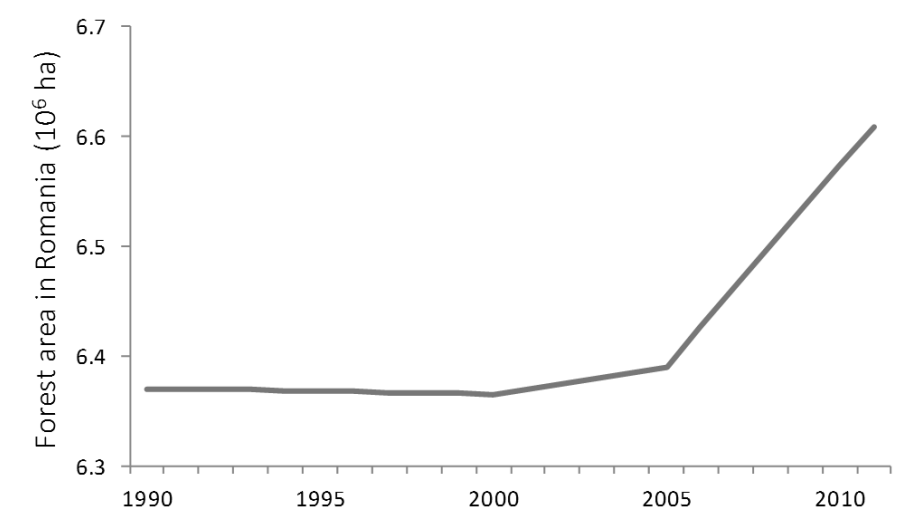

Figure 3.8.: Romanian forest area between 1990 and 2011 in ha (own processing, data: FAO, 2010; FAOSTATS, 2013a; Worldbank, 2013).

Non-protected as well as protected forest areas changed of owner during three restitution phases in 1991, 2000 and 2005 (Abrudan et al., 2009; Knorn et al., 2012a). As stated above, many owners were uncertain of their property rights after the second phase in 2000, and feared to loose their land again in the next restitution phase. As a consequence, more unsustainable logging was observed after this second phase (Olofsson et al., 2011). Most of the restituted forests were immediately cleared by the new owners and this tendency was further clear-cuttings were stimulated by weakened institutions and increased economic hardship (Mantescu and Vasile, 2009; Knorn et al., 2012a). A study by Griffiths et al. (2013a) investigated the influence of three restitution laws on Romanian forest cover in a Landsat footprint between 1984 and 2000. The forest disturbance was highest after implementation of the three restitution laws. The laws of 1991, 2000 and 2005 resulted in forest disturbance levels of respectively 34%, 21% and 32%. After law implementation, forest harvesting increased due to a low Gross Domestic Product (GDP), weak implementation and insecurity of the

property laws. The disturbance was higher in areas of private ownership (Griffiths et al., 2013a). The main reason for natural disturbances were wind-throw and bark beetle attacks (Anfodillo et al., 2008).

A national scale study on deforestation and forest degradation between 2000 and 2011 was conducted by Greenpeace (2012). The analysis was based on freely available Landsat TM and ETM+ images, and HR satellite images from Google Earth. The total forest area of Romania in 2000 was 8,171,399 ha. This number is an overestimation compared to the total forest area of FAO (2010). Total area of deforestation and forest degradation between 2000-2011 was 280,108 ha (approximately 28,000 ha per year). This means that 3.4% of Romania forest cover was lost or degraded in the recent 10 years (Greenpeace, 2012). However, the afforestation area was not calculated and forest was defined as 20% or greater canopy cover for trees of 5 m or more in height. Another national scale study estimated land cover changes between 1990 and 2006 using CORINE Land Cover products, based on satellite images from three different years: 1990, 2000 and 2006. Two major land cover-change types were considered: from forest to other land cover (i.e. deforestation) and from a different land cover to forest (i.e. afforestation). Using the CORINE model, 2,871 ha was affected by afforestation between 1990 and 2006, while 3,267 ha was deforested. So based on the CORINE maps, the Romanian landscape experienced an increased forest cover between this period. However, since the average size of forest properties was small, land cover changes in Romania occurred often on small areas. Most of these areas could not be quantified in the model, leading to an underestimation (Dutca and Abrudan, 2010).

Similar trends were presented by studies in smaller Romanian study areas. A local scale study by Kuemmerle et al. (2008a) analyzed land cover changes using Landsat TM/ETM+ images between 1990 and 2005 in the Romanian Argeş County (6,824 km^2). The results revealed that there was almost no change in forest cover between 1990 and 2005. Cropland on the other hand showed an abandonment rate of 21.1% (512 km^2; Kuemmerle et al., 2008a). Furthermore, no large scale logging was observed. Müller et al. (2009) also examined cropland abandonment in Argeş county between 1990 and 2005. A major cropland abandonment was recorded in the hilly areas, which might trigger natural reforestation. In contrast, less farmland abandonment was discovered in the plain areas. A recent study by Müller et al. (2013) examined cropland abandonment in Argeş County during the post-socialist transitional period from 1990 to 2005. This time period following the collapse of socialism was dominated by extensive cropland abandonment in areas where agricultural production was no longer profitable. Gradual changes were observed in later stages of the transition period. Overall, 28% of all cropland was abandoned in Romania between 1990 and 2005 (Müller et al., 2013).

As explained in section 3.1.6, the Romanian nature is protected by a national and international network of protected areas**.** However, after the fall of the communist regime, the protected areas were neglected due to weakened institutions (Soran et al., 2000). Knorn et al. (2012b) detected old-growth forest disturbances between 2000 and 2010 near the border of Ukraine and in the northwestern part of the Romanian Carpathian Ecoregion. Furthermore, Knorn et al. (2012b) reported a continued loss of old-growth forests in the Romanian Carpathians despite an increasing protected area network. About 72% of the old-growth forest disturbances was found within protected areas and was partly related to institutional land reforms, insufficient protection and ownership changes since the collapse of communism in 1989 (Knorn et al., 2012b). Knorn et al.

(2012a) also assessed disturbance patterns between 1987 and 2009 in the northern Romanian Carpathians. Forest disturbance rates increased sharply in two waves after 1995 and 2005. Substantial disturbances were detected in protected areas and even within core reserve areas (Knorn et al., 2012a). Moreover, logging rates were largely triggered by rapid ownership and institutional changes. Corruption and lack of transparency was also a major problem, leading to cases where sanitary or salvage logging has been misused to harvest healthy forest stands (Brandlmaier and Hirschberger, 2005; Knorn et al., 2012a). Finally, a study of Ioja et al. (2010) reported an overall decrease in the efficacy of Romania's protected areas following the creation of the Natura 2000 sites. Administrative bodies were generally under-staffed and poorly financed, conditions that were reflected in a poor enforcement and implementation of conservation goals (Ioja et al., 2010).

Forest ecosystems were also affected by pollution over the past decades. Rapid industrialization after World War II induced increasing environmental pollution, resulting in widespread deterioration of forest health. After the communist era, these polluting industries were halted and emissions were reduced drastically. By comparing emission between 1990 and 2010, CO_2 emission was predicted to drop by 10%, SO_2 by 68%, NO_x by 42%, and particulate matter (< 10 µm) by 67% (Van Vuuren et al., 2006). Hostert et al. (2010) concluded that the socialist history of eastern European countries has caused a totally different abandonment process than that of western Europe. In the post-socialist countries, land abandonment and additionally forest transition was a result of rapid institutional and economic changes. Whereas in the western European countries, the process resulted from slow socio-economic transformations such as industrialisation.

3.2.2 Arable land dynamics

Starting from 1989, a sharp decline occurred in the arable land percentage in Romania (Figure 3.9; FAOSTATS, 2013a; Worldbank 2013). Hereby, arable land was defined as the land under temporary agricultural crops (multiple-cropped areas were counted only once). The abandoned land resulting from shifting cultivation was not included in this category (FAOSTATS, 2013b). In contrast, the adherence to the EU in 2007 and the implementation of the EU-regulations in environmental and agricultural policies stimulated the agriculture in Romania (Van Dessel, 2008). The production was intensified by increasing expenditure and expanding cultivated land, as shown in Figure 3.9. Smaller and less efficient farms with an unfavourable location for a function change failed to keep up with the competition and were left fallow or were afforested (Lowicki, 2008).

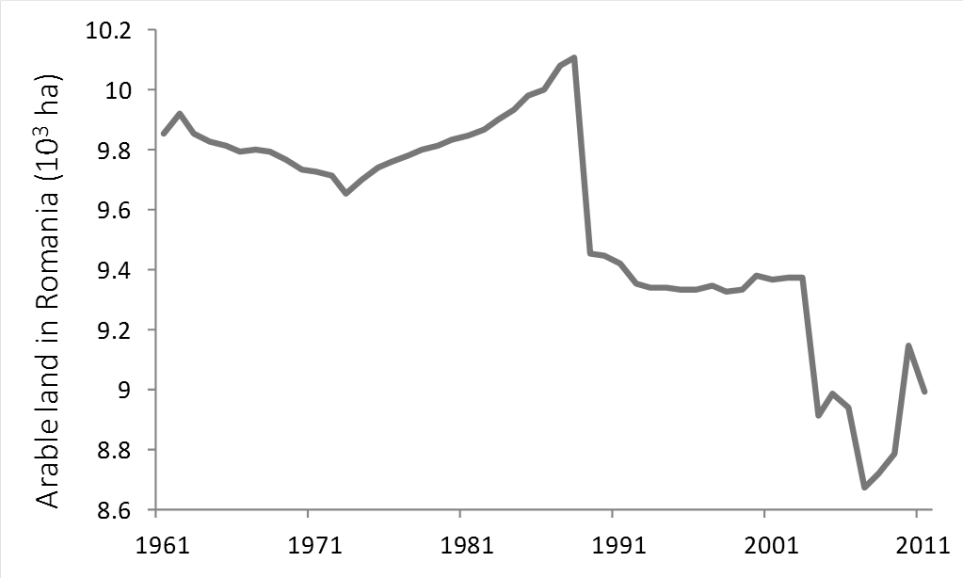

Figure 3.9.: Arable land in Romania between 1961 and 2012 in ha (own processing, data: FAOSTATS, 2013a; Worldbank 2013).

A study by Griffiths et al. (2013c) covering the entire Carpathian Mountains compared cropland abandonment, grassland conversion, afforestation and forest expansion in different countries. Generally, agricultural abandonment was the largest change process between 1985 and 2010. For example, more than 67% of all cropland-grassland-cropland conversions was mapped in Romania. Furthermore, grassland conversion persisted during 1995-2010 in western Romania. Finally, the most extensive afforestation in the total Carpathian Ecoregion during the EU accession period occurred in Romania (28%) (Griffiths et al., 2013c).

3.3 Study areas

3.3.1 Regional scale study area

The regional scale study area of this PhD research is situated in the Romanian Carpathian Ecoregion, which constitute more than half of the total Carpathian region (52.9%; Oszlányi et al., 2004). About 60% of the forest cover in the Carpathian mountain range is located in Romania (Webster et al., 2001). During field campaigns in May 2010 and July 2011, the regional scale study area was explored in three contrasting Romanian study sites. The main characteristics of the test sites are summarized in Table 3.2. The first site is located around the town Gheorgheni in the northern part of the Romanian Carpathian Ecoregion and is indicated as the most northern polygon in Figure 3.1. In this study site, arable land has been partially abandoned. The second study site is located in the forested area south of the town Brașov (central polygon in Figure 3.1). The last study site is part of the Făgăraș mountains on the southern ridge of the Romanian Carpathian Ecoregion (most western polygon in Figure 3.1). This study site is part of a protected Natura 2000 area and is located at the intersection between the counties Brașov, Sibiu and Argeș.

Table 3.2.: Characteristics of the three test sites on the regional scale study area.

	Study site 1	**Study site 2**	**Study site 3**
Name	Gheorgheni	Brașov	Făgăraș
Average elevation (m)	1,100	820	680
Dominant land cover type	Forest and arable land	Forest and urban	Forest, grassland and bare soil
Dominant forest type	Coniferous	Broadleaved	Broadleaved and coniferous
Influence of nearby city	No	Yes (ski slopes)	No
Protected	No	No	Yes (Natura 2000)

In Figure 3.10, the Carpathian Ecoregion is delineated by an irregular and green polygon. The Romanian part of the Ecoregion is covered by nine Landsat footprints. The regional scale study area comprises ±107,000 km² (Figure 3.10) and consists of a mountainous terrain with elevations up to 2,544 m and a temperate-continental climate. The growing season is between April and October, and varies in response to annual rainfall and elevation (Rotzer and Chmielewski, 2001). Both temperature and precipitation are highly inversely correlated with elevation. This mountain area is characterized by a mean annual temperature of ±7°C and a mean annual rainfall ranging between 750 and 1,400 mm (Mihai et al., 2007; Müller et al., 2009). Warm summers alternate with cold winters and high precipitation rates, mostly as snow (Stancioiu and O'Hara, 2006). In summer, showers and thunderstorms occur frequently, reaching peak intensity in June (Perzanowski and Jerzy, 2001). The bedrock in this area consists of crystalline schist, sedimentary rock deposits as limestone and volcanic layers (Griffiths et al., 2013a). Major soils include *Podzols* in the mountain zone and *Cambisols* in the foothill zone (FAO/UNESCO, 1988).

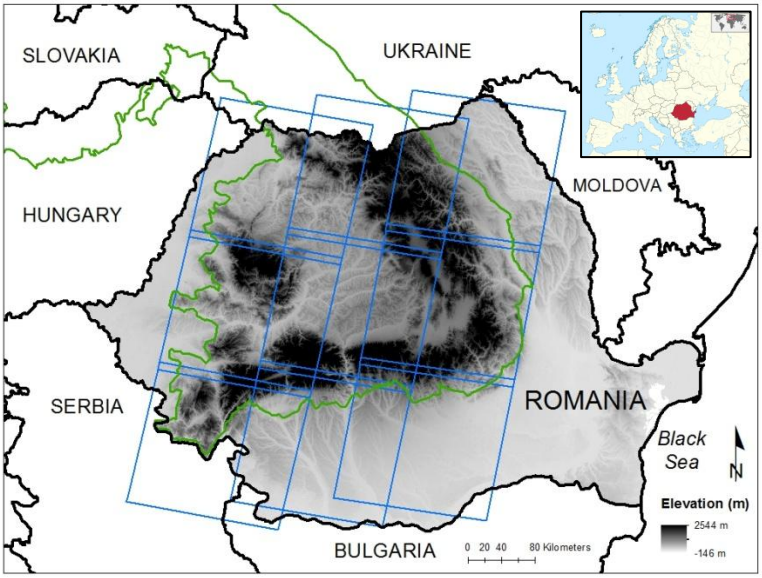

Figure 3.10.: Location of Romania in Europe and indication of the Carpathian Ecoregion (irregular and green polygon) and the nine Landsat footprints comprising the Romanian Carpathian Ecoregion (blue rectangles). Also the elevation data from the Shuttle Radar Topography Mission elevation data are shown in Romania.

In the regional scale study area, several forest clearings (Figure 3.12a and b) and specially even-aged silvicultural systems were observed: the alternate strip clearcutting system and the patch cut system. In the alternate strip clearcut system (Figure 3.12a and b), a stand is harvested over a period of three to seven years by removing several strips rather than harvesting the entire stand at once (British

Colombia Ministry of Forests, 2001). Strip clearcutting was developed to take advantage of natural seeding from the leave-strips. The patch cut system (Figure 3.13a and b) involves removal of an entire stand of trees less than one hectare in size from an area and each patch is managed as a distinct even-aged opening (British Colombia Ministry of Forests, 2001). Both management strategies allow natural regeneration in the cleared patches - which normally takes about 7 to 9 years - before the surrounding mature forest is cut (Matthews, 1989).

Figure 3.11.: (a) and (b) Examples of forest clearings in Gheorgheni(photos: Steven Vanonckelen, 2012).

Figure 3.12.: (a) Alternate strip clearcutting system (Google Earth, 2011), and (b) View in a cleared forest stripe clearcut (Gheorgheni; photos: Iris Deliever, 2012).

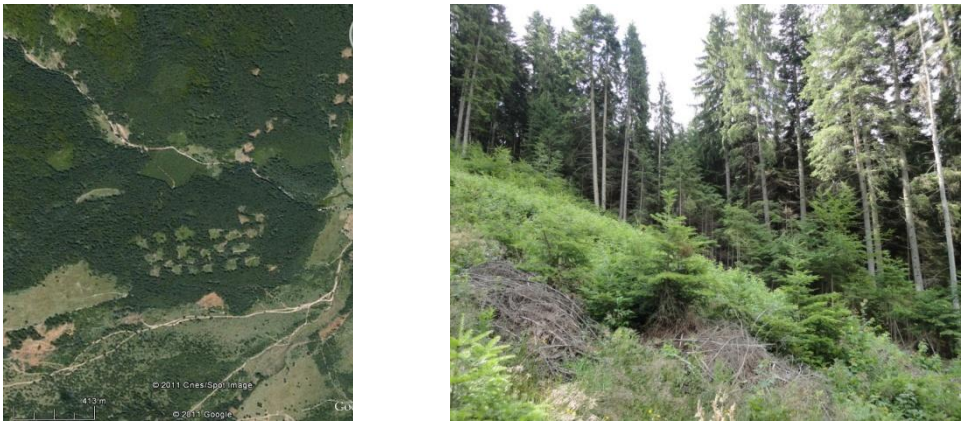

Figure 3.13.: (a) Patch cut system (Google Earth, 2011), and (b) View in a cleared forest patch (Gheorgheni; photos: Iris Deliever, 2012).

3.3.2 Local scale study area

The local scale study area consists of a Landsat-5 Thematic Mapper image (path 183/row 28) located in the central-eastern Romanian Carpathian Ecoregion (Figure 3.14). The study area covers 185 x 185 km and elevation ranges between 53 and 2,545 m with a mean elevation of 570 m. The total population in the study area is estimated at 2,667,000 people of which 277,000 live in Braşov and 175,500 in Bacau (NIS Romania, 2013).

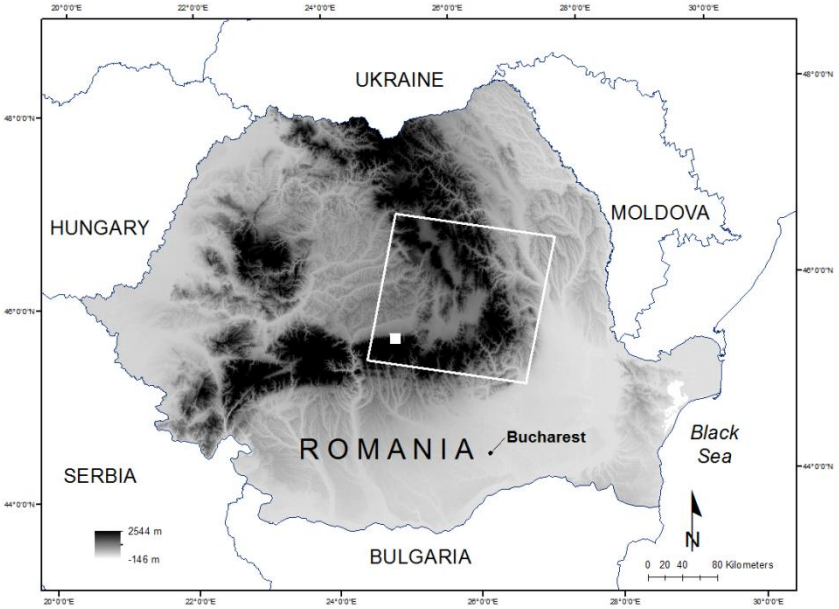

Figure 3.14.: Romania with indication of the bordering countries. The white-outlined rectangle delineates the local study area of Chapter 4 and 5, the solid white rectangle a zoom in the study area. Also the elevation data from the Shuttle Radar Topography Mission elevation data are shown in Romania.

PART 2: Atmospheric and topographic correction

Chapter 4: Performance of atmospheric and topographic correction methods on Landsat imagery in mountain areas*

*This chapter is accepted as: Vanonckelen′ S., Lhermitte, S., Balthazar, V., Van Rompaey, A.Performance of atmospheric and topographic correction methods on Landsat imagery in mountain areas. International Journal of Remote Sensing.

4.1 Introduction

Worldwide, mountain areas are experiencing rapid land cover changes that affect a set of ecosystem services, such as soil and water conservation, biodiversity preservation and carbon sequestration (DeFries et al., 2004; Foley et al., 2005; Lambin and Meyfroidt, 2010; World Health Organization, 2005). Not surprisingly, increasing efforts are invested in land cover monitoring and mapping of mountain areas. The relative inaccessibility of mountain areas favors remote sensing techniques as a monitoring tool (Lambin and Geist, 2006; Turner et al., 2007). Implementation of remote sensing tools is, however, often hampered by problems originating from atmospheric and topographic distortions (Singh et al., 2011). Therefore, preprocessing techniques are an essential step to improve interpretation of satellite imagery.

As stated In Chapter 2, atmospheric correction (AC) methods aim at removing radiometric distortions caused by the interaction between radiance and atmosphere. AC methods can be divided in two major types: empirical and radiative transfer modelling methods (Gao et al., 2009). Topographic correction (TC) aims at removing radiometric distortions by deriving the radiance that would be observed in flat terrain. A list of topographic correction methods is shown in Table 2.3. As explained in Chapter 2, three major types of topographic correction methods have been developed: empirical, Lambertian geometrical andnon-Lambertian geometrical methods.

During the past 30 years, AC and TC methods have mainly been evaluated individually, which is shown in Table 2.4. However, a maximum of five individual AC and/or TC methods has been tested (Table 2.4). In principle, many more 'new' combined models can be built with individual atmospheric and topographic methods. Appropriate combined corrections are selected according to the study area, available data, research goals and implementation time. In order to select the most appropriate preprocessing steps, the performance of combined corrections should be evaluated based on different individual AC and TC components.

The added value of this study is the decomposition of combined models in an AC and a TC component, and the evaluation of their combined corrections. Most studies to date lack a thorough comparison between different AC and TC methods. This chapter systematically evaluates the effects of all possible combinations of two AC and four TC methods, along with uncorrected imagery. Thereby, a variety of representative methods – 2 atmospheric and 4 topographic correction methods - is selected based on their data input requirement and automation complexity. This selected correction methods are automated in the ENVI/IDL software. Since ATCOR3 is a popular combined model, the evaluation of this combined model is also included in the analyses.

4.2 Study Area and Dataset

The study area consists of a Landsat-5 Thematic Mapper image (path 183/row 28) located in the central-eastern Carpathian mountains in Romania (Figure 4.1). The study area covers 185 x 185 km and comprises parts of the eastern Carpathian mountains and the Transylvanian Plateau. Elevation ranges between 53 and 2,545 m with a mean elevation of 570 m.

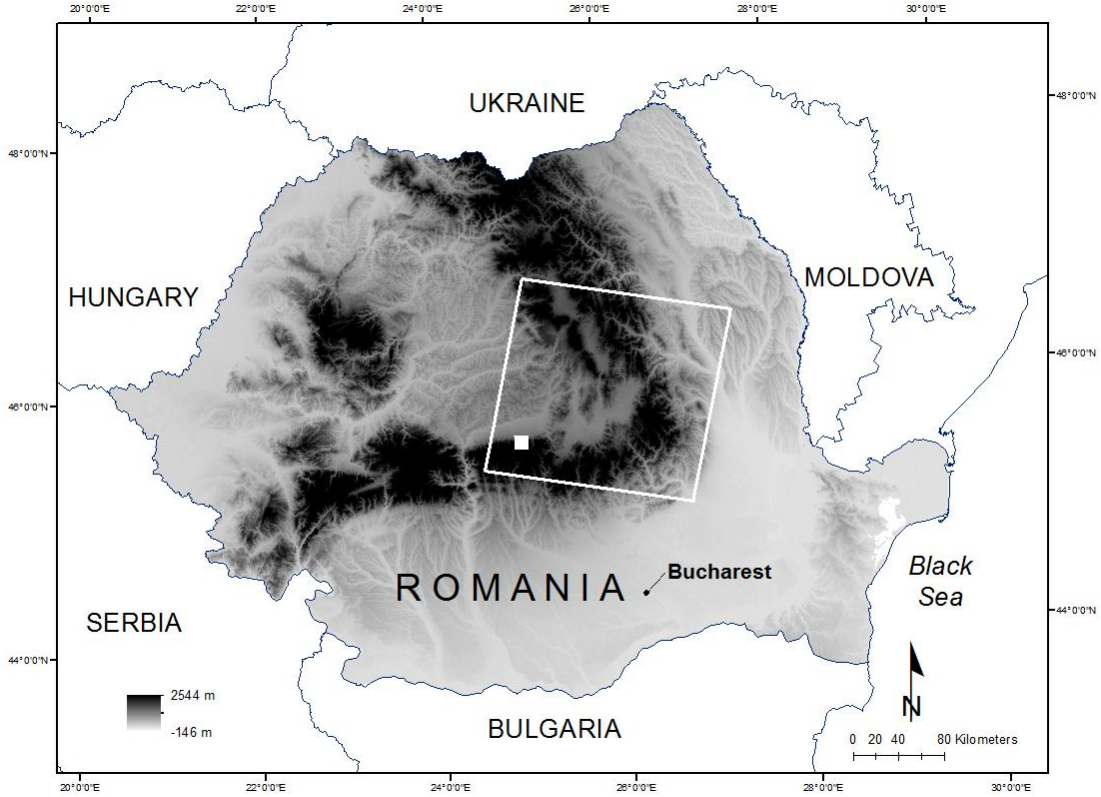

Figure 4.1.:Romania with indication of the bordering countries. The white-outlined rectangle delineates the local study area of Chapter 4 and 5, the solid white rectangle a zoom in the study area. Also the elevation data from the Shuttle Radar Topography Mission elevation data are shown in Romania (Vanonckelen et al., accepted).

The elevation ranges in study area are between 53 and 2,545 m with a mean elevation of 570 m. The area is characterized by a temperate mountain climate with an average yearly rainfall volume of about 635 mm and a mean annual temperature of about 11°C in the centre of the study area. The ridges of the eastern Carpathians consist of crystalline schist, sedimentary and volcanic rock. The steep hillslopes are covered with mixed forests consisting of coniferous (e.g. *Abies alba* and *Picea abies*) and broadleaved trees (e.g. *Betula pendula, Carpinus betulus* and *Fagus sylvatica*) (Kuemmerle et al., 2008a). Footslopes and plateaus are used for farming and cattle herding. Total population in the study area is estimated at 2,667,000 people, of which 277,000 live in Braşov and 175,500 in Bacau (NIS Romania, 2013). The majority of the population earns an income from farming.

The Landsat sensor was used in Chapters 4 to 7 since long-term vegetation mapping is best achievable with medium to low resolution imagery. The Landsat sensor has multiple advantages: a 16-day repeat cycle (NASA, 2013b), an extended operation time (USGS, 2013b), revised calibration and the entire image archive is freely downloadable (Chander et al., 2010; Loveland and Dwyer,

2012). In this study, a Landsat-5 image was selected since the Landsat archive is freely available (Loveland and Dwyer, 2012), Landsat images have been calibrated (Chander et al., 2010) and the spatial resolution is 30m. The Landsat-5 image from 24 July 2009 was obtained from the archive of the United States Geological Survey and covers 185 x 185 km. In this analysis, all corrections were performed on six non-thermal bands: three visible bands (0.45–0.52 µm, 0.52–0.60 µm and 0.63–0.69 µm) and three infrared bands (0.76–0.90 µm, 1.55–1.75 µm and 2.08–2.35 µm). The image was orthorectified with precision terrain correction level L1T by the United States Geological Survey and no cloud masking was performed, since cloud coverage in the study area was below 1%. The solar elevation and azimuth angles were 57.8° and 136.9°, respectively. The digital elevation model (DEM) was the space shuttle radar topography mission (SRTM) version 4.1 from CGIAR-CSI/NASA (2013), which was co-registered with the Landsat image using automatic tie matching and considering both Landsat displacement and acquisition geometry (RMSE < 0.5pixels; Leica Geosystems, 2006). The SRTM was preferred since it provided a high-quality DEM at resolution levels of 1 arc sec (30 x 30 m) in the US or 3 arc sec (90 x 90 m) worldwide (Rabus et al., 2003). Though the ASTER GDEM from the METI/NASA is characterized by a worldwide 1 arc sec resolution, several analyses have indicated that the ASTER GDEM was more subject to artifacts such as stripes or cloud anomalies (Hirt et al., 2010; Van Ede, 2004). Therefore, the SRTM was resampled to a pixel size of 30 x 30 m by means of a bicubic spline interpolation to match the resolution of the Landsat image.

4.3 Methodology

First, digital numbers (DN) of each spectral band were calibrated to at-satellite radiances ($L_{as,\lambda}$) based on gain and offset values included in the metadata and as described in Equation 2.8. A cloud masking was not applied in the analyses of Chapter 4 and 5, since cloud coverage in all images of the study area was below 1%. Secondly, the calibrated radiance values were atmospherically corrected by means of different atmospheric correction methods which are described in section 4.3.1. After atmospheric correction, the at-satellite radianceswere converted to at-surface reflectances with Equation 2.9. According to the Landsat 5 sensor values of Chander et al. (2009), the mean exo-atmospheric solar irradiance per band was respectively: 1,983, 1,796, 1,536, 1,031, 220, 83 W/(m^2 µm). In a final step, the normalized reflectance of a horizontal surface ($\rho_{H,\lambda}$) was calculated using different topographic correctionmethods as described in section 4.3.2.

4.3.1 Atmospheric corrections

In this chapter, an empirical AC, an AC based on radiative transfer models and no correction were compared on one Landsat footprint. Table 4.1 provides the implemented equations of the AC methods. The implemented empirical AC method is the DOS correction, which assumes that observed radiances from dark objects are a good assessment of atmospheric scattering (path radiance). Thereby, a uniform atmosphere across the image is assumed and DOS only considers the effect of atmospheric scattering (Bruce and Hilbert, 2004). The at-satellite radiance was computed by subtracting a minimum radiance value (L_{min}, in W/(m^2 µm)) from each pixel value, as shown in Equation 4.2 of Table 4.1 (Song et al., 2001). The minimum value was calculated for each band as the 1^{th} percentile radiance value over the entire image and accounts for the atmospheric effect (Chavez, 1996).

Table 4.1.: Equations and references of the two applied atmospheric corrections (Vanonckelen et al., accepted).

AC	Equation		Reference
DOS	$L_{s,\lambda} = L_{as,\lambda} - L_{min}$	(4.2)	Chavez, 1996
TF	$L_{s,\lambda} = \frac{L_{as,\lambda} - L_{min}}{0.5(1+T_{r,\lambda})T_{r,\lambda}T_{w,\lambda}^2}$	(4.3)	Kobayashi and Sanga-Ngoie, 2008
	$T_{r,\lambda} = \exp\left[-\frac{P}{P_0}M\frac{1}{115.6406\lambda^4 - 1.335\lambda^2}\right]$	(4.4)	
	$M = \frac{1}{\cos\theta_s + 0.15(93.885-\theta_s)^{-1.253}}$	(4.5)	
	$T_{w,\lambda} = \exp\left[-\frac{0.2385a_wWM}{(1+20.07a_wWM)^{0.45}}\right]$	(4.6)	

Note: DOS is the dark object subtraction method and TF is the atmospheric correction based on transmittance functions. $L_{s,\lambda}$(in W/(m^2 μm)) is the atmospherically corrected at-satellite radiance of the image and $L_{as,\lambda}$ is the atmospherically uncorrected radiance of the image. L_{min} represents the minimum radiance value of the image, calculated as the 1th percentile. $T_{r,\lambda}$ is the Rayleigh scattering transmittance function, including sea-level atmospheric pressure (P_0; in mbar), ambient atmospheric pressure (P; in mbar) and band wavelength (λ). M is the relative air mass and ϑ_s is the solar zenith angle (in degrees). $T_{w,\lambda}$ is the water-vapor transmittance function, calculated with the precipitable water vapor (W; in cm), relative air mass (M) and water-vapor absorption coefficients (a_w).

The second method is the TF atmospheric correction, which implements the atmospheric part of the IRC method of Kobayashi and Sanga-Ngoie (2008). This correction removes the effects of Rayleigh scattering and water-vapor absorption. TF correction extends the DOS method with a denominator containing normalized and band specific transmittance functions of water-vapor absorption and Rayleigh scattering, as shown in Equation 4.3 of Table 4.1. Transmittance functions were calculated for each wavelength and normalized per band. Here, a simplified approach was implemented, calculating the normalized transmittance function for each band based on the mean wavelength. The Rayleigh scattering transmittance function ($T_{r,\lambda}$) was calculated by Equation 4.4, which is based on sea-level atmospheric pressure (P_0; in mbar), ambient atmospheric pressure (P; in mbar) and wavelength (λ). The value of sea-level atmospheric pressure was assumed to be 1,013 mbar and the ambient atmospheric pressure value (995 mbar) was obtained from daily mean surface pressures in NASA's atmospheric Giovanni portal (2013). Relative air mass M was calculated using Equation 4.5.This value was constant across the study area, since M was only dependent on the solar zenith angle (ϑ_s). The water-vapor transmittance function ($T_{w,\lambda}$) was calculated with Equation 4.6 in Table 4.1 based on the following parameters: precipitable water vapor (W; in cm), relative air mass (M) and water-vapor absorption coefficients (a_w) given as a function of wavelength (Bird and Riordan, 1986). The precipitable water vapor (1.39 cm) was obtained from the Aqua satellite in NASA's atmospheric Giovanni portal (2013) and based on the central point in the image at acquisition. Values of W and P were selected for the center of the image and were assumed constant across the study area. Therefore, central values were compared with values in the four corners of the image. The minima and maxima of these values were only varying 1 to 5% of the central value.

4.3.2 Topographic corrections

Four different topographic corrections were evaluated in this analysis. Table 4.2 provides the implemented equations of all TC methods. The first method, band ratioing, is based on the assumption that reflectance values vary proportionally in all bands. The observed reflectance on an inclined terrain ($\rho_{t,\lambda}$) was obtained by calculating the arithmetic mean of observed reflectances over all spectral bands, as shown in Equation 4.7 of Table 4.2.

Table 4.2.: Equations and references of the four applied topographic corrections (Vanonckelen et al., accepted).

TC	Equation		Reference
Band ratio	$\rho_{h,\lambda}^{(i)} = \frac{\rho_{t,\lambda}^{(i)}}{\frac{1}{N}\sum_{j=1}^{N}\rho_{t,\lambda}^{(j)}}$	(4.7)	Ono et al., 2007
Cosine	$\rho_{h,\lambda} = \rho_{t,\lambda}\frac{\cos\theta_s}{\cos\beta}$	(4.8)	Teillet et al., 1982
PBM	$\rho_{h,\lambda} = \rho_{t,\lambda}\frac{\cos\theta_n}{(\cos\theta_n \cos\beta)^{k,\lambda}}$	(4.9)	Lu et al., 2008
PBC	$\rho_{h,\lambda} = \rho_{t,\lambda}\frac{\cos\theta_s + C_\lambda h_0^{-1}}{\cos\beta + C_\lambda h_0^{-1}h}$	(4.10)	Kobayashi and Sanga-Ngoie, 2008

Note: PBM is the pixel-based Minnaert correction and PBC is the pixel-based C-correction. $P_{h,\lambda}$(dimensionless or %) stands for the normalized reflectance of a horizontal surface for a specific spectral band number (N) and $\rho_{t,\lambda}$ for the observed reflectance on an inclined terrain. ϑ_s is the solar zenith angle and β is the incident solar angle. ϑ_n is the slope angle of the terrain and$k_{,\lambda}$ is the slope of the regression between x= log(cos ϑ_n cos β) and y= log($\rho_{T,\lambda}$cos ϑ_n). Parameter C_λ is the quotient of intercept (b_λ) and slope (m_λ) of the regression line between x and y. The h-factor represents a topographic parameter derived from the SRTM (h = 1-ϑ_n/π) and the h_0-factor an empirical parameter derived from the regression line between reflectance and cos β (h_0= (π +2ϑ_s)/2π).

The second method, cosine correction, assumes a uniform reflectance of incident solar energy in all directions (Lu et al., 2008).The cosine of the incident solar angle is calculated with Equation 4.11 and varies between -1 and +1:

$$\cos\beta = \cos\vartheta_s \cos\vartheta_n + \sin\vartheta_s \sin\vartheta_n \cos(\phi_t - \phi_a) \quad (4.11)$$

where ϑ_n, ϕ_t and ϕ_a, are slope angle of the terrain, solar azimuth angle andaspect angle of the terrain, respectively. This illumination parameter is the basis of the cosine correction formula, which is provided in Equation 4.8 of Table 4.2. The cosine correction only includes direct solar irradiance on the ground and ignores diffuse irradiance from the sky and adjacent terrain reflected irradiance (Teillet et al., 1982). Furthermore, the standard cosine correction is subject to overcorrection which is most pronounced in low illuminated areas (Moran et al., 1992; Soenen et al., 2008; Richter et al., 2009). The third implemented method is the pixel-based Minnaert correction (PBM), which accounts for non-Lambertian reflectance behavior by means of an empirical Minnaert constant k. In this study, the k-value was assessed for each band following the regression analysis between x = log(cos ϑ_n cos β) and y = log($\rho_{T,\lambda}$cos θ_n) (Equation 4.9 in Table 4.2; Lu et al., 2008; Meyer et al., 1993; Jensen, 1996). More sophisticated approaches assessed wavelength-dependent k-values (Bishop and Colby, 2002; Bishop et al., 2003). The fourth implemented method, pixel-based C-correction (PBC), consisted of the topographic part of the radiometric correction applied in the analysis of Kobayashi and Sanga-

Ngoie in 2008. The PBC method adds an additional factor C_λ to the cosine correction in Equation 4.10 of Table 4.2 to account for diffuse sky irradiance. The factor C_λ is the quotient of the intercept (b_λ) and the slope (m_λ) of the regression line. This additional factor is function of terrain slope, solar zenith angle, topographic parameters derived from the SRTM (β and h-factor) and empirical parameters derived from the regression line between reflectance and cos β (C_λ and h_0-factor).

4.3.3 ATCOR3 correction

Many so-called combined correction methods are presented and/or evaluated which consist of an atmospheric and a topographic component. For example, problems of overcorrection in the cosine correction are solved by the Hay's model (Hay, 1979). This model implements transmittance functions and the inclination and orientation of the surface to accounts for the anisotropic distribution of the diffuse irradiance (Richter, 1997; Guanter et al., 2008). Moreover, the so-called ATCOR3 correction integrates a MODTRAN atmospheric radiative transfer code and a modified Minnaert topographic method. This correction is similar to the combination of TF with PBM correction, though the atmospheric part of ATCOR3 implements MODTRAN and the k value is calculated differently. For reasons of comparison and visualisation, ATCOR3 results are shown in parentheses within the TF and PBM combination in all tables. The atmospheric part consists of an interactive and an automatic part (Richter, 1996). In the interactive part, sensor type and relevant acquisition information were chosen, such as solar zenith angle, calibration information and date. Secondly, a reference target (dense dark vegetation or water) was defined. The automatic phase calculated the visibility of the reference areas for the selected atmospheric characteristics and linked these characteristics with results obtained from the MODTRAN atmospheric radiative transfer code (Balthazar et al., 2012). Preset ATCOR look-up tables were implemented to calculate the radiation components, as well as molecular and particulate absorption and scattering (Frey and Parlow, 2009). The topographic ATCOR3 part is a modified Minnaert model based on a set of empirical rules (Richter et al., 2009). The normalized reflectance $\rho_{H,\lambda}$ is calculated with the correction factor $(\cos \beta / \cos \beta_T)^b$ in equation 4.12, where b is function of wavelength and vegetation cover, and β_T is a threshold value depending on ϑ_s:

$$\rho_{h,\lambda} = \rho_{t,\lambda} \left(\frac{\cos \beta}{\cos \beta_T} \right)^b \tag{4.12}$$

with b is function of the vegetation cover and wavelength. The ATCOR3 method combines two empirical parameters to calculate the bidirectional reflectance distribution function model: the lower boundary threshold of the factor $(\cos\beta / \cos\beta_T)^b$ and the threshold β_T (0 - 90°). The first parameter regulates the intensity of the correction by adapting the correction factor. When β exceeds the threshold β_T (i.e. in low illuminated areas), the corrected surface reflectance is converted according to Richter and Schläpfer (2013):

b = 1/2 for non-vegetation;
b = 3/4 for vegetation in the visible spectrum (λ< 720 nm);
b = 1/3 for vegetation if $\lambda \geq$ 720 nm.

Furthermore, if the correction factor is smaller than 0.25, it will be reset to 0.25 to prevent a too strong reduction (Richter and Schläpfer, 2011). The second parameter β_T is a threshold value of the local illumination angle below which Lambertian correction is applied ($\rho_{H,\lambda} = \rho_{T,\lambda}$) (Balthazar et al.,

2012). This threshold was calculated based on ϑ_s plus an increment that depends on its initial value, as described in Equations 4.13 to 4.15 (Richter et al., 2009):

$$\beta_T = \vartheta_s + 20° \text{ if } \vartheta_s < 45° \quad (4.13)$$

$$\beta_T = \vartheta_s + 15° \text{ if } 45° < \vartheta_s < 55° \quad (4.14)$$

$$\beta_T = \vartheta_s + 10° \text{ if } \vartheta_s > 55° \quad (4.15)$$

4.3.4 Evaluation of combined corrections

The combined correction methods were evaluated based on three analyses that test the homogeneity of reflectance values within a land cover class or within the entire image. Since forest was the dominant land cover class, most statistical analyses were carried out on a set of 4,000 forest pixels. These pixels were delineated on the basis of ground control points collected during field visits in May 2010 and July 2011 and visual interpretation of high resolution satellite imagery (WorldView-2, 8 bands, 46 cm resolution, acquisition date 13 October 2010). Forest pixels were classified in two groups, based on visual inspection of the satellite data and the value of cos β: illuminated (cos β> 0.8) and shaded forest pixels (cos β< 0.6). Visual inspection was performed by comparing the illuminated (sun-oriented) and shaded land units on true color composites before and after correction.

The combined correction methods were evaluated based on the following three analyses:

(1) By comparing differences in reflectance values between shaded and illuminated slope groups, where each group was represented by 2,000 forest pixels. These differences are expected to decrease after successful correction. Furthermore, the reflectance values between all pairs of shaded and illuminated slope groups before and after correction were tested with a dependent *t*-test for paired samples. Equation 4.16 was implemented where $\bar{z}$ is difference in average reflectance values for shaded and illuminated slope groups, *s* is the sample standard deviation and *n* is the sample size (i.e. the 15 combined corrections and ATCOR3). The *t*-test was performed at the significance level 0.05.

$$t = \frac{\bar{z}}{s}\sqrt{n} \quad (4.16)$$

(2) By calculating the coefficient of variation (CV) of reflectance values within the selected forest pixels with Equation 4.17. The CV is expected to decrease after a successful combined correction.

$$\mathrm{CV} = 100\,\frac{\mathrm{SD}}{\mathrm{mean}} \quad (4.17)$$

where SD is the standard deviation of the reflectance values within the forest class. To allow for a better interpretation, average CV values over all bands and $CV_{difference}$ values were calculated ($CV_{difference} = CV_{before\ correction} - CV_{after\ correction}$).

(3) By examining the dependency between reflectance values and cos β before and after correction on a stratified sample of 5,000 points over the entire image and on the selected forest pixels. This statistic was evaluated based on the regression slope and the P-value for testing the hypothesis of no dependency before and after correction. The dependency is expected to decrease after a successful

correction and correlations are significant if P-values are larger than the significance level 0.05. In this analysis, band 4 was selected based on the large differences in average reflectance values between illuminated and shaded slopes in the first statistical analysis.

4.4 Results

All analyses were performed on the 15 combined methods and ATCOR3. The tables show results for all combinations. In contrast, it was impractical to show all combinations in the figures. Therefore, six representative combinations were presented: (a) no AC and no TC; (b) DOS without TC; (c) DOS with band ratio; (d) TF with cosine; (e) TF with PBM; and (f) TF with PBC. These six combinations were selected since all single AC and TC methods were included and represented the range data requirement and thus modeling complexity.

4.4.1 Differences in reflectances (shaded versus illuminated)

Figure 4.2 shows reflectance values on illuminated (squares) and shaded slopes (circles) of the six bands and representative combinations for the selected forest pixels. In bands 1 to 3 of Figure 4.2a, small differences were present between average uncorrected reflectance values of illuminated and shaded areas. In contrast, average reflectance values were less homogenous in bands 4, 5 and 7. Combination of DOS without TC especially diminished the differences between reflectance values of shaded and illuminated slopes in bands 4, 5 and 7 (Figure 4.2b). Similar outputs were obtained for TF without TC. Application of DOS with band ratio overcorrected average reflectance values of visual bands and the difference in average reflectance values was reduced in bands 4 to 7 (Figure 4.2c). After cosine with TF correction (Figure 4.2d), average reflectance values of shaded slopes were higher than illuminated slopes for bands 1 to 3, which indicated an overcompensation of reflectance values of shaded slopes. ATCOR3 and the TF with PBM combination showed a reduction of differences between average illuminated and shaded reflectances in all bands (Figure 4.2e). Implementation of TF with PBC correction performed best (Figure 4.2f), since average reflectance values of illuminated and shaded areas were similar.

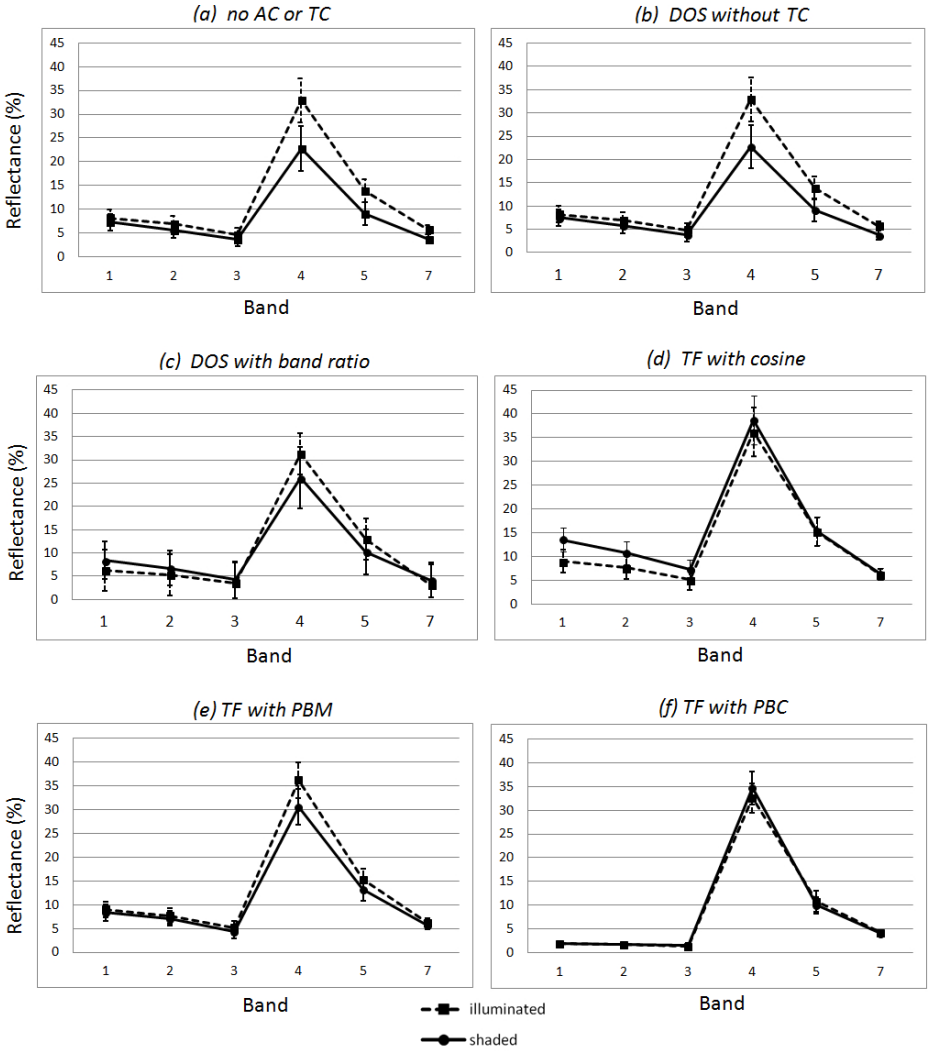

Figure 4.2.: Average reflectance (%) calculated in the forest class as a function of spectral band: (a) no AC or TC; (b) DOS without TC; (c) DOS with band ratio; (d) TF with cosine; (e) TF with PBM and (f) TF with PBC. The dashed line with square dots denotes the illuminated areas, the solid line with round dots the shaded areas. The whiskers represent the standard deviations(Vanonckelen et al., accepted).

The largest differences in reflectance values between illuminated and shaded forest slopes were observed in band 4. Table 4.3 shows that topographic corrections had a stronger impact on the reflectance values than atmospheric correction in this band. Differences after TC without AC ranged between -1.91% and 5.56%, while differences after only AC ranged between 8.54% and 9.86%. Furthermore, combination of AC and TC methods resulted in the smallest differences with a minimum of -0.83% (TF with PBC) and a maximum of 5.83% (TF with band ratio). Results of the TF with PBM method (4.14%) were comparable to the results of ATCOR3 (3.73%). The smallest differences were found after TF with PBC correction (-0.83%). When the *t*-test was significant, an asterisk was added in Table 4.3. Significant results were present for the ATCOR3 method and for combined corrections with a PBM or a PBC topographic correction. The PBM method was only significant in combination with the transmittance based atmospheric correction. In contrast, the PBC correction was significant in combination with all atmospheric corrections.

Table 4.3.: Average reflectance differences (%) between illuminated and shaded forest slopes of band 4 for the 15 combined corrections and ATCOR3 (in parentheses). The asterisks indicate a significant t-test between all pairs of shaded and illuminated slope groups before and after correctionat the significance level 0.05 (Vanonckelen et al., accepted).

	No TC	**Band ratio**	**Cosine**	**PBM**	**PBC**
No AC	10.16	5.56	-2.36	4.65	-1.91*
DOS	9.86	5.12	-2.34	5.04	-1.62*
TF	8.54	5.83	-1.56	4.14* (3.73*)	-0.83*

4.4.2 Coefficient of variation

Table 4.4 shows CV values for the selected forest pixels of each spectral band. Furthermore, average CV and $CV_{difference}$ values over all bands are presented. There was only an increase in CV for bands 2, 3 and 5 after band ratioing without AC. All other combined corrections decreased the CV values. Results after TC without AC emphasized the effectiveness of topographic corrections. The $CV_{difference}$ value after implementation of band ratio without AC was low (1.09). Furthermore, $CV_{difference}$ values increased after implementation of the three other TCs without AC. The $CV_{difference}$ value was highest for PBC (5.57), followed by PBM (4.65), and cosine (2.57), respectively. Table 4.4 also shows the performance of the two AC methods without TC. TF correction resulted in higher homogeneity than DOS correction, since the $CV_{difference}$ value after TF (1.85) was higher than the value after DOS (1.04). Best results were obtained after combined corrections. Combination of TF with PBC correction resulted in the highest homogeneity ($CV_{difference}$ of 8.60), closely followed by ATCOR3 ($CV_{difference}$ of 8.48) and TF with PBM correction ($CV_{difference}$ of 8.17).

Table 4.4.: CV values for each band, average CV and $CV_{difference}$ values over all bands (dimensionless) of the 15 combined corrections and ATCOR3 (in parentheses) for the selected forest pixels (Vanonckelen et al., accepted).

CV		**TM1**	**TM2**	**TM3**	**TM4**	**TM5**	**TM7**	**Average**	**Difference**
No AC	No TC	45.66	54.16	71.46	33.58	41.21	40.98	47.84	/
	Band ratio	42.44	57.74	75.51	30.32	45.49	42.08	48.93	1.09
	Cosine	44.68	54.32	67.82	24.81	40.97	39.05	45.27	2.57
	PBM	41.55	48.73	64.37	30.55	36.98	36.96	43.19	4.65
	PBC	41.51	46.56	62.71	30.14	35.09	37.60	42.27	5.57
DOS	No TC	44.93	53.60	67.18	34.90	40.78	39.40	46.80	1.04
	Band ratio	41.71	51.68	65.84	31.03	37.31	37.83	44.23	3.61
	Cosine	43.69	52.57	67.76	30.79	37.98	38.00	45.13	2.71
	PBM	41.28	49.53	63.86	27.77	36.98	37.40	42.80	5.04
	PBC	40.62	49.80	60.66	26.62	34.82	37.13	41.61	6.23
TF	No TC	43.80	52.85	65.86	33.18	40.26	39.98	45.99	1.85
	Band ratio	41.16	49.87	64.87	30.26	37.62	38.41	43.70	4.14
	Cosine	41.02	50.28	67.92	27.53	36.81	36.44	43.33	4.51
	PBM	40.05 (39.74)	46.58 (46.89)	63.53 (62.87)	23.45 (23.16)	33.55 (33.87)	30.84 (29.61)	39.67 (39.36)	8.17 (8.48)
	PBC	39.26	46.50	61.58	24.39	34.80	28.91	39.24	8.60

4.4.3 Correlation analysis

Correlation coefficients between cos β and reflectance values before and after correction were computed on the selected forest pixels and the stratified sampling over the entire image. Tables 4.5 and 4.6 show results of both sampling strategies for all combined corrections in band 4. Before correction, correlation between cos β and reflectance values of both sampling strategies was positive. This is shown in Tables 4.5 and 4.6 by slope values of 16.3 and 14.6 respectively, and significance levels less than 0.05. The dependency of reflectance values on terrain illumination was reduced after correction. All tested corrections decreased slope values of the regression line, though correlations remained significant for a number of combinations. After combining DOS without TC, positive correlation was still present. Slope values decreased from 16.3 to 13.9 and from 14.6 to 12.6, respectively. A significant correlation was still present for both samplings after combination of an AC with band ratio or cosine correction. In Tables 4.5 and 4.6, P-values were lower than the significance level and slope values were negative. Implementation of DOS with band ratio and TF with cosine resulted negative slope values in both scenarios. Combination of PBM or PBC without an AC resulted in a small dependency, with slope values smaller than 3.0 and P-values between 0.31 and 0.39. Dependency of reflectance values on terrain illumination was reduced after implementation of an AC with PBM or PBC method. For the forest pixels (Table 4.5), slope values ranged between 2.2 and 2.5, and P-values indicated that data were uncorrelated (P > 0.05). Table 4.6 shows that sampling over the entire image was even performing better than the forest sample, with slope values approximating 0 and P-values larger than 0.05. Results were improved most after ATCOR3 and combination of TF with PBM and PBC correction. Reflectance values and cos β were uncorrelated with reduced slope values of 1.1, 1.3 and 0.7, respectively.

Table 4.5.: Slope and P value of correlation analysis of the selected forest pixels in band 4 for the 15 combined corrections and ATCOR3 (in parentheses)(Vanonckelen et al., accepted).

	No TC		**Band ratio**		**Cosine**		**PBM**		**PBC**	
	slope	P	slope	P	slope	P	slope	P	slope	P
No AC	16.3	<0.001	-3.6	<0.001	-10.7	<0.001	3.0	0.312	2.9	0.326
DOS	13.9	<0.001	-3.3	<0.001	-9.8	<0.001	2.5	0.351	2.5	0.355
TF	12.5	<0.001	-3.0	<0.001	-9.4	<0.001	2.2	0.378	2.3	0.384
							(2.1)	(0.386)		

Table 4.6.: Slope and P value of correlation analysis of the stratified sample in band 4 over the entire image for the 15 combined corrections and ATCOR3 (in parentheses)(Vanonckelen et al., accepted).

	No TC		**Band ratio**		**Cosine**		**PBM**		**PBC**	
	slope	P	slope	P	slope	P	slope	P	slope	P
No AC	14.6	<0.001	-2.5	<0.001	-9.3	<0.001	2.1	0.365	2.3	0.386
DOS	12.6	<0.001	-2.1	0.001	-8.5	<0.001	1.8	0.403	1.6	0.412
TF	11.4	<0.001	-1.9	0.001	-8.7	<0.001	1.3	0.465	0.7	0.483
							(1.1)	(0.474)		

Figure 4.3 shows true color composite images (TM 3, 2, 1) before and after implementation of the six representative combined corrections. These images provide a better understanding of the study area and depict the removal of shading effects after combined correction. The image shows a 120 km² representative zoom of the study area as indicated in Figure 4.1. Without any corrections applied, there are clear differences between sun-oriented and opposite slopes in Figure 4.3a. The output after DOS without a TC did not result in visual differences compared to no AC or TC and shown in Figure

4.3b. A comparable output was obtained for TF without TC. In contrast, combined AC and TC methods changed the appearance of the images. Band ratioing resulted in an overall lowering of reflectance values as expected after implementation of Equation 4.7 (Figure 4.3c). Combined TF and cosine correction resulted in a reduction of shades on poorly illuminated areas in Figure 4.3d, though an overcorrection in the visible bands appeared. Best results were obtained after combination of TF with PBM or PBC correction in Figures 3e and f. Differential illumination effects were reduced and spectral characteristics of sun-oriented and opposite slopes were similar.

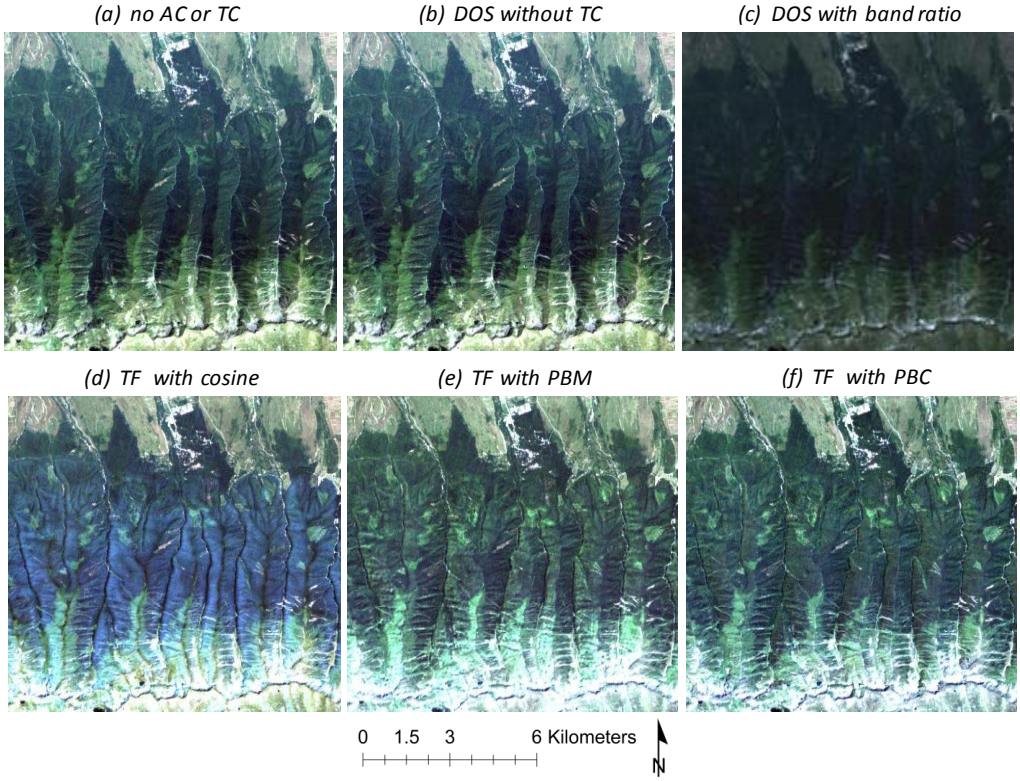

Figure 4.3.: True color composite images (RGB: band 3, 2 and 1) of the zoom in the study area with a linear stretching: (a) no AC or TC; (b) DOS without TC; (c) DOS with band ratio; (d) TF with cosine; (e) TF with PBM and (f) TF with PBC (Vanonckelen et al., accepted).

4.5 Discussion

This analysis provided an analysis of fifteen combinations of two atmospheric and/or four topographic corrections along with uncorrected imagery. Generally, visible bands presented small differences between average reflectance values of illuminated and shaded areas. These differences indicated that especially bands 1 to 3 were not strongly affected by topographical effects. Furthermore, it is a possible indication that atmospheric distortions had a larger influence than topographic distortions in these bands due to scattering and diffusion, which was confirmed by results of previous research (Kobayashi and Sanga-Ngoie, 2008; Schroeder et al., 2006; Vicente-Serrano et al., 2008). Implementation of TF with cosine indicated an overcorrection of reflectance values of shaded slopes since cos β is smaller in these non-illuminated areas and since the diffuse sky irradiance was ignoraned which resulting in an overestimation of the output radiance data (Teillet et al., 1982). The overcorrection of areas under low illumination conditions, especially steep terrain

where incident angles approach 90°, has been observed in several analyses (Hantson and Chuvieco, 2011; Meyer et al., 1993; Teillet et al., 1982).

This was ATCOR3 and combination of TF with PBM and PBC showed a reduction of differences between average reflectance values in all bands and significant *t*-test results. These results were comparable to experiments conducted by Huang et al. in 2008, Wen et al. in 2009 and Vicente-Serrano et al. in 2008. Average $CV_{difference}$ values increased after implementation of advanced TCs without AC. The average $CV_{difference}$ value was highest for PBC, followed by PBM and cosine correction. Correlation analysis showed that PBM or PBC without an AC resulted in a small dependency. However, this dependency was even reduced after combined correction, which proved that TC methods had a larger impact on the results than AC methods. A valid explanation for these results was the application of only one Landsat footprint in this analysis. The dependency between cos θ and reflectance values was decreased most after ATCOR3 and the combination of TF with PBM or PBC. Similar results were obtained in a previous analysis by Kobayashi and Sanga-Ngoie in 2008. Largest illumination effects were observed in the forest class, which explained an improved performance of sampling over the entire Landsat image.

Considering overall results, this analysis showed that most complex combined corrections were most effective but also most difficult to automate since they require more input data which need to be derived from look-up tables or regression analyses. Relative simple AC methods failed compared to the more advanced AC methods since the last methods were more capable to simulate the atmospheric processes of scattering and diffusion by implementing parameters such as the water vapor and ambient atmospheric pressure. This was also true for the TC methods, in which the more advanced TC method included parameters that were derived from regression analyses or from a DEM. Furthermore, the added value of complex TC methods was high, while the added value of AC methods was limited. These results confirmed findings of previous analyses by Eiumnoh and Shrestha in 2000 and Hale and Rock in 2003, where topographic effects had a larger impact on reflectance values than atmospheric effects. Therefore, application of a combined correction based on a complex TC component and a rather straightforward AC component was justified in this local scale study.

4.6 Conclusions

In this analysis, the performance of the combination of three atmospheric and five topographic correction methods and the ATCOR3 method was evaluated along with uncorrected Landsat imagery. Most similar studies to date missed a thorough comparison between different AC and TC methods, while this analysis decomposed combined models in an AC and a TC component and systematically evaluated effects of all combinations. Statistical comparison of illuminated versus shaded reflectance values of forested pixels without any correction indicated that major differences were present in bands 4 to 7. After implementation of combined corrections, these differences were reduced. The smallest differences in reflectance values were present after ATCOR3 correction or combination of an atmospheric correction with PBM or PBC. Furthermore, most ofthese combined corrections resulted in significant *t*-test results. Comparable conclusions were drawn from the analysis of the coefficients of variation for the forest sampling. The CV of each spectral band decreased after combined

correction. Overall results indicated that TC had a larger impact on the reflectance values than AC. Added value of AC methods was relatively low, since only one Landsat image was implemented. Results of the AC methods were included since these methods are essential in time series analyses. In this study, ATCOR3 and combinations of TF with PBM or PBC performed best, though these methods required the largest amount of input data.

The added value of this study was the decomposition of combined models and the systematic evaluation along with uncorrected imagery. This local scale study demonstrated that the benefits in reduction of atmospheric and topographic distortions justified automation of more complex corrections in mountain areas.

Chapter 5: Effect of atmospheric and topographic correction methods on land cover classification accuracy in mountain areas*

*This chapter is published as: Vanonckelen, S., Lhermitte, S., Van Rompaey, A., 2013. The effect of atmospheric and topographic correction methods on land cover classification accuracy, International Journal of Applied Earth Observation and Geoinformation, 24, 9-21.

5.1 Introduction

Assessing the rate and spatial pattern of land cover changes is challenging given the ruggedness and inaccessibility of mountain areas (Lambin and Geist, 2006). Remote sensing techniques are privileged monitoring tools and yet suffer from methodological challenges that need to be resolved by correction methods (Balthazar et al., 2012; Lhermitte et al., 2011). A typical image preprocessing includes sensor calibration, atmospheric and topographic correction and relative radiometric normalization (Vicente-Serrano et al., 2008). Remote sensing-based land cover mapping in mountain areas is especially affected by atmospheric and topographic effects on recorded sensor signals (Soenen et al., 2008). Topographic effects are caused by differences in illumination angles at the moment of image acquisition and result in a variation of reflectance response for similar terrain features (Veraverbeke et al., 2010). During the past 10 years, several atmospheric correction (AC) and topographic correction (TC) methods have been evaluated individually. Table 2.3 summarizes the most frequently used correction methods. Some authors (e.g. Richter, 1996; 1998; Kobayashi and Sanga-Ngoie, 2008) have evaluated the influence of combined AC and TC corrections. The combined methods that have been developed include a specific combination of an atmospheric and a topographic correction. In literature, though, only a limited number of combined AC and TC corrections has been tested and described so far (Table 2.3). Nevertheless, at present, a systematic comparison of the performance of different combined corrections on classification accuracy is lacking.

Several authors examined the influence of atmospheric and/or topographic corrections on land cover classification in mountain regions. In Table 5.1, an overview of recent studies that examine the influence of different correction methods on classification accuracy is presented. Depending on the correction methods used, there was no improvement in classification accuracy (e.g. Blesius and Weirich, 2005; Zhang et al., 2011) or an increase in the overall classification accuracy (OA) up to 40% (e.g. Gitas and Devereux, 2006). However, it is difficult to compare these studies since the input files and parameters are varying: study areas, vegetation types, sensors, DEMs, AC and TC corrections, etc.

Table 5.1.: Reference, study area and land cover, classification method, AC and TC, and improvement in accuracy after correction (Vanonckelen et al., 2013).

Reference	Study area and land cover (LC)	Classification method	AC and TC	Improvement in accuracy after correction
Conese et al., 1993	Italy, all LCs	Supervised (ML*)	Inverse technique + topographic normalization	Kappa increase from 0.56 to 0.62
Meyer et al., 1993	Switzerland,	Not specified	No AC + statistical, Minnaert	Overall accuracy

	(non)-forest		and C	(OA) increase with 10-30%
Sandmeier and Itten, 1997	Switzerland, all LCs	Supervised (ML)	6S + DEM	OA increase between 1-7%
Coburn and Roberts, 2004	Canada, all LCs	Supervised (ML)	No AC + different statistical texture measures	Not specified
Hale and Rock, 2003	USA, all LCs	Supervised (ML)	No AC + band ratios, Minnaert, aspect partitioning and combinations of these corrections	OA increase with 4-13%
Mitri and Gitas, 2004	Greece, all LCs	Fuzzy classification	ATCOR2 + multi-resolution segmentation	OA of 98.85%
Blesius and Weirich, 2005	USA, all LCs	Supervised	No AC + Minnaert	No improvement
Gitas and Devereux, 2006	Greece, all LCs	Supervised (ML)	DOS + Minnaert	OA increase of maximum 40%
Huang et al., 2008	USA, all LCs	Support vector machines	MODTRAN + SCS and a revised correction	OA increase from 85.5% to 89.1%
Soenen et al., 2008	Canada, all LCs	Supervised (ML)	Empirical line + cosine, C, Minnaert, statistical-empirical, SCS, b, SCS+C and MFM-TOPO	Class accuracy increase between 13-62%
Gao and Zhang, 2009	China, all LCs	Supervised (ML)	DOS + Minnaert and SCS	OA increase from 88.1% to 89.7%
Cuo et al., 2010	Thailand, all LCs	Supervised	Simplified normalization	OA from 55% to 85% and 51% to 91%
Zhang et al., 2011	China, all LCs	Artificial neural networks	No AC + cosine, Minnaert, C, SCS, two stage normalization and slope matching	No improvement

* ML is the Maximum Likelihood classification algorithm.

In order to allow a good comparison between the existing AC and TC methods, a systematic analysis is essential. The overall research question of this chapter is therefore the evaluation of the impact of fifteen combined AC and TC corrections on the accuracy of land cover classifications in mountain areas. A land cover classification analysis is performed on the image outputs after implementation of fifteen AC and TC combinations. The selected atmospheric and topographic correction methods are frequently used and have a different degree of complexity. The methods differ from relatively straightforward to complex with a highdata and computation requirement. The study area is a Landsat-5 Thematic Mapper (TM) image in the Romanian Carpathians.

Four aspects of the overall research question are examined for two validation sets:

- Which AC and TC combinations result in the best overall classification accuracy?
- What is the influence of different AC and TC combinations on class accuracies?
- Does the influence of combined corrections on overall classification accuracy vary under different illumination conditions?
- Does the influence of combined corrections on classification accuracy vary under different atmospheric conditions?

These four aspects help us to conclude what the individual and combined effect of the different AC and TC components is on classification accuracy.

5.2 Material and methods

5.2.1 Study area and data acquisition

Study area

In order to address the research questions described above, a local scale study area of 915 km² in the Romanian Carpathian mountains was selected (Figure 4.1, white-outlined rectangle). The study area consists of rugged terrain with an elevation varying between 690 and 2,540 m above mean sea level. The Făgăraș mountains which are located at the intersection between the counties Brașov, Sibiu and Argeș are included in the study area.

The dominant lithology of the Făgăraș mountains is crystalline rock with occasional occurrence of limestone. Major soils include *Podzols* in the mountain zone and *Cambisols* in the foothill zone (FAO/UNESCO, 1988). Three natural vegetation zones are present: a foothill zone with mixed and broadleaved forests between 250 and 1,500 m with *Betula pendula*, *Carpinus betulus* and *Fagus silvatica* (Figure 5.1a); a mountain zone (1,500–2,200 m; Figure 5.1b and c) with coniferous forests (e.g. *Abies alba*, *Picea abies*, *Pinus mugo*); and an alpine zone (>2,200 m; Figure 5.1d) above the tree line dominated by *Carex curvula*, *Festuca supine* and *Juncus trifidus* (Enescu, 1996; Kuemmerle et al., 2008a; Mihai et al., 2007). The majority of the land cover comprises forests as forestry has traditionally been an important component of the regional economy and a major source of rural income (Ioras and Abrudan, 2006). Forests provide important ecosystem services and are being affected by natural and human induced threats: bark-beetle infestations (Knorn et al., 2012a), wind-throws (Anfodillo et al., 2008), extensive salvage logging after wind-throws (Macovei, 2009) and land restitutions (Kuemmerle et al., 2008a).

Figure 5.1.: (a) Foothill zone (1,020 m) with mixed and broadleaved forests. (b) Mountain zone (1,640 m) with coniferous forests. (c) Mountain zone (2,050 m) with small vegetation. (d) Alpine zone (2,360 m) above the tree line with grasses (Vanonckelen et al., 2013).

Satellite and elevation data

The recent opening of the global Landsat archive by the United States Geological Survey (USGS) provides opportunities to advanced land cover studies. The released archive of Landsat imagery is temporally and spatially extensive and freely available for download (Knudby et al., 2010). For this study, Landsat-5 TM images (path 183/row 28) with acquisition days July 24, 2009 and August 12, 2010 were selected (see white-outlined rectangle in Figure 4.1). In this chapter, all analyses were performed on the SRTM and the 6 Landsat bands of Chapter 4. The images were orthorectified with precision terrain correction level L1T by the USGS. Clouds and cloud shadows were ignored since cloud coverage in the study area was below 1%. The solar elevation angle at image capture was respectively 57.8° and 53.8° for the 2009 and 2010 images. The difference between the atmospheric parameters of both images is explained in the methodology.

Ground Control Points

GCPs for land cover classification training and validation were gathered through field visits and the analysis of highresolution satellite imagery. Training data were gathered systematically over the total image in order to collect the spectral range of the different classes. Pixels were chosen not too close together in order to avoid spatial autocorrelation (Campbell, 1981; Labovitz and Masuoka, 1984). First, eighty-three usable GCPs were recorded through transect walks in the study area during field visits in May 2010 and July 2011 (Figure 5.2, red dots). The dominant vegetation type and topographic information, such as slope and elevation, was recorded for each point. Secondly, since the number of field-registered points was insufficient to serve as training and validation data for image classification, extra land cover data were derived by a visual interpretation based on high resolution satellite imagery (WorldView-2, 8 bands, 46 cm resolution, acquisition date October 13, 2010).

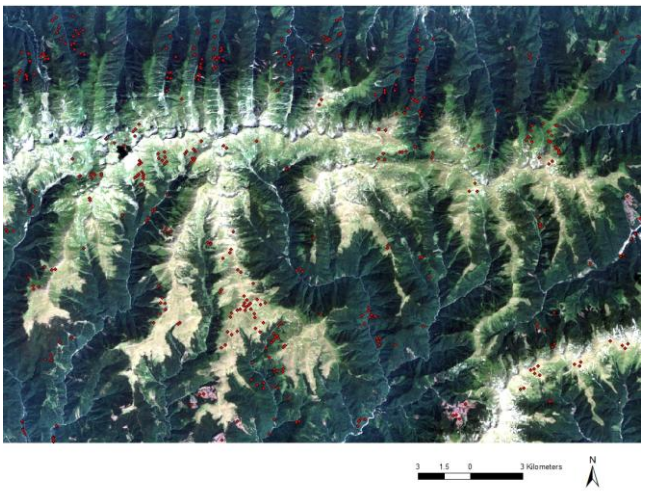

Figure 5.2.: True color composite image (RGB: band 3, 2 and 1) of the local scale study area: the red dots indicate the registered reference points (Vanonckelen et al., 2013).

On the basis of the WorldView-2 image and field expertise, 322 extra reference points were identified. In order to check whether the land cover types for the selected reference points in 2010-2011 were equal in 2009, two Landsat images from the same season and acquired around identical dates (July 24, 2009 and August 12, 2010) were selected. Furthermore, the consistency of the land cover types throughout the years 2009-2011 was checked based on Google Earth.

5.2.2 Methodology

Figure 5.3 presents an overview of the applied methodology. After data acquisition, the input images were corrected by applying the fifteen combinations of AC and TC corrections (including scenarios without atmospheric and/or topographic correction). Secondly, each corrected image is classified. Thirdly, the land cover maps are evaluated by comparing overall classification accuracies, class accuracies and overall accuracies for three illumination conditions.

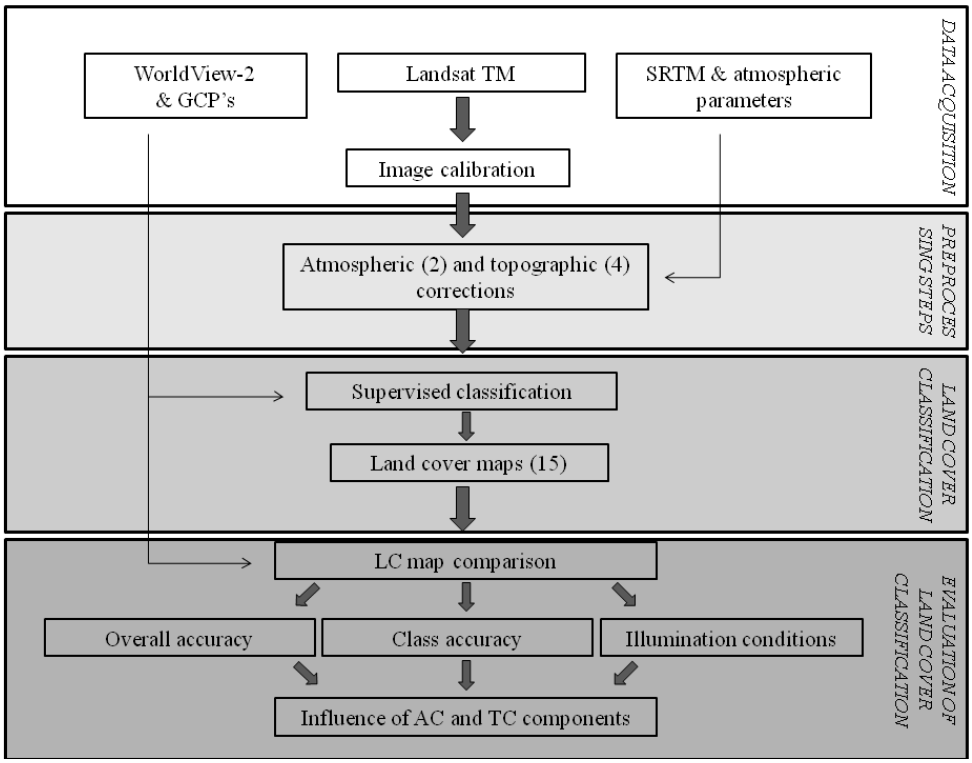

Figure 5.3.: Overview of the methodology: data acquisition, preprocessing steps, land cover classification and evaluation of the land cover classification (Vanonckelen et al., 2013).

Preprocessing steps

The preprocessing steps were similar as described in the methodology section in Chapter 4. Hereby, the 3 different AC methods of section 4.3.1 were implemented. Furthermore, the five TC methods of section 4.3.2 were implemented: i) no TC, ii) band ratioing, iii) cosine correction, iv) pixel-based Minnaert correction (PBM), and v) pixel-based C-correction (PBC). These three AC and five TC methods – including no AC and no TC – were combined to fifteen different combinations of AC and TC methods. The combination of no topographic and no atmospheric correction was considered as the baseline scenario. The L_{min} values (in W/(m^2 µm)) per band for the 2009 and 2010 images were respectively: [37.50, 26.12, 14.50, 36.16, 2.76, 0.44] and [40.60, 27.57, 16.58, 44.92, 3.60, 0.57]. The ambient atmospheric pressure (*P*, in mbar) was respectively 995 and 925 mbar for the 2009 and 2010 image. The value of *P* was obtained for the central point in the image and at acquisition time. Precipitable water vapor values (*W*) were respectively 1.39 and 2.99 cm. The most complex combined correction (TF-PBM) simulated the total radiance pathway through the atmosphere and implemented the path radiance, solar direct irradiance, sky diffuse irradiance and adjacent terrain reflectance. In contrast to Chapter 4, the ATCOR3 procedure was not implemented in Chapter 5. Finally, the uncorrected images and the fourteen corrected images provide the input for the classification protocol described below.

Land cover classification

In order to obtain classification accuracies, an appropriate classification algorithm is required. Since this study concentrates on the effect of atmospheric and topographic corrections on land cover accuracy, a relatively straightforward classifier was chosen. When detailed information of the study area exists and good training data are available, a supervised classification is preferable (Kuemmerle et al., 2006). The supervised maximum likelihood (ML) classifier based on the Gaussian distribution of the elements in the coherent scattering matrix is used in this study (Foody, 2002). The maximum likelihood decision rule is relatively convenient to implement in ENVI when sufficient GCPs are available. It is at present still the most widely applied classification technique because of its relative simplicity and robustness (Gao and Zhang, 2009). Furthermore, the classifier utilizes means, variances and covariances of training site statistics, where most other decision rules are based on simpler statistics (Chen et al., 2004). Moreover, Table 5.1 shows that ML classification is still frequently implemented in recent assessments of land cover accuracy (e.g. Gao and Zhang, 2009; Soenen et al., 2008). The classification procedure is based on a 10-fold cross validation (Kohavi, 1995) where the image is repeatedly trained with two-thirds of the reference points and validation is based on the remaining one-third of reference points. Thereby, the 405 reference points are repeatedly and randomly subdivided in training and validation datasets. First, the classification is performed on the uncorrected and corrected images of 2010. Secondly, reflectance spectra are modeled as the linear combination of a finite number of spectrally unique signatures of pure ground components, referred to as endmembers (Bateson et al., 2000). Therefore, the endmember spectra of the 2009 image are collected based on the GCPs of the 2010 image and applied on the 2009 image. Endmember spectra are easier to interpret than DNs, and, therefore, provide a more intuitive link between image measurements and observations in the field (Adams et al., 1995; Martinez et al., 2006). The land cover classes used for image classification are described in Table 5.2. In total, six classes are discerned, including two non-vegetation classes (bare soil and water surface).

Table 5.2.: Land cover classes, code and dominant species in the study area (Vanonckelen et al., 2013).

Land cover classes	Code	Dominant species
Broadleaved forest	BL	*Carpinus betulus, Fagus sylvatica, Quercus petraea Quercus robur*
Bare soil	BS	/
Coniferous forest	CF	*Abies alba, Picea abies, Pinus mugo, Pinus sylestris*
Grassland	GRASS	
Mixed forest	MX	*Mixture of the dominant BL and CF forest species*
Water surface	WT	/

Bare soil (BS), grassland (GRASS), water (WT), and broadleaved (BL), coniferous (CF) and mixed forest (MX). Mixed forests are stands where neither broadleaved nor coniferous trees account for more than 75% of the tree crown area (UN-ECE/FAO, 2000).

Evaluation of land cover classification

The performance of land cover classification maps for each of the correction methods is examined based on four statistical analyses:

(1) Class reflectance values separability;
(2) Overall classification accuracy to determine the best combination of AC and TC;
(3) Land cover class accuracies to understand the effect on each class;

(4) Classification accuracies to examine the effect of different illumination conditions.

One of the most popular measures of classification accuracy derived from the confusion matrix is the percentage of cases correctly allocated (Foody, 2002). A problem is that some cases are allocated to the correct class purely by chance (Congalton, 1991; Pontius, 2000; Rosenfield and Fitzpatrick-Lins, 1986; Turk, 1979). To accommodate for the effects of chance agreement, Cohen's kappa coefficient has often been used and a number of commentators argue that it should, in some circumstances, be adopted as a standard measure of classification accuracy (Cohen, 1960; Congalton et al., 1983; Foody, 2002; Smits et al., 1999). Kappa became popularized in the field of remote sensing and map comparison by Congalton (1981), Monserud and Leemans (1992), Congalton and Green (1999), Smits et al. (1999) and Wilkinson (2005). The kappa coefficient has many attractive features as an index of classification accuracy. In particular, it performs a compensation for chance agreement and a variance term can be calculated to enable the statistical testing of the significance of the difference between two coefficients (Rosenfield and Fitzpatrick-Lins, 1986; Foody, 2002). However, Pontius (2000) documented some conceptual problems with the standard Kappa since it is frequently complicated to compute, difficult to understand and unhelpful to interpret. Therefore, multiple variations on Kappa were proposed in an attempt to remedy the flaws of the standard Kappa (Pontius; 2000). Although, the use of Kappa continues to be pervasive in spite of criticisms from many authors (Foody, 1992; Foody, 2002; Turk, 2002; Jung, 2003; Di Eugenio and Glass, 2004; Foody, 2004; Allouche et al., 2006; Foody, 2008; Pontius and Millones, 2011).

First, average reflectance values per wavelength and land cover type for the all combined corrections are analyzed to understand the differences in accuracy. Secondly, average kappa coefficientsof the 2009 and 2010 images are derived as a measure of classification accuracy. The range of classification accuracies between both dates is shown through the whiskers on the bars and illustrates the difference in accuracy between the two dates. In this context, two validation datasets are used: a set containing all validation pixels and a so called difference subset. This subset includes the validation pixels that are classified differently between the classification of one of the combined corrections and the classification of the uncorrected image. Thirdly, at class level, differences of average 2009-2010 kappa values (δkappa)for each class are calculated using the following equation (Zhang et al., 2011):

$$\delta\text{kappa}_i = \text{kappa}_{i,\ \text{corrected}} - \text{kappa}_{i,\ \text{uncorrected}} \quad (5.1)$$

where: $\text{kappa}_{i,\ \text{corrected}}$ is the kappa value of class *i* based on a corrected image classification; and $\text{kappa}_{i,\ \text{uncorrected}}$ is the kappa value of class *i* derived from theuncorrected image classification. In this section, the overall δkappa over all fourteen correction methods is also calculated to provide a general perspective on the performance of all combined corrections. Fourthly, the effect of AC/TC methods on classification accuracy is evaluated for three different levels of illumination separately. Therefore, both validation sets are divided in three illumination zones based on the illumination parameter cos β that is calculated using Equation 4.11 and varies between -1 and +1 (maximum illumination) (Civco, 1989). The three illumination zones are: low illumination [cos $\beta \leq 0.65$], moderate illumination [$0.65 < \cos\beta < 0.85$], and high illumination [$\cos\beta \geq 0.85$]. The spatial distribution of each zone is illustrated in Figure 5.4. An equal area subdivision in thirds of the total area is approximated with these class boundaries. Finally, based on all accuracy criteria, the

individual effect of the two components (AC and TC) within a combined correction is evaluated and the influence of combined corrections under different atmospheric conditions is examined.

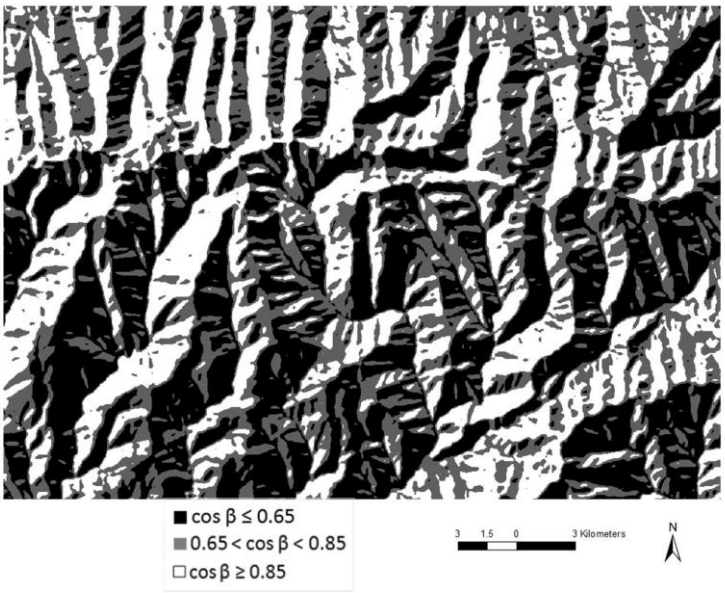

Figure 5.4.: The study area divided in three illumination zones: black is the low illumination zone [cos β ≤ 0.65], gray is moderate illumination [0.65 < cos β < 0.85] and the high illumination zone is indicated in white [cos β ≥ 0.85] (Vanonckelen et al., 2013).

5.3 Results

5.3.1 Class reflectance separability

Figure 5.5 shows average reflectance values per wavelength and land cover type for: (a) the uncorrected images and (b) after TF-PBM correction of 2009 (solid line) and 2010 (dashed line). The spectra for all land cover types of both dates before correction are overlapping (Figure 5.5a). Therefore, it is difficult to differentiate land cover classes in all bands before correction. On the contrary, the different land cover spectra of all bands show less overlap after TF-PBM correction. In band 1, 2, 3 and 7; the reflectance values per land cover class are less overlapping and the overlap between land cover classes also diminishes for bands 4 and 5. Especially the reflectance values of the GRASS, BL and WT classes are discernable after correction, which is shown by a large gap between the reflectance values of both dates. There is also an improvement between the differentiation of the three other land cover classes: values between the different land cover types are less corresponding.

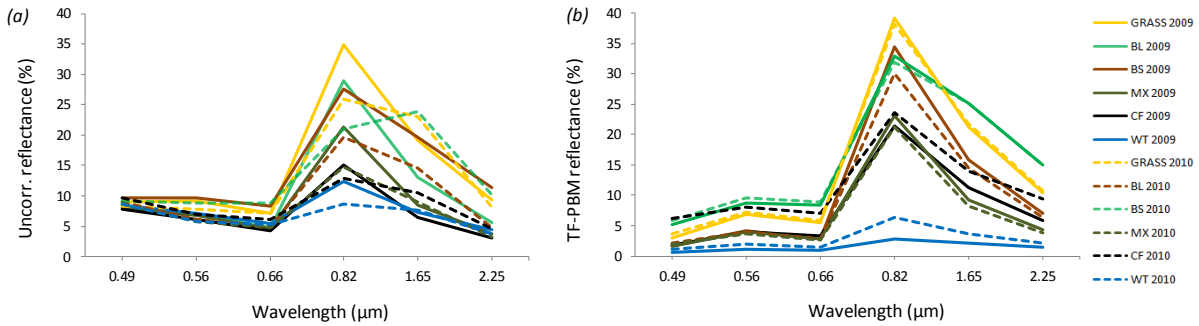

Figure 5.5.: (a) Average reflectance values per wavelength (band) and land cover type for the uncorrected images of 2009 (solid line) and 2010 (dashed line). (b) Average values for the most advanced method (TF-PBM) of 2009 (solid line) and 2010 (dashed line) (Vanonckelen et al., 2013).

5.3.2 Overall accuracy

Figure 5.6 presents average 2009-2010 kappa values of the uncorrected and corrected classifications using the full validation set (black) and the difference subset (white). For the full validation set, average kappa coefficients are generally high, varying between 0.87 (no AC and no TC; range 0.017) and 0.94 (TF-PBM; range 0.007). In this study, all combined corrections result in higher average kappa values. The land cover maps of methods that combine an atmospheric correction (DOS or TF) with a PBC or PBM topographic method are performing best. For these combinations, average kappa values are 0.94 (Figure 5.6; range respectively 0.006 and 0.007). Application of an atmospheric correction (DOS or TF) without TC correction increased average value with respectively +0.03 and +0.04 for the full validation set. Implementation of topographic corrections without AC correction resulted in higher average kappa values: +0.008 for band ratio, +0.015 for cosine, +0.027 for PBC and +0.022 for PBM correction. The range of classification accuracies provides information of the difference in classification accuracy between the 2009 and 2010 classification. Therefore, the range of the average kappa coefficients of both dates is able to provide valuable information. In this study, the average accuracy range over all five topographic corrections for the scenarios without AC, with DOS and TF correction is calculated. For the combined corrections without AC, the average difference of classification accuracy between both dates is larger (~0.017) than for the DOS (~0.015) and TF (~0.007) corrections respectively. This implies that the difference in classification accuracy between different dates is larger when no AC is applied, whereas it is smallest for TF corrections, with the TF-PBC method performing best (range 0.006).

In this study, an analogue analysis was carried out on the difference pixels. The implementation of a so-called 'difference subset of pixels' had the major advantage that differences in accuracies and ranges were more pronounced. The white bars in Figure 5.6 show average kappa values in the difference area. The average kappa value of the uncorrected image in the difference area (0.22; range 0.025) is lower than the value of the entire image (0.87; range 0.017). Increases in average kappa value after application of topographic corrections without AC correction were the following: +0.10 for band ratio, +0.19 for cosine, and +0.23 for PBC and PBM correction. Implementation of DOS and TF without TC correction resulted in average kappa increases of respectively +0.13 and +0.20 for the difference subset. The highest average kappa values in the difference area with lowest range were achieved after implementation of TF-PBC correction (average 0.77; range 0.012) and TF-PBM correction (average 0.76; range 0.023).

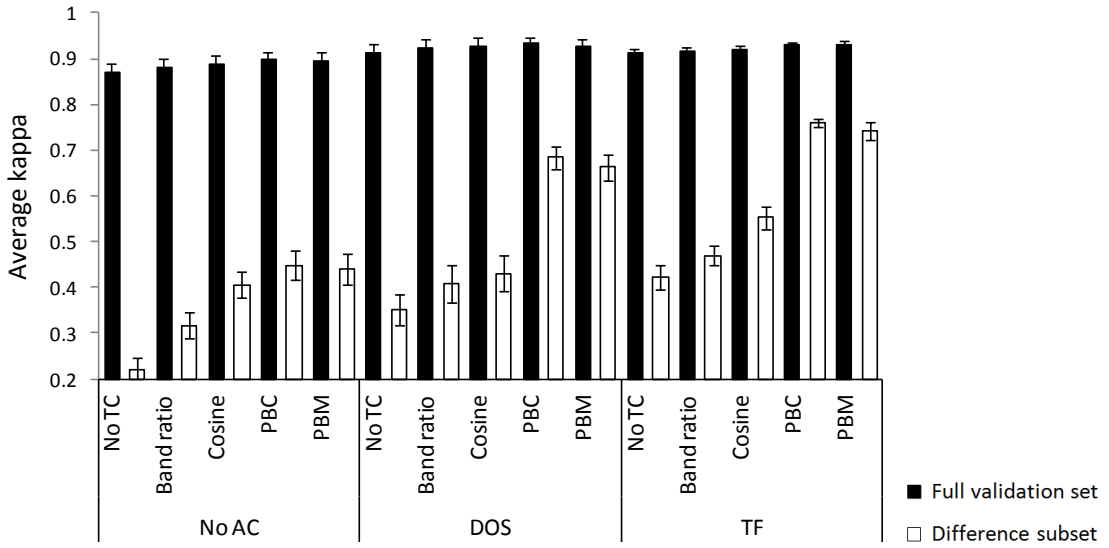

Figure 5.6.: Average kappa coefficients of the 2009 and 2010 images using the full validation set (black) or difference subset (white) of the 15 combinations of corrections. The range of classification accuracies between both dates is shown through the whiskers on the bars (Vanonckelen et al., 2013).

To illustrate the effect of the different combinations, outputs of three representative techniques are shown for the 2009 land cover maps in Figure 5.7: the baseline scenario (i.e. the uncorrected image), a combination with a low classification accuracy (i.e. a TF and cosine combination) and a scenario with high accuracy (i.e. a TF and PBC combination). Figure 5.7a-c shows the resulting true color composites and classified images. The difference in illumination is clearly visible for points 1 and 2 in the composite without correction (Figure 5.7a) and combination of TF and cosine correction causes overcorrection in the visible bands (Figure 5.7b). The TF-PBC correction (Figure 5.7c) reduces the differential illumination effects: the same land cover types have comparable spectral values for similar terrain features on opposite facing slopes. As a result, illumination differences between points 1 and 2 in Figure 5.7c on opposite facing slopes have disappeared. The classification results show no clear differences between land cover maps resulting from the uncorrected (Figure 5.7a) and the TF-cosine corrected image (Figure 5.7b). Table 5.3 shows the percentages of 2009 LC classes for the three combinations of correction methods and confirms this finding. There is only a minor difference of ±3% in the broadleaved and mixed forest class that is hardly to distinguish on the indicated points 3 and 4 in Figure 5.7a and b. Compared to these two maps, the LC map resulting from TF-PBC correction shows less BL and MX forest (Figure 5.7c). This is confirmed by the data in Table 5.3: the decrease in the BL and MX classes after TF-PBC correction and compared to the baseline scenario is respectively 7% and 12%. The BS class is decreasing with 3% and in contrast, the CF and GRASS classes are increasing with respectively 8% and 14%. The difference is also shown by comparison between points 3 and 4 on the LC maps. For point 3, the MX forest type in Figure 5.7 a and b has disappeared and is replaced by CF forest in Figure 5.7c. The dominant BL forest type in point 4 is replaced by grasslands and bare soil in Figure 5.7c.

Table 5.3.: Percentage of the six land cover classes present in 3 combinations of 2009 AC and TC correction methods (%)(Vanonckelen et al., 2013).

	No AC - no TC	TF - cosine	TF - PBC
Broadleaved forest	26	29	19
Bare soil	19	19	16
Coniferous forest	12	11	20
Grassland	15	16	29
Mixed forest	27	24	15
Water surface	1	1	1

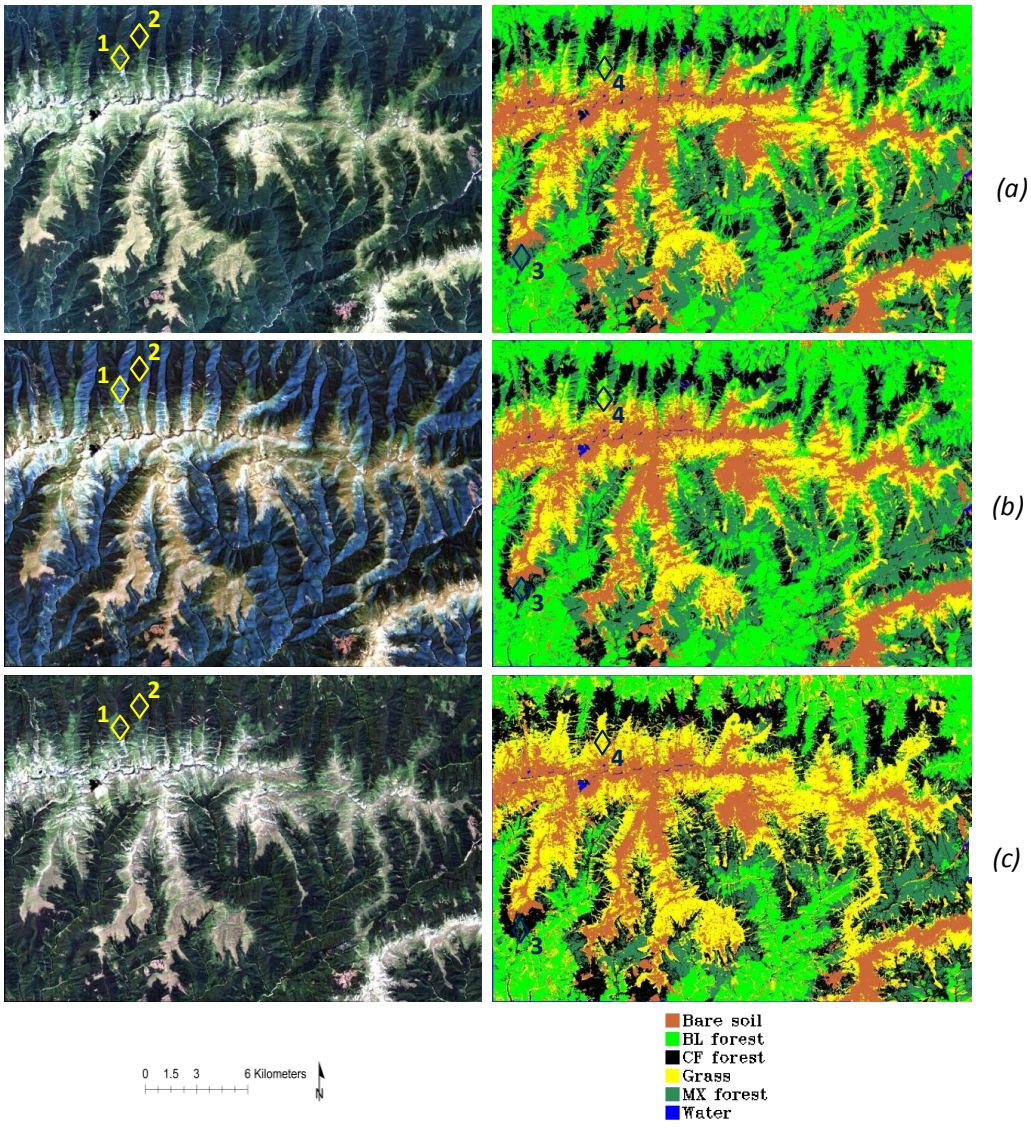

Figure 5.7.: True color composite with a linear stretching (RGB: band 3, 2 and 1) and ML classification of the 2009 image with visualization of contrasting points delineated by numbers 1 and 2: (a) no AC or TC; (b) TF with cosine correction and (c) TF with PBC correction (Vanonckelen et al., 2013).

5.3.3 Class accuracy

Figure 5.8 shows average 2009-2010 *δ*kappa values per class between uncorrected and corrected image using the full validation set for the 14 combinations of corrections and anoverall value per class over the 14 combinations of corrections. The results are included in a bubble chart, in which the size of the bubble represents the average 2009-2010 *δ*kappa value. A red color represents a negative *δ*kappa value and a blue color a positive *δ*kappa value. Positive average *δ*kappa values indicate a more accurate classification of a specific land cover class compared to the baseline scenario. The results show positive average *δ*kappa values for the CF and MX classes which implies that combined corrections improve classification accuracy for these LC categories. The combination of TF-PBM correction produces the best results: increases in average kappa values of respectively 0.17 and 0.18 for the CF and MX forest types. The overall *δ*kappa values over all fourteen correction methods are also shown in Figure 5.8. The overall value increases with 0.09 for the CF and MX forest types and with 0.01 for the GRASS class. For the three other LC types (BS, BL and WT), mapping accuracy is not increasing after correction: difference values of the WT and BL class have not been changed and there is even a small negative overall *δ*kappa value (-0.03) for the BS class.

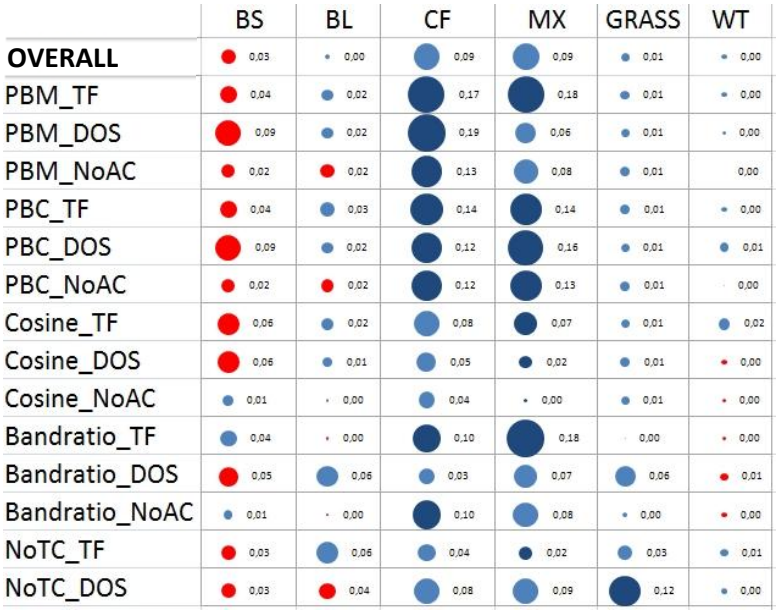

Figure 5.8.: Average 2009-2010 δkappa values per class between uncorrected and corrected image using the full validation set for the 14 combinations of corrections and anoverall value per class over the 14 combinations of corrections. The size of the bubble represents the average 2009-2010 δkappa value. A red color represents a negative δkappa value and a blue color a positive δkappa value. BS = bare soil; BL = broadleaved forest; CF = coniferous forest; MF = mixed forest; GRASS = grassland; WT = water (Vanonckelen et al., 2013).

The average 2009-2010 accuracy of the six classes is also evaluated within the difference area (Figure 5.9). Average *δ*kappa values of the CF and MX forest types are especially improving after correction. The trend for the CF and MX forest class is similar as the trend for the full validation set but almost all average *δ*kappa values have increased. The maximum average *δ*kappa value for the CF class is 0.30 (TF-PBC combination), compared to the maximum average value of 0.17 for the CF class using the full validation set. The MX forest class has a maximum average *δ*kappa value of 0.20 (TF-PBM combination), an increase with 0.02 compared to the maximum average value of 0.18 for the full validation set. Trends for the other classes are not uniform. The overall *δ*kappa values (Figure 5.9) over all fourteen correction methods per LC class are pinpointing to general increases of respectively

0.19 and 0.10 for the CF and MX forest types. For the four other LC types (BS, BL, GRASS and WT), overall *δ*kappa values are not increasing or even slightly decreasing in the difference zone. Compared to the full validation set, BS and GRASS classes are performing slightly worse in the difference zone (overall *δ*kappaof -0.01). The overall class accuracy of WT is slightly positive (0.01) and the BL class is performing equal before and after correction.

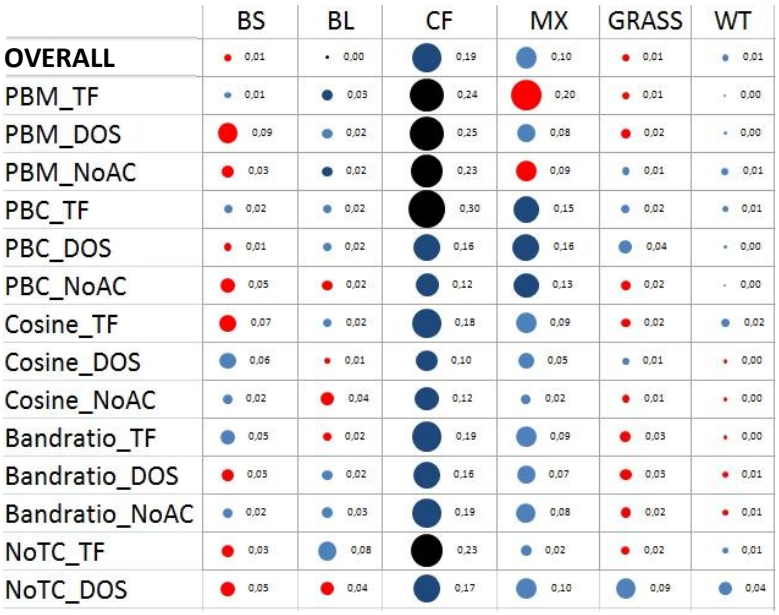

Figure 5.9.: Average 2009-2010 δkappa values per class between uncorrected and corrected image using the validation subset for the 14 combinations of corrections and anoverall value per class over the 14 combinations of corrections. The size of the bubble represents the average 2009-2010 δkappa value. A red color represents a negative δkappa value and a blue color a positive δkappa value. BS = bare soil; BL = broadleaved forest; CF = coniferous forest; MF = mixed forest; GRASS = grassland; WT = water (Vanonckelen et al., 2013).

5.3.4 Illumination conditions

Figure 5.10 shows that the average 2009-2010 accuracy of the uncorrected image is small in the low illumination zone (kappa value of 0.23; range 0.018). After correction the accuracy is improving, especially for the combination of TF-PBC or TF-PBM. For those two combinations, average kappa values are increasing from 0.23 to 0.72 (range respectively 0.011 and 0.012). The range of classification accuracies between both dates is smallest after implementation of the TF with a topographic correction method: 0.013 (band ratioing), 0.014 (DOS), 0.011 (PBC) and 0.012 (PBM). Results in the difference area of the low illumination zone also show that highest average kappa values with lowest ranges are achieved after implementation of TF-PBC (average 0.72; range 0.011) and TF-PBM correction (average 0.72; range 0.012).The same trends are visible in the moderate and high illumination zone. Here, the accuracies are also improving, though the increases are smaller (respectively +0.45 and +0.42 between no AC/TC and TF-PBM) than in the low illumination zone (+0.49 between no AC/TC and TF-PBM). In the moderate zone, the largest improvement in accuracy is an increase in average kappa from 0.33 (baseline scenario; range 0.015) to 0.84 (TF-PBM; range 0.007). Overall, the accuracy is largest in the high illumination zone with average kappa value of 0.85 for the TF-PBM combination (range 0.007).

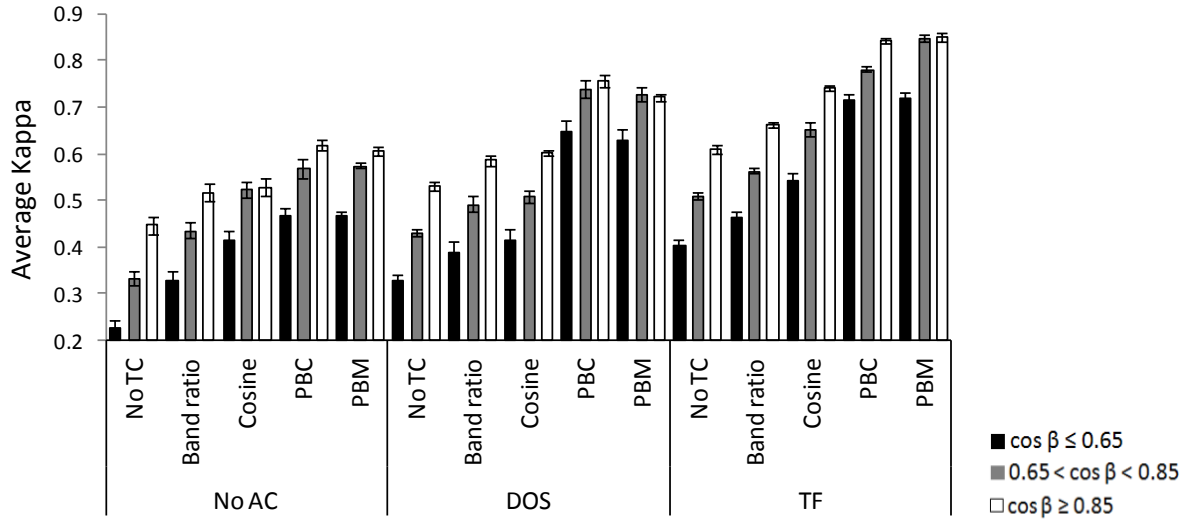

Figure 5.10.: Average kappa coefficients of the 2009 and 2010 images using the 15 combinations of corrections for three different illumination characteristics (black represents the low illumination zone, gray stands for the moderate illumination zoneand white is the high illumination zone). The range of classification accuracies between both dates is shown through the whiskers on the bars(Vanonckelen et al., 2013).

5.4 Discussion

This study provided an impact analysis of fourteen combinations of atmospheric and topographic correction methods on the accuracy of land cover classification. Adding and comparing the effect of AC/TC correction in combination with different classification algorithms would generate so many data and to some extent hide the single effect of AC/TC correction. Therefore, two Landsat-5 TM images from July 24 2009 and August 12 2010 were selected and compared. The characteristics of the study area (steep slopes, no intensive human influence, few roads and low population) were favorable to discourage large changes in land cover between both dates. The land cover classification accuracy under the baseline scenario (no topographic and no atmospheric correction) was relatively high because of the high quality of the Landsat image and the availability of a large number of land cover calibration data that were collected during fieldwork.

First, the differentiation between land cover classes was relatively difficult before correction: there was an overlap between average reflectance values of both dates per land cover type and the differences between average class reflectance values was small (Figure 5.5a). On the contrary, the different land cover spectra of all bands showed less overlap after TF-PBM correction (Figure 5.5b). However, the class separability of the BS class remained poor after correction, which can be explained by the remaining large differences in reflectances after correction (Figure 5.5b) and by location of the bare soil land cover in the landscape. This bare soil land cover class was mainly present at the highest elevations where artifacts were visible in the shaded zones, also after correction (Figure 5.7). Secondly, considering overall accuracies of the full validation set, average kappa values were generally high. The overall high accuracies were achieved through the implementation of a high-quality image and a high number of reference data sampled on the ground by means of field work. The results indicated that average land cover classification accuracy increased more after combined AC/TC correction than when an individual AC or TC correction was

applied. The average kappa coefficients varied between 0.87 for the baseline scenario and 0.94 for TF-PBM correction.

Compared to other studies performed by Hale and Rock (2003), Gitas and Devereux (2004) and Cuo et al. (2010), overall accuracies were high and the increases in accuracy were therefore lower. Comparable results were achieved by a study of Huang et al. (2008). There, overall accuracy increased from 85.5% to 89.7% after a combination of a MODTRAN and SCS correction. Gao and Zhang (2009) described an OA increase from 51% to 91% after a simplified normalization.A small variety in accuracy range between both dates was expected since there were changes between the land cover types of 2009 and 2010. The range in classification accuracy between both dates was larger when no AC was applied (0.017), whereas the range was smallest for TF-PBM correction (0.007). The ranges for the accuracies after DOS (~0.015) and no AC (~0.017) were comparable. However, a larger variability in the range for DOS correction was expected since the overall accuracies were higher after DOS correction. In contrast, a large accuracy range of land cover maps without AC correction was observed since the atmospheric parameters between both images were different. After combined AC and TC correction, there was a smaller range in accuracies since the effect of diverse atmospheres and illumination was removed. In general, the TF-PBC method was performing best with a range of only 0.006.

Thirdly, the class accuracies showed positive average δkappa values for CF and MX classes and no classification improvements for the other land cover classes (BS, BL, GRASS and WT). The study of Zhang et al. (2011) at class level showed that δkappa values of pine forests on sunny and shaded slopes increased by a maximum of about 0.12 using topographically corrected images. On the contrary, δkappa values of oak and mixed forests on sunny and shaded slopes decreased up to 0.7 after correction. The MFM-TOPO correction of Soenen et al. (2008) increased pine class accuracy by 62% over shaded slopes and spruce class accuracy by 13% over moderate slopes. Finally, classification accuracies were evaluated for three illumination conditions separately. Average accuracy of the uncorrected image was smallest in the low illumination zone and largest in the high illumination zone. The largest improvements in accuracy were achieved in the low illumination zone, where the average kappa value increased from 0.23 (baseline scenario; range 0.018) to 0.73 (TF-PBM; range 0.012). This comparison showed that the correction methods performed best on steep slopes in mountain areas.

The composite without correction (Figure 5.7a) showed differences in illumination on opposite slopes. Furthermore, combination of TF and cosine correction (Figure 5.7b) caused an overcorrection in the visible bands. This was explained by the ignorance of the diffuse sky irradiance, resulting in an overestimation of the output radiance data (Teillet et al., 1982). Finally, combination of the TF-PBC and TF-PBM corrections (Figure 5.7c) reduced the differential illumination effects on opposite facing slopes and solved the problem of overcorrection. The natural catena from broadleaved forest on the footslopes over mixed and coniferous forest to grasslands at the highest altitudes (as described in the study area section) was best depicted on the TF-PBC map. This result was explained by the location of the different land cover types in the landscape: the forest classes (BL, MX and CF) covered the steepest slopes dominated by differences in illumination (Figure 5.1a-c). On the contrary, the other land cover types (BS, GRASS and WT) were located on the mountain ridge where illumination was high. As a consequence, it was harder to improve the differentiation between these three land cover classes since the class accuracy before correction was already high. In less mountainous areas and

when atmospheric variables between the dates are larger, atmospheric corrections have a larger impact on classification accuracy. Therefore, it is recommended to invest in AC and TC methods for multi-temporal studies. A balance must be found between the benefits of AC/TC correction in terms of increased classification accuracy and decreased automation potential. Such balance depends on: size of the study area, number of footprints, number and location of available GCPs, location and spectral signatures of the land cover types that need to be mapped.

Considering overall results, the study showed that the most complex combined corrections (TF-PBC and TF-PBM) performed best since these methods simulate the radiance pathway through the atmosphere in the most accurate way. In general, results indicated that the topographic component had a higher influence on classification accuracy than the atmospheric component. This was shown by the difference in overall classification accuracies in Figure 5.6 for the full and difference subset. In a study by Prishchepov et al. (2012), no atmospheric correction was implemented in a multi-temporal analysis since classification accuracy was not significantly improved. The observed accuracy differences were explained by relative large differences in elevation (690 to 2,540 m above mean sea level) and solar elevation angles (respectively 57.8° and 53.8°) between both dates. There were relative small differences in atmospheric parameters (minimum radiance, ambient atmospheric pressure and precipitable water vapor) as described in the preprocessing steps section.In a multi-temporal study with more pronounced variations in atmospheric parameters, the impact AC methods becomes more important.

5.5 Conclusions

A wide range of atmospheric and topographic correction methodologies is available in literature. However, application of combined corrections is labor and data intensive, especially for the most advanced techniques. It is therefore important to examine the added value of these corrections on land cover classification. In this chapter, the added value of fifteen combined corrections (including the scenarios without atmospheric and/or topographic correction) was evaluated on a dataset and based on four criteria: class reflectance separability, overall classification accuracy, class accuracy and illumination specific accuracy. The statistical analysis was performed for two validation sets: a set containing all validation pixels and a subset containing the difference pixels between the classified, uncorrected image and one of the classified, corrected images.

Analysis of average reflectance values per wavelength and land cover type of the uncorrected and corrected images of 2009 and 2010 showed that differentiation between all land cover classes improved after combined correction. The accuracy results also showed that overall classification accuracies of all corrected land cover maps increased after combined correction. Average kappa coefficients for the full validation sets differed between 0.87 for the scenario without corrections (range 0.017) and 0.94 for the atmospheric correction based on transmittance functions (TF) combined with the pixel-based Minnaert (PBM) correction (range 0.023). Higher increases in average kappa values were present for all combined corrections when the difference validation subset was used. The results also indicated that average land cover classification accuracy increased more after combined AC/TC correction than after an individual AC or TC correction. After combined AC/TC correction, the differences in range between both dates and images were removed and an identical

and optimal classification was performed. Results of the class accuracies showed positive average *δ*kappa values for coniferous and mixed classes and no classification improvements for the four other land cover classes. In this study, the impact of combined AC/TC corrections was especially effective to increase the mapping accuracy of the different forest types. AC/TC corrections were less effective in increasing mapping accuracies of land cover types above the tree line since these areas were well illuminated. Considering the analysis in the different illumination zones, combined correction methods performed best in the low illuminated areas. In this study between two dates, results indicated that the influence of the topographic component on classification accuracy was higher than the atmospheric component. This was explained by relative small variations in atmospheric parameters and relative large differences in topographic parameters within the scene.

The topographic component influenced the accuracy more than the atmospheric component. However, it was worthwhile to invest in both atmospheric and topographic corrections in a multi-temporal study. For each application, a balance must be found between the benefits of AC and TC corrections in terms of increased classification accuracy and decreased automation potential of the preprocessing procedure. Furthermore, application of a combined correction based on a complex TC component (PBC or PBM) and a TF atmospheric component was justified in this study. Best overall classification results were achieved after TF-PBM or TF-PBC since the pathway through the atmosphere was simulated in the most accurate way. However, drawbacks of these advanced methods were their data requirements that impeded fully automated application and integration in image preprocessing chains. Further research should focus on the application of the combined corrections to other study areas and larger temporal series.

PART 3: MULTI-TEMPORAL ANALYSIS

Chapter 6: Integration of topographic correction in a pixel-based compositing algorithm and forest cover change detection in the Romanian Carpathian Ecoregion*

*A part of this chapter was presented at the Multitemp 2013 Conference and will be published as:Vanonckelen, S., Griffiths, P., Lhermitte, S., Van Rompaey, A., 2013. Integration of topographic correction in a pixel-based compositing algorithm for large scale land cover mapping. Proceedings of Multitemp 2013, 7th International Workshop on the Analysis of Multi-temporal Remote-Sensing Images, Banff, Alberta, Canada, 26-28 June 2013.

The research in this chapter was carried out in collaboration with Prof. Patrick Hostert and Dr. Patrick Griffiths from the Geography Department at the Humboldt-University in Berlin. The pixel-based compositing procedure was developed, calibrated and applied for the entire Carpathian Mountains by Griffiths et al. (2013). The results from this study build further on their work, by adding a topographic correction after the compositing procedure. The research team of Prof. Hostert is greatly acknowledged for their willingness to share their codes and the time spent on running the procedures including the topographic correction module.

6.1 Introduction

The opening of the Landsat archive in 2009 provided opportunities to reconstruct LULCC for large areas (Loveland and Dwyer, 2012). Apart from the topographic and atmospheric distortions discussed in the previous chapters, large area land cover mapping poses some challenges. Firstly,Landsat footprints have a footprint size of 185 x 185 km which requires image mosaicking for areas larger than one footprint. Secondly, Landsat satellites have a 16-day repeat cycle. However, especially in mountain and tropical areas, it is possible that only a few unclouded footprints are provided per yearly growing season (Ju and Roy, 2008; Griffiths et al., 2013a). This poses a problem since land cover classifications should be based on phenologically consistent datasets (Masek et al., 2006). Finally, data availability can be further limited by discontinuities due to sensor or data related errors (e.g. the failure of scan line correction in Landsat 7; Arvidson et al., 2006). There is a need for accurate, reliable and timely estimates of LULCC at medium scale spatial resolution (30 m; Giri et al., 2013). Therefore, pixel-based image compositing (PBIC) techniques have been developed to improve large area change monitoring at medium spatial resolutions (Gutman et al., 2008).

A PBIC technique selects the most suitable pixel for each location from a series of available source images. The history and principles of PBIC are explained in Chapter 2 (section 2.2.6). The free access to the Landsat archive (Loveland and Dwyer, 2012), 16-day repeat cycle, extended Landsat operation time (Ju and Roy, 2008), revised Landsat calibration (Chander et al., 2010) and improvements in computational resources (Plaza et al., 2011; Richards, 2005) allowed the application of PBIC techniques with Landsat imagery at medium scale resolution. At present, however, it is unknown to what extent the results of PBIC can be improved if topographic preprocessing is applied on the source images. Therefore, a PBIC algorithm is combined with a topographic correction in this chapter, which results in topographically corrected composites based on Landsat source images of target years 1985, 1995 and 2010 covering the Romanian Carpathian Ecoregion. Next, the accuracy of the derived land cover and land cover change maps is examined.

6.2 Study area

As described in Chapter 3, the regional study area is located in the Romanian part of the Carpathian Ecoregion (Figure 6.1). In this figure, the Carpathian Ecoregion is indicated by an irregular polygon and the nine considered Landsat footprints are shown by rectangles.

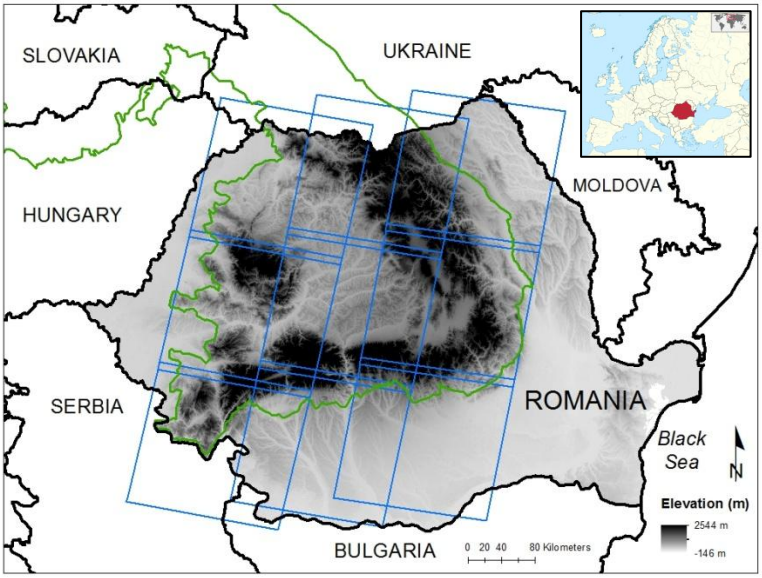

Figure 6.1: Location of Romania in eastern Europe and indication of the Carpathian Ecoregion (irregular polygon) and the nine Landsat footprints comprising the Romanian Carpathian Ecoregion (rectangles). Romania was overlaid with the Shuttle Radar Topography Mission elevation data.

Different studies have examined Romanian land and forest cover changes on a regional and local scale. On a local scale of one Landsat footprint, Knorn et al. (2012a) mapped the land cover in the northern Romanian Carpathians based on 8 topographically uncorrected Landsat TM/ETM+ images between 1987 and 2009. Results suggested that forest disturbances increased, especially in two waves after 1995 and 2005 (Knorn et al., 2012a). Another local scale study by Griffiths et al. (2012) investigated the Romanian forest cover and the influence of forest restitution on an atmospherically corrected Landsat footprint between 1984 and 2010. The results indicated that forest cover increased with 1,100 km² between 1987 and 2010 and increased forest disturbances were observed since 1989.

Local forest cover changes are influenced by different transition trajectories than regional changes. However, the results of the above mentioned local scale studies were confirmed by studies on larger scales. On a national scale, the Global Forest Resources Assessment of FAO (2010) estimated the total Romanian forest area 6,371,000 ha in 1990 and 6,573,000 ha in 2010 (Figure 3.15). Between 1990 and 2000, the forested area declined slightly with ±5,000 ha. Turnock (2002) also observed a decrease in forest cover in the Carpathians after 1989. These forest cover assessments also suggest that this downward trend reversed in 1990: current logging rates are substantially lower than logging rates during and immediately after the communist regime, and forests are expanding on unused or abandoned land (Olofsson et al., 2011). According to FAO (2010), after the minor forest increase of ±25,000 ha between 2000 and 2005, there was a major forest increase of 200,000 ha between 2005 and 2011 (Figure 3.15). New change detection approaches based on time series of Landsat images offer several methodological advantages, including robustness against spectral variations arising

from topography and phenology (Griffiths et al., 2013a). Recently, large scale land cover change mapping across the entire Carpathians based on pixel-based Landsat compositing between 2000 and 2010 has been presented by Griffiths et al. (2013a). Results indicated that the compositing algorithm succeeded in constructing seasonally consistent large area composites (Griffiths et al., 2013a). Based on an atmospherically corrected PBIC between 1985 and 2010, Griffiths et al. (2013b) also examined forest disturbances across the entire Carpathian Ecoregion. Results showed that large changes in forest composition occurred in Romania: coniferous forests decreased with 7% or 197,330 ha between 1985 and 2010, while broadleaved and mixed forests increased with 12% and 2% or respectively 1,095,030 ha and 233,290 ha (Griffiths et al., 2013b). The total forest area increased from 6,027,370 ha in 1985 to 7,158,360 ha in 2010.

However, topographically corrected composites of the Romanian Carpathians are still missing and the influence of topographic correction on large scale pixel-based compositing has not been examined. Therefore, in this chapter, a pixel-based topographic correction was integrated in the compositing algorithm of Griffiths et al. (2013a), applied on the Romanian Carpathians and compared to the topographically uncorrected composites. Results were evaluated by the calculation of overall and land cover specific classification accuracies. Furthermore, land cover changes between 1985, 1995 and 2010 were mapped.

6.3 Materials and methods

In order to test the results of Chapter 5, a pixel-based image composite for each year (1985, 1995 and 2010) was constructed. The basic concepts of a PBIC procedure were already explained in Chapter 2. However, the PBICs were constructed and topographically corrected in this chapter following five steps.

First, all available Landsat TM and ETM+ images from the USGS Landsat archive with a precision terrain correction L1T and covered by less than 70% clouds were considered (Griffiths et al., 2013a). Furthermore, all images acquired within a two year range of the target years 1985, 1995 and 2010, and between mid-February and mid-November (Figure 6.2a). The range of acquisition months was included to avoid low sun elevation angles, shadowing and high snow coverage. Figure 6.2a represents is a simplification of the PBIC procedure since the first step only contains 3 available input images, while in this study more than 1000 images were available for the three years.

Secondly, all footprints were georeferenced and atmospherically corrected with the Landsat Ecosystem Disturbance Adaptive Processing System (LEDAPS) algorithm (Masek et al., 2006) and masked for clouds using the FMASK algorithm (Zhu and Woodcock, 2012). Hereby, georeferencing of all images was crucial since an optimal pixel will be selected for each cell in the next step.

Thirdly, a pixel-based composite was constructed for each year by sampling the most suitable pixel for each cell from the all available imagery (Figure 6.2b). The principle of pixel-based image compositing (PBIC) algorithms has been explained in Chapter 2 (section 2.2.6). In this Chapter, the most suitable observation was selected for each cell based on a suitability assessment that was elaborated by Patrick Griffiths and presented in Griffiths et al. (2013a). This suitability assessment was automated in an ENVI/IDL workflow using scripts. A single value and not an average value was

extracted for each cell, since pixel and scene specific metadata (solar zenith angle, solar azimuth angle, etc.) were also stored for usage in the next steps.

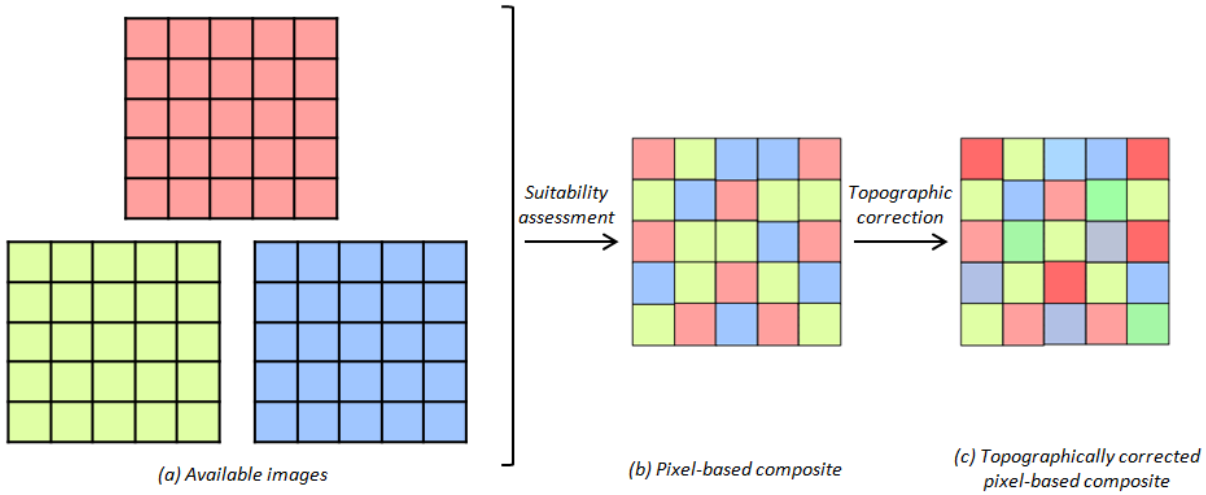

Figure 6.2.: Pixel-based compositing with (a) selection of all available images (in this example there are only 3 images available), (b) construction of the pixel-based composite with selection of the best pixel for each cell after a suitability assessment, and (c) topographically corrected pixel-based composite.

In this study, the suitability for each cell was assessed based on 3 parameters, for which a pixel score was calculated. Afterwards, the total weighting of the pixel scores was obtained. As the study focused on temperate forest mapping, composites with high scoring weights in the period of main photosynthetic activity were preferred. Therefore, images as close as possible to the middle day of year - namely day 183 which is an approximation of the peak leaf-on state in Romania - were selected. Normally, day 183 is each year on July 2, except for a leap year. For each pixel, the suitability was assessed based on scoring weights for three parameters: day of year (DOY, i.e. seasonal suitability), acquisition year (i.e. annual suitability), and distance of a pixel to the next cloud (i.e. risk of atmospheric disturbance) (Griffiths et al., 2013a). Highly suitable pixels have: (1) a DOY nearby 183, (2) an acquisition year close to 2010, and (3) no adjacent clouds. The different factors were weighted according to a flexible parametric weighting scheme proposed by Griffiths et al. (2013a). In this weighting scheme, scores were calculated according to the year median DOY, preferred seasonal window and the distance to clouds. Next, the scores were summed up andafter selection of the pixels with the highest final score, the composite was constructed for the 6 spectral bands (Griffiths et al., 2013a). The PBIC procedure was applied on the total Landsat archive to generate three composites for target years 1985, 1995 and 2010.

Fourthly, an alternative composite was constructed by correcting the pixel-based composite for shadowing effects due to topography (Figure 6.2c). The selection of the appropriate topographic correction method for implementation and automation in an image processing chain is not straightforward since the most complex methods demand the highest number of input data. The automation potential of corrections normally decreases with the number and complexity of input data. Therefore, it is possible to define a complexity range in the input data: (a) single value input parameters available in image metadata (e.g. solar zenith and azimuth angle), (b) single value input parameters available in external data sources (e.g. sea-level atmospheric pressure, slope and azimuth angle), (c) single value input parameters derived from regression models (e.g. *k*- and *C*-factor), and (d) data layers available in external data sources (e.g. DEM and NDVI). In a previous study

by Vanonckelen et al. (2013), three atmospheric and five topographic corrections were applied in all possible combinations on two Landsat acquisition (2009 and 2010) in the Romanian Carpathians. The results showed that a pixel-based Minnaert correction (PBM) resulted in a more accurate detection of land cover in mountain areas. Therefore, the pixel-based compositing procedure was combined with a PBM correction as shown in Figure 6.2c. The PBM of Chapter 4 and 5 implemented a regression analysis between cos ϑ and (un)corrected radiances for each band based on selected sample data. This sampling scheme and regression analysis was impossible to include in the automated PBIC procedure. Therefore, the topographic part of the ATCOR3 correction described in Chapter 4 (section 4.3.3) was included in this analysis.

The differentiation between vegetation and non-vegetation in this Chapter was based on the pixel-based NDVI value (Equation 6.1). In this study, an NDVI value lower than 0.7 was considered as non-vegetation and a higher value as vegetation. This threshold value was determined by trial and error runs, field knowledge and comparison of the outputs with existing vegetation maps. Thereby, the threshold value 0.7 was the best boundary between vegetation and non-vegetation.

$$NDVI = \frac{\rho_{NIR} - \rho_{red}}{\rho_{NIR} + \rho_{red}} \tag{6.1}$$

where ρ_{red} and ρ_{NIR} are reflectance measurements in % for the red and NIR bands.

The lower boundary threshold of the factor $(\cos\beta / \cos\vartheta_T)^b$ prevents an excessive reduction of the reflectances if the local solar zenith angle is substantially higher than the threshold angle (Richter and Schläpfer, 2013). Though a value of 0.25 is the standard threshold (Richter et al., 2009), the user is encouraged to optimize the parameter to obtain adequate results for a specific study area (Balthazar et al., 2012). In this study, an optimal lower boundary of 0.05 was derived by trial and error. Thereby, especially under- and overcorrection problems were improved in the natural and false color composites.

Finally, based on the generated composites, large scale land cover maps were compiled for the three target years using the Maximum Likelihood (ML) and Support Vector Machine (SVM) classifiers. The ML was explained in Chapter 5. The non-parametric and supervised SVM is well suited to map spectrally complex classes, such as in forest change analysis (Vapnik, 1999; Melgani and Bruzzone, 2004; Huang et al., 2008). The basic principle of a SVM classifier is to identify a hyperplane that optimally separates two classes in the feature space. The hyperplane is constructed in an iterative way by maximizing the distance among class boundaries (Huang et al., 2002; Pal and Mather, 2005; Foody et al., 2007; Alcantara et al., 2012). To determine this hyperplane, only the edges between the class distributions are described based on a relatively small amount of training data (Foody and Mathur, 2004; Mathur and Foody, 2008). SVMs are non-parametric classifiers since the distribution of the training data is not modeled (Anthony et al., 2008). In contrast to parametric classifiers such as ML, the different classes are separated by directly searching for adequate boundaries between the classes (Keuchel et al., 2003).

SVMs frequently outperform other non-parametric and parametric classifiers (Foody and Mathur, 2004) while requiring few training data (Huang et al., 2002; Pal and Mather, 2005; Guo et al., 2005; Dixon and Candade, 2008; Knorn et al., 2009). SVMs are well suited to separate multimodal classes, which are difficult for parametric-based classifiers to classify accurately due to the violation of the

assumption of a normal distribution of reflectance values within one class (Foody and Mathur, 2004; Pal and Mather, 2005; Kuemmerle et al., 2009a; Prishchepov et al., 2012). To separate classes with non-linear boundaries, kernel functions are used to transform training data into a higher-dimensional space, where linear class separation is possible (Huang et al., 2002). SVMs have been successfully applied to map forest cover changes over large areas (Huang et al., 2008; Kuemmerle et al., 2008b, Sieber et al., 2013).

The parametric ML classifier was implemented using ENVI/IDL and the EnMAP Box software to differentiate 8 land cover classes (Table 6.1): arable land, bare soil, urban land, grassland, water and forest. Since the dominant LC class in this study area was forest, this class was divided in three categories: broadleaved, coniferous and mixed forest. The ML classifier of 2010 was trained with randomly sampled points from three different sources: (1) GCP-collection during field visits in May 2010 and July 2011, (2) GCP-identification on high-resolution satellite imagery (WorldView-2, 8 bands, 46 cm resolution, acquisition date October 13, 2010), and (3) GCP-identification on high resolution imagery from Google Earth. An average of 800 training points was randomly sampled per land cover class with a minimum distance of 1 km to minimize spatial autocorrelation (Campbell, 1981; Labovitz and Masuoka, 1984), except for the water class since the study area lacked large water bodies (Table 6.1). About 500 training points were sampled for the relative less present classes water and urban. Points were gathered systematically in order to collect the spectral range of the different classes. For the scenarios of 1985 and 1995, ground truth data were unavailable. In order to train the ML classifier, the 2010 training data were selected and verified on false and natural color composites of the 1985 and 1995 pixel-based composites. Training was performed with ±90% of the samples and validation with the remaining ±10%.

Table 6.1.: Land cover classes, code, dominant species and average training and test samples in the study area.

Land cover classes	Code	Dominant species	Average training samples	Average test samples
Arable land	AR	/	900	100
Broadleaved forest	BL	*Carpinus betulus, Fagus sylvatica, Quercus petraea Quercus robur*	900	100
Bare soil	BS	/	900	100
Coniferous forest	CF	*Abies alba, Picea abies, Pinus mugo, Pinus sylestris*	900	100
Grassland	GRASS	/	900	100
Mixed forest	MX	*Mixture of the dominant BL and CF forest species*	900	100
Urban land	UR	/	500	50
Water surface	WT	/	500	50

Urban land (UR), arable land (AR), bare soil (BS), grassland (GRASS), water (WT), and broadleaved (BL), coniferous (CF) and mixed forest (MX). Mixed forests are stands where neither broadleaved nor coniferous trees account for more than 75% of the tree crown area (UN-ECE/FAO, 2000). Arable land is the land under temporary agricultural crops (multiple-cropped areas are counted only once). The abandoned land resulting from shifting cultivation is not included in this category (FAOSTATS, 2013b).

The SVM classifier was implemented to discern the 8 land cover classes of Table 6.1. Furthermore, all non-forest classes were grouped and SVM classification was performed on only 4 land cover classes: non-forest, broadleaved forest, mixed forest, and coniferous forest. A similar and successive separation of classes was performed by Griffiths et al. (2013b), Main-Knorn et al. (2013) and Olofsson

et al. (2013). The SVM training and validation principles were similar as ML classification. However, the SVM classifier for 2010 was trained with randomly sampled points based on high resolution imagery from Google Earth. About 900 training points were sampled for the three forest classes and 2000 points for the non-forest class. Validation was performed with independently and randomly sampled GCP points from two sources: fieldwork and high-resolution WorldView-2 imagery. The SVM parameterization, image classification, and accuracy assessment was carried out with the EnMAP Box software (www.hu-geomatics.de).

In order to evaluate the results, overall accuracy (OA) and land cover specific producer's and user's accuracies were assessed as presented by Congalton (1991) and Foody (2002). The accuracies were assessed for five different scenarios:

1) ML with 8 classes – topographically uncorrected;
2) ML with 8 classes – topographically corrected;
3) SVM with 8 classes – topographically corrected;
4) SVM with 4 classes – topographically uncorrected.
5) SVM with 4 classes – topographically corrected.

Finally, the main land cover trends related to forest cover changes were mapped and areal statistics were calculated for the two periods: 1985-1995 and 1995-2010. Table 6.2 summarizes the different land cover change types that were included in the main land cover trends: stable broadleaved forest, stable mixed forest, stable coniferous forest, deforestation, afforestation, disturbance and non-forest. Afforestation is the establishment of trees on land that is not covered by forest (IPCC, 2013). The disturbance class contains the conversions from one forest class in another forest class.

Table 6.2.: The land cover change types that were included in the main land cover trends

Land cover trend	Land cover change types
Stable BL	BL-BL
Stable MX	MX-MX
Stable CF	CF-CF
Deforestation	BL-NF, MX-NF, CF-NF
Afforestation	NF-BL, NF-MX, NF-CF
Disturbance	CF-BL, BL-CF, CF-MX, MX-CF, BL-MX, MX-BL
Non-forest	All other land cover change types

Broadleaved forest (BL), mixed forest (MX), coniferous forest (CF) and non-forest (NF).

6.4 Results

6.4.1 Land cover accuracies

The classification accuracy matrices of the topographically uncorrected ML classification of 1985, 1995 and 2010 are presented in Table 6.3. The produced land cover maps have overall accuracy values of 66% (1985), 75% (1995) and 78% (2010). The highest producer's accuracies are present in the CF and UR classes, with accuracy values ranging between 85% to 89%, and 82% to 99% respectively. The accuracies are lowest for the AR and MX classes, with producer's accuracies ranging from 44% till 57% and from 54% till 60%, respectively. The results of Table 6.3 indicate that especially the differentiation between the AR, BS and GRASS classes is less accurate, which is indicated by the

low producer's and/or user's accuracy (PA and UA) values. This can be explained by a similar spectral signature of these three land cover classes since arable lands are regularly left fallow and hayfields or grasslands are hard to distinguish from arable lands. In contrast, the classification accuracy of the forest classes (BL, MX and CF) is relatively high. Also the WT and UR classes are consistent land cover types with high producer's accuracies ranging between 82% and 99% since both land cover classes have a specific and easily discernable spectral signature. Finally, a remarkable trend in the accuracy of the AR class is noticeable: the producer's accuracy is decreasing from 57% in 1985 to 44% in 2010. In the final stage, 33% from the AR class is classified as the GRASS class (Table 6.3).

Table 6.3.: Classification accuracy assessment of a topographically uncorrected Maximum Likelihood classification of 1985, 1995 and 2010 (separated by commas and in %).

Reference	**Classification**							
	AR	BL	BS	UR	CF	GRASS	MX	WT
AR	*57,58,44*	2,1,1	2,7,6	6,5,2	0,1,0	6,4,5	2,2,2	3,2,0
BL	2,3,2	*77,92,88*	0,3,0	0,0,0	0,0,0	8,4,3	5,4,14	0,0,0
BS	13,13,13	6,0,1	*64,61,72*	4,5,5	1,1,0	4,3,3	3,2,0	4,1,0
UR	7,5,3	0,0,0	5,5,13	*83,86,90*	0,1,1	0,0,0	1,1,0	4,2,0
CF	2,0,0	1,0,1	9,8,1	1,0,0	*89,85,88*	2,0,0	25,25,29	4,0,0
GRASS	17,14,33	7,5,1	16,13,8	0,0,0	1,0,0	*74,85,87*	3,2,0	2,0,0
MX	2,5,2	7,1,8	0,1,0	0,1,0	8,10,11	5,4,1	*60,64,54*	0,0,0
WT	1,3,2	0,0,0	3,1,0	4,2,1	1,1,0	0,2,0	1,0,0	*82,93,99*
PA	57,58,44	77,92,88	64,61,72	83,86,90	89,85,88	74,85,87	60,64,54	82,93,99
UA	94,60,61	29,45,51	62,88,90	51,77,75	52,64,75	39,61,64	56,66,69	89,95,97
OA								**66,75,78**

Urban land (UR), arable land (AR), bare soil (BS), grassland (GRASS), water (WT), and broadleaved (BL), coniferous (CF) and mixed forest (MX). Producer's Accuracy (PA), User's Accuracy (UA) and Overall Accuracy (OA). Note: accuracy values are provided as integers, consequently it is possible that the sum over all land cover classes is not exactly 100.

Table 6.4 presents the classification accuracy matrices of the topographically corrected ML classification of 1985, 1995 and 2010. Compared to the uncorrected ML classification (Table 6.3), the overall accuracy values have increased with respectively 4% (1985), 4% (1995) and 3% (2010). Furthermore, the accuracies of the classes with lowest PA values in Table 6.3 (AR, BS and MX) show a larger accuracy increase compared to the other land cover types.

Table 6.4.: Classification accuracy assessment of a topographically corrected Maximum Likelihood classification of 1985, 1995 and 2010 (separated by commas and in %).

Reference	**Classification**							
	AR	BL	BS	UR	CF	GRASS	MX	WT
AR	*60,62,48*	2,1,1	2,6,5	5,2,3	0,1,0	5,4,4	3,1,2	3,2,1
BL	2,3,2	*80,91,88*	0,4,1	0,1,1	2,1,0	6,4,4	5,7,11	1,0,0
BS	12,10,14	7,0,1	*67,64,73*	5,5,3	1,2,0	3,2,2	4,2,3	3,1,1
UR	5,6,4	0,0,0	7,5,13	*85,85,91*	0,1,1	1,1,0	1,1,2	4,0,1
CF	4,2,2	1,2,2	8,7,1	1,0,0	*89,84,88*	2,1,1	17,22,23	3,1,0
GRASS	14,10,26	8,3,1	12,12,9	1,1,1	1,0,0	*77,88,87*	3,2,1	2,1,0
MX	2,6,3	7,1,7	1,0,1	0,1,1	8,10,10	5,3,1	*62,65,57*	0,0,0
WT	1,4,1	0,0,0	3,1,1	3,2,0	1,1,1	0,3,1	1,0,0	*84,94,97*

PA	60,62,48	80,91,88	67,64,73	85,85,91	89,84,88	77,88,87	62,65,67	84,94,97	
UA	89,59,64	37,46,53	66,87,91	60,75,76	57,64,77	41,56,64	57,63,69	87,95,97	
OA									**70,79,81**

Urban land (UR), arable land (AR), bare soil (BS), grassland (GRASS), water (WT), and broadleaved (BL), coniferous (CF) and mixed forest (MX). Producer's Accuracy (PA), User's Accuracy (UA) and Overall Accuracy (OA). Note: accuracy values are provided as integers, consequently it is possible that the sum over all land cover classes is not exactly 100.

The classification accuracy matrices of the topographically corrected SVM classification of 1985, 1995 and 2010 are presented in Table 6.5. Compared to the uncorrected SVM classification (Table 6.4), there is a small increase in overall accuracy with respectively 3% (1985), 0% (1995) and 1% (2010). The low producer's accuracies of the AR, BS and GRASS classes in Table 6.5 indicate that the differentiation between the classes is still hard. The misclassification between these classes has improved compared to the ML classifier and uncorrected scenarios, but remains problematic. Since this study is focusing on forest cover dynamics, all non-forest classes were grouped in a 'non-forest' class and the classification analysis was performed on the topographically uncorrected and corrected SVM scenarios.

Table 6.5.: Classification accuracy assessment of a topographically corrected Support Vector Machine classification of 1985, 1995 and 2010 (separated by commas and in %).

Reference	**Classification**							
	AR	BL	BS	UR	CF	GRASS	MX	WT
AR	*61,61,50*	2,1,1	3,6,3	4,2,2	1,2,0	5,4,4	4,1,1	4,2,1
BL	2,3,2	*81,91,88*	0,5,1	1,1,1	0,1,1	5,3,5	3,7,9	1,0,0
BS	10,10,13	5,0,0	*69,63,74*	3,5,2	2,1,0	4,2,2	5,2,1	3,1,0
UR	4,5,3	1,1,0	5,5,13	*86,85,93*	0,1,1	1,1,1	1,1,3	3,0,0
CF	5,1,2	2,3,3	9,8,1	1,0,0	*89,84,90*	2,0,1	17,19,23	3,1,0
GRASS	14,11,24	5,3,2	11,11,8	0,1,0	0,0,1	*77,89,88*	3,2,1	1,0,0
MX	1,4,3	6,1,6	2,1,1	0,1,1	7,10,7	4,5,0	*65,67,61*	0,0,0
WT	1,4,1	0,0,1	1,1,2	2,2,1	1,1,1	1,3,1	1,1,0	*85,95,98*
PA	61,61,50	81,91,88	69,63,74	86,85,93	89,84,90	77,89,88	65,67,61	85,95,98
UA	89,59,63	36,45,52	65,87,91	60,75,76	58,64,76	76,79,87	58,64,70	88,95,98
OA								**73,79,82**

Urban land (UR), arable land (AR), bare soil (BS), grassland (GRASS), water (WT), and broadleaved (BL), coniferous (CF) and mixed forest (MX). Producer's Accuracy (PA), User's Accuracy (UA) and Overall Accuracy (OA). Note: accuracy values are provided as integers, consequently it is possible that the sum over all land cover classes is not exactly 100.

Table 6.6 shows the classification accuracy matrices of the topographically corrected SVM classification of 1985, 1995 and 2010 with 4 land cover classes. Compared to the uncorrected SVM classification with 8 classes (Table 6.4), there is a large improvement in overall accuracy with respectively 10% (1985), 4% (1995) and 7% (2010). The accuracies of the three forest classes has increased, but the largest increase is present in the non-forest (NF) class. This increase is explained by the omittance of the AR, GRASS and BS classes, which were hard to differentiate between each other. In Table 6.6, the MX forest class has the lowest producer's accuracies ranging between respectively 70% (1985), 67% (1995) and 85% (2010).

Table 6.6.: Classification accuracy assessment of a topographically uncorrected Support Vector Machine classification of 1985, 1995 and 2010 (separated by commas and in %).

Reference	**Classification**				
	NF	BL	MX	CF	
NF	*82,81,94*	8,2,4	5,5,1	1,4,1	
BL	7,6,9	*84,97,89*	8,6,4	1,1,3	
MX	3,6,2	2,1,5	*70,67,85*	1,10,10	
CF	5,7,1	5,0,1	17,23,9	*89,86,87*	
PA	82,81,94	84,97,89	70,67,85	89,86,87	
UA	93,94,90	75,85,83	57,61,80	63,78,74	
OA					**83,83,89**

Non-forest (NF), broadleaved forest (BL), coniferous forest (CF) and mixed forest (MX). Producer's Accuracy (PA), User's Accuracy (UA) and Overall Accuracy (OA). Note: accuracy values are provided as integers, consequently it is possible that the sum over all land cover classes is not exactly 100.

The classification accuracy matrices of the topographically corrected SVM classification with 4 land cover classes of 1985, 1995 and 2010 are presented in Table 6.7. Compared to the uncorrected SVM classification with 4 classes (Table 6.6), the overall classification accuracies increase with respectively 2% (1985), 0% (1995) and 2% (2010). The CF forest class has the highest producer's accuracies (respectively 92%, 86% and 88%) and the MX forest class shows the lowest PAs (respectively 72%, 66% and 86%).

Table 6.7.: Classification accuracy assessment of a topographically corrected Support Vector Machine classification of 1985, 1995 and 2010 (separated by commas and in %).

Reference	**Classification**				
	NF	BL	MX	CF	
NF	*85,83,97*	7,1,2	5,5,1	1,4,1	
BL	5,5,1	*85,97,89*	6,5,4	0,1,1	
MX	3,5,1	1,2,8	*72,66,86*	6,10,11	
CF	4,6,1	6,0,1	17,25,10	*92,86,88*	
PA	85,83,97	85,97,89	72,66,86	92,86,88	
UA	98,96,93	76,85,84	59,62,81	64,77,75	
OA					**85,83,91**

Non-forest (NF), broadleaved forest (BL), coniferous forest (CF) and mixed forest (MX). Producer's Accuracy (PA), User's Accuracy (UA) and Overall Accuracy (OA). Note: accuracy values are provided as integers, consequently it is possible that the sum over all land cover classes is not exactly 100.

6.4.2 Land cover maps

As expected, the classification accuracies of the composites with 8 land cover classes (Table 6.3, 6.4 and 6.5) are lower than the accuracies with only 4 land cover classes (Table 6.6 and 6.7). Furthermore, since the differences in classification accuracy of the topographically uncorrected and corrected SVM composites with 4 classes are small and especially visually difficult to analyze, only the resulting land cover maps of the topographically composites 1985, 1995 and 2010 are presented in Figures 6.3a, b and c. Figure 6.3a presents the land cover map of 1985. The Romanian Carpathian

mountain range is dominated by the forest classes, with broadleaved forest in light green, coniferous forest in dark green and mixed forest in between. Lower elevated areas - located in the centre and northwest corner of the map - are dominated by the non-forest class, especially arable land and grassland. In general, no major changes are present in the three figures. However, it is possible to discern a gradual greening of some areas in 1995 (Figure 6.3b) and 2010 (Figure 6.3c). In order to support the visual results, the statistics of the land cover types were calculated and presented.

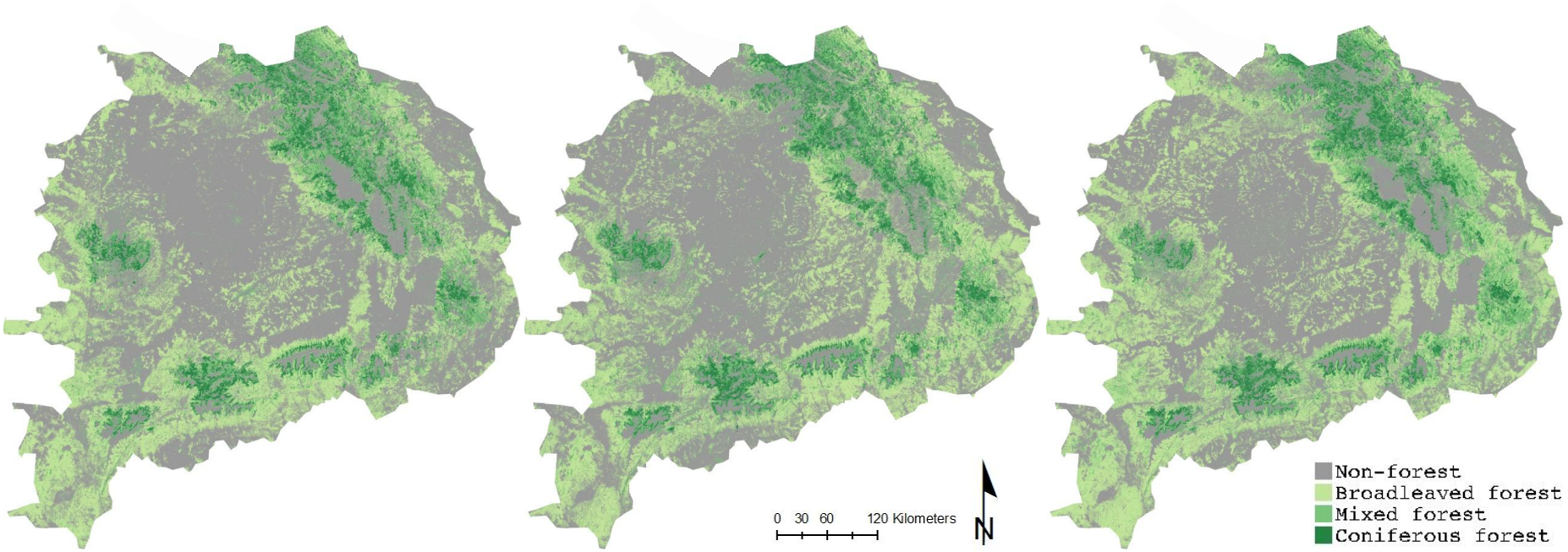

Figure 6.3.: Land cover maps in the Romanian Carpathian Ecoregion of (a) 1985, (b) 1995 and (c) 2010.

Figure 6.4 shows the statistics in percentage of the topographically corrected SVM classification with 4 land cover classes in the Romanian Carpathian Ecoregion. The general trends between 1985 and 2010 show a decrease of ±5% in the non-forest class and consequently a similar increase in the forest class. In 1985, the land cover map consisted for 57% of NF, 27% of BL, 10% of MX and 7% of CF. Compared to 1985, Figure 6.4 denotes an increase in the BL and MX forest cover classes in 1995 and 2010. The CF forest class remains stable. The increase from 10% to 13% between 1985 and 2010 was largest in the mixed forest class, followed by an increase from 27% to 29% in the similar period for the BL class. In contrast, CF forest remained stable between 1985 and 2010, with a minor increase between 1985 and 1995.

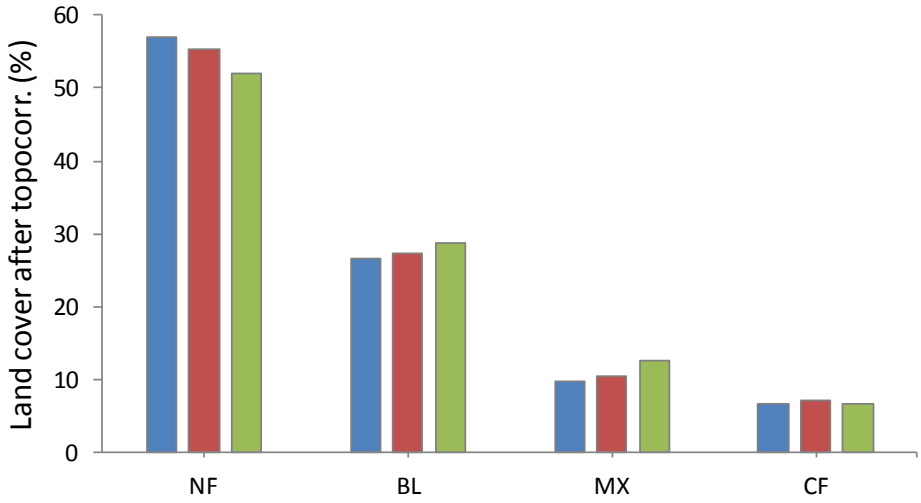

Figure 6.4.: Statistics of the cover change maps of 1985, 1995 and 2010 in the Romanian Carpathian Ecoregion. The average standard deviation over all land cover types and bands for the 3 years was respectively 1.85 for 1985, 1.64 for 1995 and 1.38 for 2010. Non-forest (NF), and broadleaved (BL), mixed (MX) and coniferous (CF) and forest.

In Table 6.8, these statistics are also summarized in ha for the Romanian Carpathian Ecoregion. The non-forest class accounts for more than half of the surface area, followed by the BL, MX and CF class. The decrease in the non-forest class between 1985 and 2010 (-516,072 ha) is especially compensated by an increase in the BL and MX forest classes with respectively increases of 302,784 ha and 217,162 ha. The CF forest class experienced a small decline of 3,874 ha between 1985 and 2010. Table 6.8 also shows that the total forest area increased from ±4,614,864 ha in 1985 to ±5,130,936 ha in 2010.

Table 6.8.: Land cover area in ha of the 4 land cover classes of 1985, 1995 and 2010.

Land cover area (ha)	**1985**	**1995**	**2010**
NF	6,100,236	5,927,443	5,584,164
BL	2,859,076	2,920,346	3,076,238
MX	1,034,334	1,111,709	1,337,118
CF	721,453	755,602	717,579
Total forest	4,614,864	4,787,657	5,130,936

Broadleaved forest (BL), mixed forest (MX), coniferous forest (CF) and non-forest (NF).

6.4.3 Land cover change maps

Based on the topographically corrected SVM classification with 4 land cover classes, land cover change maps between 1985-1995 and 1995-2010 were constructed. In order to assess the spatial pattern of land cover conversions, the main land cover trends related to forest cover changes between 1985, 1995 and 2010 were determined and visualized: afforestation, deforestation and disturbance. Furthermore, the three stable forest classes were included in the change map. Figure 6.5 shows the main land cover trends between 1985 and 2010. Table 6.9 provides an overview of the land cover change types that were included in the main land cover trends.

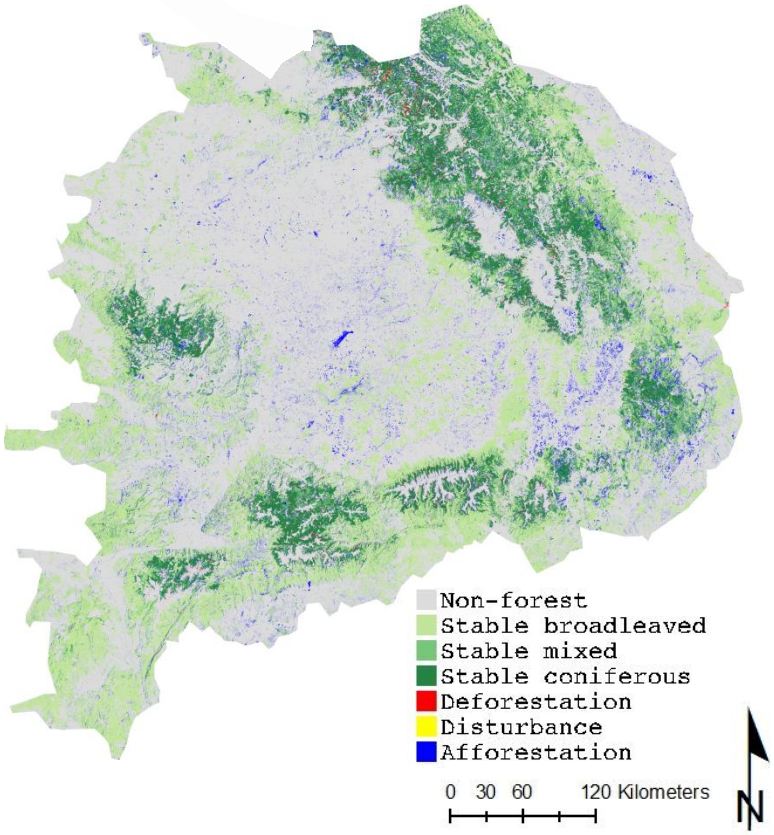

Figure 6.5.: Non-forest (grey), stable broadleaved, mixed and coniferous forest (green), deforestation (red), disturbance (yellow) and afforestation (light green) between 1985-1995.

Table 6.9.: The main land cover trends and their areal change between 1985-1995 and 1995-2010 (in ha).

Land cover trend	**Area 1985-1995 (ha)**	**Area 1995-2010 (ha)**
Stable BL	2,287,758	2,467,323
Stable MX	1,089,086	1,267,481
Stable CF	1,020,613	997,483
Deforestation	292,383	322,380
Afforestation	426,086	478,727
Disturbance	54,653	34,368
Non-forest	5,544,520	5,147,338

Broadleaved forest (BL), mixed forest (MX), coniferous forest (CF) and non-forest (NF).

The 1985-1995 change map shows that the forest classes remain fairly stable with ±2 million ha of stable BL forest and ±1 million ha of stable MX and CF forest. In contrast, the land cover change types

- deforestation, afforestation and disturbance – are underrepresented. The afforestation class covers about 425,000 ha (blue color in Figure 6.5) and occurs mainly in lower elevated areas or at the edges of the stable forests in higher elevated areas. The Carpathian Ecoregion was greening in the period 1985-1995 since deforestation is lower than afforestation and is only occurring on ±290,000 ha (red color in Figure 6.5). The disturbance class is hard to distinguish in Figure 6.5 (yellow color), since it only accounts for ±55,000 ha and shows a scattered pattern nearby the edges of the stable forest classes.

The change map of 1995-2010 in Figure 6.6 shows an increased presence of deforestation and afforestation. Deforestation is especially present in the southern and western corners of the Carpathian Ecoregion and accounts for ±320,000 ha. The afforestation class covers about 479,000 ha in Figure 6.6. Both land cover trends occur mainly at the fringes of the stable forests. Furthermore, the NF class between 1995 and 2010 decreased with about 400,000 ha compared to the period 1985-1995. Compared to 1985-1995, the stable BL and CF forest classes increased in the second change period, with a presence of ±2.5 million ha of stable BL forest and ±1.25 million ha of stable CF forest. The disturbance class only accounted for ±35,000 ha.

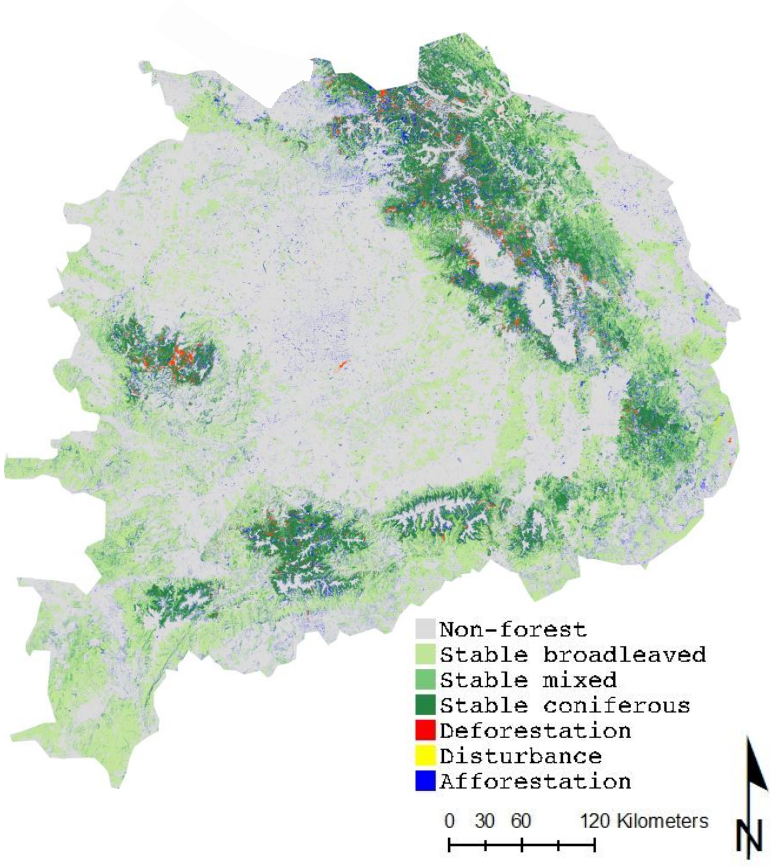

Figure 6.6.: Non-forest (grey), stable broadleaved, mixed and coniferous forest (green), deforestation (red), disturbance (yellow) and afforestation (light green) between 1995-2010.

6.5 Discussion

Hitherto, forest cover dynamics in the Romanian Carpathians were described by means of local scale case studies and topographically corrected Landsat composites were missing at regional scale. In this chapter, classification accuracies were assessed for five different scenarios in which 3 components were altered: classifier (ML or SVM), number of classes (4 or 8) and topographic correction (uncorrected or corrected).

First, land cover accuracies were assessed and compared for the five scenarios. The topographically uncorrected classification for 8 land cover classes resulted in overall accuracies of respectively 66% (1985), 75% (1995) and 78% (2010). The topographic correction improved the ML classification with respectively 4% (1985), 4% (1995) and 3% (2010). Therefore, a SVM classification was performed on the topographically corrected composites which resulted in an accuracy increase of respectively 3% (1985), 0% (1995) and 1% (2010). These results presented an indication that the implementation of a topographic correction had a smaller influence on the classification accuracies than the selection of a classifier. Compared to the results of Chapter 5, the accuracies were lower and the influence of the topographic correction was less pronounced. This was mainly explained by: (1) the larger extent of and more heterogeneous land cover classes in the study area of Chapter 6, and (2) the overall less pronounced topography in the study area of Chapter 6. In contrast, Chapter 5 only assessed accuracy values for one Landsat footprint located in a steeper study area of the Romanian Carpathian mountains.

Therefore, the influence of topographic correction on classification accuracy was larger. Furthermore, Chapter 5 only examined the accuracy for six land cover classes, compared to eight land cover classes in Chapter 6. The arable land and urban class were not included in Chapter 5, which resulted in higher accuracies since especially the subtle differentiation between arable land and grassland was not included. However, the overall accuracy of the land cover maps produced in this study were higher than a similar large scale study of Griffiths et al. (2013a) which obtained an OA of 65% for the pixel-based image composites without topographic correction. Furthermore, UA values were ranging between 9% and 94%, and PA values varied between 36% and 96%. For example, the UA for the PBIC of grassland was 14%, the PA was 50% and bare soil class was not included in the analysis of Griffiths et al. (2013a). Another local scale study on one multi-temporal Landsat TM footprint in Oregon by Kennedy et al. (2007) selected the most suitable pixels based on the temporal signatures of spectral values that are associated with different land cover changes. Here, the automated method labeled the year of disturbance with 90% overall accuracy in clear-cuts and with 77% accuracy in partial-cuts.

Nevertheless, even after optimization of the classifier and inclusion of a topographic correction procedure, the identification of 8 different land cover types, still involved considerable levels of uncertainty. Especially the differentiation between the classes arable land, bare soil and grassland resulted in low producer's and/or user's accuracy values. This low separation of land cover classes is caused by similar spectral signatures of these three land cover classes. Since only one optimal pixel near the median DOY of 183 was selected for each year, phenology-related errors due to missing effects of crop cycles were included in the analysis. In a comparable analysis of Griffiths et al. (2012) on one Romanian Landsat footprint, the acquisition dates of some images between mid-October and

late-May explained lower accuracies due to strong phenology and illumination differences. Therefore, future versions of the PBIC algorithm should address the potential of different phenology measures by including specific temporal and spectral observations (Griffiths et al., 2012). The accuracies of the classes with lowest accuracy values before correction (arable land, bare soil and grassland) showed a larger accuracy increase compared to the other land cover types. The accuracies of the topographically uncorrected and corrected Support Vector Machine classifications for 4 land cover classes resulted in significant improvements of the accuracies. Compared to the uncorrected SVM classification with 8 classes (Table 6.4), there was a large improvement in overall accuracy for the scenario with 4 classes of respectively 10% (1985), 4% (1995) and 7% (2010). Furthermore, the influence of the topographic correction was again smaller than the influence of the classifier. Compared to the uncorrected SVM classification with 4 classes (Table 6.6), the overall classification accuracies of the corrected SVM classification increased with respectively 2% (1985), 0% (1995) and 2% (2010).

Generally, the main land cover conversion between 1985-1995 and 1995-2010was the conversion of non-forest in forest. A steady greening of the Romanian Carpathian Ecoregion was observed since afforestation was larger than deforestation in the two periods. Between 1985 and 2010, a decrease of ±5% in the non-forest class was compensated by an increase in the forest class (Table 6.8). The decrease in the non-forest class between 1985 and 2010 (-516,072 ha) was especially compensated by an increase in the BL and MX forest classes with respectively increases of ±302,784 ha and ±217,162 ha. The CF forest class experienced a small decline of ±3,874 ha between 1985 and 2010. Table 6.8 also showed that the total forest area increased from ±4,614,864 ha in 1985 to ±5,130,936 ha in 2010. Griffiths et al. (2013b) examined forest disturbances across the Romanian Carpathian Ecoregion in a similar way. Results showed that large changes in forest composition between 1985 and 2010 occurred in Romania: coniferous forests decreased with 7% or ±197,330 ha between 1985 and 2010, while broadleaved and mixed forests increased with 12% and 2% or respectively ±1,095,030 ha and ±233,290 ha (Griffiths et al., 2013b). In general, the total forest area increased from ±6,027,370 ha in 1985 to ±7,158,360 ha in 2010. Moreover, the Global Forest Resources Assessment of FAO (2010) reported ±6,573,000 ha of Romanian forest area in 2010. Based on this comparison, our results reflect conservatives estimates of forest cover and forest cover change.

The change detection analysis showed that stable forests were present on higher elevations. The 1985-1995 change statistics in Table 6.8 showed that afforestation occurred on±425,000 ha and was larger than deforestation (±290,000 ha) in the Carpathian Ecoregion. The disturbance class only accounted for ±55,000 ha. In the 1995-2010 change statistics, an increased presence of deforestation and afforestation was observed. Deforestation accounted for ±320,000 ha and afforestation covered ±479,000 ha. Both land cover trends occurred mainly at the fringes of the stable forests. Compared to 1985-1995, the stable BL and CF forest classes experienced a larger increase between 1995 and 2010. An area of ±2.5 million ha of stable BL forest and ±1.25 million ha of stable CF forest was present in this second period (Table 6.9). However, this second period was five years longer than the first period. The deforestation was especially triggered by the weak implementation of the property laws during the different restitution phases, as explained in Chapter 3. The increasing forest area in Romania was confirmed by other studies. As indicated in Chapter 3, a national scale study of Greenpeace (2012) estimated the total area of deforestation and forest degradation ±280,108 ha between 2000 and 2011. However, in this study, forest was defined as 20% or greater canopy cover

for trees of 5 m or more in height. Another national scale study that was mentioned in Chapter 3 estimated land cover changes between 1990 and 2006 using CORINE Land Cover products. Thereby ±2,871 ha was affected by afforestation and ±3,267 ha was deforested. However, since the average size of forest properties was small, most of these areas could not be quantified in the model, leading to underestimations (Dutca and Abrudan, 2010).

The conversion from non-forest to a forest class was triggered by the abandonment of cropland and a slow afforestation. A similar study by Olofsson et al. (2011) in the Romanian Carpathians between 1990 and 2010 showed that grasslands and forests were expanding on unused or abandoned farmland after 1989. A study by Griffiths et al. (2013c) in the Romanian Carpathian Ecoregion showed grassland abandonment rates between 60% and 70% between 1985 and 2010. Moreover, grassland conversion persisted during 1995-2010 in western Romania. Furthermore, afforestation occurred after the EU accession and was especially concentrated in areas favorable for farming (Griffiths et al., 2013c). In this study, the afforestation was mainly present in the northwestern corner of the study area which is also a suitable region for farming practices.The locations of deforestation in Romania also overlapped with the mapped areas of 'full canopy removal' in other studies. Knorn et al. (2012a) assessed these patterns between 1987 and 2009 in the northern Romanian Carpathians. Largest deforestation was present near the Ukranian border in between 1994 and 2009, which overlapped with the deforestation patterns between 1990 and 2010 (Figure 6.6). Another study by Knorn et al. (2012b) also detected old-growth forest disturbances between 2000 and 2010 near the border of Ukraine and in the northwestern part of the Romanian Carpathian Ecoregion, as detected in Figure 6.6. Moreover, Griffiths et al. (2012) determined areas of deforestation between 1985 and 2010 on a Landsat footprint in central-eastern Romania. Thereby, main deforestation patterns were observed during the first restitution phase between 1991 and 1999. Furthermore, these patterns were present at the borders of the forest and the plateaus, and overlapped more or less with observed patterns in Figure 6.6.

In a following step, pixel-based compositing procedure can be improved, e.g. by implementation of variability metrics to alleviate scan line correction-off errors which was also tested successfully by Griffiths et al. (2013a). Such metrics can be produced to capture relevant phenologic states in the seasonal cycle of vegetation (Hansen et al., 2002; Griffiths et al., 2013a). Furthermore, the decision for image selection during compositing was based on a flexible parametric weighting scheme that evaluated available observations for their suitability. However, this decision system lacks a parameter that quantifies the atmospheric or topographic distortion. For example, the observation with the lowest reflectance in the blue band can be selected to minimize the atmospheric effects (Griffiths et al., 2013a).

6.6 Conclusion

So far, multi-temporal change analyses in the Carpathian mountains were performed with mosaicked satellite data or with pixel-based image composites. However, at present, the inclusion of a topographic correction in the compositing of Landsat data was still lacking. In this chapter, a topographic correction was included in the pixel-based image compositing algorithm and tested between 1985 and 2010. The multi-temporal analysis in the Romanian Carpathian Ecoregion

provided large scale topographically corrected maps and accuracy results. Thereby, the classification accuracy was assessed for five different scenarios in which 3 components were altered: classifier (ML or SVM), number of classes (4 or 8) and topographic correction (uncorrected or corrected).

Generally, the overall accuracies for 8 land cover classes was between 66% and 82% for all years. The overall accuracy values were highest for the land cover maps of 2010. Furthermore, results presented an indication that the implementation of a topographic correction had a smaller influence on the classification accuracy than the selection of a classifier. However, after topographic correction and improvement of the classifier, the differentiation between the eight different land cover classes remained difficult. Therefore, accuracies of the topographically uncorrected and corrected Support Vector Machine classifications were determined for 4 land cover classes. This resulted in significant improvements of the accuracies. The overall classification accuracies of the corrected SVM classification were respectively 85% (1985), 83% (1995) and 91% (2010).

A steady greening of the Romanian Carpathian Ecoregion was observed between 1985 and 2010 since afforestation was larger than deforestation. Between 1985 and 2010, a decrease of ±5% in the non-forest class was compensated by an increase in the forest class. This decrease in the non-forest class was especially compensated by an increase in the broadleaved and mixed forest classes. The change detection analysis showed that the afforestation and deforestation trends were larger in the second period (1995-2010). In contrast, the disturbance trend was more important in the first period (1985-1995) but was only present on a small area. As shown in the next chapter, the examination of the main land cover trends can result in interesting research questions for large scale studies.

The further development of automatic detection methods based on time series with a high temporal resolution is helpful for the identification of forest cover changes. In a following step, pixel-based compositing procedure can be improved by implementation of variability metrics, as explained in the discussion of Chapter 6. Moreover, the determination of the optimal lower boundary threshold of the factor $(\cos\beta / \cos\theta_T)^b$ can be improved, e.g. by an optimization procedure of the as performed by Balthazar et al. (2012). Finally, the application of topographic correction before the pixel-based image compositing deserves further elaboration. This application would allow the inclusion of a parameter that quantifies the illumination effects and improves the input map for classification. Especially change detection studies in mountain areas could profit from such improvements.

Chapter 7: Controlling factors of forest cover changes in the Romanian Carpathian Ecoregion

7.1 Introduction

Forest cover changes are complex processes with different possible pathways and controlling factors. A better insight in the factors that control forest cover change can support the development of sustainable conservation plans. Moreover, forest cover change data can be used to evaluate whether an implemented forest conservation policy was successful or not.

Due to the lack of reliable and consistent data at larger spatial scales, many studies have evaluated controlling factors of forest cover change at local scale levels. The drawback of this approach is that it is unknownwhether the extent of the local scale study is representative for a larger area. Moreover, such local scale studies can only partially reveal the complex interactions of controlling factors that operate at different scale levels. Controlling factors such as soil type, soil gradient and accessibility can vary from parcel to parcel and are therefore typically important at local scale levels. Other controlling factors such as land use policy, forest protection and regional economic development show a variation over longer distances and can only be analyzed at regional scale levels. Based on the land cover data produced in the previous chapters of this work, such a regional scale analysis of the controlling factors of forest cover change will be carried out in the Romanian Carpathian Ecoregion. The selected period between 1985 and 2010 will allow to evaluate the impact of the policy changes that occurred following the fall of the communist regime in 1990.

In Romania, several natural and anthropogenic factors have influenced the forest cover changes. Land zoning and changes in ownership regimes have been major drivers of forest cover changes during the past decades. Land reforms affected large areas of forest land that altered from state-owned to private ownership. Non-protected as well as protected forest areas changed of owner during the three restitution phases (Knorn et al., 2012a). Three factors explained increased logging rates after the implementation of forest restitution laws. First, the economic recession provided an incentive for the new owners to immediately clear-cut their forests for short-term returns (Ioras and Abrudan 2006; Strimbu et al., 2005). Secondly, Romania's forest restitution was a slow and complex process, with many new owners fearing that their property rights were not permanent (Sikor et al., 2009), leading to rapid deforestation. Thirdly, the post-socialist period in Romania was characterized by weak institutional strength and law enforcement, which resulted in increased illegal logging rates (Ioja et al., 2010; Strimbu et al., 2005). Results of a similar study in the northern part of Romania by Knorn et al. (2012a) suggested that the decline of the forest area was largely triggered by institutional changes. Moreover, new forest owners often lacked capacity and knowledge for sustainable forest management and nature conservation (Knorn et al., 2012a). Natural stand-replacing disturbance events also occurred in the Romanian Carpathians and included avalanches, wind-throw and insect infestation (Schelhaas et al., 2003; Toader and Dumitru, 2005). Informal interviews pointed out that corridors in forests were deliberately placed to inflict wind-throw and thereafter allow salvage logging (Knorn et al., 2012a). Forest fires, on the other hand, were not widespread and were always occurring in small areas (Anfodillo et al., 2008; Rozylowicz et al., 2011).

The objective of this study in the Romanian Carpathian Ecoregion is the assessment of the relative importance of local and regional scale controlling factors. In Chapter 6, a multi-temporal land cover dataset was produced by integrating a topographic correction procedure in pixel-based Landsat compositing procedure. The reconstruction of the main land cover changes between 1985, 1995 and 2010 showed particular patterns of an overall land cover greening, though deforestation was observed at a number of locations. At present, it is unclear to what extent such patterns are caused by variations in the biophysical environment, regional socio-economic settings or land use policy implemented at a national scale. Therefore, an exploratory analysis of possible controlling factors of the regional scale land cover change patterns will be carried out based on the image composites produced in the previous chapter. Firstly, possible controlling factors of the observed land cover changes are selected. Next, their relative importance and the significance of these factors will be evaluated by means of a logistic regression analyses for the periods 1985-1995 and 1995-2010.

7.2 Materials and Methods

7.2.1 Study Area

The study area of this chapter was the Romanian Carpathian Ecoregion, which was described in Chapter 6 (Figure 6.1).

7.2.2 Analysis of controlling factors of forest cover change

Variables that could possibly explain the observed land cover changes in the periods 1985-1995 and 1995-2010 were selected based on two criteria. First, the observed land change processes were linked with possible explanatory variables mentioned in literature (Table 7.1). This resulted in the formulation of hypotheses on possible controlling factors which were related to accessibility, demography, land use policy and the biophysical environment. A second criterion was the nation-wide availability of categorical and numerical data that could be considered as proxy-variables for the controlling factors.

Table 7.1.: Studies on controlling factors of land cover changes: study area, period, topic of interest, explanatory variables and reference.

Study Area	Period	Topic of interest	Explanatory variables	Reference
Belize	1989-1995	Deforestation	Accessibility	Chomitz and Gray, 1996
Republic of Congo	1987-1995	Deforestation	Accessibility	Wilkie et al., 2000
Czech Republic	1850-2000	Land cover change	Land use policy and economic condition	Bicik et al., 2001
Belgium	1774-1990	Soil erosion	Slope gradient and soil type	Van Rompaey et al., 2002
Hungary	1784-2002	Sediment fluxes	Land cover change	Jordan et al., 2005
France	1834-2001	Deforestation	Land use policy, technological progress and rural exodus	Vandendael, 2007
Belgium	1775-1929	Land cover change	Land use policy and technological progress	Petit and Lambin, 2002
Ecuador	1963-2002	River channel	Land cover change	Vanacker et al., 2005

		response		
Greece	1886-1996	Land cover change	Soil erosion	Bakker et al., 2005
Europe	2001-2010	Cropland	Land use policy	Van Meijl et al., 2006
Czech Republic	1992-1998	Sediment fluxes	Field size	Van Rompaey et al., 2007
Worldwide	1984-2010	Cropland abandonment	Socio-economic factors	Benayas et al., 2007
Poland, Slovakia and Ukraine	1986-2000	Cropland abandonment	Land use policy and demography	Kuemmerle et al., 2008b
Romania	1990-2002	Cropland abandonment	Land use policy	Kuemmerle et al., 2008a
Romania	1990-2005	Cropland abandonment	Elevation and slope gradient	Müller et al., 2009
Europe	2000-2030	Cropland abandonment	Land cover change and macro-economic condition	Verburg and Overmars, 2009
Hungary	1981-2006	Land cover change	Soil type	Szillassi et al., 2010
Uganda	1989-2010	Urban growth	Land use policy	Vermeiren et al., 2012
Ethiopia	1957-2007	Deforestation	Elevation and slope gradient	Getahun et al., 2013
Ethiopia	1965-2007	Deforestation	Land use policy and slope gradient	Teka et al., 2013
Albania/ Romania	1990-2005	Cropland abandonment	Elevation and slope gradient in both countries, accessibility in Albania	Müller et al., 2013
Belgium and France	6000 before Christ - 1850	Deforestation	Soil type and slope gradient	De Brue and Verstraeten, 2013

First, various studies identified the role of accessibility as an important controlling factor of both deforestation and afforestation. The spatially explicit model of von Thünen (1826) demonstrated that physical accessibility affected the land cover by including a transportation cost in the model that simulated the profit of peri-urban farmers. If forest is considered as a non-productive land cover, it will remain only in inaccessible places, according to the von Thünen model. However, if timber wood is an important product to be sold at a central market, timber will be harvested in accessible places (and possibly compensated by new plantations). This process is confirmed by manylocal scale studies reporting higher rates of deforestation along roads (e.g. Belize, Chomitz and Gray, 1996; Republic of Congo, Wilkie et al., 2000; Table 7.1). Higher deforestation rates were also related to different non-market factors such as immigrants that settled along new road systems or a rise in logging for fuelwood. In contrast, a study of Getahun et al. (2013) in Ethiopia reported the opposite trend: deforestation occurred in relatively remote places away from the road systems, where isolated communities had no link with the regional market and were locked in to a system of self-subsistence agriculture. Since accessibility can steer a forest cover change in two directions, the variables distance to roads and distance to settlements were included as proxy-variables for accessibility in the analysis.

Secondly, demographical variables can also be linked with deforestation and afforestation, where the relation is obvious at first sight: more people put a higher pressure on the land, resulting in less forest. Normally, changes in population density are related with accessibility, e.g. people migrate from inaccessible to accessible places. However, recent research by Teka et al. (2013) showed that

the opposite relation was valid for remote areas in northern Ethiopia: natural population growth was higher in inaccessible villages which resulted in a higher land pressure. In this study, population density change was therefore included as a possible factor explaining the spatial pattern of the observed land cover changes.

Thirdly, socio-economic changes and its related land use policy are considered as an essential controlling factor of forest changes. The Romanian land use policy is interesting since a communist period with a central policy and collective farming was followed by a transition phase and the start of a free-market system. This socio-economic transition initially induced uncertainties related to land tenureship and private land ownership since a new forest protection policy system was installed following EU-guidelines. The three restitution laws of 1985, 1995 and 2010 affected large forest areas and non-protected as well as protected forest areas changed of owner during phases. The consequences of this transition period has been described for other countries in eastern Europe. A study of Bicik et al. (2001) reported the economic condition and especially the land use policy as the main social controlling factors over the past 150 years in the Czech Republic. Van Rompaey et al. (2007) described a transition from arable land to grassland and forest due to the abandonment of state farms along the borders of the Czech Republic. Szilassi et al. (2010) described similar processes for Hungary and was able to show that the soil type was an important controlling factors. Hereby, land of the former state farms with fertile soils was often bought by foreign investors to continue and intensify farming, while state farms with unfertile soils were completely abandoned. Decollectivization policies and the migration from rural to urban areas were considered as the main causes of cropland abandonment in Poland, Slovakia and Ukraine (Kuemmerle et al., 2008b). In Romania, cropland abandonment between 1990 and 2005 was mainly triggered by policy reforms where by steep lands at high elevations were the first to be taken out of production (Kuemmerle et al., 2008a; Müller et al., 2009 and 2013).

The decollectivization triggered land abandonment and simultaneously it was held responsible for forest cover disturbances. Kuemmerle et al. (2009b) compared forest cover dynamics on public and the decollectivized private forests stands in Poland on the basis of Landsat images between 1988 and 2000. Results showed that disturbance peaked in both public and private forests inthe transition period after the collapse of communism (Kuemmerle et al., 2009b). However, disturbance rates in private forests were about five times higher than on public lands. Furthermore, the spatial pattern of disturbances was similaracross ownership types, but private forests were more fragmented than state and National Park forests (Kuemmerle et al., 2009b). A complete overview of the forest clearings following the change in political regime in the Romanian Carpathians is, however, not yet available due to the absence of a central cadastral system. At present, land ownership data are still stored in decentralized records at communal level. Therefore, it was impossible to compile a national scale landownership map for this study. The analysis of possible policy effects on the forest cover dynamics was therefore restricted to the evaluation of the forest protection levels imposed by the Natura 2000 protection programme, which were described in Chapter 3.

Finally, the biophysical environment is a key variable that controls the spatial pattern of land use change. In a phase of expansion of farming land, the most suitable land units for agriculture will firstly be taken in production, leaving the less suited land units under forest. In contrast, in a phase of farmland abandonment, the less suited arable fields will be abandoned first. A range of land cover

studies described this process over various time scales and in different regions worldwide (Van Rompaey et al., 2002; Müller et al., 2009; Szillassi et al., 2010; De Brue and Verstraeten, 2013; Getahun et al., 2013; Müller et al., 2013; Teka et al., 2013). The biophysical factors that are the most frequently linked with suitability for arable farming are slope gradient, climate, soil type and soil fertility.

Eight explanatory variables, available for the whole Romanian Carpathian Ecoregion were selected and grouped in four categories: (1) accessibility, (2) demography, (3) land use policy and (4) biophysical environment (Table 7.2). The following eight factors were assessed for the Romanian Carpathian Ecoregion: distance to primary and secondary roads, distance to most nearby settlement, demographic evolution, protection level, slope gradient, elevation and soil type (Table 7.2). In the next paragraphs, the selected explanatory variables are briefly discussed.

Table 7.2.: Variable description: variable, unit and category.

Variable	**Unit**	**Category**
Distance to primary roads (DPR)	Meter	Accessibility
Distance to secondary roads (DSR)	Meter	Accessibility
Distance to nearby settlement (DNS)	Meter	Accessibility
Demographic evolution (DE, 1986-2010)	Change in number of inhabitants/km^2	Demography
Protection level (PL) 0 = Not protected 1 = Special Protection Area (SPA) 2 = Area of Special Conservation Interest (SCI)	Categorical	Land use policy
Slope gradient (SG)	Degrees	Biophysical environment
Elevation (EV)	Meter a.s.l.	Biophysical environment
Soil type (ST) 1 = *Andosol* (AN) 2 = *Cambisol* (CM) 3 = *Fluvisol* (FL) 4 = *Leptosol* (LP) 5 = *Luvisol* (LV) 6 = *Phaeozem* (PH) 7 = *Podzo*l (PZ)	Categorical	Biophysical environment

Accessibility

For each pixel, the Euclidean distance to the most nearby settlement, the most nearby primary and secondary road was calculated. The location of roads and settlements was extracted from the 2003 NUTS-database (Nomenclature of territorial units for statistics), developed by the European Commission and presented in Figure 7.1 (European Commission, 2013b).

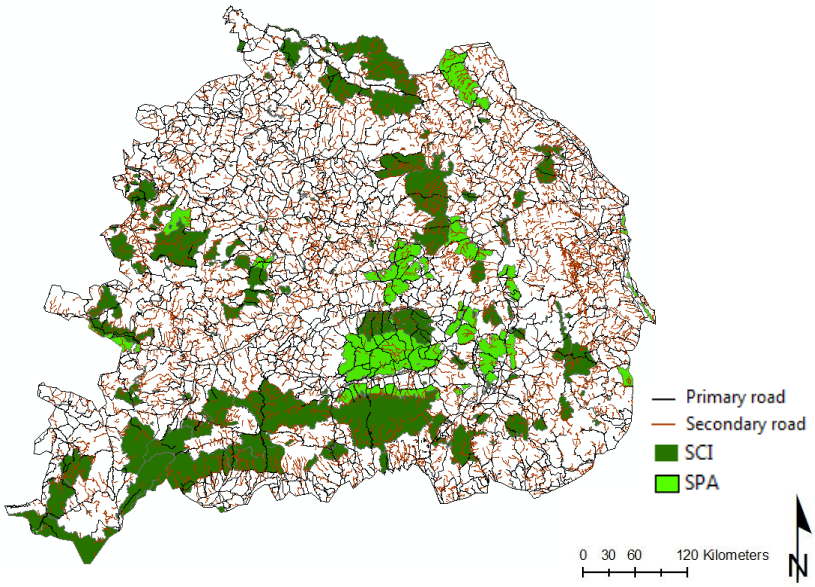

Figure 7.1.: Primary roads (black line), secondary roads (brown line) and protected area (SCI in dark green and SPA in light green) in the Romanian Carpathian Ecoregion. SCI is an area of Special Conservation Interest and SPA is a Special Protection Area (European Commission, 2013b).

Land use policy

The Romanian legislation to safeguard valuable regions dates back to the communist times (1948-1989) in which the protected area expanded. Between 1940 and 1991, the number of protected areas increased from 36 to 539 and their total areas were expanded about 13 times from 1,551 ha to 1,140,388 ha (Cristea 1995 and 1996b; Soran et al., 2000). This was especially possible after the publication of Ministry Council Resolution no. 518 in 1954 which was the basis for legal activity for nature protection in Romania (Soran et al., 2000). After the fall of this regime, the protected areas were neglected due to weakened institutions. However, since 2001, Romania participated in the Natura 2000 network that comprises two different protection zones: SPAs and SCIs (Natura 2000, 2012). This protection zones were discussed in Chapter 2. The Birds Directive requires SPAs and the Habitats Directive requests the establishment of SCIs for species other than birds and also habitats on itself. In total, 34,830 km^2 or 18% of Romania falls under one of these two protection statuses (Matei, 2011).

Implementing the NATURA 2000 network in Romania is rather difficult due to the lack of trained experts, data availability and/or their chaotic dispersion (Biriş et al., 2006). Therefore, considerable concerns about the status of nature protection remain: protected areas are sometimes subject to illegal logging and poaching, and many protected areas lack professional management, financing, and scientific support (Soran et al., 2000; Ioja et al., 2010; Knorn et al., 2012a). The categorical variable 'protection level' consists therefore of three categories: not protected (0), under the SPA (1) or SCI (2) protection level. In Figure 7.1, the SPAs are shown in light green and the SCIs in dark green.

Demography

As in most Carpathian countries, the national Romanian population number has been decreasing over the last 15 years (NIS Romania, 2013). Census data, however, show that this decline is relatively recent: Romania's population was strongly increasing between 1960 and 1992, stimulated by the family policy of the central government (NIS Romania, 2013). During the communist regime,

especially the rural population was affected by high unemployment rates and poverty. Consequently, a major part of the rural population abandoned their land and moved to the cities, in a number of cases stimulated by organized resettlement programmes (Turnock, 1991). After the fall of communism in 1989, the migration to the urban areas continued. However, this trend was inversed after 1997 and an net urban-rural movement was detected. People returned to the rural areas since the city life became more expensive and the job uncertainty increased (Guran-Nica et al., 2010).In this study, population data were analyzed at communal level (Solovastru, 2010). Population data of 1986 and 2010 were provided by the NIS of Braşov (NIS Romania, 2013). Figure 7.2 shows the demographic evolution in change in inhabitants per km^2 between 1986 and 2000. Results show that the population is declining in the major part of the study area. Absolute population change in the communes of the high mountains is relatively low due to the very low population density in this mountain area.

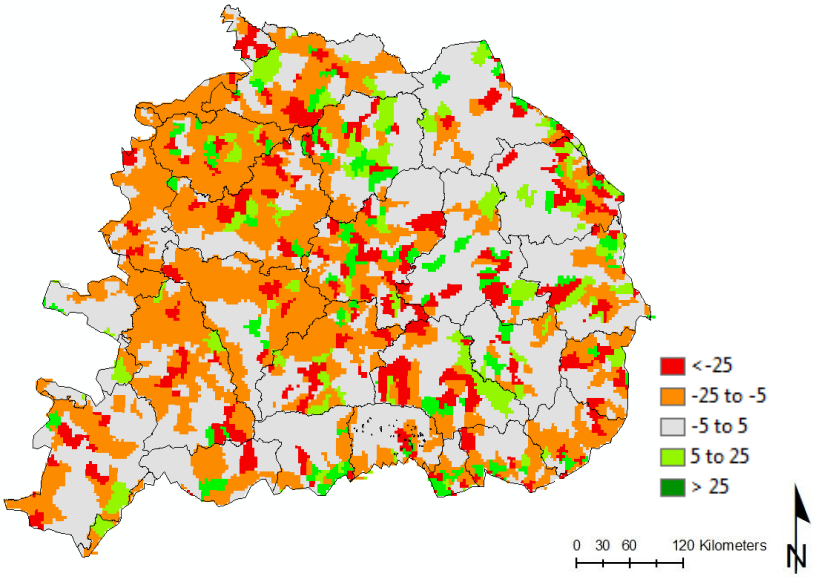

Figure 7.2.: Demographic evolution (change in inhabitants per km^2) between 1986 and 2000 in the Romanian Carpathian Ecoregion (NIS Romania, 2013).

Biophysical environment

Elevation and slope values were derived from an SRTM with an original spatial resolution of 90 x 90 m (CGIAR-CSI/NASA, 2013). As explained in Chapter 4, this resolution was resampled to 30 x 30 m by means of a bicubic spline interpolation to match the resolution of the Landsat data (Figure 6.1). According to the WRB full soil code, 30 different classes were present in the Romanian Ecoregion. In order to reduce the level of detail, these 30 classes were merged in 8 main WRB soil types: *Andosol* (AN), *Cambisol* (CM), *Fluvisol* (FL), *Leptosol* (LP), *Luvisol* (LV), *Phaeozem* (PH), *Podzol* (PZ) and *Regosol* (RG) (FAO/UNESCO/WRB, 1998). The main soil types in the lower lying areas are *Luvisols* and *Phaeozems* which are fertile soils and suitable for a wide range of agricultural uses (FAO, 2006). *Fluvisols* are occurring around water bodies and also have a good natural fertility (Figure 7.3). In contrast, higher elevated areas are dominated by *Cambisols*, *Podzols* and *Andosols*. *Cambisols* generally result in good agricultural land and are used intensively, while *Podzols* are unattractive soils for arable farming due to their low nutrient status, low level of available moisture and low pH (FAO, 2006). *Andosols* are generally fertile soils and have a high potential for agricultural production (FAO, 2006). Furthermore, *Leptosols* have a resource potential for wet-season grazing and as forest land, and many *Regosols* are used for extensive grazing (FAO, 2006). Arable land in Romania, opposed to

forest, is normally expected land units with gentle slopes with fertile soils, at lower elevation ranges types (e.g. *Luvisols* and *Phaeozems*).

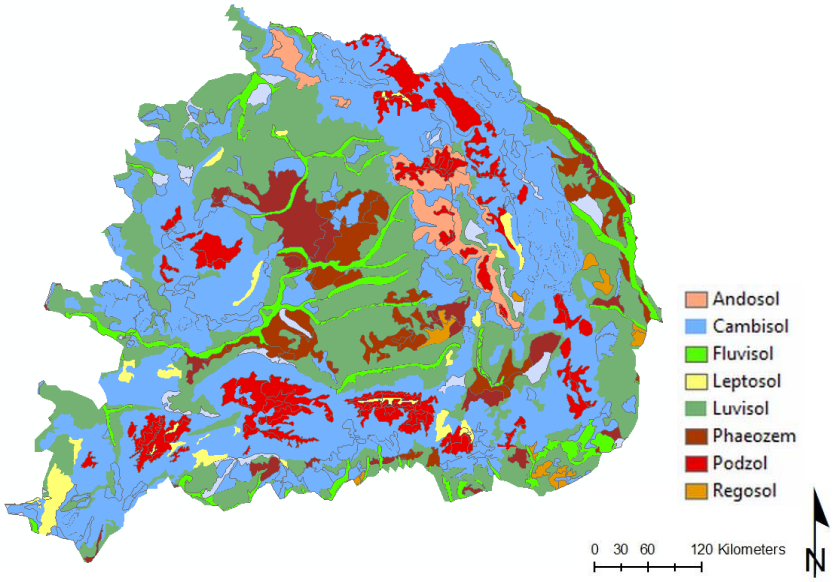

Figure 7.3.: Eight main WRB soil types in the Romanian Carpathian Ecoregion: *Andosol* (AN), *Cambisol* (CM), *Fluvisol* (FL), *Leptosol* (LP), *Luvisol* (LV), *Phaeozem* (PH), *Podzol* (PZ) and *Regosol* (RG) (FAO/UNESCO, 1998).

7.2.3 Logistic regression

A wide range of methods is available to evaluate the relation between an observed land cover change and a potential explanatory variable. First, the most straightforward approach is based on frequency analyses of a crosstabulation tables in which the observed number of land cover changes in a certain category of a explanatory variable is compared with the expected number of land cover changes (Van Rompaey et al., 2001). A significant over- or under representation of a change type in a given class of a categorical variable can then be interpreted as a correlation.

Though this method allows to test individual variables, simultaneous analysis of the effect of multiple variables is often impossible since correlation between explanatory variables is not allowed in crosstabulation analysis. A second drawback is the need to categorize each numerical variable, which automatically leads to a loss of information. An alternative technique is a logistic regression that links at set of explanatory variables (numerical and/or categorical) with the probability of occurrence of a certain event, in this case a specific land cover change (Hosmer and Lemeshow, 2000). The advantages of logistic regression analyses are: (1) calibration is possible with a relatively limited number of input data, (2) both categorical and numerical variables can be included simultaneously, (3) there is no need to categorize numerical variables, and (4) correlated explanatory variables can be included (Baker, 1989; Nelson and Geoghegan, 2001; Serneels and Lambin, 2001; Van Rompaey et al., 2001; Munroe et al., 2002; Verburg et al., 2004; Van Dessel et al., 2008). However, some disadvantages are the following: an implicit assumption of linearity of the land cover change process in terms of the logit function and between dependent and independent variables, the prerequisite of selecting explanatory variables, and the limitation of application to studies using between-subject designs (Tu, 1996; Steyerberg et al., 2001).

Therefore, more advanced model approaches include neighborhood effects in which e.g. the progression of a deforestation front is simulated. Neighborhood effects are typically modeled with cellular automata that describe potential pull and push effects between various land cover types by a range of parameters (Clarke et al., 1997; Verburg et al., 2004; Poelmans and Van Rompaey, 2009). Finally, the most advanced approach consists of agent-based models that simulate land cover changes by modeling the behavior of individual agents (land users) based on the goal and the characteristics of the agents and the characteristics of the environment in which they can operate (Parker and Meretsky, 2004). Though this technique is promising from a conceptual point of view, the practical application has been limited to a few case studies since a large database describing the individual behavior of land users or agents is required for model calibration (e.g. Brown and Robinson, 2006; Rui and Ban, 2010). These examples were mainly based on data derived from interviews with households and stakeholders.

Given the possibilities and drawbacks of the available techniques and data, a logistic regression analysis was selected for the further analysis of the observed land cover change in the Romanian Carpathians. In this study, a stepwise Multiple Logistic Regression (MLR) was implemented using ArcMap 10 and SAS 9.2. Thereby, a MLR-equation was derived for the two main observed land cover changes: deforestation and afforestation (respectively DEFOR and AFFOR; see Chapter 6). The forest disturbance class was not included in the analysis since Chapter 6 showed that disturbance occurred only in a few fragmented locations in the Romanian Carpathian Ecoregion. Furthermore, the MLR analysis was performed for the two time periods, respectively 1985-1995 and 1995-2010. Probabilities for the two main land cover change types were assessed using the standard logistic regression equation 7.1. By applying these equation, it is possible to assess the probability of the occurrence of a land cover change at pixel level.

$$P(AFFOR) = \frac{EXP\left[a + b*DPR + c*DSR + d*DNS + e*DE + f*SPA + g*SCI + h*SG + i*EV + j*AN + k*CM + l*FL + m*LP + n*LV + o*PH + p*PZ\right]}{1 + EXP\left[a + b*DPR + c*DSR + d*DNS + e*DE + f*SPA + g*SCI + h*SG + i*EV + j*AN + k*CM + l*FL + m*LP + n*LV + o*PH + p*PZ\right]} \quad (7.1)$$

with P(AFFOR), the probability that a pixel will be afforested; DPR, distance to primary roads (in meters); DSR, distance to secondary roads (in meters); DNS, distance to nearby settlement (in meters); DE, demographic evolution (inhabitants/km^2); protection level (SPA, SCI); SG, slope gradient (in degrees); EV, elevation (in meters); ST, soil type [*Andosol* (AN), *Cambisol* (CM), *Fluvisol* (FL), *Leptosol* (LP), *Luvisol* (LV), *Phaeozem* (PH), and *Podzol* (PZ)]; a, b, c, d, e, f, g, h, i, j, k, l, m, n, o, p: regression coefficients. The categorical variables soil type (9 categories) and protection level (3 categories) were coded with binary dummy variables: a value of 0 (absence of the category) or 1 (presence of the category) (Hosmer and Lemeshow, 2000). The number of dummy variables was one less than the number of categories per categorical predictor, so 8 dummy variables for the soil type and 2 dummy variables for the protection level. The reference category for soil type was *Regosol* and the reference for protection level was 'no protection'. A similar analysis was performed for the deforestation land cover change.

Since the Natura 2000 network in Romania only started in 2001, the predictor 'protection level' was not included in the MLR-models for the period 1985-1995. In a stepwise MLR, the model coefficients

are assessed by maximizing the likelihood of the observed land cover changes (deforestation or afforestation) through an iterative procedure. Parameters that are not significant at a 95% confidence level are left out of Equation 7.1, after which new parameters are calibrated for the remaining variables.

Positive values for the coefficients imply that the probability of the land cover change increases with increasing values for the explanatory variable. In order to calculate the regression coefficients, 25,000 points were selected separately for the two dependent variables (AFFOR and DEFOR). The sampling was based on the land cover changes that were examined in Chapter 6 (Figure 6.6 and 6.7) and the values of the corresponding explanatory variables were extracted for each pixel. Hereby, half of the sample (about 12,500 points) was selected in the area where the land cover change was absent (coded with '0') and the other 12,500 pixels were chosen in the area where the land cover change occurred (and coded with '1'). For example, the spatial pattern of the sample points for afforestation is shown in Figure 7.4, where afforestation occurred in the green points and was absent in the red points. Thereby, all afforestation sampling points were selected from points which were originally non-forest. In contrast, all deforestation sampling points were chosen from points that were originally forest.

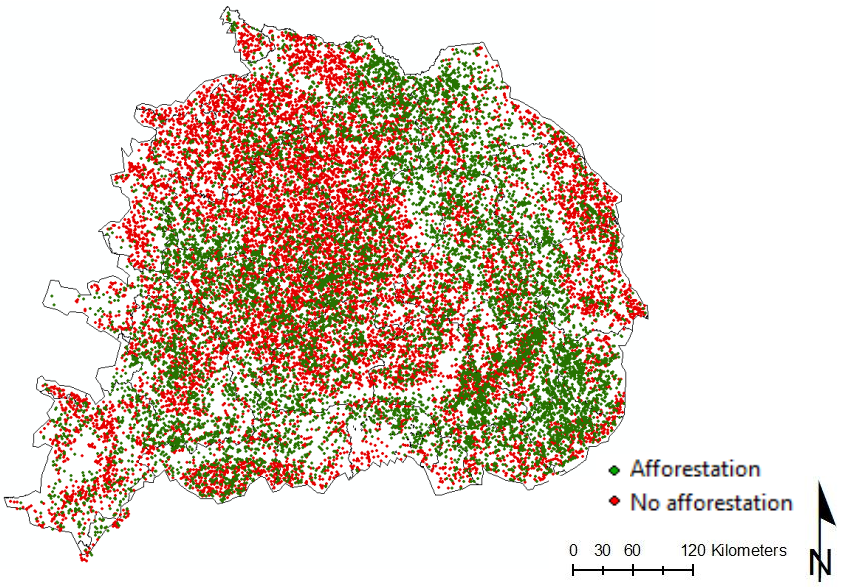

Figure 7.4.: Spatial pattern of the sample points for afforestation. Afforestation occurred in the green points and was absent in the red points.

After the MLR analysis, probability maps were constructed using Equation 7.1 for each MLR-model (AFFOR and DEFOR). Afterwards, the goodness of fit was evaluated using a Relative Operation Characteristic procedure (Hall et al., 1995; Schneider and Pontius, 2001; Pontius and Schneider, 2001). This analysis was performed to evaluate whether the MLR-models described the observed land cover changes better than random models. In a ROC-analysis, true positives (i.e. pixels correctly predicted) were plotted against false positives (i.e. pixels incorrectly predicted) for different land cover changes (Pontius and Schneider, 2001). The ROC-curve of a significant model has more true positives for the same level of false positives. In the case of a random model without any predictive power, a scatter around the 1:1 line is expected. In contrast, low false positive values would correspond to very high true positive values for a near-perfect model. The overall ROC-value is

defined as the area under the ROC-curve (AUC), which is an indication of the model performance. Therefore, a significant model is characterized by an AUC-value larger than 0.5 while a random model corresponds with an AUC-value of 0.5 (Pontius and Schneider, 2001).

7.3 Results

7.3.1 1985-1995

Table 7.3 provides an overview of all MLR coefficients, Wald Chi-square and the P-values for both afforestation and deforestation in the study area between 1985 and 1995. Afforestation is correlated with 5 explanatory variables at a 95% confidence level. Significant predictors for afforestation are the slope gradient, elevation, distance to nearby settlements, and distance to primary and secondary roads with P values smaller than 0.05 (Table 7.3). All significant predictors are positively correlated with afforestation since the corresponding coefficients are positive, apart from distance to secondary roads. This means that afforestation in 1985-1995 rather occurred on steep slopes at high elevations, away from settlements and primary roads but nearby secondary roads. The Wald Chi-square values show that slope gradient and elevation are the most influential predictors (Table 7.3).

Deforestation in the period 1985-1995 is positively correlated with elevation, but negatively with distance to settlements and distance to primary and secondary roads. This implies that forests were mainly removed at high elevations and in relatively accessible places. Furthermore, also *Podzols* were significantly correlated with deforestation (Table 7.3), whereby forests were rather avoided for deforestation on *Podzols.* The most influential predictor of deforestation model 1985-1995 was elevation with a Wald Chi-square value of 2,041 in Table 7.3.

Table 7.3.: Coefficients and the P-value of the stepwise multiple logistic regression equation between 1985-1995 where a = intercept, b(DPR) = coefficient of distance to primary roads, c(DSR) = coefficient of distance to secondary roads, d(DNS) = coefficient of distance to nearby settlement, e(DE) = coefficient of demographic evolution, f(SPA) = coefficient of special protected area, g(SCI) = coefficient of area of special conservation interest, h(SG) = coefficient of slope gradient, i(EV) = coefficient of elevation, j(AN) = coefficient of *Andosols,* k(CM) = coefficient of *Cambisols,* l(FL) = coefficient of *Fluvisols,* m(LP) = coefficient of *Leptosols*, n(LV) = coefficient of *Luvisols,* o(PH) = coefficient of *Phaeozems,* p(PZ) = coefficient of *Podzols*.

	Afforestation			**Deforestation**		
	Coefficient	Wald Chi-square	P-value	Coefficient	Wald Chi-square	P-value
Intercept (a)	-1.39	838	<0.0001	-0.24	1,248	<0.0001
b(DPR)	0.000033	27	<0.0001	-0.000030	27	<0.0001
c(DSR)	-0.000060	53	0.0023	-0.00011	139	<0.0001
d(DNS)	0.000031	52	<0.0001	-0.00004	147	<0.0001
e(DE)	NS	/	/	NS	/	/
f(SPA)	NA	NA	NA	NA	NA	NA
g(SCI)	NA	NA	NA	NA	NA	NA
h(SG)	0.050	863	<0.0001	NS	/	/
i(EV)	0.00088	225	<0.0001	0.0026	2,041	<0.0001
j(AN)	NS	/	/	NS	/	/
k(CM)	NS	/	/	NS	/	/
l(FL)	NS	/	/	NS	/	/
m(LP)	NS	/	/	NS	/	/

n(LV)	NS	/	/	NS	/	/
o(PH)	NS	/	/	NS	/	/
p(PZ)	NS	/	/	-0.0017	6	0.027

NS: non-significant at the 95% confidence level; NA: not applicable since the Natura 2000 network in Romania only started in 2001.

The goodness of fit of the modeling approach was evaluated with ROC-curves and AUC-values. The results for the deforestation and afforestation between 1985 and 1995 are shown in Figure 7.5a and b. The final model ROC curve is presented in green and compared against the 1:1 line (in orange). AUC-values of 0.76 for deforestation and 0.71 for afforestation show that the MLR model describes observed transitions better than a random model.

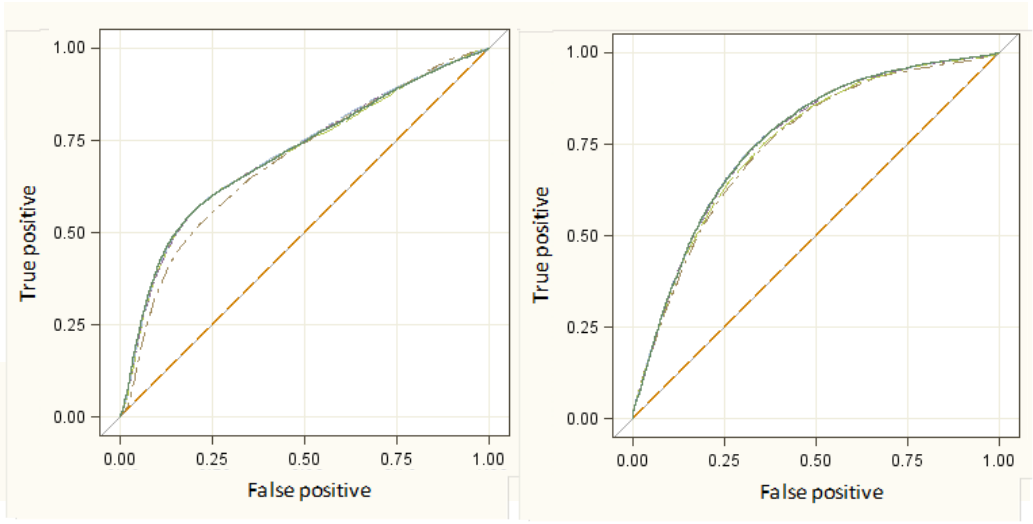

(a) Afforestation *(b) Deforestation*

Figure 7.5.: ROC curves showing the true and false positives between 1985-1995 for (a) afforestation, and (b) deforestation.

7.3.2 1995-2010

The MLR coefficients, Wald Chi-square and the P-values for afforestation and deforestation at the 95% confidence level are shown in Table 7.4. Afforestation is significantly correlated with 10 explanatory variables, including 5 soil types. Afforestation between 1995 and 2010 was correlated with: slope gradient, elevation, distance to primary and secondary roads, demographic evolution, *Cambisols, Fluvisols, Luvisols, Phaeozems* and *Podzols* (Table 7.4). This implies that land units with steep slopes at high elevations, away from primary roads but nearby secondary roads were preferred for afforestation. Afforestation in this period was also significantly correlated with population increase. *Cambisols, Luvisols, Fluvisols* and *Podzols* were preferred for afforestation while *Phaeozems* were avoided. The most influential predictors for afforestation were elevation and slope gradient with Wald Chi-square value of respectively 2,322 and 1,107 (Table 7.4).

Deforestation in the period 1995-2010 was significantly correlated with all evaluated predictors except two soil types (*Fluvisols* and *Leptosols*). The coefficients show that deforestation probabilities were higher than average on land units with steep slopes, at high elevations, nearby settlements, nearby roads (primary and secondary), in places with an increasing population and in zones with SPA or SCI protection. Furthermore, *Andosols, Cambisols, Phaeozems* and *Podzols* were preferred over

Luvisols. The most influential predictor for afforestation in the period 1995-2010 was elevation as indicated with a Wald Chi-square value of 2,041.

Table 7.4.: Coefficients and the P-value of the stepwise multiple logistic regression equation between 1995-2010 where a = intercept, b(DPR) = coefficient of distance to primary roads, c(DSR) = coefficient of distance to secondary roads, d(DNS) = coefficient of distance to nearby settlement, e(DE) = coefficient of demographic evolution, f(SPA) = coefficient of special protected area, g(SCI) = coefficient of area of special conservation interest, h(SG) = coefficient of slope gradient, i(EV) = coefficient of elevation, j(AN) = coefficient of *Andosols,* k(CM) = coefficient of *Cambisols,* l(FL) = coefficient of *Fluvisols,* m(LP) = coefficient of *Leptosols*, n(LV) = coefficient of *Luvisols,* o(PH) = coefficient of *Phaeozems,* p(PZ) = coefficient of *Podzols*.

	Afforestation			**Deforestation**		
	Coefficient	Wald Chi-square	P-value	Coefficient	Wald Chi-square	P-value
Intercept (a)	-2.40	2,044	<0.0001	-0.25	937	<0.0001
b(DPR)	0.000080	132	<0.0001	-0.000050	80	<0.0001
c(DSR)	-0.000060	37	0.0023	-0.000010	88	<0.0001
d(DNS)	NS	/	/	-0.000090	520	<0.0001
e(DE)	0.00051	5	0.028	0.0014	13	0.0003
f(SPA)	NS	/	/	0.12	31	<0.0001
g(SCI)	NS	/	/	0.24	152	<0.0001
h(SG)	0.068	1,107	<0.0001	0.014	76	<0.0001
i(EV)	0.001	2,322	<0.0001	0.0034	2,697	<0.0001
j(AN)	NS	/	/	0.76	95	<0.0001
k(CM)	0.36	89	<0.0001	0.14	6	0.015
l(FL)	0.62	92	<0.0001	NS	/	/
m(LP)	NS	/	/	NS	/	/
n(LV)	0.30	56	<0.0001	-0.52	53	<0.0001
o(PH)	-0.55	104	<0.0001	0.66	61	<0.0001
p(PZ)	0.37	33	<0.0001	0.95	89	<0.0001

NS: non-significant at the 95% confidence level.

Figure 7.6a and b show the ROC curves for the modeled afforestation and deforestation between 1995 and 2010. The AUC-values are higher than the models describing forest cover change in 1985-1995 period: 0.81 for the deforestation model and 0.80 for afforestation.

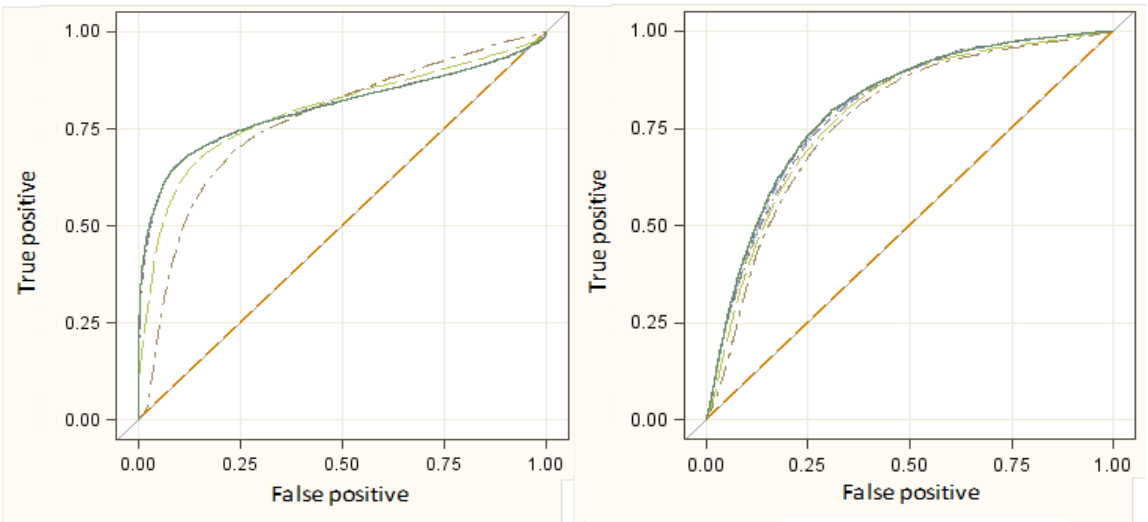

(a) Afforestation *(b) Deforestation*

Figure 7.6.: ROC curves showing the true and false positives between 1995-2010 for (a) afforestation, and (b) deforestation.

7.3.3 Comparison between 1985-1995 and 1995-2010

Table 7.5 shows a comparison between the coefficients for afforestation and deforestation for the time periods 1985-1995 and 1995-2010. A comparison shows that both deforestation and afforestation occurred at the same places in both time periods. For the period 1995-2010, more predictors were found to be significantly correlated with deforestation or afforestation. For most predictors, a similar correlation with deforestation or afforestation was found for both periods. Table 7.5 also shows that the sign of most coefficients (+/-) was consistent between 1985-1995 and 1995-2010. Only one inconsistency was observed: *Podzols* were negatively correlated with afforestation in the period 1985-1995 and positively correlated in 1995-2010.

Table 7.5.: Comparison of the coefficients for afforestation and deforestation between 1985-1995 and 1995-2010, with: b(DPR) = coefficient of distance to primary roads, c(DSR) = coefficient of distance to secondary roads, d(DNS) = coefficient of distance to nearby settlement, e(DE) = coefficient of demographic evolution, f(SPA) = coefficient of special protected area, g(SCI) = coefficient of area of special conservation interest, h(SG) = coefficient of slope gradient, i(EV) = coefficient of elevation, j(AN) = coefficient of *Andosols,* k(CM) = coefficient of *Cambisols,* l(FL) = coefficient of *Fluvisols,* m(LP) = coefficient of *Leptosols*, n(LV) = coefficient of *Luvisols,* o(PH) = coefficient of *Phaeozems,* p(PZ) = coefficient of *Podzols.*

	Coefficients for Afforestation model		**Coefficients for Deforestation model**	
	’85-‘95	’95-‘10	’85-‘95	’95-‘10
b(DPR)	+	+	-	-
c(DSR)	-	-	-	-
d(DNS)	+	NS	-	-
e(DE)	NS	+	NS	+
f(SPA)	NA	NS	NA	+
g(SCI)	NA	NS	NA	+
h(SG)	+	+	NS	+
i(EV)	+	+	+	+
j(AN)	NS	NS	NS	+
k(CM)	NS	+	NS	+
l(FL)	NS	+	NS	NS
m(LP)	NS	NS	NS	NS
n(LV)	NS	+	NS	-
o(PH)	NS	-	NS	+
p(PZ)	NS	+	-	+

NS: non-significant at the 95% confidence level; NA: not applicable since the Natura 2000 network in Romania only started in 2001.

7.4 Discussion

In this chapter, eight explanatory variables describing accessibility, demography, land use policy and the biophysical environment were linked with observed land cover changes in the Romanian Carpathian Ecoregion. By a logistic regression model, the main explanatory variables of deforestation and afforestation were detected for two periods: 1985-1995 and 1995-2010. Model validation showed a good fit between observed afforestation and deforestation patterns and the predicted probabilities. The area under the curve ranged from 0.71 to 0.81 over the two periods and was highest for the deforestation scenario between 1995 and 2010. In the following section, the results were summarized for the 4 categories: biophysical environment, accessibility, demography and land use policy.

7.4.1 Biophysical environment

In general, the variables linked to the biophysical environment (e.g. slope gradient and elevation) were positively linked to both land cover changes (Table 7.5). The biophysical environment was the most influential predictor in the multiple regression models. The results of the MLR showed that both deforestation and afforestation occurred at relatively high elevations and on steep slopes. For afforestation, this observation was in line with the theory that land units with a low suitability for farming were firstly abandoned. Following the same logic, deforestation should have occurred at lower elevations and on weaker slopes, which was however not the case. A possible hypothesis could be that the forests were not harvested for the creation of new agricultural land but for their timber yield. Under this assumption, forest that provide the highest yield will be deforested first. In the Carpathian Ecoregion, many forests in the lower areas were the result of a recent regreening due to land abandonment and recent tree plantations after the regime change. In contrast, the forests at higher elevations were on average more mature and worthwhile harvesting. Further fieldwork and forest age mapping should confirm this hypothesis.

Moreover, the results showed that *Phaeozems* were avoided for afforestation, while *Podzols* were preferred. This result is in line with the intrinsic suitability of these soil types. The *Phaeozems*, rich in nutrients and organic material, are highly suitable for grassland and arable land (FAO, 2006). *Podzols* on the other hand are considered as unattractive soils for arable farming and suitable soils for forests (FAO, 2006), which made them attractive for new plantations in the period after the decollectivization. Furthermore, the correlation of afforestation with the occurrence of *Podzols* that occurred mainly at higher elevations in the study area, may partly explain the positive correlation between afforestation and elevation.

7.4.2 Accessibility

Distance to settlements, distance to primary and secondary roads were taken as proxy variables for accessibility. The results showed that deforestation mainly occurred in relatively accessible places nearby settlements, primary roads and secondary roads in both periods. This finding may confirm the von Thünen model in which timber is considered as a market product, whereby transportation costs and accessibility control the deforestation patterns to a certain extent. The afforestation process seems to follow a different logic since afforestation probabilities were further away from settlements and primary roads in both periods. This may be explained by the fact that afforestation results from the natural regeneration of trees due to the forest transition which mainly occurs on abandoned fields which are often located in rather remote places (Kuemmerle et al., 2006 and 2008a). Griffiths et al. (2013c) observed an extensive afforestation in the Romanian Carpathian Ecoregion during the EU accession period. Furthermore, another explanation could be the obliged replanting of young trees in the second year after a cut when the natural regeneration was insufficient (Dumitriu et al., 2003). Further field observations are necessary to validate these hypotheses.

7.4.3 Demography

In the first period, the demographic evolution (population growth or decrease) was not significantly correlated with the observed deforestation and afforestation patterns. However, both forest cover trends were positively correlated with population growth between 1995 and 2010. This might be

explained by the fact that an increasing population leads to a more intensive management of the Romanian forest with frequent clear-cuts followed replanting, while the landscape in the depopulating areas is more stable. Due to a mismatch between the available population data (1986 and 2000) and the observed land cover patterns (1985, 1995 and 2010), further field observations are necessary to validate this hypothesis.

7.4.4 Land use policy

The end of the communist regime resulted in new political and economical conditions and a change in land tenureship after the decollectivization process in the 1990s. Crucial evolutions in the Romanian forestry sector were the implementation of three restitution laws between 1991 and 2005, the accession to the EU and the construction of protected areas. However, weak implementation of the property laws resulted in increasing forest disturbance rates and nation-wide data to research the impact of the restitution laws were unavailable.

Therefore, data on the Natura 2000 network in Romania were used as a controlling factor for the impact of land use policy. Since both protection levels (SPA and SCI) started in 2001, they were only considered in the second period (1995-2010). It might be expected that the Natura 2000 policy instrument led to a slowing down of deforestation in the delineated zones. However, the opposite was observed: both protection levels were significantly positively correlated to deforestation between 1995 and 2010. This means that both in SCI and SPA zones, relatively more forest disappeared than outside these zones. A possible explanation for this finding might be an accelerated deforestation in the SPA and SCI zones between 1995-2001. In this period, the Natura 2000 policy instrument was not yet implemented. Furthermore, Biriş et al. (2006) reported that the implementation of the Natura 2000 network in Romania is rather difficult due to the lack of trained experts, data availability and/or their chaotic dispersion.

This finding are also in line with finding from other researchers that analyzed forest cover dynamics at local scale levels during and just after the fall of the communist regime (Soran et al., 2000; Brandlmaier and Hirschberger, 2005; Ioja et al., 2010; Knorn et al., 2012a and b). Knorn et al. (2012b) detected old-growth forest disturbances between 2000 and 2010 near the border of Ukraine and in the northwestern part of the Romanian Carpathian Ecoregion. The same study also reported a continued loss of old-growth forests in the Romanian Carpathians despite an increasing protected area network. 72% of the old-growth forest disturbances was found within protected areas and was partly related to institutional land reforms, insufficient protection and ownership changes since the collapse of communism in 1989. In another study, Knorn et al. (2012a) assessed disturbance patterns between 1987 and 2009 in the northern Romanian Carpathians. Forest disturbance rates increased sharply in two waves after 1995 and 2005. Substantial disturbances were detected in protected areas and even within core reserve areas. Furthermore, logging rates were largely triggered by rapid ownership and institutional changes. Corruption and lack of transparency were also mentioned as a major problem, leading to cases where sanitary or salvage logging has been misused to harvest healthy forest stands (Brandlmaier and Hirschberger, 2005; Knorn et al., 2012a). Finally, a study of Ioja et al. (2010) reported an overall decrease in the efficacy of Romania's protected areas following the creation of the Natura 2000 sites. Administrative bodies were generally under-staffed and poorly

financed, conditions that were reflected in a poor enforcement and implementation of conservation goals (Ioja et al., 2010).

7.4.5 Are the Romanian Carpathians in a forest transition phase?

Despite the disappearance of forest over the past decades in the Romanian Carpathians and according to the observed inefficiency of the land use policy, it could be concluded that the Romanian Carpathians are experiencing an overall greening. The afforestation patterns observed and described in this study show to a certain extent a similarity with the positive forest cover change in mountain regions of western Europe such as the French Alps. Remote areas, marginal arable fields and grasslands are being abandoned and are gradually replaced by natural regrowth or plantation forest. This trend is quite similar with observation made at the beginning of the 20th century in e.g. the Swiss and French Alps and the Pyrenees (Freeman, 1994; Mather et al., 1999; Mather and Fairbairn, 2000; Mather, 2001; Liébault et al., 2005).

The delay with which the Romanian Carpathians experienced a forest transition can be explained by the fact that western Europe transformed much earlier to an industrial society, while Romania remained a society based on agriculture for a longer period. At present, still 29% of Romania's population is employed in the agricultural sector (Eurostat, 2012), which is the highest percentage in Europe. The communist period further delayed the entrance of Romania in a global market system which sustained the agriculture on from global economic point of view non-profitable land units.

7.5 Conclusion

Hitherto, former studies on land cover change patterns and their controlling factors were conducted at a local scale. These studies were able to reveal certain relations between local conditions and land cover change or focused on a specific land cover change. However, local scale studies were limited since no regional scale variables were included such as demographic trends and regional policy regulations. This study aimed to produce new insights in the mechanisms of land cover change by including both local and regional scale variables. Regional scale land cover maps produced with advanced pixel-based compositing techniques were combined to map the main land cover changes.

In order to acquire a better insight in the controlling factors of the forest cover dynamics, the observed dynamics were linked with 8 explanatory variables. The results show that deforestation follows to a certain extent a von Thünen logic in which the accessible places are logged first, while the deforestation patterns seem to occur in more remote locations, possibly related to the abandonment of remote fields. Land suitability for farming and forestry could be identified as a crucial factor. Afforestation is dominant on *Podzols,* while the *Phaeozems* are avoided.

Furthermore, this study showed that the implementation of the Natura 2000 network missed its goal since more deforestation was observed in the protected areas than outside. This could partly be explained by the lawless period following the fall of the communist regime and before the installation of the protected zones. A second explanation were the concerns on the difficult implementation of the Natura 2000 network in Romania and the status of nature protection. The

most important finding was the observation that the Romanian Carpathians are greening, despite local reports of deforestation and illegal logging. The observed forest cover trends can therefore be considered as a delayed forest transition similar to transition phases in the western European mountain ranges at the beginning of the 20th century.

PART 4: GENERAL DISCUSSION, CONCLUSIONS AND PROSPECTS

Chapter 8: General discussion, conclusions and prospects

8.1 General conclusions and discussion

Forest cover changes have essential implications on a variety of landscape functions and their associated ecosystem services. Obviously, there is a need for reliable assessments of forest cover dynamics in order to assess future levels of ecosystem services. From scientific point of view there is an increasing interest in reliable data on forest cover dynamics that may provide a better insight in the drivers and mechanisms of forest cover change. Policy makers that are trying to steer forest cover dynamics in a certain direction developed a range of instruments such as land zoning, payment systems for the conservation of ecosystem services and product certification for sustainable production processes. Not surprisingly, there is a need for the evaluation of those instruments to check whetherthe protection by certain policiesis efficient.

The detection and mapping of forest dynamics is, however, rather challenging since landscapes in the transition phases typically consist of patchy structures. Moreover, many hotspots of change are located in remote mountain areas. Finally, forest cover changes in the turnover phase from net deforestation to net afforestation are often characterized by subtle up- and downward trends. Remote sensing techniques seem to be proper tools for the analysis of forest cover changes in mountain areas and yet suffer from methodological problems. Many forest cover maps derived from remote sensing imagery are unreliable due to atmospheric and topographic distortions, especially in mountain areas. Moreover, for large scale studies, there is a strong need for reliable techniques to develop homogeneous image mosaicks. A range of techniques and methods has been developed but a systematic comparison of their efficiency for mapping forest cover dynamics was lacking till now.

This thesis evaluated the existing atmospheric and topographic correction techniques based on assessments of reflectance homogeneity and classification accuracy. Furthermore, a topographic correction procedure was integrated in a pixel-based image compositing (PBIC) algorithm for the analysis of forest cover change on a large scale. Thereby, the detection of forest cover change in the Romanian Carpathian Ecoregion between 1985 and 2010 was taken as an example application.

The scientific challenges related to large scale monitoring of forest cover change were addressed by following four research questions. Here, the main findings of this thesis are summarized:

1. To what extent do available atmospheric and topographic corrections improve the homogeneity of reflectance values of medium resolution imagery in mountain areas? Do complex procedures perform better than simplified approaches?

Most radiometric correction methods described in literature are presented as integrated methods although they consist of a sequential application of an atmospheric and topographic correction. In this study, it was decided to evaluate the basic topographic and atmospheric components for such models. Firstly, a typology of atmospheric and topographic correction methods was developed. Next, the performance of 15 atmospheric and topographic combinations was assessed. In order to do so,

three validation techniques were developed: (1) assessment of differences in reflectance between illuminated and shaded land units before and after correction, (2) statistical homogeneity tests for pixels with equal land cover before and after correction, and (3) correlation analysis between observed reflectance and terrain illumination. The analyses were performed on a Landsat footprint in the Romanian Carpathian mountains. First, results showed a reduction of the differences between average illuminated and shaded reflectance values after correction. Significant improvements were found for methods with a pixel-based Minnaert (PBM) or a pixel-based C (PBC) topographic correction. Secondly, the analysis of the coefficients of variation showed that the homogeneity for the selected forest pixels increased after correction. Finally, the dependency of reflectance values on terrain illumination was reduced after implementation of an atmospheric correction combined with the PBM or PBC method.

Considering the overall results, this analysis showed that the complex combined corrections were most accurate but also most difficult to automate. Furthermore, the added value of complex topographic methods was high, while the added value of atmospheric methods was limited. Therefore, application of a combined correction based on a complex topographic component and a rather straightforward atmospheric component was justified in this case study. The added value of this study was the decomposition of combined models and the systematic evaluation along with uncorrected imagery.

2. Does image preprocessing lead to more accurate land cover classification?

In order to address this research question, all combinations of two atmospheric corrections, four topographic corrections and the uncorrected scenarios were applied on two acquisitions (2009 and 2010) of a Landsat image in the Romanian Carpathian mountains. First, results showed that all corrected images resulted in higher overall classification accuracies than the uncorrected images. Secondly, class accuracies of especially the coniferous and mixed forest classes were enhanced after correction. Finally, combined correction methods showed most efficient on weakly illuminated slopes ($\cos i \leq 0.65$). The highest classification accuracy was achieved after combination of the transmittance functioncorrection with PBM or PBC topographic correction. Results of this study also indicated that the topographic component had a higher influence on classification accuracy than the atmospheric component.

3. To what extent does topographic correction and pixel-based compositing improve large area (change) mapping?

Recently, pixel-based image compositing algorithm have been developed to produce homogeneous land cover maps for larger areas, such as Griffiths et al. (2013b) for the Carpathians and Hansen et al. (2013) for the world. It is clear that these methods interact with preceding or following radiometric correction. Although, the added value of the combination of these methods was not examined till now. In this work, the results of pixel-based image compositing with and without topographic correction was examined. Therefore, the classification accuracy was assessed for five different scenarios in which 3 components were altered: classifier (Maximum Likelihood or Support Vector Machine, SVM), number of classes (4 or 8) and topographic correction (uncorrected or corrected). The results were evaluated by the calculation of overall and land cover specific accuracies. The overall accuracy for 8 land cover classes was between 66% and 82% for all years. Furthermore, the

implementation of a topographic correction had a smaller influence on the classification accuracy than the selection of a classifier. In contrast, overall classification accuracies of the corrected SVM classification for 4 land cover classes were higher, respectively 85% (1985), 83% (1995) and 91% (2010). The change analysis observed a steady greening of the Romanian Carpathians between 1985 and 2010 due to a larger afforestation than deforestation.

4. What is the pattern and what are the controlling factors of forest cover changes in the Romanian Carpathians?

An analysis of the produced forest cover change maps for the Romanian Carpathians showed an overall greening of the landscape since more afforestation than deforestation occurred. In this final part, the observed land cover change patterns were linked with 8 controlling factors in four categories: accessibility, demography, land use policy and biophysical environment. The most important finding was the observation that the Romanian Carpathians are greening, despite local reports of deforestation and illegal logging. The observed forest cover trends can therefore be considered as a delayed forest transition similar to transition phases in the western European mountain ranges at the beginning of the 20th century.

The multiple logistic regression also concluded that afforestation and deforestation were mainly positively related to the biophysical environment (elevation and slope gradient) for both periods. In contrast, the distance to secondary roads was negatively related to both land cover changes in these periods. Furthermore, land suitability for farming and forestry was identified as a crucial factor since afforestation was dominant on *Podzols,* while *Phaeozems* were avoided. Finally, this study showed that more deforestation was observed in forests protected by the Natura 2000 network than outside these forests. This was explained by the lawless period following the fall of the communist regime and the difficult implementation of the Natura 2000 network in Romania.

8.2 Prospects and recommendations for further research

This study aimed at contributing to a better detection of forest cover dynamics, especially in mountain areas. Therefore, available preprocessing methods were examined, evaluated with novel evaluation techniques and integrated in chain processing. Nevertheless, this research revealed that several additional procedures could be developed and evaluated.

The approach adopted in this study consisted of the decomposition of so-called 'combined correction methods'in their basic topographic and atmospheric components. In this way, the performance of each component could be evaluated separately. The case study proved that the benefits in reduction of atmospheric and topographic distortions justified the automation of more complex corrections in mountain areas. Preprocessing methods that were complex to automate in a processing chain were unattractive for integration in regional scale analyses though. This was especially valid for pixel-based compositing algorithms which need to preprocess large image archives. Therefore, a larger focus on the automation potential of correction methods is desired in further studies. The automation potential of different corrections decreases with the complexity of input parameters. Therefore, indicators that quantify the automation potential should be developed. Such indicators should

include a distinction between: (a) single value input parameters available in image metadata (high automation potential), (b) single value input parameters available in external data sources (medium automation potential), (c) single value input parameters derived from regression models (low automation potential), and (d) data layers available in external data sources (low automation potential). Consequently, the automation difficulty could be assessed for each combined correction by summing the scores of all input variables. Such an automation indicator could then be used in an expert system that helps a user to select the appropriate techniques given the accuracy criteria and the manpower available in the project.

The integration of different scale levels of satellite imagery will also play an important role in future research since the costs of high and very high resolution imagery is expected to decrease. This will provide additional data for regional scale land cover studies. For example, high and very high resolution imagery can be used for the accurate selection and verification of ground control points to improve accuracy assessments of land cover mapping. The techniques that were implemented in this research can also support the improvement of the direct monitoring of ecosystem services. Moreover, this research can provide a basis for the evaluation of policy instruments and conservation measures. In the future, new analyzing techniques will be necessary to evaluate programmes such as eco-certificates and payments for ecosystem services.

In this thesis, pixel-based compositing and topographic correction were integrated in a rather straightforward procedure: topographic correction of the imagery after compositing. The decision for image selection during compositing devised by Griffiths et al. (2013a) was based on a flexible parametric weighting scheme that evaluated available observations for their suitability. A more sophisticated integration could be developed by extending the flexible parametric weighting scheme with e.g. the local solar incidence angle and off-nadir position. In mountain areas, the inclusion of parameters that quantify the illumination effect could be interesting for an adapted topographic and/or atmospheric correction. Griffiths et al. (2013a) suggested the selection of the observation with the lowest reflectance in the blue band to minimize the atmospheric effects. Furthermore, in such a scheme, topographic and atmospheric correction should be performed before the composting procedure since the compositing will depend on the preprocessing. Results in this study and the study by Griffiths et al. (2013a) showed that compositing artifacts related to SLC-off scan line errors were visible in some areas of the land cover map when using the uncorrected PBIC. These artifacts were still visible in the map resulting from the topographically corrected PBIC. However, Griffiths et al. (2013a) showed that the inclusion of variability metrics is able to alleviate the SLC-off errors.

Finally, this study focused on the impact of atmospheric and topographic corrections on a single study area: the Romanian Carpathian Ecoregion. Further research should therefore focus on the application of the techniques on other mountain study areas and larger temporal series.

References

Abrudan, I.V., Codrin, C., Ignea, G., Marinescu, V., 2005. Present situation and trends in the Romanian Forestry, Proceedings of the 6th international symposium, Legal Aspects of European Forest Sustainable Development, April 2005, Poiana, Brasov. 180 pp.

Abrudan, I.V., Marinescu, V., Ionescu, O., Ioras, F., Horodnic, S.A., Sestras, R., 2009. Developments in the Romanian forestry and its linkages with other sectors, Notulae Botanicae Horti Agrobotanici Cluj-Napoca, 37, 2, 14-21.

Ackerman, S.A., Strabala, K.I., Menzel, W.P., Frey, R.A., Moeller, C.C., Gumley, L.E., Baum, B.A., Schaaf, C., Riggs, G., 2002. Discriminating Clear-Sky from Cloud with MODIS – Algorithm Theoretical Basis Document, Products: MOD35, 121 pp.

Adams, J.B., Sabol, D.E., Kapos, V., Filho, R.A., Roberts, D.A., Smith, M.O., Gillespie, A.R., 1995. Classification of multispectral images based on fractions of endmembers: Application to land-cover change in the Brazilian Amazon, Remote Sensing of Environment, 52, 2, 137–154.

Adler–Golden, S.M., Matthew, M.W., Bernstein, L.S., Levine, R.Y., Berk, A., Richtsmeier, S.C., Acharya, P.K., Anderson, G.P., Felde, G., Gardner, J., Hoke, M., Jeong, L.S., Pukall, B., Mello, J., Ratkowski, A., Burke., H.H., 1999. Atmospheric correction for short-wave spectral imagery based on MODTRAN4, SPIE Proceeding, Imaging Spectrometry V, 3753, 1-10.

Alcantara, C., Radeloff, V.C., Prishchepov, A.V., Kuemmerle, T., 2012. Mapping abandoned agriculture with multi-temporal MODIS satellite data, Remote Sensing of Environment, 124, 334–347.

Aldhous, J.R., 1997. British forestry: 70 years of achievement, Forestry, 70, 283- 291.

Ammer, U., Breitsameter, J., Zander, J., 1995. Contribution of mountain forests towards the prevention of surface runoff and soil erosion, Forstwissenschaftliches Centralblatt, 114, 232–249.

Anfodillo, T., Carrer, M., Valle, E.D., Giacoma, E., Lamedica, S., Pettenella, D., 2008. Current State of Forest Resources in the Carpathians. Activity 2.7: Forestry and Timber Industry, 20 January 2008, Università Degli Studi Di Padova, Dipartimento Territorio e Sistemi Agro-Forestali, Legnaro, 158 pp.

Angelsen, A., Rudel, T., 2013. Designing and Implementing Effective REDD+ Policies: A Forest Transition Approach, Review of Environmental Economics and Policy, 7, 1, 91–113.

Anthony, G., Gregg, H., Tshilidzi, M., 2008. A SVM multi-classifier approach to land cover mapping, ASPRS 2008 Annual Conference, May 2 2008, Portland, Oregan, USA, 6 pp.

Achard, F., Eva, H., Mollicone, D., Popatov, P., Stibig, H.-J., Turubanova, S., Yaroshenko, A., 2009. Detecting intact forests from space: hot spots of loss, deforestation and the UNFCCC. In: Old-Growth Forests, Wirth, C., Gleixner, G., Heimann, M. (Ed.), Berlin and Heidelberg, Germany, Springer, 411–427.

Allouche, O., Tsoar, A., Kadmon, R., 2006. Assessing the accuracy of species distribution models: prevalence, kappa and true skill statistic, Journal of Applied Ecology, 43,. 1223–1232.

Arvidson, T., Gasch, J., Goward, S.N., 2001. Landsat 7's long term acquisition plan – an innovative approach to building a global archive, Special Issue on Landsat 7, Remote Sensing of Environment, 78, 13–26.

Arvidson, T., Goward,, S., Gasch, J., Williams, D., 2006. Landsat-7 long-term acquisition plan: Development and validation, PhotogrammetricEngineering and Remote Sensing, 72, 1137–1146.

ASFOR, 2010. The Romanian Forest Resources, Recent Developments and Future Prospects. Available at http://www.metla.fi/hanke/7395/pdf/Asfor.pdf (accessed 8 January 2014).

Asmala, A., Shaun, Q., 2012. Cloud Masking for Remotely Sensed Data Using Spectral and Principal Components Analysis, Engineering, Technology & Applied Science Research, 2, 3, 221-225.

Aspinall, R., 2002. A land-cover data infrastructure for measurement, modeling, and analysis of land-cover change dynamics, Photogrammetric Engineering and Remote Sensing ,68, 10, 1101−1105.

Asrar, G., Fuch, M., Kanemasu, E.T., Hatfield, J.L., 1984. Estimating absorbed photosynthetic radiation and leaf area index from spectral reflectance in wheat, Agronomy Journal, 76, 300–6.

ASTRIUM, 2013. SPOT 6 and SPOT 7. Available at http://www.astrium-geo.com/en/147-spot-6-7 (Accessed 19 January 2014).

Baker, W.L., 1989. A review of models of landscape change, Landscape Ecology, 2, 2, 111–133.

Bakker, M.M., Govers, G., Kosmas, C., Vanacker, V., van Oost, K., Rounsevell, M., 2005. Soil erosion as a driver of land-use change, Agriculture Ecosystems and Environment, 105, 467-481.

Baldi, G., Paruelo, J.M., 2008. Land-Use and Land Cover Dynamics in South American Temperate Grasslands, Ecology and Society, 13, 1-20.

Balthazar, V., Vanacker V., Lambin, E., 2012. Evaluation and parameterization of ATCOR3 topographic correction method for forest cover mapping in mountain areas, International Journal of Applied Earth Observation and Geoinformation, 18, 436–450.

Bannari, A., Morin, D., Bonn, F., Huete, A.R., 1995. A review of vegetation indices, Remote Sensing Reviews, 13, 1-2, 95–120.

Baret, F., Guyot, G. 1991. Potentials and limits of vegetation indices for LAI and PAR assessment, Remote Sensing of Environment, 35, 161– 173.

Baret, F., Guyot, G., Major, D., 1989. TSAVI: a vegetation index which minimizes soil brightness effects on LAI and APAR estimation, 12th Canadian Symposium on Remote Sensing and IGARSS'90, 10- 14 July 1989, Vancouver, Canada, 4 pp.

Barney, K., 2005. Central Plans and Global Exports: Tracking Vietnam's Forestry Commodity Chains and Export Links to China, Forest Trends, Washington, DC, 77 pp.

Bateso,, C.A., Asner, G.P., Wessman, C.A., 2000. Endmember bundles: a new approach to incorporating endmember variability into spectral mixture analysis, IEEE Transactions on Geoscience and Remote Sensing, 38**,** 2, 1083- 1094.

Beeri, O., Phillips, R., Hendrickson, J., Frank, A.B., Kronberg, S., 2007. Estimating forage quantity and quality using aerial hyperspectral imagery for northern mixed-grass prairie, Remote Sensing of Environment, 110, 216–25.

BELSPO, 2011. PROBA-V, GMES Global Land, Lisbon, Portugal, 12 December 2011, 16 pp.

Benayas, J.M.R., Martins, A., Nicolau, J.M., Schulz, J.J., 2007. Abandonment of agricultural land: an overview of drivers and consequences, Reviews: Perspectives in Agriculture, Veterinary Science, Nutrition and Natural Resources, 2, 57, 2-14

Bendix, J., Rollenbeck, R., Palacios, W.E., 2004. Cloud detection in the Tropics – a suitable tool for climate – ecological studies in the high mountains of Equador, International Journal of Remote Sensing, 25, 21, 4521 – 4540.

Bennet, G., 2000. Ecoregion-Based Conservation in the Carpathians: Final Reconnaissance Report, WWF International Danube–Carpathian Programme, Vienna, 43 pp.

Berk, A, Bernstein, L.S., Anderson, G.P., Robertson, D.C., Chetwynd, J.H., Adler-Golden, S.M., 1998. MODTRAN Cloud and multiple scattering upgrades with application to AVIRIS, Remote Sensing of Environment, 65, pp. 367–375.

Berlik, M.M., Kittredge, D.B., Foster, D.R., 2002. The illusion of preservation: A global environmental argument for the local production of natural resources, Journal of Biogeography, 29, 1557–1568.

Bernstein, L.S., Adler-Goldon, S.M., Sundberg, R.L., Levine, R.Y., Perkins, T.C., Berk, A., Ratkowski, A.J., Felde, G., Hoke, M.L., 2005. A new method for atmospheric correction and aerosol optical property retrieval for VIS-SWIR multi- and hyperspectral imaging sensors: QUAC (Quick Atmospheric Correction), IEEE International Geoscience and Remote Sensing Symposium, 5, 3549-3552.

Bicik, I., Jelecek, L., Stepanek, V., 2001. Land-use changes and their social driving forces in Czechia in the 19th an 20th centuries, Land Use Policy, 18, 1, 65-73.

Bird, R.E., Riordan, C., 1986. Simple solar spectral model for direct and diffuse irradiance on horizontal and tilted planes at the earth's surface for cloudless atmospheres, Journal of Climate and Applied Meteorology, 25,87–97.

Biriş, I.-A., Veen, P., 2005. Virgin Forests in Romania, inventory and strategy for sustainable management and protection of virgin forest in Romania, ICAS and KNNV, 61 pp.

Biriş, I.-A., Marin, G., Stoiculescu, C., Maxim, I., Verghelet, M., Apostel, J., 2006. COST Action E 27: protected forest areas in Europe (PROFOR)—country report Romania, Forest Research and Management Institute ICAS, Bucharest, Romania, 19 pp.

Bishop, M.P., Colby, J.D., 2002. Anisotropic reflectance correction of SPOT-3 HRV imagery, International Journal of Remote Sensing, 23, 2125–2131.

Bishop, M.P., Shroder, J.F., Colby, J.D, 2003. Remote sensing and geomorphometry for studying relief production in high mountains, Geomorphology, 55,345–361.

Björnsen G.A., Bokwa, A., Chelmicki, W., Elbakidze, M., Hirschmugl, M., Hostert, P., Ibisch, P., Kozak, J., Kuemmele, T., Matei, E., Ostapowicz, K., Pociask-Katerczka, J., Schmidt, L., van der Linden, S., Zebisch, M., 2009. Mountain Research and Development, 29, 282-288.

Blesius, L., Weirich, F., 2005. The use of the Minnaert correction for land-cover classification in mountainous terrain, International Journal of Remote Sensing, 26,3831–3851.

Borlea, G.F., Brad, R., Merce, O., Turcu, D., 2004. Wood energy in Romania, Anale I.C.A.S., 46, 6 pp.

BOS+, 2013. 10 Miljoen bomen voor Vlaanderen. Available at http://www.10miljoenbomen.be/hoe-werkt-het (accessed 21 August 2013).

Bradshaw, R.H.W., 2004. Past anthropogenic influence on European forests and some possible genetic consequences. Forest Ecology and Management, 197, 203-212.

Brandlmaier, H., Hirschberger, P., 2005. Illegal logging in Romania, WWF European Forest Programme and Danube Carpathian Programme, 116, 1-17.

British Colombia Ministry of Forests, 2001. Introduction to silvicultural systems. Available at http://www.for.gov.bc.ca/hfp/training/00014/chap2frt.htm (accessed 11 January 2013).

Broich, M., Hansen, M.C., Potapov, P., Adusei, B., Lindquist, E., Stehman, S.V., 2011. Time-series analysis of multi-resolution optical imagery for quantifying forest cover loss in Sumatra and Kalimantan, Indonesia, International Journal of Applied Earth Observation and Geoinformation, 13, 277–291.

Broszeit, A., Ashraf, S., 2013. Using different atmospheric correction methods to classify remotely sensed data to detect liquefaction of the February 2011 earthquake in Christchurch, August 29th – 30th 2013, SIRC NZ – GIS and Remote Sensing Research Conference, University of Otago, Dunedin, New Zealand, 6 pp.

Bruce, C.M., Hilbert, D.W., 2004. Pre-processing methodology forapplication to Landsat TM/ETM+imagery of the wet Tropics. Research report, Cooperative research centre fortropical rainforest ecology andmanagement,Cairns, Australia. Available at http://www.rrrc.org.au/rfcrc/downloads/44_landsat_preprocessing.pdf (Accessed 13 July 2013)

Brünig, E., Mayer, H., 1980. Waldbauliche Terminologie. Universität für Bodenkultur, Wien.

Bud, N., 2000. Silvicultura Romaniei in 200 de ani, Baia Mare, Romania, 225 pp.

Burkhard, B., Kroll, F., Nedkov, S., Müller, F., 2012. Mapping ecosystem service supply demand and budgets, Ecological Indicators, 21, 17–29.

Burns, P., Nolin, A., 2014. Using atmospherically-corrected Landsat imagery to measure glacier area change in the Cordillera Blanca, Peru from 1987 to 2010. Remote Sensing of Environment, 140, 165–178.

Campbell, J.B., 1981. Spatial correlation effects upon accuracy of supervised classification of land cover, Photogrammetric Engineering and Remote Sensing, 47, 355–363.

CGIAR-CSI/NASA, 2013. SRTM 90m Digital Elevation Database v4.1. Available at http://www.cgiar-csi.org/data/srtm-90m-digital-elevation-database-v4-1 (Accessed 16 January 2013).

Chazdon, R.L., 2008. Beyond deforestation: restoring forests and ecosystem services on degraded lands, Science, 320, 1458–1460.

Chhabra, A., Palria, S., Dadhwal, V.K., 2002. Growing stock-based forest biomass estimate for India, Biomass Bioenergy, 22, 181-194.

Chhabra, A., Dadhwal, V.K., 2004. Assessment of Major Pools and Fluxes of Carbon in Indian Forests, Climatic Change, 64, 341-360.

Chander, G., Markham, B.L., Helder, D.L., 2009. Summary of current radiometric calibration coefficients for Landsat MSS, TM, ETM and EO-1 ALI sensors, Remote Sensing of Environment, 113,893-903.

Chander, G., Xiong, X., Choi, T., Angal, A., 2010. Monitoring on-orbit calibration stability of the Terra MODIS and Landsat 7 ETM+ sensors using pseudo-invariant test sites, Remote Sensing of Environment, 114, 925–939.

Chavez, P.S., 1975. Atmospheric, solar, and MTF corrections for ERTS digital imagery, Proceedings of American Society of Photogrammetry Fall Conference, Phoenix, Arizona, USA, 69 pp.

Chavez, P.S., 1996. Image-based atmospheric correction-revisited and improved, Photogrammetric Engineering and Remote Sensing, 62, 1025–1036.

Chen, D., Stow, D.A., Gong, P., 2004. Examining the effect of spatial resolution and texture window size on classification accuracy: an urban environment case, International Journal of Remote Sensing 25, 2177–2192.

Chevrel, M., Courtois, M., Weill, G., 1980. The SPOTsatellite remote sensing mission, American Photogrammetric Engineering and Remote Sensing, 47, 1163-1171.

Chomitz, K.M., Gray, D.A., 1996. Roads, land use, and deforestation: a spatial model applied to Belize, The World Bank Economic Review, 10, 3, 487–512.

Cihlar, J., Manak, D., Diorio, M., 1994. Evaluation of compositing algorithms for AVHRR data over land,IEEE Transactions on Geoscience and Remote Sensing, 32, 427–437.

Cismaru, I., 2003. Wood Industry in Romania - Present and Perspectives. In: Proceedings of the 8th International IUFRO Wood Drying Conference, 24-29 August 2003, Brasov, Romania, pp. 3-8.

Civco, D.L., 1989. Topographic normalization of Landsat Thematic Mapper digital imagery, Photogrammetric Engineering and Remote Sensing, 55, 1303–1309.

Clapp, R.A., 2001. Tree farming and forest conservation in Chile: do replacement forests leave any originals behind? Society and Natural Resources, 14, 341-356.

Clarke, K.C., Hoppen, S., Gaydos, L., 1997. A self-modifying cellular automaton model of historical urbanization in the San Francisco Bay area, Environment and Planning B: Planning and Design, 24, 247-261.

Clawson, M., 1979. Forests in the Long Sweep of American History, Science, 204, 1168-1174.

Coburn, C.A., Roberts, A.C.B., 2004. A multiscale texture analysis procedure for improved forest stand classification, International Journal of Remote Sensing, 25, 4287–4308.

Cohen, J., 1960. A coefficient of agreement for nominal scales, Educational and Psychological Measurement 20, 37–46.

Cohen, W.B., Goward, S.N., 2004. Landsat's role in ecological applications of remote sensing, Bioscience, 54, 535–545.

Colby, J.D., 1991. Topographic normalization in rugged terrain, Photogrammetric Engineering and Remote Sensing, 57, 531-537.

Colby, J.D., Keating, P.L., 1998. Land cover classification using Landsat TM imagery in the tropical highlands: the influence of anisotropic reflectance, International Journal of Remote Sensing, 19,1479–1500.

Cole, C.V., Burke, I.C., Parton, W.J., Schimel, D.S., Stewart, J.W.B., 1989. Analysis of historical changes in soil fertility and organic matter levels of the North American Great Plains, Proceedings of the International Conference on Dryland Farming, January 1989, College Station, Texas A&M, pp. 436-438.

Commission of the European Communities, 1995**.** CORINE land cover. 163 pp.

Committee on Global Change Research, National Research Council, 1999. Global Environmental Change: Research Pathways for theNext Decade. National Academy Press, Washington, DC. 603 pp.

Conel, J.E., Green, R.O., Vane, G., Bruegge, C.J., Alley, R.E., 1987. AIS-2 radiometry and a comparison of methods for the recovery of ground reflectance. In: Vane, G. (Ed.), Proceedings of the 3rd Airborne Imaging Spectrometer Data Analysis Workshop JPL Publ., 2-4 June 1987, Jet Propulsion Laboratory, Pasadena, CA, 29 pp.

Conese, C., Gilabert, M.A., Maselli, F., Bottai, L., 1993. Topographic normalization of TM scenes through the use of an atmospheric correction method and digital terrain models, Photogrammetric Engineering and Remote Sensing, 59, 1745-1753.

Congalton, R.G., 1981. The use of discretemultivariate analysis for the assessment of Landsat classification accuracy. M.Sc. thesis, Virginia Polytechnic Institute and State University, Blacksburg, VA, USA; 132 pp.

Congalton, R.G., 1991. A review of assessing the accuracy of classifications of remotely sensed data, Remote Sensing of Environment 37, 35–46.

Congalton, R.G., Green, K., 1999. Assessing the Accuracy of Remotely Sensed Data: Principles and Practices, Boca Raton, Florida, USA, 129 pp.

Congalton, R.G., Oderwald, R.G., Mead, R.A., 1983. Assessing Landsat classification accuracy using discrete multivariate analysis statistical techniques, American Society of Photogrammetry, 49, 1671–1678.

COP3, 2011. Protocol on sustainable forest management to the framework convention on the protection and sustainable development of the Carpathians, Third meeting of the conference of the parties to the Carpathian convention, Bratislava, Slovakia, 27 May 2011, 12 pp.

Coppin, P., Nackaerts, K., Queen, L., Brewer, K., 2001. Operational monitoring of green biomass change for forest management, Photogrammetric Engineering and Remote Sensing, 67, 5, 603-611.

Costanza, R., d'Arge, R., de Groot, R., Farberk, S., Grasso, M., Hannon, B., Limburg, K., Naeem, S., O'Neill, R.V., Paruelo, J., Raskin, R.G., Suttonk, P., van den Belt, M., 1997. The value of the world's ecosystem services and natural capital, Nature, 387, 253-260.

Courtois, M., Weill, G., 1985. The SPOTsatellite system, Monitoring earth's ocean, land, and atmosphere from space - Sensors, systems, and applications, 14, 493-523.

Crawford, J.J., Manson, S.M., Bauer, M.E., Hall, D.K., 2013. Multitemporal snow cover mapping in mountainous terrain for Landsat climate data record development, Remote Sensing of Environment, 135, 224–233.

Crippen, E.R., 1988. The dangers of underestimating the importance of data adjustments in band ratioing, International Journal of Remote Sensing, 9, 4, 767–776.

Cristea, V., 1995. La conservation de la nature en Roumanie, Camerino (Macerata), Universita degli Studi, Italy, 39, 95-97.

Cristea, V., 1996a. Nature and environment protection – main problems of contemporary world. In: Cristea, V., Denaeyer, S., Herremans, I.P., Goia, I. (Eds.), Ocrotirea naturii si protectia mediului în România, Cluj University Press, Cluj-Napoca, Romania [in Romanian], 13–102.

Cuo, L., Vogler, J.B., Fox, J.M., 2010. Topographic normalization for improving vegetation classification in a mountainous watershed in Northern Thailand, International Journal of Remote Sensing, 31, 3037-3050.

De Brue, H., Verstraeten, G., 2013. Impact of the spatial and thematic resolution of Holocene anthropogenic land cover scenarios on modeled soil erosion and sediment delivery rates. The Holocene. DOI 10.1177/0959683613512168.

Deliever, I., 2012. Exploring the forest cover in the Romanian Carpathians (1986-2010), a remote sensing analysis using medium resolution Landsat and very high resolution WordlView-2 imagery, Unpublished M.Sc. thesis, KU Leuven, Belgium, 145 pp.

DeFries, R.S., Foley, J.A., Asner, G.P., 2004. Land-use choices, balancing human needs and ecosystem function, Frontiers in Ecology and the Environment, 2,249-257.

DeFries, R.S., Pandey, D., 2010. Urbanization, the energy ladder and forest transitions in India's emerging economy, Land Use Policy, 27, 130-138.

Dendoncker, N., Rounsevell, M., Bogaert, P., 2007. Spatial analysis of modeling of land use distributions in Belgium, Computers, Environment and Urban Systems, 31, 188-205.

Devasthale, A., Karlsson, K.G., Quaas, J., Grassl, H., 2012. Correcting orbital drift signal in the time series of AVHRR derived convective cloud fraction using rotated empirical orthogonal function, Atmospheric Measurement Techniques, 5, 267–273.

Diaci, J., 1998. Virgin forests and forest reserves in central and east European countries. History, present status and future development. COST Action E4, Ljubljana, Slovakia, 25-28 April 1998, Romania, 183 pp.

Dial, G., Bowen, H., Gerlach, F., Grodecki, J., Oleszczuk, R., 2003. IKONOS satellite, imagery, and products, Remote Sensing of Environment, 88, 1-2, 23–36.

Diaz-Briquets, S., Perez-Lopez, J.F., 2000. Conquering nature: the environmental legacy of socialism in Cuba, Pittsburgh, University of Pittsburgh Press, 157 pp.

Diaz, G.I., Nahuelhual, L., Echeverria, C., Marin, S., 2011. Drivers of land abandonment in southern Chile and implications for landscape planning, Landscape and Urban Planning, 99, 207-217.

Di Eugenio, B., Glass, M., 2004. The kappa statistic: a second look. Computational Linguistics, 30, 95–101.

Dumitriu, G., Pirnuta, G., Biris, O., Florian, G.B., 2003. The sound use of wood and other resources in Romania. Seminar on Strategies for the Sound Use of Wood, Poiana Brasov, Romania, 11 pp.

Dixon, B., Candade, N., 2008. Multispectral land use classification using neural networks and support vector machines: One or the other, or both? InternationalJournal of Remote Sensing, 29, 1185−1206.

Dupouey, J. L., Dambrine, E., Laffite, J.D., Moares, C., 2002. Irreversible impact of past land use on forest soils and biodiversity, Ecology, 83, 2978–2984.

Dutca, I., Abrudan, I.V., 2010. Estimation of forest land-cover change in Romania, between 1990 and 2006, Bulletin of the Transilvania University of Brasov, 3, 52, 4 pp.

Echeverria, C., Coomes, D.A., Hall, M., Newton, A.C., 2008. Spatially explicit models to analyze forest loss and fragmentation between 1976 and 2020 in southern, Chile, Ecological Modelling, 212, 439-449.

EEA, 1995. CORINE Land and forest cover maps. Available at http://www.eea.europa.eu/publications/COR0-landcover (Accessed 2 October 2013).

Egbert, S.L., Park, S., Price, K.P., Lee, R.-Y., Wu, Y., Nellis, M.D., 2002. Using conservation reserve program maps derived from satellite imagery to characterize landscape structure, Computers and Electronics in Agriculture, 37, 141–56.

Ehrlich, D., Estes, J.E., Singh, A., 1994. Applications of NOAA-AVHRR 1 km data for environmental monitoring, International Journal of Remote Sensing, 15, 1, 145-161.

Eidenshink, J.C., Faundeen, J.L., 1994. The 1 km AVHRR global land data set: first stages in implementation, International Journal of Remote Sensing, 15, 17, 3443-3462.

Eiumnoh, A., Shrestha, R.P., 2000. Application of DEM data to Landsat image classification: evaluation in tropical wet-dry climate, Photogrammetric Engineering and Remote Sensing, 66, 297-304.

Ekstrand, S., 1996. Landsat TM-based forest damage assessment: correction for topographic effects, Photogrammetric Engineering and Remote Sensing, 62, 151–161.

Elvidge, C.D., Chen, Z., 1995. Comparison of broad-band and narrow-band red and near-infrared vegetation indices, Remote Sensing of Environment, 54, 1, 38–48.

Enescu, V., 1996. Forest Genetic Resources Conservation in Romania. Food and Agriculture Organization of the United Nations (FAO), Rome. 132 pp.

Epiphanio, J.C.N., 2005. Joint China-Brazil remote sensing satellites: CBERS-2. GIM Interational, 19, 68–71.

Ericsson S., Östlund, L., Axelsson, A.L., 2000. A forest of grazing and logging: Deforestation and reforestation history of a boreal landscape in central Sweden, New Forest, 19, 227-240.

ESA, 2012. PROBA-V mission. Available at http://www.esa.int/Our_Activities/Technology/Proba_Missions/Mission (Accessed 2 February 2014).

Eumetrain, 2010. Monitoring vegetation from space. Available at http://www.eumetrain.org/data/3/36/index.htm (Accessed 12 July 2013).

European Commission, 2012. NUTS Nomenclature of territorial units for statistics. Available at http://epp.eurostat.ec.europa.eu/portal/page/portal/nuts_nomenclature/introduction (Accessed 14 August 2013).

European Commission, 2013a. Global Land Cover 2000. Available at http://bioval.jrc.ec.europa.eu/products/glc2000/glc2000.php (Accessed 5 October 2013).

European Commission, 2013b. Management of Natura 2000 sites. Available athttp://ec.europa.eu/environment/nature/Natura 2000/management/(Accessed 13 October 2013).

Eurostat, 2012. Statistics by theme. Available athttp://epp.eurostat.ec.europa.eu/portal/page/portal/statistics/themes (Accessed 16 April 2013).

FAO, 1997. Issues and Opportunities in the Evolution of Private Forestry and Forestry Extension in Several Countries with Economies in Transition in Central and Eastern Europe. Available at http://www.fao.org/docrep/w7170e/w7170e0f.htm (Accessed 8 January 2014).

FAO/UNESCO/WRB, 1998. Soil Map of the World, Revised Legend. World Soil Resources Report 60, Rome, 146 pp.

FAO, 2001. Global Forest Resources Assessment 2000. Rome, Italy, 511 pp.

FAO, 2006. World reference base for soil resources 2006: A framework for international classification, correlation and communication, Rome, Italy, 145 pp.

FAO, 2008. Technical Review of FAO's Approach and Methods for National Forest Monitoring and Assessment (NFMA), National Forest Monitoring andAssessment Working Paper NFMA 38, Rome, 96 pp.

FAO, 2010. Global Forest Resources Assessment 2010. Rome, Italy. 340 pp.

FAOSTATS, 2013a. Resources per country. Available athttp://faostat.fao.org/site/377/default.aspx#ancor (Accessed 3 September 2013).

FAOSTATS, 2013b. Concepts and definitions, glossary. Available athttp://faostat.fao.org/site/375/default.aspx (Accessed 15 October 2013).

Feranec, J., Jaffrain, G., Soukup, T., Hazeu, G., 2010. Determining changes and flows in European landscapes 1990–2000 using CORINE land cover data, Applied Geography, 30, 1, 19–35.

Filippi, A.M., Carder, K.L., Davis, C.O., 2006. Vicarious calibration of the Ocean PHILLS hyperspectral sensor using a coastal tree-shadow method, Geophysical Research Letters, 33, 2605-2610.

Fisher, J., Baumback, M.M.,Bowles, J.H., Grossmann, J.M., Antoniades, J.AJ., 1998. Comparison of low-cost hyperspectral sensors, Proceedings of Imaging Spectrometry IV, 23, 14 pp.

Foley, J.A., DeFries, R., Asner, G.P., Barford, C., Bonan, G., Carpenter, S.R., Chapin, F.S., Coe, M.T., Daily, G.C., Gibbs, H.K., Helkowski, J.H., Holloway, T., Howard, E.A., Kucharik, C.J., Monfreda, C., Patz, J.A., Prentice, I.C., Ramankutty, N.,Snyder, P.K., 2005. Global consequences of land use, Science, 309,570-574.

Foody, G.M., 1992. On the compensation for chance agreement in image classification accuracy assessment, Photogrammetric Engineering and Remote Sensing, 58, 1459–1460.

Foody, G.M., 2002. Status of land cover classification accuracy assessment, Remote Sensing of Environment 80, 185–201.

Foody, G.M., 2004. Thematic map comparison: evaluating the statistical significance of differences in classification accuracy, Photogrammetric Engineering and Remote Sensing, 70, 627–633.

Foody, G.M., Mathur, A., 2004. Toward intelligent training of supervised image classifications: directing training data acquisition for SVM classification, Remote Sensing of Environment, 93, 107–117.

Foody, G.M., Boyd, D.S., Sanchez-Hernandez, C., 2007. Mapping a specific class with an ensemble of classifiers, International Journal of Remote Sensing, 28, 1733– 1746.

Foody, G.M., 2008. Harshness in image classification accuracy assessment, International Journal of Remote Sensing, 29, 3137–3158.

Foster, D.R., 1992. Land-use history (1730–1990) and vegetation dynamics in central New England, USA, Journal of Ecology, 80, 753–71.

Foster, D.R., Motzkin, G., Slater, B., 1998. Land-Use History as Long-Term Broad-Scale Disturbance: Regional Forest Dynamics in Central New England, Ecosystems, 1, 96-119.

Foster, A.D., Rosenzweig, M.R., 2003. Economic growth and the rise of forests, Quarterly Journal of Economics, 118, 601-637.

Frank, D., Finckh, M., Wirth, C., 2009. Impacts of land use on habitat functions of old-growth forests and their biodiversity. In: Old-Growth Forests, Wirth, C., Gleixner, G., Heimann, M. (Ed.), Berlin and Heidelberg, Germany, Springer, pp. 429–450.

Franya, G.B., Cracknell, A.P., 1995. A simple cloud masking approach using NOAA AVHRR daytime data for tropical areas, International Journal of Remote Sensing, 16, 9, 1697–1705.

Freeman, J.T., 1994. Forest Conservancy in the Alps of Dauphiné, 1287-1870, Forest and Conservation History, 38, 171-180.

Frey, C., Parlow, E., 2009. Geometry effect on the estimation of band reflectance in an urban area, Theoretical and Applied Climatology, 96, 395–406.

Frey, G.E., Fassola, H.E., Nahuel Pachas, A., Colcombet, L., Lacorte, S.M., Perez, O., Renkow, M, Warren, S.T., Cubbage, F.W., 2012. Perceptions of silvopasture systems among adopters in northeast Argentina, Agricultural systems, 105, 21-32.

Gancz, V., Hostert, P., 2012. Forest restitution and protected area effectiveness in post-socialist Romania, Biological Conservation, 146, 204-212.

Gao, B.C., Heidebrecht, K.B., Goetz, A.F.H., 1993. Derivation of scaled surface reflectances from AVIRIS data, Remote Sensing of Environment, 44, 165−178.

Gao, B.-C., Montes, M.J., Davis, C.O., Goetz, A.F.H., 2009. Atmospheric correction algorithms for hyperspectral remote sensing data of land and ocean, Remote Sensing of Environment, 113, 17–24.

Gao, Y., Zhang, W., 2009. A simple empirical topographic correction method for ETM+ imagery, International Journal of Remote Sensing, 30,2259–2275.

Garcia-Haro, F.J., Gilabert, M.A., Melia, J., 2001. Monitoring fire affected areas using Thematic Mapper data, InternationalJournal of Remote Sensing, 22, 533–549.

Garcia-Quijano, J., Peters, J., Cockx., L., van Wyk, G., Rosanov, A.,Deckmyn, G., Ceulemans, R., Ward, S.M., Holden, N.M., Van Orshoven, J., Muys., B., 2007. Carbon sequestration and environmental effects of afforestation with Pinus radiata D. Don in the Western Cape, South Africa. Climate Change, 83, 3, 323-355.

Gardner, W.B.R., 1993. Cloud detection using satellite measurement of infrared and visible radiances for ISCCP, Journal of Climate, 6, 2341 – 2369.

Garret, H.E., Kerley, M.S., Ladyman, K.P., Walter, W.D., Godsey, L.D., Van Sambeek, J.W., Brauer, D.K., 2004. Hardwood silvopasture management in North-America, Agroforestry Systems, 61, 21-33.

Getahun, K., Van Rompaey, A., Van Turnhout, P., Poesen, J., 2013. Factors controlling patterns of deforestation in moist evergreen Afromontane forests of Southwest Ethiopia, Forest Ecology and Management, 304, 171-181.

Gibson, L., Lee, T.M., Koh, L.P., Brook, B.W., Gardner, T.A., Barlow, J., Peres, C.A., Bradshaw, C.J.A., Laurance, W.F., Lovejoy, T.E., Sodhi, N.S., 2011. Primary forests are irreplaceable for sustaining tropical biodiversity, Nature,478, 7369, 378–381.

Gilabert, M.A., Conese, C., Maselli, F., 1994. An atmospheric correction method for the automatic retrieval of surface reflectances from TM images, International Journal of Remote Sensing, 15, 2065-2086.

Giovanni portal, 2012. Interactive Visualization and Analysis. Goddard Earth Sciences, Data and Information Services Center, Washington, DC. Available at http://disc.sci.gsfc.nasa.gov/giovanni/overview/index.html (Accessed 16 July 2013).

Giri, C., Zhu, Z., Reed, B., 2005. A comparative analysis of the Global Land Cover 2000 and MODIS land cover data sets, Remote Sensing of Environment, 94, 1, 123–132.

Giri, C., Pengra, B., Long, J., Loveland, T.R., 2013. Next generation of global land cover characterization, mapping, and monitoring, International Journal of Applied Earth Observation and Geoinformation, 25, 30–37.

Gitas, I.Z., Devereux, B.J., 2006. The role of topographic correction in mapping recently burned Mediterranean forest areas from Landsat TM images, International Journal of Remote Sensing, 27,41–54.

Global Land Project, 2005. Science plan and implementation strategy. IGB Report 53/IHFP Report 19. Stockholm, 74 pp.

Global Witness, 1999. Made in Vietnam—Cut in Cambodia: How the Garden Furniture Trade Is Destroying Rainforests, Global Witness, Washington, DC., 21 pp.

Goetz, S.J., Wright, R.K., Smith, A.J., Zinecker, E., Schaub, E., 2003. IKONOS imagery for resource management: Tree cover, impervious surfaces, and riparian buffer analyses in the mid-Atlantic region, Remote Sensing of Environment, 88, 1-2, 195–208.

Google Earth, 2011. Available at http://www.google.com/earth/ (Accessed 12 August 2011).

Goudie, A., 2013. The human impact on the natural environment, past, present and future, John Wiley & Sons, Inc., UK, 424 pp.

Goward, S.N., Haskett, J., Williams, D., Arvidson, T., Gasch, J., Lonigro, R., Reeley, M., Irons, J., Dubayah, R., Turner, S., Campana, K., Bindschadler, R., 1999. Enhanced Landsat capturing all the Earth's land areas, EOS, 80, 26, 289–293.

Grainger, A., Malayang, B.S., 2006. A model of policy changes to secure sustainable forest management and control of deforestation in the Philippines, Forest Policy and Economics, 8, 67-80.

Grau, H.R., Aide, T.M., Zimmerman, J.K., Thomlinson, J.R., Helmer, E., Zou, X., 2003. The EcologicalConsequences of Socioeconomic and Land-Use Changes in Postagricultural Puerto Rico, Bioscience, 53, 1159-1168.

Grau, H.R., Aide, T.M., Zimmerman, J.K., Thomlinson, J.R., 2004. Trends and scenarios of the carbon budget in postagricultural Puerto Rico (1936–2060), Global Change Biology, 10, 1163-1179.

Green, K., 2006. Landsat in context: The land remote sensing business model, Photogrammetric Engineering and Remote Sensing, 72, 10, 1147-1153.

Greenpeace, 2012. Forest cover change in Romania in 2000-2011. Available at http://www.greenpeace.org/romania/Global/romania/paduri/Despaduririle%20din%20Romania/Forestcover%20change%20in%20Romania%202000-2011.pdf (Accessed 17 December 2013).

Gretchen, C.D., 1997. Nature's services: societal dependence on natural ecosystems, Washington, DC, 421 pp.

Griffiths, P., Kuemmerle, T., Kennedy, R.E., Abrudan, I.V., Knorn, J., Hostert, P., 2012. Using annual time-series of Landsat images to assess the effects of forest restitution in post-socialist Romania, Remote Sensing of Environment, 118, 199-214.

Griffiths, P., van der Linden, S. Kuemmerle, T., Hostert, P., 2013a. A Pixel-Based Landsat Compositing Algorithm for Large Area Land Cover Mapping, IEEE Journal of Selected Topics in Applied Earth Observations and Remote Sensing, 1-14.

Griffiths, P., Kuemmerle, T., Baumann, M., Radeloff, V.C., Abrudan, I.V., Lieskovsky, J., Munteanu, C., Ostapowicz, K., Hostert, P., 2013b. Forest disturbances, forest recovery, and changes in forest types across the Carpathian ecoregion from 1985 to 2010 based on Landsat image composites. Remote Sensing of Environment. http://dx.doi.org/10.1016/j.rse.2013.04.022.

Griffiths, P., Mueller, D., Kuemmerle, T., Hostert, P., 2013c. Agricultural land change in the Carpathian ecoregion after the breakdown of socialism and expansion of the European Union. Environmental Research Letters, 8, 1-12. Doi 10.1088/1748-9326/8/4/045024.

Gu, D., Gillespie, A., 1998. Topographic normalization of Landsat TM images of forest based on subpixel sun-canopy-sensor geometry, Remote Sensing of Environment, 64,166−175.

Guanter, L., Gomez-Chova, L., Moreno, J., 2008. Coupled retrieval of aerosol optical thickness, columnar water vapor and surface reflectance maps from ENVISAT/MERIS data over land, Remote Sensing of Environment, 112, 2898–2913.

Guo, Q., Kelly, M., Graham, C.H., 2005. Support vector machines for predicting distribution of Sudden Oak Death in California, Ecological Modelling, 182, 75–90.

Guran-Nica, L., Marin, C., Todică-Ştefan, N., 2010. Migration Movements in the Romanian Rural Space (1990-2008), Proceedings of the 5th WSEAS International Conference on Economy and Management Transformation, 2, 503-507.

Gutman, G., Byrnes, R., Masek, J., Covington, S., Justice, C., Franks, S., Headley, R., 2008. Towards monitoring land-cover and land-use changes at a global scale: The Global Land Survey 2005. Photogrammetric Engineering and Remote Sensing, 74, 6−10.

Gutman, G., 2012. On the use of long-term global data of land reflectances and vegetation indices derived from the advanced very high resolution radiometer, Journal of Geophysical Research: Atmospheres (1984–2012), 104, D6, 6241–6255.

Haines-Young, R., Potschin, M., Kienast, F., 2012. Indicators of ecosystem servicepotential at European scales. Mapping marginal changes and trade-offs, Ecological Indicators, 21, 39–53.

Hale, S.R., Rock, B.N., 2003. Impact of topographic normalization on land-cover classification accuracy, Photogrammetric Engineering and Remote Sensing, 69, 785-791.

Hall, C.A.S., Tian, H., Qi, Y., Pontius, G., Cornell, J., 1995. Modelling spatial and temporal patterns of tropical land use change, Journal of Biogeography, 22, 753–757.

Hall, J.M., Van Holt, T., Daniels, A.E., Balthazar, V., Lambin, E.F., 2012. Trade-offs between tree cover, carbon storage and floristic biodiversity in reforesting landscapes, Landscape Ecology, 27, 1135–1147.

Hansen, M., Dubayah, R., DeFries, R., 1996. Classification trees: an alternative to traditional land-cover classifiers, International Journal of Remote Sensing, 17, 5, 1075−1081.

Hansen, M.C., DeFries, R.S., Townshend, J.R.G., Sohlberg, R., Dimiceli, C., Carroll, M., 2002. Towards an operational MODIS continuous field of percent tree cover algorithm: Examples using AVHRR and MODIS data, Remote Sensing of Environment, 83, 303–319.

Hansen, M.C., Roy, D.P., Lindquist, E., Adusei, B., Justice, C.O., Altstatt, A., 2008. A method for integrating MODIS and Landsat data for systematic monitoring of forest cover and change in the Congo Basin, Remote Sensing of Environment, 112, 2495–2513.

Hansen, M.C., Egorov, A., Roy, D.P., Potopov, P., Ju, J., Turubanova, S., Kommareddy, I., Loveland, T.R., 2011. Continuous fields of land cover for the conterminous United States using Landsat data: First results from the Web-Enabled Landsat Data (WELD) project, Remote SensingLetters, 2, 279–288.

Hansen, M.C., Loveland, T.R., 2012. A review of large area monitoring of land cover change using Landsat data, Remote Sensing of Environment, 122, 66-74.

Hansen, M.C., Potapov, P.V., Moore, R., Hancher, M., Turubanova, S.A., Tyukavina, A., Thau, D., Stehman, S.V., Goetz, S.J.,Loveland, T.R., Kommareddy, A., Egorov, A., Chini, L., Justice, C.O., Townshend, J.R.G., 2013.High-Resolution Global Maps of 21st-Century Forest Cover Change, Science, 342, 6160, 850-853.

Hantson, S., Chuvieco, E., 2011. Evaluation of different topographic correction methods for Landsat imagery, International Journal of Applied Earth Observation and Geoinformation,13,691-700.

Hay, J.E., 1979. Calculation of monthly mean solar radiation for horizontal and inclined surfaces, Solar Energy, 23, 301−307.

He, C., Zhang, Q., Li, Y., Li, X., Shi, P., 2005. Zoning grassland protection area using remote sensing and cellular automata modeling—a case study in Xilingol steppe grassland in northern China, Journal of Arid Environments, 63, 814–26.

Hecht, S., Kandel, S., Gomes, I., Cuellar, N., Rosa, H., 2006. Globalization, forest resurgence, and environmental politics in El Salvador, World Development, 34, 308-323.

Hecht, S., Saatchi, S.S., 2007. Globalization and Forest Resurgence: Changes in Forest Cover in El Salvador, BioScience, 57,6 63-672.

Hecht, S., 2010. The new rurality: globalization, peasants and the paradoxes of landscapes, Land Use Policy, 27, 161–69.

Hersperger, A.M., Burgi, M., 2009. Going beyond landscape change description: Quantifying the importance of driving forces of landscape change in a Central Europe case study, Land Use Policy, 26, 640-648.

Higgins, S.I., Scheiter, S., 2012. Atmospheric CO_2 forces abrupt vegetation shifts locally, but not globally, Nature, 488, 209-212.

Hirt, C., Filmer, M.S., Featherstone, W.E., 2010. Comparison and validation of the recent freely-available ASTER GDEM ver1, SRTM ver4.1 and GEODATA DEM-9S ver3 digital elevation models over Australia, Australian Journal of Earth Sciences, 57, 337–347.

Ho, D., Asem, A., 1986. NOAA AVHRR image referencing, International Journal of Remote Sensing, 7, 7, 895-904.

Hofstede, R.G.M., 2011. Un árbol no siempre es más agua: a propósito de las políticas de (re)forestación. Consorcio para el Desarrollo Sostenible de la Ecorregión Andina (CONDESAN), Propuestas Andinas 3, Lima, Perú. 4 pp.

Holben, B.N., 1986. Characteristics of maximum-value composite images fromtemporal AVHRR data, International Journal of Remote Sensing, 7, 1417–1434.

Holeksa, J., Saniga, M., Szwagrzyk, J., Czerniak, M., Staszynska, K., Kapusta, P., 2009. A giant tree stand in the West Carpathians, an exception or a relic of formerly widespread mountain European forests?, Forest Ecology and Management, 257, 7, 1577–1585.

Hosmer, W.D., Lemeshow, S., 2000. Applied Logistic Regression. John Wiley & Sons, Inc., Canada, 528 pp.

Hostert, P., Kuemmerle, T., Baumann, M., 2010. The Carpathian Mountains in Transformation, Mountain Research Initiative Newsletter, 6-8.

Houghton, R., Hackler, J.L., 2000. Changes in terrestrial carbon storage in the United States: The roles of agriculture and forestry, Global Ecology and Biogeography, 9, 125-144.

Houghton, R., Skole, D., Nobre, C., Hackler, J., Lawrence, K., Chementowski, W., 2000. Annual fluxes of carbon from deforestation and regrowth in the Brazilian Amazon, Letters to Nature, 403, 301-304.

Huang, C., Davis, L. S., Townshend, J.R.G., 2002. An assessment of support vector machines for land cover classification, International Journal of Remote Sensing, 23, 725−749.

Huang, H., Gong, P., Clinton, N., Hui, F., 2008. Reduction of atmospheric and topographic effect on Landsat TM data for forest classification, International Journal of Remote Sensing, 29,5623–5642.

Huang, C., Goward, S.N., Masek, J.G., Thomas, N., Zhu, Z., Vogelmann, J E., 2010. An automated approach for reconstructing recent forest disturbance history using dense Landsat time series stacks, Remote Sensing of Environment, 114, 183–198.

Huete, A.R., 1988. A soil-adjusted vegetation index (SAVI), Remote Sensing of Environment, 25, 295-309.

Huete, A.R., Liu, H.Q., Batchily, K., van Leeuwen, W., 1997. A comparison of vegetation indices over a global set of TM images for EOS-MODIS. Remote Sensing of Environment, 59, 3, 440–451.

Huete, A., Didan, K., Miura, T., Rodriguez, E.P., Gao, X., Ferreira, L. G., 2002. Overview of the radiometric and biophysical performance of the MODIS vegetation indices, Remote Sensing of Environment, 83, 195-213.

Huete, A.R., 2012. Vegetation Indices, Remote Sensing and Forest Monitoring, Geography Compass, 6, 9, 513-532.

Hyde, W.F., Amacher, G.S., Magrath, W., 1996. Deforestation and forest land use: theory, evidence and policy implications, World Bank Research Observer, 11, 223-248.

Inampudi, R.B., 1998. Geoscience and Remote Sensing Symposium Proceedings, IGARSS 1998, 5, 2363 – 2365.

Ioja, C.I., Patroescu, M., Rozylowicz, L., Popescu, V.D., Verghelet, M., Zotta, M.I., Felciuc, M., 2010. The efficacy of Romania's protected areas network in conserving biodiversity, Biological Conservation, 143, 2468–2476.

Ionov, N., Plugtschieva, M., Milev, M., 2000. Afforestation Programmes in Bulgaria. In NEWFOR – New Forests for Europe: Afforestation at the Turn of the Century, EFI Proc. 35, Weber, N. (Ed.), Joensuu, pp. 213—220.

Ioras, F., Abrudan, I.V., 2006. The Romanian forestry sector: privatization facts, International Forestry Review, 8, 361–367.

Ioras, F., Abrudan, I.V., Dautbasic, M., Avdibegovic, M., Gurean, D., Ratnasingam, J., 2009. Conservation gains through HCVF assessments in Bosnia-Herzegovina and Romania, Biodiversity and Conservation, 18, 3395–3406.

IPCC, 2013. Afforestation, reforestation and deforestation. Available at http://www.ipcc.ch/ipccreports/sres/land_use/index.php?idp=47 (Accessed 16 October 2013).

Irland, L., 2008. State failure, corruption, and warfare: challenges for forest policy, Journal of Sustainable Forestry, 27, 189–223.

IUCN, 2008. Guidelines for protected area management categories, Dudley, N. (Ed.), Gland Switzerland, 87 pp.

Izac, A.M.N., Swift, M.J., Andriesse, W., 1991. A strategy for inland valley agroecosystems research in West and Central Africa. RCMP Research Monograph. IITA, Resource and Crop Management Program, Ibadan, 208 pp.

Jack, B.K., Kousky, C., Sims, K.R.E., 2008. Designing payments for ecosystem services: Lessons from previous experience with incentive-based mechanisms, Proceedings of the National Academy of Sciences of the United States of America, 105, 28, 9465-9470.

Jaskowiek, B., 2013. Assessment of land cover changes in the Carpathian Mountains with MODIS data. The Carpathians: Integrating Nature and Society Towards Sustainability Environmental Science and Engineering, 639-653.

Jenkins, C.N., Joppa, L., 2009. Expansion of the global terrestrial protected area system, Biological Conservation, 142, 2166-2174.

Jensen, J.R., 1996. Introduction digital image processing: a remote sensing perspective. Prentice-Hall, Englewood Cliffs, New Jersey, 526 pp.

Johnson, G.E., van Dijk, A., Sakamoto, C.M., 1987. The use of AVHRR data in operational agricultural assessment in Africa, Special Issue: Remote Sensing and Biomes, 2, 1, 41-60.

Johnson, D.M., Mueller, R., 2010. The 2009 cropland data layer, Photogrammetric Engineering and Remote Sensing, 11, 1201–1205.

Jordan, G., Van Rompaey, A., Szilassi, P., Mannaerts, C., Woldai, T., 2005. Historical landuse change and their impact on sediment fluxes in the Balaton basin (Hungary), Agriculture, Ecosystems and Environment, 108, 119-133.

Ju, J., Roy, D.P., 2008. The availability of cloud-free Landsat ETM plus data over the conterminous United States and globally, Remote Sensing of Environment, 112, 1196–1211.

Jung, H.W., 2003. Evaluating interrater agreement in SPICE-based assessments, Computer Standards and Interfaces, 25, 477–499.

Jung, M., Churkina, G., Henkel, K., Herold, M., 2006. Exploiting synergies of global land cover products for carbon cycle modeling, Remote Sensing ofEnvironment, 101, 534–53.

Justice, C.O., Vermote, E.F., Townshend, J.R.G., DeFries, R., Roy, D.P., Hall, D.K., Salamonson, V.V., Privette, J.L., Riggs, G., Strahler, A. , Lucht, W. , Myneni, R.B. , Knyazikhin, Y. , Running, S.W., Nemani, R.R., Wan , Z., Huete, A.R., Van Leeuwen, W., Wolfe, R.E. , Giglio, L. , Muller, J.P. , Lewis, P. , Barnsley, M.J., 1998. The Moderate Resolution Imaging Spectroradiometer (MODIS): land remote sensing for global change research, Geoscience and Remote Sensing, 36, 4, 1228-1249.

Justice, C.O., Townshend, J.R.G., Vermote, E.F., Masuoka, E., Wolfe, R. E., Saleous, N., Roy, D.P., Monsette, J.P., 2002. An overview of MODIS Land data processing and product status, Remote Sensing of Environment, 83, 3–15.

Kandler, O., 1992. Historical decline and dieback of Central European forests and present conditions, Environmental Toxicology and Chemistry, 11, 1077-1093.

Kastner, T., 2009. Trajectories in human domination of ecosystems: Human appropriation of net primary production in the Philippines during the 20th century, Ecological Economics 69, 260-269.

Kauppi, P.E., Ausubel, J.H., Fang, Y.I., Mather, A.S., Sedjo, R.A., Waggoners, P.E., 2006. Returning forests analyzed with the forest identity, Proceedings of the National Academy of Sciences of the United States of America, 103, 17574-17579.

Keeton, W.S., Crow, S.M., 2009. Sustainable forest management for the Carpathian Mountain region: providing a broad array of ecosystem service. In: Soloviy, I. and Keeton, W.S. (eds.), Ecological Economics and Sustainable Forest Management: Developing a trans-disciplinary approach for the Carpathian Mountains, Ukrainian National Forestry University Press, Lviv, Ukraine, pp. 109-126.

Keeton, W.S., Chernyavskyy, M., Gratzer, G., Main-Knorn, M., Shpylchak, M., Bihun, Y., 2010. Structural characteristics and aboveground biomass of old-growth spruce–fir stands in the eastern Carpathian mountains, Ukraine, Plant Biosystems., An International Journal Dealing with all Aspects of Plant Biology,144, 1, 148–159.

Keeton, W.S., Whitman, A.A., McGee, G.C., Goodale, C.L., 2011. Late-successional biomass development in northern hardwoodconifer forests of the northeastern United States, Forest Science, 57, 6, 489–505.

Kennedy, R.E., Cohen, W.B., Schroeder, T.A., 2007. Trajectory-based change detection for automated characterization of forest disturbance dynamics, Remote Sensing of Environment, 110, 370–386.

Kennedy, R.E., Yang, Z., Cohen, W.B., 2010. Detecting trends in forest disturbance and recovery using yearly Landsat time series: 1. LandTrendr - temporal segmentation algorithms, Remote Sensing of Environment, 114, 2897–2910.

Keuchel, J., Naumann, S., Heiler, M., Siegmund, A., 2003. Automatic land cover analysis for Tenerife by supervised classification using remotely sensed data, Remote Sensing of Environment, 86, 530–541.

Kim, E., Kim, D., 2005. Historical Changes and Characteristics of Rehabilitation, Management and Utilization of Forest Resources in South Korean, Journal of Mountain Science, 2, 164-172.

Kleinn, C., Corrales, L., Morales, D., 2002. Forest Area in Costa Rica: a Comparative Study of Tropical Forest Cover Estimates Over Time, Environmental Monitoring and Assessment, 73, 17-40.

Kline, J.D., Mazzotta, M.J., 2012. Evaluating trade-offs among ecosystem services in the management of public lands, Department of Agriculture, Forest Service, Pacific Northwest Research Station, Corvallis, USA, 54 pp.

Klock, J., 1995. The Advancement of South Korean Forestry: National development and forest policy from 1910 to present, Korea Journal, 35, 119-132.

Kneizys, F.X., Shettle, E.P., Abreu, L.W., Chetwynd, J.H., Anderson, G.P., Gallery, W.O., Selby, J.E.A., Clough, S.A., 1988. User's Guide to LOWTRAN-7. Air Force Geophysics Laboratory, Hanscom, Massachusetts, 146 pp.

Knight, J., 2000. From timber to tourism: recommoditizing the Japanese forest, Development and Change, 31, 341-359.

Knight, C., 2009. The paradox of discourse concerning deforestation in New Zealand: A historical survey, Environment and History, 15, 323-342.

Knight, J.F., Lunetta, R.S., Ediriwickrema, J., Khorram, S., 2006. Regional scale land cover characterization using MODIS-NDVI 250m multi-temporal imagery: a phenology-based approach, GIScience Remote Sensing, 43, 1, 1–23.

Knohl, A., Schulze, E.-D., Wirth, C., 2009. Biosphere–atmosphere exchange of old-growth forests: processes and pattern. In: Old-Growth Forests, Wirth, C., Gleixner, G., Heimann, M. (Ed.), Berlin and Heidelberg, Germany, Springer, 141–158.

Knorn, J., Rabe, A., Radeloff, V.C., Kuemmerle, T., Kozak, J., Hostert, P., 2009. Land cover mapping of large areas using chain classification of neighboring Landsat satellite images, Remote Sensing of Environment, 113, 957-964.

Knorn, J., Kuemmerle, T., Radeloff, V.C., Szabo, A., Mindrescu, M., Keeton, W.S., Abrudan, I., Griffiths, P., Gancz, V., Hostert, P., 2012a. Forest restitution and protected area effectiveness in post-socialist Romania, Biological Conservation 146, 204–212.

Knorn, J., Kuemmerle, T., Radeloff, V.C., Keeton, W.S., Gancz, V., Biris, I.A., Svoboda, M., Griffiths, P., Hagatis, A., Hostert, P., 2012b. Continued loss of temperate old-growth forests in the Romanian Carpathians despite an increasing protected area network, Environmental Conservation 40, 2, 182–193.

Knudby, A., Newman, C., Shaghude, Y., Muhando, C., 2010. Simple and effective mon-itoring of historic changes in nearshore environments using the free archive of Landsat imagery, International Journal of Applied Earth Observation and Geo-information, 12, S116–S122.

Kobayashi, S., Sanga-Ngoie, K., 2008. The integrated radiometric correction of optical remote sensing imageries,. International Journal of Remote Sensing, 29, 5957-5985.

Kogan, F.N., 1995. Application of vegetation index and brightness temperature for drought detection, Advances in Space Research, 15, 11, 91-100.

Kozak, J., Estreguil, C., Troll, M., 2007a. Forest cover change in the northern Carpathians in the 20th century: a slow transition, Journal of Land Use Science, 2, 2, 127-146.

Kozak, J., Estreguil, C., Vogt, P., 2007b. Forest cover and pattern changes in the Carpathians over the last decades, European Journal of Forest Research, 126, 77-90.

Krausmann, F., 2001. Land use and industrial modernization: an empirical analysis of human influence on the functioning of ecosystems in Austria 1830- 1995, Land Use Policy, 18, 17–26.

Krieger, D.J., 2001. Economic value of forest ecosystem services – a review, The Wilderness Society, 40 pp.

Kruse, F.A., 1988. Use of airborne imaging spectrometer data to map minerals associated with hydrothermally altered rocks in the northern Grapevine Mountains, Nevada and California, Remote Sensing of Environment, 24, 31−51.

Kruse, F.A., 2004. Comparison of ATREM, ACORN, and FLAASH atmospheric corrections using low-altitude AVIRIS data of Boulder, CO. In: Summaries of 13th JPL Airborne Geoscience Workshop, 31 March – 2 April 2004, Jet Propulsion Lab, Pasadena, CA, USA, 7 pp.

Kuemmerle, T., Radeloff, V.C., Perzanowski, K., Hostert, P., 2006. Cross-border comparison of land cover and landscape pattern in Eastern Europe using a hybrid classification technique, Remote Sensing and the Environment, 103, 449-464.

Kuemmerle, T., Hostert, P., Radeloff, V.C., Perzanowski, K., Kruhlov, I., 2007. Post-socialist forest disturbance in the Carpathian border region of Poland, Slovakia, and Ukraine, Ecological Applications, 17, 5, 1279-1295.

Kuemmerle, T., Müller, D., Griffiths, P., Rusu, M., 2008a. Land use change in Southern Romania after the collapse of socialism, Regional Environmental Change, 9, 1, 1-12.

Kuemmerle, T., Hostert, P., Radeloff, V.C., van der Linden, S., Perzanowski, K., Kruhlov, I., 2008b. Cross-border comparison of post-socialist farmland abandonment in the Carpathians, Ecosystems, 11, 614-628.

Kuemmerle, T., Chaskovskyy, O., Knorn, J., Radeloff, W.C., Kruhlov, I., Keeton, W.S., Hostert, P., 2009a. Forest cover change and illegal logging in the Ukrainian Carpathians in the transition period from 1988 to 2007, Remote Sensing of Environment, 113, 1194-1207.

Kuemmerle, T., Kozak, J., Radeloff, V.C., Hostert, P., 2009b. Differences in forest disturbance among land ownership types in Poland during and after socialism, Journal of Land Use Science, 4, 1-2, 73-83.

Kull, C.A., Ibrahim, C.K., Meredith, T.C., 2007. Tropical Forest Transitions and Globalization: Neo-Liberalism, Migration, Tourism, and International Conservation Agendas, Society and Natural Resources, 20, 723-737.

Labovitz, M.L., Masuoka, E.J., 1984. The influence of autocorrelation in signature extraction: an example from a geobotanical investigation of Cotter Basin, Montana, International Journal of Remote Sensing 5, 315–332.

Lambin, E.F., Turner, B.L., Helmut, J., Geist, H.J., Agbola, S.B. ,Angelsen, A. ,Bruce, J.W., Coomes,O.T., Dirzo, R., Fisher, G., Folke, C., George, P.S., Homewood,K., Imbernon, J., Leemans, R., Li, X., Moran, E.F., Mortimore, M., Ramakrishnan, P.S., Richards, J.F., Skånes, H., Steffen, W., Stone,G.D., Svedin, U., Veldkamp, T.A., Vogel, C., Xu, J., 2001. The causes of land-use and land-cover change: moving beyond the myths, Global EnvironmentalChange, 11, 261–9.

Lambin, E.F., Geist, H.J., 2006. Land-Use and Land-Cover Change. Local Processes and Global Impacts, third ed., Springer-Verlag, Heidelber/Berlin/New York, 222 pp.

Lambin, E.F., Meyfroidt, P., 2010. Land use transitions: socio-ecological feedback versus socio-economic change, Land Use Policy, 27, 108–18.

Langley, S.K., Cheshire, H.M., Humes, K.S., 2001. A comparison of single date and multitemporal satellite image classifications in a semi-arid grassland, Journal of Arid Environment, 49, 401–11.

Latifovic, R., Pouliot, D., Dillabaugh, C., 2012. Identification and correction of systematic error in NOAA AVHRR long-term satellite data record, Remote Sensing of Environment, 127, 84–97.

Lawrence, A., Szabo, A., 2005. Forest Restitution in Romania: Challenging the Value System of Foresters and Farmers, European forests in ethical discourse, Berlin, Germany, 16 pp.

Lawrence, A., 2009. Forestry in transition: imperial legacy and negotiated expertise in Romania and Poland, Forest Policy and Economics, 11, 429-436.

Lee, Z.P., Casey, B., Parsons, R., Goode, W., Weidemann, A., Arnone, R., 2005. Bathymetry of shallow coastal regions derived from space-borne hyperspectral sensor, Oceans 2005 MTS/IEEE, September 18–23, Washington, DC.

Leica Geosystems, 2006. Imagine AutoSync.White Paper, Leice Geosystems Geospatial Imaging, Georgia, USA. Available at http://geospatial.intergrapgh.com/products/ERDASIMAGINE/IMAGINEAutoSync/Details.aspx (Accessed 25 June 2013).

Lenot, X., Achard, V., Poutier, L., 2009. SIERRA: a new approach to atmospheric and topographic corrections for hyperspectral imagery, Remote Sensing of Environment, 113, 1664-1677.

Lhermitte, S., Verbesselt, J., Verstraeten, W.W., Coppin, P., 2011. A comparison of time series similarity measures for classification and change detection of ecosystem dynamics, Remote Sensing of Environment 115, 3129–3152.

Liang, S., Fang, H., 2004. An improved atmospheric correction algorithm for hyperspectral remotely sensed imagery, IEEE Geoscience and RemoteSensing Letters, 1,112-117.

Liang, S., Fang, H., Chen, M., 2001. Atmospheric correction of Landsat ETM+ land surface imagery – part I, methods, IEEE Transactions on Geoscience and RemoteSensing, 39, 2490–2498.

Liebault, F., Gomez, B., Page, M., Marden, M., Peacock, D., Richard, D., Trotter, C.M., 2005. Land-use change, sediment production and channel response in upland regions, River Research and Applications, 21, 739-756.

Ligtenberg, A., Bregt, A.K., van Lammeren, R., 2001. Multi-actor-based land use modelling: spatial planning using agents, Landscape and Urban Planning, 56, 21-33.

Lillesand, T.M., Kiefer, R.W., Chipman, J.W., 2004. Remote Sensing and Image Interpretation. John Wiley and Sons, New York, USA, 763 pp.

Liquete, C., Zulian, G., Delgado, I., Stips, A., Maes, J., 2013. Assessment of coastalprotection as an ecosystem service in Europe, Ecological Indicators, 30, 205–217.

Liu, H.Q., Huete, A., 1995. A feedback based modification of the NDVI to minimize canopy background and atmospheric noise, IEEE Transactions on Geoscience andRemote Sensing, 33, 2, 457-465.

Logar, A.M., Lloyd, D.E., Corwin, E.M., Penaloza, M.L., Feind, R.E., Berendes, T.A., Kuo, K., Welch, R.M., 1998. The ASTER polar cloud mask, IEEE Transactions on Geoscience and Remote Sensing, 36, 4, 1302 – 1312.

Loveland, T.R., Reed, B.C., Brown, J.F., Ohlen, D.O., Zhu, Z., Yang, L., Merchant, J.W., 2012. Development of a global land cover characteristics database and IGBP DISCover from 1 km AVHRR data, International Journal of Remote Sensing, 21, 6-7, 1303-1330.

Loveland, T.R., Dwyer, J.L., 2012. Landsat: Building a strong future, Remote Sensing of Environment, 122, 22–29.

Lowicki, D., 2008. Land use changes in Poland during transformation Case study of Wielkopolska region, Landscape and Urban Planning, 87, 279-288.

Lu, D., Ge, H., He, S., Xu, A., Zhou, G.,Du, H., 2008. Pixel-based Minnaert correction method for reducing topographic effects on a Landsat-7 ETM+ image, Photogrammetric Engineering and Remote Sensing, 74, 1343–1350.

Lugo, A.E., Helmer, E., 2004. Emerging forests on abandoned land: Puerto Rico's new forests, Forest Ecology and Management, 190, 145-161.

LUI, 2013. Land use impact on soil quality. Available at http://soilweb.landfood.ubc.ca/luitool/one-origin (Accessed 10 October 2013).

Luyssaert, S., Schulze, E.D., Borner, A., Knohl, A., Hessenmoller, D., Law, B.E., Ciais, P., Grace, J., 2008. Old-growth forests as global carbon sinks, Nature, 455, 7210, 213–215.

MacCleery, D.W., 1994. Resiliency and Recovery: A Brief History of Conditions and Trends in U.S. Forests, Forest and Conservation History, 38, 135-139.

Macovei, C., 2009. The wind as a climatic risk factor for the forestry fund of Suceava county, Present Environment and Sustainable Development 3, 275–286.

Maes, J., Paracchini, M.L., Zulian, G., 2011. A European assessment of the provisionof ecosystem

services – towards an atlas of ecosystem services. JRC Scientificand Technical Reports. European Commission, Joint Research Centre, Institutefor Environment and Sustainability, 82 pp.

Maggi, M., Stroppiana, D., 2002. Advantages and drawbacks of NOAA-AVHRR and SPOT-VGT for burnt area mapping in a tropical savanna ecosystem, Canadian Journal of Remote Sensing, 28, 2, 231-245.

Main-Knorn, M., Cohen, W.B., Kennedy, R.E., Grodzki, W., Pflugmacher, D., Griffiths, P., Hostert, P., 2013. Monitoring coniferous forest biomass change using a Landsat trajectory-based approach, Remote Sensing of Environment, 277–290.

Main-Knorn, M., Hostert, P., Kozak, J., Kuemmerle, T., 2009. How pollution legacies and land use histories shape post-communist forest cover trends in the Western Carpathians, Forest Ecology and Management, 258, 60-70.

Mantescu, L., Vasile, M., 2009. Property Reforms in Rural Romania and Community based Forests, Romanian Sociology, 7, 95–113.

Markham, B.L., Barker, J.L., 1986. Landsat MSS and TM Post-calibration Dynamic Ranges, Exoatmospheric Reflectances and At-satellite Temperatures. Earth Observation Satellite Co., August 1986, Lanham, MD, Landsat Tech. Note 1.

Martínez, P.J., Pérez, M.R., Plaza, A., Aguilar, P.L., Cantero, M.C., Plaza, J., 2006. Endmember extraction algorithms from hyperspectral images, Annals of Geophysics, 49, 1, 93-101.

Masek, J.G., Vermote, E.F., Saleous, N.E., Wolfe, R., Hall, F.G., Huemmrich, K.F., Gao, F., Kutler, J., Lim, T.K., 2006. A Landsat surface reflectance dataset for North America, 1990–2000, IEEE Geoscience and Remote Sensing Letters, 3, 68–72.

Mather, A.S., 1992. The forest transition, Area, 24, 367-379.

Mather, A.S., Needle, C.L., 1998. The forest transition: a theoretical basis, Area, 30, 2, 117-124.

Mather, A.S., Needle, C.L., Coull, J.R., 1998. From resource crisis to sustainability: the forest transition in Denmark, International Journal of a Sustainable Development and World Ecology, 5, 182–93.

Mather, A.S., Fairbairn, J., Needle, C.L, 1999. The Course and Drivers of the Forest Transtion: the case of France, Journal of rural studies, 15, 65-90.

Mather, A.S., Fairbairn, J., 2000. From Floods to Reforestation: The Forest Transition in Switzerland, Environment and History, 6, 399-421.

Mather, A.S., 2001. The Transition from Deforestation to Reforestation in Europe. In: Agricultural technologies and tropical deforestation, Angelsen, A., Kaimowitz, D.(Ed.), Wallingford: CAB International, pp. 35-52.

Mather, A.S., 2004. Forest transition theory and the reforesting of Scotland, Scottish Geographical Journal, 120, 83–98.

Mather, A.S., 2007. Recent Asian forest transitions in relation to forest-transition theory, International Forestry Review, 9, 491–502.

Mathur, A., Foody, G.M., 2008. Crop classification by support vector machine with intelligently selected training data for an operational application, InternationalJournal of Remote Sensing, 29, 2227−2240.

Matthews, E., Grainger, A., 2002. Evaluation of FAO's Global Forest Resources Assessment from the user perspective, Unasylva, 53, 42-55.

Matthews, J.D., 1989. Silvicultural Systems, Oxford University Press Inc., Oxford, New York, 285 pp.

Mayer, A.L., Kauppi, P.E., Angelstam, P.K., Zhang, Y., Tikka, P.M., 2005, Ecology. Importing timber, exporting ecological impact, Science, 308, 359–360.

Mayer, A.L., Kauppi, P.E., Tikka, P.M., Angelstam, P.K., 2006. Conservation implications of exporting domestic wood harvest to neighboring countries, Environmental Scienceand Policy, 9, 228–236.

Melgani, F., Bruzzone, L., 2004. Classification of hyperspectral remote sensing images with support vector machines, IEEE Transactions on Geoscience and RemoteSensing, 42, 1778−1790.

Mertens, B., Lambin, E.F., 1997. Spatial modeling of deforestation in southern Cameroon, Applied Geography 17, 143–162.

Meyer, P., Itten, K.L., Kellenberger, T., Sandmeier, S.,Sandmeier, R., 1993. Radiometric corrections of topographically induced effects on Landsat TM data in alpine environment, ISPRS Journal of Photogrammetry and Remote Sensing, 48, 17–28.

Meyfroidt, P., Lambin, E.F., 2008a. Forest transition in Vietnam and its environmental impacts, Global Change Biology, 14, 1319-1336.

Meyfroidt, P., Lambin, E.F., 2008b. The causes of the reforestation in Vietnam, Land Use Policy, 25, 182-197.

Meyfroidt, P., 2009. Forest Transition in Vietnam; Evidence, Theory and Social- Ecological Feedbacks, Ph.D. Dissertation, Université catholique de Louvain, Louvain-la-Neuve, Belgium, 187 pp.

Meyfroidt, P., Lambin E.F., 2010. Forest transition in Vietnam and Bhutan: causes and environmental impacts. Reforesting Landscapes: Linking Pattern and Process, Nagendra, H. (ed.), Southworth, Springer Landscape Series vol. 10. Dordrecht, Springer, pp. 315-339.

Meyfroidt, P., Rudel, T.K., Lambin, E.F., 2010. Forest transition, trade, and the global displacement of land use, PNAS, 107, 20917-20922.

Meyfroidt, P., Lambin, E.F., 2011. Global Forest Transition: prospects for an end to deforestation, Annual Review of Environment and Resources, 36, 343-371.

Mihai, B., Savulescu, I., Sandric, I., 2007. Change detection analysis (1986–2002) of vegetation cover in Romania: a study of alpine, subalpine, and forest landscapes in the Lezer mountains, Southern Carpathians, Mountain Research and Development 27, 250–258.

Millennium Development Goals Report, 2013, United Nations, June 2013, New York, 68 pp.

Minnaert, N., 1941. The reciprocity principle in lunar photometry. Astrophysical Journal, 93,403–410.

Mitri, G.H., Gitas, I.Z., 2004. A performance evaluation of a burned area object-based classification model when applied to topographically and non-topographically corrected TM imagery, International Journal of Remote Sensing, 25, 2863-2870.

Monserud, R.A., Leemans, R., 1992. Comparing global vegetation maps with the kappa statistic, Ecological Modelling, 62, 275–293.

Moran, M.S., Jackson, R.D., Slater, P.N., Teillet, P.M., 1992. Evaluation of simplified procedures for retrieval of land surface reflectance factors from satellite sensor output, Remote Sensing of Environment, 41,169-184.

Müller, D., Kuemmerle, T., Rusu, M., Griffiths, P., 2009. Lost in transition: determinants of post-socialist cropland abandonment in Romania, Journal of Land Use Science, 4, 1-2, 109-129.

Müller. D., Leitão, P.J., Sikor, T., 2013. Comparing the determinants of cropland abandonment in Albania and Romania using boosted regression trees, Agricultural systems, 117, 66-77.

Munroe, D.K., Southworth, J., Tucker, C.M., 2002. The dynamics of land-cover change in western Honduras: exploring spatial and temporal complexity, Agricultural Economics, 27, 3, 355–369.

Muys, B., Achten, W., Verbist, B., Aerts, R., Kint, V., Hermy, M., Poppe, J., Marx, A., Verheyen, K., De Tavernier, J., Fanta, J., Van Rompaey, A., Vranken, L., Dondeyne, S., Lenaerts, L., Nabuurs, G.-J., 2011. Conservation and management of forests for sustainable development: where science meets policy, Forests2011 symposium, Leuven, Belgium, 24 November 2011, 47 pp.

Myllyntaus, T., Mattila, T., 2002. Decline or increase? The standing timber stock in Finland, 1800-1997. Ecological Economics, 27, 271-288.

National Agricultural Statistics Service, 2011. Cropland data layer. Washington, DC, U.S. Department of Agriculture. Available at www.nass.usda.gov/research/Cropland/SARS1a.htm (Accessed 14 January 2013).

National Research Council, 2011. Assessment of Impediments to Interagency Collaboration on Space and Earth Science Missions, Washington, 81 pp.

NASA, 1997. Global Land Cover Facility dataset. Available at http://glcf.umd.edu/research/ (Accessed 14 Ocober 2013).

NASA, 2013a. Measuring vegetation (NDVI and EVI). Available at http://earthobservatory.nasa.gov/Features/MeasuringVegetation/ (Accessed 3 October 2013).

NASA, 2013b. Landsat processing details. Available at http://landsat.usgs.gov/Landsat_Processing_Details.php (Accessed 4 September 2013).

NASA, 2013c. Giovanni portal. Available at http://disc.sci.gsfc.nasa.gov/giovanni/overview/index.html (Accessed 8 January 2013).

Navulur, K., 2006. Multispectral Image Analysis Using the Object-Oriented Paradigm. New York, Taylor and Francis, 214 pp.

Nelson, G.C., Geoghegan, J., 2001. Deforestation and land use change: sparse data environments, Agricultural Economics, 27, 201–216.

Nichiforel, L., Schanz, H., 2011. Property rights distribution and entrepreneurial rent-seeking in Romanian forestry: a perspective of private forest owners, European Journal of Forest Research, 130, 369–381.

NIS Romania, 2013. Database of Localities. National Institute of Statistics, Bucharest, Romania. Available at http://www.insse.ro/ (Accessed 12 March 2013).

Nordberg, M.L., Evertson, J., 2003. Vegetation index differencing and linear regression for change detection in a Swedish mountain range using Landsat TM and ETM+ imagery, Land Degradation and Development, 16, 139–149.

Olofsson, P., Kuemmerle, T., Griffiths, P., Knorn, J., Baccini, A., Gancz, V., Blujdea, V., Houghton, R.A., Abrudan, I.V., Woodcock, C., 2011. Carbon implications of forest restitution in post-socialist Romania, Environmental Research Letters, 6, 1-10.

Ono, A., Kajiwara, K., Honda, Y., 2007. Development of vegetation index using radiant spectra normalized by their arithmetic mean, Proceedings 42nd Conference of the Remote Sensing Society of Japan, 10-11 May 2007, Tokyo, Japan, 99-100.

Osborn, M., 2003. The Weirdest of all Undertakings: The Land and the Early Industrial Revolution in Oldham, England, Environmental History, 8, 246–269.

Oszlanyi, J., Grodzinska, K., Badea, O., Shparyk, Y., 2004. Nature conservation in Central and Eastern Europe with a special emphasis on the Carpathian Mountains, Environmental Pollution, 130, 127–134.

Pal, M., Mather, P.M., 2005. Support vector machines for classification in remote sensing, International Journal of Remote Sensing, 26, 1007−1011.

Parcak, 2009. Satellite Remote Sensing for Archaeology, Routeledge, New York, USA, 320 p.

Parker, D.C., Meretsky, V., 2004. Measuring pattern outcomes in an agent-based model of edge-effect externalities using spatial metrics? Agriculture, Ecosystems and Environment, 101, 2–3, 233–250.

Parviainen, J., 2005. Virgin and natural forests in the temperate zone of Europe. Forest Snow and Landscape Research, 78, 9–18.

Pax-Lenney, M., Woodcock, C.E., Macomber, S.A., Gopal, S., Song, C., 2001. Forest mapping with a generalized classifier and Landsat TM data, Remote Sensing of Environment, 77, 241–250.

Perz, S.G., 2007. Grand theory and context-specificity in the study of forest dynamics: forest transition theory and other directions, The Professional Geographer, 59, 105–14.

Petek, F., 2002. Methodology and evaluation of changes in land use in Slovenia between 1896 and 1999, Geografski Zbornik, 52, 61–97.

Petit, C.C., Lambin, F., 2002. Long-term land-cover changes in the Belgian Ardennes (1775-1929): model-based reconstruction versus historical maps. Global Change Biology, 8, 616-630.

Pfaff, A., Walker, R., 2010. Regional interdependence and forest transitions: Substitute deforestation limits the relevance of local reversals, Land Use Policy, 27, 119–29.

Phillips, O.L., Malhi, Y., Higuchi, N., Laurance, W.F., Nunez, P.V., Vasquez, R.M., Laurance, S.G., Ferreira, L.V., Stern, M., Brown, S., Grace, J., 1998. Changes in carbon balance of tropical forests: evidence from long-term plots, Science, 282, 439–441.

Pisani, D.J., 1985. Forests and conservation, 1865-1890, Journal of American History, 72, 340-359.

Pisani, D.J., 1993. Forests and Reclamation, 1891-1911, Forest and Conservation History, 37, 68-79.

Piussi, P., Pettenella, D., 2000. Spontaneous Afforestation of Fallows in Italy. In NEWFOR - New Forests for Europe: Afforestation at the Turn of the Century, EFI Proc. 35, ed. N Weber, Joensuu, EFI, pp. 151—163.

Plaza, A., Du, Q., Chang, Y.-L., King, R.L., 2011. High performance computing for hyperspectral remote sensing, IEEE Journal of Selected Topics on Applied Earth Observation and Remote Sensing, 4, 528–544.

Poelmans, L., Van Rompaey, A., 2009. Detecting and modelling spatial patterns of urban sprawl in the Flanders–Brussels region (Belgium), Landscape and urbanplanning, 93, 645-675.

Poelmans, L., Van Rompaey, A., 2010. Complexity and performance of urban expansion models, Computers, Environment and Urban Systems, 34, 17–27.

Pontius, R.G., 2000. Quantification error versus location error in comparison of categorical maps, Photogrammetric Engineering and Remote Sensing 66, 1011–1016.

Pontius, R.G., Schneider, L.C., 2001. Land-cover change model validation by an ROC method for the Ipswich watershed, Massachusetts, USA. Agriculture,Ecosystems and Environment, 85, 239-248.

Pontius, R.G., 2000. Quantification error versus location error in comparison of categoricalmaps, Photogrammetric Engineering and Remote Sensing, 66, 1011–1016.

Pontius, R.G., Millones M., 2011. Death to Kappa: birth of quantity disagreement and allocation disagreement for accuracy assessment, International Journal of RemoteSensing, 32, 15, 4407–4429.

Ponzoni, F.J., Junior, J.Z., Lamparelli, R.A.C., 2006. In-flight absolute calibration of the CBERS-2 IRMSS sensor data, International Journal of Remote Sensing, 27, 799–804.

Potapov, P.V., Turubanova, S.A., Hansen, M.C., 2011. Regional-scale boreal forest cover and change mapping using Landsat data composites for European Russia, Remote Sensing of Environment, 115, 548–561.

Potapov, P.V., Turubanova, S. A., Hansen, M.C., Adusei, B., Broich, M., Altstatt, A., Mane, L., Justice, C.O., 2012. Quantifying forest cover loss in Democratic Republic of the Congo, 2000–2010, with Landsat ETM+ data, Remote Sensing of Environment, 122, 106-116.

Preston, D., 1998. Changed household livelihood strategies in the cordillera of Luzon, Tijdschrift voor Economische and Sociale Geografie, 89, 371-383.

Prishchepov, A.V., Radeloff, V.C., Baumann, M., Kuemmerle, T., Müller, D., 2012. Effects of institutional changes on land use: agricultural land abandonment during the transition from state-command to market-driven economies in post-Soviet Eastern Europe, Environmental Research Letters, 7, 13.

Puetz, A.M., Lee, K., Olsen, R.C., 2009. WorldView-2 data simulation and analysis results, Proceeding Algorithms and Technologies for Multispectral, Hyperspectral, and Ultraspectral Imagery XV, 12 pp.

Qi, J., Kerr, Y., 1997. On Current Compositing Algorithms, Remote Sensing Reviews, 15. 235-256.

Qu, Z., Kindel, B.C., Goetz, A.F.H., 2003. The high accuracy atmospheric correction for hyperspectral data (HATCH) model, IEEE Transactions on Geoscience and Remote Sensing, 41, 1223−1231.

Rabus, B., Eineder, M., Roth, A., Bamler, R., 2003. The shuttle radar topography mission - a new class of digital elevation models acquired by spaceborne radar, ISPRS Journal of Photogrammetry and Remote Sensing, 57,241– 262.

Radkau, J., 2008. Nature and power: a global history of the environment. Cambridge, Cambridge University Press, 448 pp.

Rahman, H., Dedieu, G., 1994. SMAC: a simplified method for the atmospheric correction of satellite measurements in the solar spectrum, International Journal of Remote Sensing, 15, 123-143.

Ramankutty, N., Heller, E., Rhemtulla, J., 2010. Prevailing myths about agricultural abandonment and forest regrowth in the United States, Annals of the Association of American Geographers, 100, 502–12.

Reinersman, P.N., Carder, K.L., Chen, R.F., 1998. Satellite-sensor calibration verification with the cloud-shadow method, Applied Optics, 37, 5541−5549.

Report of the High-Level Panel of Eminent Persons on the Post-2015 Development Agenda, a new global partnership: eradicate poverty and transform economies through sustainable development,United Nations, 84 pp.

Riaño, D., Chuvieco, E., Salas, F.J., Aguado, I., 2003. Assessment of different topographic corrections in Landsat TM data for mapping vegetation types, IEEE Transactions on Geoscience and Remote Sensing, 41,1056–1061.

Ribaudo, M.O., Hoag, D.L., Smith, M.E., Heimlich, R., 2001. Environmental indices and the politics of the Conservation Reserve Program,Ecological Indicators, 1, 1, 11–20.

Richards, J.A., Xiuping, J.A., 1999. Remote Sensing Digital Image Analysis. An Introduction, 3rd revised and enlarged edition. 363 pp. Berlin, Heidelberg, New York, London, Paris, Tokyo, Hong Kong: Springer-Verlag, Cambridge University Press, pp. 335-342.

Richards, J.A., 2005. Analysis of remotely sensed data: The formative decades and the future, IEEE Transactions on Geoscience and Remote Sensing, 43, 422–432.

Richardson, and Wiegand, 1977. Distinguishing vegetation from soil background information, Photogrammetric Engineering and Remote Sensing,43, 1541-1552.

Richter, R., 1996. Atmospheric correction of satellite data with haze removal including a haze/clear transition region, Computers and Geosciences, 22,675–681.

Richter, R., 1997. Correction of atmospheric and topographic effects for high spatial resolution satellite imagery, International Journal of Remote Sensing, 18, 1099–1111.

Richter, R., 1998. Correction of satellite imagery over mountainous terrain, Applied Optics, 37, 4004-4015.

Richter, R., Schläpfer, D., 2002. Geo-atmospheric processing of airborne imaging spectrometry data. Part 2. Atmospheric/topographic correction, International Journal of Remote Sensing, 23, 2631–2649.

Richter, R., Kellenberger, T., Kaufmann, H., 2009. Comparison of topographic correction methods, Remote Sensing, 1, 184-196.

Richter, R., Schläpfer, D., 2011. Atmospheric/topographic correction for satellite imagery. ATCOR 2/3 User Guide. Version 8.0.2, 215 pp.

Richter, R., Schläpfer, D., 2013. Atmospheric/Topographic Correction for Satellite Imagery. Atcor-2/3 User Guide, version 8.2.1., February 2013. Available at http://www.rese.ch/pdf/atcor3_manual.pdf (Accessed 26 January 2013).

Roberts, D.A., Yamaguchi, Y., Lyon, R., 1986. Comparison of various techniques for calibration of AIS data. In: Vane, G. and Goetz, A.F.H.(Eds.), Proceedings of the 2nd Airborne Imaging Spectrometer Data Analysis Workshop JPL Publication, 8, 35. 21−30. Pasadena, CA, Jet Propulsion Lab, pp. 21-30.

Rockström, J., Steffen, W., Noone, K., Persson, Å, Chapin, F.S., Lambin, E.F., Lenton, T.M., Scheffer, M., Folke, C., Schellnhuber, H.C., Nykvist, B., de Wit, C.A., Hughes, T., van der Leeuw, S., Rodhe, H., Sörlin, S., Snyder, P.K., Costanza, R., Svedi, U., Falkenmark, M., Karlberg, L., Corell, R.W., Fabry, V.J., Hansen, J., Walker, B.,Liverman, D., Richardson, K., Crutzen, P., Foley, J.A., 2009. A safe operating space for humanity, 461, 24, 472-475.

Rogan, J., Chen, D., 2004. Remote sensing technology for mapping and monitoring land cover and land use change, Progress in Planning, 61, 301−325.

Rogan, J., Franklin, J., Stow, D., Miller, J., Woodcock, C., Roberts, D., 2008. Mapping landcover modifications over large areas: a comparison of machine learning algorithms, Remote Sensing of Environment, 112, 2272–2283.

Rosenfield, G.H., Fitzpatrick-Lins, K., 1986. A coefficient of agreement as a measure of thematic classification accuracy, Photogrammetric Engineering and Remote Sensing, 52, 223–227.

Rotzer, T., Chmielewski, F.M., 2001. Phenological maps of Europe, Climate Research, 18, 249–257.

Rounsevell, M.D.A., Annetts, J.E., Audsley, E., Mayr, T., Reginster, I., 2003. Modelling the spatial distribution of agricultural land use at the regional scale. Agriculture, Ecosystems and Environment, 95, 465-479.

Rouse, J.W., Haas, R.H., Schell, J.A., Deering, D.W., 1973. Monitoring vegetation systems in the Great Plains with ERTS. Third ERTS Symposium, NASA SP-351, I, 309-317.

Roy, D.P, Ju, J., Kline, K., Scaramuzza, P.L., Kovalsky, V., Hansen, M.C., Loveland, T.R., Vermote, E., Zhang, C., 2010. Web-enabled LandsatData (WELD): Landsat ETM plus composited mosaics of the conterminous United States, Remote Sensing of Environment, 114, 35–49.

Rosenfield, G., Fitzpatrick-Lins, K., 1986. A coefficient of agreement as a measure ofthematic classification accuracy, Photogrammetric Engineering and Remote Sensing, 52,223–227.

Rozylowicz, L., Popescu, V., Troescu, M., Chi, A.G., 2011. The potential of large carnivores as conservation surrogates in the Romanian Carpathians, Biodiversity and Conservation, 20, 561-579.

Rudel, T.K., Perez-Lugo, M., Zichal, H., 2000. When fields revert to forest: Development and spontaneous reforestation in post-war Puerto Rico, The Professional Geographer, 52, 386-397.

Rudel, T.K., 2001. Did a green revolution restore the forests of the American South? In Agricultural technologies and tropical deforestation, Angelsen, A., Kaimowitz, D. (Ed.), Wallingford, CABInternational, pp. 45-57.

Rudel, T.K., Achard, F., Angelsen, A., Coomes, O.T., Lambin, E.F., Moran, E., Xu, J., 2005. Forest transitions: towards a global understanding of land use change, Global Environmental Change, 15, 23-31.

Rudel, T.K., 2009. Tree farms: driving forces and regional patterns in the global expansion of forest plantations, Land Use Policy, 26, 545–50.

Rudel, T.K., DeFries, R., Asner, G.P., Laurance, W.F., 2009. Changing drivers of deforestation and new opportunities for conservation, Conservational Biology, 23, 1396–405.

Rudel, T.K., Schneider, L., Uriarte, M., 2010. Forest transitions: An introduction, Land Use Policy, 27, 95-97.

Rui, Y., Ban, Y., 2010. Multi-agent Simulation for Modeling Urban Sprawl in the Greater Toronto Area, 13th AGILE Conference on Geographic Information Science, 10-14 May 2010, Guimaraes, Portugal. 12 pp.

Sader, S.A., Jin, S., 2006. Feasibility and accuracy of MODIS 250m imagery for forest disturbance monitoring, ASPRS 2006 Annual Conference, Reno, Nevada, USA, May 1-5, 2006, 6 pp.

Sandmeier, S., Itten, K.I., 1997. A physically-based model to correct atmospheric and illumination effects in optical satellite data of rugged terrain, IEEE Transactions on Geoscience and Remote Sensing, 35, 708-717.

Saunders, R.W., 1986. An automated scheme for the removal of cloud contamination form AVHRR radiances over Western Europe, International Journal of Remote Sensing, 7, 867 – 886.

Schelhaas, M.J., Nabuurs, G.J., Schuck, A., 2003. Natural disturbances in the European forests in the 19th and 20th centuries, Global Change Biology, 9, 1620–1633.

Schneider, L., Pontius Jr, R.G., 2001. Modeling land-use change: the case of the Ipswich watershed, Massachusetts, USA, Agriculture, Ecosystems and Environment, 85, 83–94.

Schroeder, T.A., Cohen, W.B., Song, C., Canty, M.J., Yang, Z., 2006, Radiometric correction of multi-temporal Landsat data for characterization of early successional forest patterns in western Oregon, Remote Sensing of Environment, 103, 16–26.

Schröter, D., Cramer, W., Leemans, R., Prentice, I.C., Araújo , M.B., Arnell, N.W., Bondeau, A., Bugmann, H., Carter, C.T.R. , Gracia,A., de la Vega-Leinert, A.C., Erhard, M., Ewert, F., Glendining, M., House, J., Kankaanpää, S., Reginster, I., Rounsevell, M., Sabaté, S., Sitch, S., Smith, B., Smith, J., Smith, P., Sykes, M.T., Thonicke, K., Thuiller, W., Tuck, G., Zaehle, S., Zierl, B., 2005. Ecosystem Service Supply and Vulnerability to Global Change in Europe, Science, 310, 5752, 1333-1337.

Schuck, P., Bücking, W., 1994. A review of approaches to forestry research on structure, succession and biodiversity of undisturbed and semi-natural forests and woodlands in Europe, EFI Working paper 3, Joensuu, Finland, 64 pp.

Schulz, J.J., Cayuela, L., Echeverria, C., Salas, J., Benayas, J.M.R., 2010. Monitoring land cover change of the dryland forest landscape of Central Chile (1975–2008), Applied Geography, 30, 436-447.

Schulze, E.-D., Hessenmoeller, D., Knohl, A., Luyssaert, S., Boerner, A., Grace, J., 2009. Temperate and boreal old-growth forests: how do their growth dynamics and biodiversity differ from young stands and managed forests? In: Old-Growth Forests, Wirth, C., Gleixner, G., Heimann, M. (Ed.), Berlin and Heidelberg, Germany, Springer, 343–366.

Scott, D.F., Bruijnzeel, L.A., Mackensen, J., 2005. The hydrological and soil impacts of forestation in the tropics. In: Bonell, M., Bruijnzeel, L.A. (Eds.), Forests, Water and People in the Humid Tropics, Cambridge University Press, Cambridge, 16 pp.

Serneels, S., Lambin, E.F., 2001. Proximate causes of land use change in Narok district Kenya: a spatial statistical model, Agriculture, Ecosystems and Environment, 85, 65–82.

Shively, G.E., 2001. Agricultural Change, Rural Labor Markets, and Forest Clearings: An illustrative Case from the Philippines, Land Economics, 77, 268-284.

Sieber, A., Kuemmerle, T., Prishchepov, A.V., Wendland, K.J., Baumann, M., Radeloff, V.C., Baskin, L.M., Hostert, P., 2013. Landsat-based mapping of post-Soviet land-use change to assess the effectiveness of the Oksky and Mordovsky protected areas in European Russia, Remote Sensing of Environment, 133, 38–51.

Siiskonen, H., 2007. The conflict between traditional and scientific forest management in 20th century Finland, Forest Ecology and Management, 249, 125-133.

Sikor, T., Stahl, J., Dorondel, S., 2009. Negotiating post-socialist property and state: struggles over forests in Albania and Romania, Development and Change, 40, 171–193.

Singh, S., Sharma, J.K., Mishra, V.D., 2011. Comparison of different topographic correction methods using AWiFS satellite data, International Journal of Advanced Engineering Sciences and Technologies, 7, 103-109.

Slater, P.N., Biggar, S.F., Holm, R.G., Jackson, R.D., Mao, Y., Moran, M.S., Palmer, J.M., Yuan, B., 1987. Reflectance- and Radiance-Based Methods for the in-Flight Absolute Calibration of Multispectral Sensors, Remote Sensing of Environment, 22, 11–37.

Slater, J.A., Garvey, G., Johnston, C., Haase, J., Heady, B., Kroenung, G., Little, J., 2006. The SRTM data finishing process and products, Photogrammetric Engineering and Remote Sensing, 72, 237–247.

Smith, G.M., Milton, E.J., 1999. The use of the empirical line method to calibrate remotely sensed data to reflectance, International Journal of Remote Sensing, 20, 2653-2662.

Smith, J.A., Lin, T.L., Ranson, K.J., 1980. The Lambertian assumption and Landsat data, Photogrammetric Engineering and Remote Sensing, 46, 1183-1189.

Smits, P.C., Dellepiane, S.G., Schowengerdt, R.A., 1999. Quality assessment of image classification algorithms for land-cover mapping: a review and proposal for a cost-based approach, International Journal of Remote Sensing, 20, 1461–1486.

Soenen, S.A., Peddle, D.R., Coburn, C.A., Hall, R.J., Hall, F.G., 2008. Improved topographic correction of forest image data using a 3-D canopy reflectance model in multiple forward mode, International Journal of Remote Sensing, 29, 1007–1027.

Solovastru, E., 2010. Statistical yearbook. Available at http://www.insse.ro/cms/rw/pages/anuarstatistic2010.en.do (Accessed 19 September 2013).

Solovij, I.P., 2000. Afforestation in Ukraine - Potential and Restrictions. In NEWFOR - New Forests for Europe: Afforestation at the Turn of the Century, EFI Proceeding 35, Weber, N. (Ed.), Joensuu, pp. 195-211.

Song, C., Woodcock, C.E., Seto, K.C., Lenney, M.P., Macomber, S.A., 2001. Classification and change detection using Landsat TM data: when and how to correct atmospheric effects, Remote Sensing of Environment, 75,230–244.

Song, C., Zhang, Y., 2009. Forest Cover in China from 1949 to 2006. In Reforesting Landscapes: Linking Pattern and Process, Nagendra, H. Southworth, J.(Ed.), Springer Landscape Series vol.10, Dordrecht, Springer, pp. 341-356.

Soran, V., Biro, J., Moldovan, O., Ardelean, A., 2000. Conservation of biodiversity in Romania, Biodiversity and Conservation, 9, 1187-1198.

Soudani, K., Francxois, C., Maire, G., Le Dantec, V., Dufrène, E., 2006. Comparative analysis of IKONOS, SPOT, and ETM+ data for leaf area index estimation intemperate coniferous and deciduous forest stands, Remote Sensing of Environment,102, 161–75.

Sriwongsitanon, N., Surakit, K., Thianpopirug, S., 2011. Influence of atmospheric correction and number of sampling points on the accuracy of water clarity assessment using remote sensing application, Journal of Hydrology, 401, 203-220.

Staaland, H., Holand, O., Nelleman, C., Smith, M., 1998. Time Scale for Forest Regrowth: Abandoned Grazing and Agricultural Areas in Southern Norway, Ambio, 27, 456-460.

Staenz, K., Szeredi, T., Schwarz, J., 1998. ISDAS - a system for processing/analyzing hyperspectral data; technical note, Canadian Journal of Remote Sensing, 24, 99-113.

Strassburg, B., Kelly, A., Balmford, A., Davies, R., Gibbs, H., Lovett, A., Miles, L., Orme, C.D., Price, J., Turner, R., Rodrigues, A., 2010. Global congruence of carbon storage and biodiversity in terrestrial ecosystems, Conservation Letters, 3, 98–105.

Steyerberg, E.W., Harrell Jr, F.E., Borsboom, G., Eijkemans, R., Vergouwe, Y., Habbema, J.D., 2001. Internal validation of predictive models: Efficiency of some procedures for logistic regression analysis, Journal of Clinical Epidemiology, 54, 774–781.

Strimbu, B.M., Hickey, G.M., Strimbu, V.G., 2005. Forest conditions and management under rapid legislation change in Romania, The ForestChronicle, 95, 350–358.

Stürck, J., Poortinga, A., Verburg, P.H., 2014. Mapping ecosystem services: The supply and demand of floodregulation services in Europe, Ecological Indicators, 38, 198– 211.

Stubbs, B.J., 2008. Forest Conservation and the Reciprocal Timber Trade between New Zealand and New South Wales, 1880s–1920s, Environment and History, 14, 497-522.

Szilassi, P., Jordan, G., Van Rompaey, A., Gabor, C., 2006. Impacts of historical land use changes on erosion and soil properties in the Kali basin at lake Balaton, Hungary, Catena, 68, 96-108.

Szilassi, P., Jordan, G., Kovacs, F., Van Rompaey, A., Van Dessel, W., 2010. Investigating the link between soil quality and agricultural land use change. A case study in the lake Balaton catchment, Hungary, Carpathian Journal of Earth and Environmental Sciences, 5, 2, 61-70.

Tack, G., Van Den Brempt, P., Hermy, M., 1993. Woodlands of Flanders, An historical ecology, Kirby, K.J., Watkins, C.(Ed.), Davidsfonds, Leuven, pp. 283-292.

Tan, B., Masek, J.G., Wolfe, R., Gao, F., Huang, C., Vermote, E.F., Sexton, J.O., Ederer, G., 2013. Improved forest change detection with terrain illumination corrected Landsat images, Remote Sensing of Environment, 136, 469–483.

Teka, K., Van Rompaey, A., Poesen, J., 2013. Assessing the role of policies on land use change and agricultural development since 1960s in Northern Ethiopia, Land Use Policy 30, 1, 944–951.

Teillet, P.M., Guindon, B., Goodenough, D.G., 1982. On the slope-aspect correction of multispectral scanner data, Canadian Journal of Remote Sensing, 8,84−106.

Teuber, K.B., 1990. Use of AVHHR imagery for large-scale forest inventories, Forest Ecology and Management, 33–34, 621–631.

Thome, K.J., Gellman, D.I., Parada, R.J,. Biggar, S.F., Slater, P.N., Moran, S.M., 1993. In-flight radiometric calibration of Landsat-5 Thematic Mapper from 1984 to present, Proceedings Society of Photo- Optical Instrument Engineering Symposium, Orlando, Florida, pp. 126-130.

Timisescu, 2009. Natura 2000 in Romania, study case SCI and SPA, European foresters Congress 2009, Poland. Available at http://www.european-foresters.org/PolandCongress09/Speeches/SeminarSpeeches/Natura%202000_Romania.pdf (Accessed 13 September 2013).

Toader, T., Dumitru, I., 2005. Romanian forest - national parks and natural parks. National Forest Administration ROMSILVA, Bucharest.

Toutin, T., Cheng, P., 2002. QuickBird: a milestone for high resolution mapping, Earth Observation Magazine, 11, 4. 14–18.

Tsutsui, W.M., 2003. Landscapes in the Dark Valley: Toward an Environmental History of Wartime Japan, Environmental History 8, 2, 294-311.

Tu, J.V., 1996. Advantages and disadvantages of using artificial neural networks versus logistic regression for predicting medical outcomes, Journal of Clinical Epidemiology, 49, 11, 1225-1231.

Turk, G., 1979. GT index: a measure of the success of prediction. Remote Sensing of Environment 8, 75–86. UN-ECE/FAO, 2000. Forest Resources of Europe, CIS, North America, Australia, Japan and New Zealand (industrialized temperate/boreal countries). 224 pp.

Turk, G., 2002. Map evaluation and chance correction, Photogrammetric Engineering and Remote Sensing, 68, 123–133.

Turner, B.L., Lambin, E.F., Reenberg, A., 2007. The emergence of land change science for global environmental change and sustainability, Proceedings of the National Academy of Sciences of the United States of America, 104,20666-20671.

Turnock, D., 1991. The planning of rural settlement in Romania, The Geographical Journal, 157, 3, 251-264.

Turnock, D., 2001. The Carpathian Ecoregion: A New Initiative for Conservation and Sustainable Development, Geographica Pannonica, 5, 17-23.

Turnock, D., 2002. Ecoregion-based conservation in the Carpathians and the land-use implications, Land Use Policy, 19, 47-63.

Tuttle, E.M., Jensen, R.R., Formica, V.A., Gonser, R.A., 2006. Using remote sensing image texture to study habitat use patterns: a case study using the polymorphic white-throated sparrow (Zonotrichia albicollis), Global Ecology and Biogeography, 15, 349–57.

UNDP, 2004. UNDP Project Document: Strengthening Romania's Protected Area System by Demonstrating Public-Private Partnership in Romania's Maramures Nature Park, U.N.D.P. (ed)., Government of Romania, United Nations Development Programme.

UN-ECE/FAO, 2000. Contribution to the Global Forest Resources Assessment 2000. Geneva Timber and Forest Study Papers, No. 17, United Nations, New York and Geneva.

United Nations Environmental Program, 2007. Carpathians Environment Outlook. 236 pp. Available at http://www.unep.org/geo/pdfs/KEO2007_final_FULL_72dpi.pdf (Accessed 16 July 2013).

USGS, 2013a. Global land cover characterization. Available athttp://edc2.usgs.gov/glcc/glcc.php(Accessed 13 March 2012).

USGS, 2013b. Project facts and history of Landsats 1 through 7. Available at www.landsat.usgs.gov (Accessed 19 January 2014).

Vaclavik, T., Rogan, J., 2009. Identifying Trends in Land Use/Land Cover Changes in the Context of Post-Socialist Tranformation in Central Europe: A case study of the Greater Olomouc Region, Czech Republic, GIScience and Remote Sensing, 46, 54-76.

Vanacker, V., Molina, A., Govers, G., Poesen, J., Dercon, G., Deckers, S., 2005. River channel response to short-term human-induced change in landscape connectivity in Andean ecosystems, Geomorphology, 72, 340–353.

Vanacker, V., Balthazar, V., Molina, A., 2013. Anthropogenic Activity Triggering Landslides in Densely Populated Mountain Areas, Landslide Science and Practice, 4, 163-167.

Van Beek, J., 2011. Remote sensing of vegetative systems: practical session #3. Atmospheric correction, Unpublished M.Sc. thesis, KU Leuven, Belgium, , 193 pp.

Vandendael, M., 2007. Erosie- en depositiepatronen in de vallei van de Beoux: rol van landgebruiks-veranderingen, 108 pp.

Van Dessel, W., Van Rompaey, A., Poelmans, L., Szilassi, P., 2008. Predicting land cover changes and their impact on the sediment influx in the Lake Balaton catchment, Landscape Ecology, 23, 6, 645-656.

Van Dessel, W., 2010. Evaluation of land cover change models in rural areas in central and eastern Europa. PhD Dissertation, april 2010, KU Leuven,Belgium, 155 pp.

Van Dijk, T., Kopeva, D., 2006. Land banking and Central Europe: future relevance, current initiatives, Western European past experience, Land Use Policy, 23, 3, 286-301.

Van Ede, R., 2004. Destriping and geometric correction of an ASTER Level 1A Image, Unpublished M.Sc. thesis, Utrecht University, the Netherlands, 36 pp.

Van Meijl, H., Van Rheenen, T., Tabeau, A., Eickhout, B., 2006. The impact of different policy environments on agricultural land use in Europe, Agriculture, Ecosystems and Environment, 114, 21-38.

Vanonckelen, S., Lhermitte, S., Van Rompaey, A., 2013. The effect of atmospheric and topographic correction methods on land cover classification accuracy, International Journal of Applied Earth Observation and Geoinformation, 24, 9-21.

Vanonckelen, S., Lhermitte, S., Balthazar, V., Van Rompaey, A., accepted. Performance of atmospheric and topographic correction models on Landsat imagery in mountain areas, International Journal of Remote Sensing.

Vanonckelen, S., Griffiths, P., Lhermitte, S., Van Rompaey, A., submitted. Integration of topographic correction in a pixel-based compositing algorithm for large scale land cover mapping, Proceedings of Multitemp 2013, 7th International Workshop on the Analysis of Multi-temporal Remote-Sensing Images, Banff, Alberta, Canada, 26-28 June 2013.

Van Rompaey, A., Verstraeten, G., Van Oost, K., Govers, G., Poesen, J., 2001. Modelling mean annual sediment yield using a distributed approach, Earth Surface Processes and Landforms, 26, 11, 1221-1236.

Van Rompaey, A., Govers, G., 2002. Data quality and model complexity for continental scale soil erosion modeling, International Journal of GIS, 16, 663-680.

Van Rompaey, A., Govers, G., Puttemans, C., 2002. Modelling land use changes and their impact on soil erosion and sediment supply to rivers, Earth Surface Processes and Landforms, 27, 481-494.

Van Rompaey, A., Krasa, J., Dostal, T., Govers, G., 2003. Modelling sediment supply to rivers and reservoirs in Eastern Europe during and after the collectivisation period, Hydrobiologia, 494, 1, 169-176.

Van Rompaey, A., Krasa, J., Dostal, T., 2007. Modelling the impact of land cover changes in the Czech Republic on sediment delivery, Land Use Policy, 24, 576-583.

Van Vuuren, D.P., Cofala, J., Eerens, H.E., Oostenrijk, R., Heyes, C., Klimont, Z., den Elzen, M.G.J., Amann, M., 2006. Exploring the ancillary benefits of the Kyoto Protocol for air pollution in Europe, Energy Policy, 34, 444-460.

Vapnik, V.N., 1999. An overview of statistical learning theory, IEEE Transactions on Neural Networks, 10, 988–999

Vasile, M., Mantescu, L., 2009. Property reforms in rural Romania and communitybased forests, Romanian Sociology, 7, 96–113.

Veen, P., Fanta, J., Raev, I., Biriş, I.A., de Smidt, J., Maes, B., 2010. Virgin forests in Romania and Bulgaria: results of two national inventory projects and their implications for protection, Biodiversity and Conservation, 19, 1805–1819.

Vega, E., Baldi, G., Paruelo, J., 2009. Land use change patterns in the Río de la Plata grasslands: The influence of phytogeographic and political boundaries, Agriculture Ecosystems and Environment, 134, 287-292.

Veraverbeke, S., Verstraeten, W.W., Lhermitte, S., Goossens, R., 2010. Illumination effects on the differenced Normalized Burn Ratio's optimality for assessing fire severity, International Journal of Applied Earth Observation and Geoinformation, 12, 60–70.

Veraverbeke, S., Lhermitte, S., Verstraeten, W.W., Goossens, R., 2011. A time integrated MODIS burn severity assessment using the multi-temporal differenced Normalized Burn Ratio (dNBRMT), International Journal of Applied Earth Observation and Geoinformation, 13, 52–58.

Verburg, P.H., Ritsema van Eck, J.R., de Nijs, T.C.M., Dijst, M.J., Schot, P., 2004. Determinants of land-use change patterns in the Netherlands, Environment and Planning B: Planning and Design, 31, 125-150.

Verburg, P.H., Overmars, K.P., 2009. Combining top-down and bottum-up dynamics in land use modeling: exploring the future and abandoned farmlands in Europe with the Dyna-CLUE model, Landscape Ecology, 24, 1167-1181.

Vermeiren, K., Van Rompaey, A., Loopmans, M., Eria, S., Paul, M., 2012. Urban growth of Kampala, Uganda: Pattern analysis and scenario development, Landscape and Urban Planning, 106, 199– 206.

Vermote, E.F., El Saleous, N.Z., Justice, C.O., Kaufman, Y.J., Privette, J., Remer, L., Roger, J.C., Tanré, D., 1997. Atmospheric correction of visible to middle infrared EOS-MODIS data over land surface,

background, operational algorithm and validation, Journal of Geophysical Research, 102, 17131-17141.

Vicente-Serrano, S.M., Pérez-Cabello, F.,Lasanta, T., 2008, Assessment of radiometric correction techniques in analyzing vegetation variability and change using time series of Landsat images, Remote Sensing of Environment, 112,3916–3934.

Vina, A., Gitelson, A.A., Nguy-Robertson, A.L., Peng, Y., 2011. Comparison of different vegetation indices for the remote assessment of green leaf area index of crops, Remote Sensing of Environment 115, 3468–3478.

Vincent, R.K., 1972. An ERTS Multispectral Scanner experiment for mapping iron compounds, Proceeding of the 8th International Symposium on Remote Sensing of Environment, Ann Arbor, Michigan, USA, 1239-1247.

Vincini, M., Frazzi, E., 2003. Multitemporal evaluation of topographic normalization methods on deciduous forest TM data, IEEE Transactions on Geoscience and RemoteSensing, 41, 2586-2590.

VITO, 2013a. SPOT-VEGETATION programma. Available at http://www.spot-vegetation.com/pages/VegetationProgramme/introduction.htm (Accessed 2 February 2014).

VITO, 2013b. SPOT-VEGETATION mission. Available at http://www.spot-vegetation.com/ (Accessed 2 February 2014).

Von Thünen, J.H., 1826. Der Isolierte Staat in Beziehung auf Landwirtschaft und Nationaloekonomie. Scientia Verlag, English translated reprint in 1990, Aalen, 184 pp.

Vu, K.C., Govers, G., Vanacker, V., Schmook, B., Hieu, N., 2013. Land Transitions in Northwest Vietnam: An Integrated Analysis of Biophysical and Socio-Cultural Factors, Human Ecology, 41, 37-50.

Wang, G., Innes, J.L., Lei, J., Dai, S., Wu, S.W., 2007. China's forestry reforms, Science, 318, 1556-1557.

Webster, R., Holt, S., Avis, C., 2001. The status of the Carpathians, a report developed as a part of the Carpathian Ecoregion Initiative, WWF, pp. 67.

Wen, J., Liu, Q., Liu, Q., Xiao, Q., Li, X., 2009. Parametrized BRDF for atmospheric and topographic correction and albedo estimation in Jiangxi rugged terrain, China, International Journal of Remote Sensing, 30, 2875–2896.

Wenhua, L., 2004. Degradation and restoration of forest ecosystems in China, Forest Ecology and Management, 201, 33-41.

West, A.J., 2003. Forests and National Security: British and American Forestry Policy in the Wake of World War, Environmental History, 8, 270-293.

Wilkie, D., Shaw, E., Rotberg, F., Morelli, G., Auzel, P., 2000. Roads, development, and conservation in the Congo basin, Conservation Biology, 14, 1614–1622.

Wilkinson, G.G., 2005. Results and implications of a study of fifteen years of satellite image classification experiments, IEEE Transactions on Geoscience and Remote Sensing, 43, 433–440.

Wirth, C., 2009. Old-growth forests: function, fate and value. A synthesis. In: Old-Growth Forests, Wirth, C., Gleixner, G., Heimann, M. (Ed.), Berlin and Heidelberg, Germany, Springer, 465–491.

Wofsy, S.C., Harriss, R.C., 2002. The North American Carbon Program (NACP) Report of the NACP Committee of the US Interagency Carbon Cycle Science Program, US Global Change Research Program, Washington, DC, USA, 62 pp.

Wood, V., Pawson, E., 2008. The Banks Peninsula forests and Akaroa cocksfoot: explaining a New Zealand forest transition, Environmental History, 14, 449–68.

Worldbank, 2013. Data of Romania. Available at http://data.worldbank.org/country/romania (Accessed 16 August 2013).

World Health Organization, 2005. Ecosystems and human well-being, health synthesis, Millennium Ecosystem Assessment, WHO Press, Geneva, Switzerland, 64 pp.

Wouters, H., 2012. Land cover change Detection in the Romanian Carpathians (1986-2010),Unpublished M.Sc. thesis, , KU Leuven, Belgium, 130 pp.

Wu, J., Bauer, M.E., Wang, D., Manson, S., 2008. A comparison of illumination geometry-based methods for topographic correction of QuickBird images of an undulant area, ISPRS Journal of Photogrammetry and Remote Sensing, 63, 223–236.

Wu, X., Sullivan, J.T., Heidinger, A.K., 2010. Operational calibration of the Advanced Very High Resolution Radiometer (AVHRR) visible and near-infrared channels, Canadian Journal of Remote Sensing, 36, 5, 602-616.

Wulder, M.A., Masek, J.G., Cohen, W.B., Loveland, T.R., Woodcock, C.E., 2012. Opening the archive: How free data has enabled the science and monitoring promise of Landsat, Remote Sensing of Environment, 122, 2-10.

WWF, 2005. Illegal logging in Romania.Available at http://www.forestconsulting.net/Downloads/Publications/finalromaniaillegallogging.pdf (Accessed 8 January 2014).

WWF, 2010. FSC principles spread to Bulgaria and Romania. Available at http://wwf.panda.org/?195055/FSC-principles-spread-to-Bulgaria-and-Romania (Accessed 12 January 2014).

WWF, 2012. Romania: people power protects Europ's largest virgin forest. Available at http://www.earthhour.org/romania-story (Accessed 5 January 2014).

Xiao, X.M., Zhang, Q., Braswell, B., Urbanski, S., Boles, S., Wofsy, S., Berrien, M., Ojima, D., 2004. Modeling gross primary production of temperate deciduous broadleaf forest using satellite images and climate data, Remote Sensing of Environment, 91, 256–70.

Xie, Y., Sha, Z., Yu, M., 2008. Remote sensing imagery in vegetation mapping: a review, Journal of Plant Ecology, 1, 1, 9-23.

Xu, J., Yang, Y., Fox, J., Yang, X., 2007. Forest transition, its causes and environmental consequences: An empirical evidence from Yunnan of Southwest China, Tropical Ecology, 48, 1-14.

Youn, Y.C., 2009. Use of forest resources, traditional forest-related knowledge and livelihood of forest dependent communities: Cases in South Korea, Forest Ecology and Managment, 257, 2027-2034.

Young, W.C., Kwang, 2009. Songgye, a traditional knowledge system for sustainable forest management in Choson Dynasty of Korea, Forest Ecology and Managment, 257, 2022-2026.

Zhang, Y., 2000. Deforestation and Forest Transition: Theory and Evidence in China. World Forests from Deforestation to Transition? Palo, M. Vanhanen, H. (Ed.), Dordrecht, KluwerAcademic Publishers, 25 pp.

Zhang, P., Shao, G., Zhao, G., Master, D.C.L., Parker, G.R., Dunning Jr, J.B., Li, Q., 2000. China's forest policy for the 21st century, Science, 288, 2135-2136.

Zhang, Z., De Wulf, R.R., Van Coillie, F.M.B., Verbeke, L.P.C., De Clercq, E.M., Ou, X., 2011. Influence of different topographic correction strategies on mountain vegetation classification accuracy in the Lancang Watershed, China,Journal of applied Remote Sensing, 5, 1-21.

Zhang, W., Gao, Y., 2011. Topographic correction algorithm for remotely sensed data accounting for indirect irradiance,International Journal of Remote Sensing, 32, 1807–1824.

Zhao, W., Tamura, M., Takahashi, H., 2000. Atmospheric and spectral corrections for estimating surface albedo from satellite data using 6S code, Remote Sensing of Environment, 76, 202-212.

Zhou, H., Van Rompaey, A., Wang, J., 2009.Detecting the impact of the "Grain for Green" program on the mean annual vegetation cover in the Shaanxi province, China using SPOT-VGT NDVI data, Land Use Policy, 26, 954–960.

Zhu, Z., Woodcock, C.E., 2012. Object-based cloud and cloud shadow detection in Landsat imagery, Remote Sensing of Environment, 118, 83–94.

List of publications

Articles in international journals

Vanonckelen, S., Lhermitte, S., Van Rompaey, A., 2013. The effect of atmospheric and topographic correction methods on land cover classification accuracy, International Journal of Applied Earth Observation and Geoinformation. 24, 9-21.

Vanonckelen, S., Lhermitte, S., Balthazar, V., Van Rompaey, A., accepted. Performance of atmospheric and topographic correction models on Landsat imagery in mountain areas, International Journal of Remote Sensing.

Vanonckelen, S., Griffiths, P., Lhermitte, S., Van Rompaey, A., submitted. Integration of topographic correction in a pixel-based compositing algorithm for large scale land cover mapping, Proceedings of Multitemp 2013, 7th International Workshop on the Analysis of Multi-temporal Remote-Sensing Images, Banff, Alberta, Canada, 26-28 June 2013.

In citing this research, reference should be made to these publications.

Presentations at international conferences

Vanonckelen, S., Lhermitte, S., Van Rompaey, A., 2013. Do combined atmospheric and topographic correction methods improve land cover classification accuracy in mountain areas? Multitemp 2013, 7th International Workshop on the Analysis of Multi-temporal Remote-Sensing Images, Banff, Alberta, Canada, 26-28 June 2013.

Vanonckelen, S., Lhermitte, S., Van Rompaey, A., 2012. Do combined atmospheric and topographic correction methods improve land cover classification accuracy in mountain areas? SAGEO 2012, Liège, 8November 2012.

Vanonckelen, S., Lhermitte, S., Van Rompaey, A., 2012. The added value of integrated correction models for the detection of forest transitions in mountain areas. IEEE International Geoscience and RemoteSensing Symposion (IGARSS) 2012. Munich, Germany, 22-27 July 2012.

Vanonckelen, S., Lhermitte, S., Balthazar, V., Van Rompaey, A., 2011. Atmospheric and topographic correction for the detection of forest transitions in mountain areas. Forests2011 - International Conference - Conservation and management of forests for sustainable development: where science meets policy. Leuven, 23-24 November 2011.

Vanonckelen, S., Isabirye, M., Deckers, S., Poesen, J., 2011. Land use and land use dynamics in the upper-Rwizi river catchment, Southwestern Uganda. Soil Science Society of East Africa Conference. Jinja, 21-24 November 2011.

Presentations at national conferences

Vanonckelen, S., Lhermitte, S., Van Rompaey, A., 2013. Do combined atmospheric and topographic correction methods improve land cover classification accuracy in mountain areas? Belgian Geographical Day. Louvain-La-Neuve, 24 May 2013.

Vanacker, V., Balthazar, V., Lambin, E., Hall, J., Hostert, P., Griffiths, P., Vanonckelen, S., Molina, A., Van Rompaey, A., 2012. Forest transition in mountain environments: topographic corrections andmodeling of ecosystem services. Belgian Earth Observation Day 2012. Bruges, 5 September 2012.

Van Rompaey, A., Vu, K.C., Vanonckelen, S., Molina, A., Vermeiren, K., 2011. Forest transitions in mountain areas: research challenges and some examples. Thematic days on forests and climate change.Brussels, 9-10 November 2011.

Balthazar, V., Griffiths, P., Hall, J., Hostert, P., Lambin, E., Vanacker, V., Vanonckelen, S., Van Rompaey, A., 2010. Remote sensing of the forest transition and its ecosystem impacts in mountain environments. Belgian Earth Observation Day. Chaudfontaine, 6 May 2010.

Vanonckelen, S., Deckers, J., Poesen, J., Wanyama, J., Isabirye, M., 2010. Land use and land use dynamics in the upper-Rwizi river catchment, Southwestern Uganda. Day of Young Soil Scientists 2010.Brussels, 23 February 2010.

Presentations at universities

Vanonckelen, S., Balthazar, V., 2012. Work package 1: Data acquisition, preprocessing and correction for topographic effects. Presentation at mid-term FOMO meeting. Leuven, 10 December 2012.

Vanonckelen, S., Van Rompaey, A., Lhermitte, S., 2012. The effect of combined atmospheric and topographic correction on land cover classification accuracy. Land System Science Cluster (LSSC) Colloquium. Berlin, 5 November 2012.

Vanonckelen, S., 2011. Detection and analysis of the forest transition in the Romanian Carpathians Presentation for Advisory Committee. Leuven, 16 December 2011.

Vanonckelen, S, Balthazar, V., 2011. Work package 1: Data acquisition, preprocessing and correction for topographic effects. Presentation at mid-term FOMO meeting. Leuven, 9 December 2011.

Vanonckelen, S., 2011. Combined performance of atmospheric and topographic correction models for the interpretation of satellite imagery in mountain areas. 4x4 presentation Advanced Geography. Leuven, 2 November 2011.

Vanonckelen, S., 2010. Evaluation of topographic correction methods for forest cover change mapping in mountain areas. Research Seminar at Division of Geography. Leuven, 18 February 2010.

Vanonckelen, S., Balthazar, V., 2010. Work package 1: Data acquisition, preprocessing and correction for topographic effects. Presentation at FOMO meeting. Leuven, 10 December 2010.

Supervision of M.Sc. and B.Sc. theses

Baes, A., 2013. Impact of demography, land tenure and protective measurements on forest conservation in the Romanian Carpathians. Unpublished B.Sc. thesis, KU Leuven, Belgium, 52 pp.

Bakelants, L., 2013. Forest transition in the Romanian Carpathians: a gradual conversion of agriculture to forest and their explanatory factors. Unpublished B.Sc. thesis, KU Leuven, Belgium, 57 pp.

Wouters, H., 2012. Land cover change Detection in the Romanian Carpathians (1986-2010). Unpublished M.Sc. thesis, KU Leuven, Belgium, 130 pp.

Deliever, I., 2012. Exploring the forest cover in the Romanian Carpathians (1986-2010). A remote sensing analysis using medium resolution Landsat and very high resolution WordlView-2 imagery. Unpublished M.Sc. thesis, KU Leuven, Belgium, 145 pp.

Free Remote Sensor.

This page, when rolled into a tube, makes a telescope with 1:1 magnification

FACULTY OF SCIENCE
DEPARTMENT OF EARTH AND ENVIRONMENTAL SCIENCES.
GEOGRAPHY DIVISION
Celestijnenlaan 200E box 2409
B-3001 HEVERLEE, BELGIUM
steven.vanonckelen@ees.kuleuven.be
www.ees.kuleuven.be